TOTAL SYNTHESIS OF CYANTHIWIGIN NATURAL PRODUCTS VIA DOUBLE ASYMMETRIC CATALYTIC ALKYLATION

AND

INVESTIGATIONS INTO THE NATURE OF DOUBLE ASYMMETRIC PROCESSES

Thesis by

John Andrew Enquist, Jr.

In Partial Fulfillment of the Requirements

for the Degree of

Doctor of Philosophy

CALIFORNIA INSTITUTE OF TECHNOLOGY

Pasadena, California

2011

(Defended September 28, 2010)

To my parents

ACKNOWLEDGEMENTS

Though a single thesis is often considered a personal endeavor, it is undeniable that scientific research requires the combined contributions of many different individuals. The work detailed in this thesis is no exception; it would not have been possible without the input, guidance, and support of a great many people.

First and foremost among those who have provided me with invaluable advice and opportunity is my mentor, Professor Brian Stoltz. From the first day that I had the privilege to meet Brian, his limitless enthusiasm for chemistry and his boundless creativity in addressing chemical problems have been sources of continual inspiration. During those times in my graduate career when my difficulties felt insurmountable, during those moments when chemistry felt tedious and overwhelming, a mere ten minute discussion with Brian was always enough to reenergize my interest and rekindle my motivation. In addition, Brian has been continually generous and understanding. When I initially asked to join his group, Brian's lab was already occupied to capacity. It was only through his negotiating with the department that additional lab space was secured to facilitate the members of my incoming class. Beyond even this, Brian was selfless enough to outfit those labs with completely new equipment. Brian's dedication to excellence and rigor in all aspects of scientific investigation have driven me to aspire to his example, and I have no doubt that his influence will shape the next generation of superlative chemists.

My committee chair, Professor Peter Dervan, has been an invaluable source of encouragement and advice for both my thesis and exit proposals. His energy and curiosity toward my work, and his advice looking toward the future, have bolstered my

resolve. Additionally, I must thank Professor Robert Grubbs for being an active and extremely helpful member of my committee and the chemistry department. The collaborative spirit that Professor Grubbs has fostered within his research program has considerably strengthened both the Stoltz group, and the Caltech community at large. Without the assistance and materials he and his group have provided, much of the work in this thesis would not be possible.

I also extend my gratitude to Professor Sarah Reisman, who has assisted with reviewing my proposals, served as an enthusiastic member of my thesis committee, and offered valuable advice for my pending postdoctoral studies. Furthermore she has built a dedicated, driven, and highly skilled research group to add to Caltech's chemistry department. When Professor Reisman's group first moved into the basement of Church laboratories, it was my privilege to share that space with them, and my pleasure to interact with both her and every member of her lab.

Dr. Scott Virgil has been an invaluable addition to the department, and the thorough and thoughtful regard with which he approaches all matters of chemistry have had a tremendous influence on the refinement my own technique. Without his input and assistance with the Symex robot, several critical experiments of this thesis simply would not have occurred. Additionally, Dr. Virgil provided keen insight and guidance into the refinement of the critical ring-closing cross-metathesis reaction in the cyanthiwigin synthetic sequence, and in so doing was instrumental in the completion of the work described in this thesis.

I also wish to thank Professor Jay Siegel for introducing me to synthesis. When I first enrolled in classes at UCSD as an undergraduate in the fall of 2000, I was

exceptionally apprehensive about taking organic chemistry at all. Professor Siegel's enthusiasm and teaching style allayed my fears completely. Rather than being overwhelming, his course was both an exciting and informative view into the field of synthetic chemistry. In his dedication to teaching, Professor Siegel held regular study sessions for his course on every Saturday afternoon. It was during these informal gatherings that I gained an appreciation for the science and an insight into its practical application that no textbook could cover. The subsequent classes taught by and advice that I received from Professor Siegel helped to shape my path toward graduate school, and I remain grateful for his influence.

Professor Yitzhak Tor was generous enough to accept me into his lab as an undergraduate student at UCSD, and it is thanks to his assistance that I was able to truly get my start in chemical research. While under his tutelage, was I introduced to the fundamentals of organic chemistry, and was continually inspired by the manner in which he applied the tools of synthesis to address biological questions. Also, Dr. Haim Weizman was a fantastic mentor during my time in the Tor lab, and I wish to thank him specifically for his assistance in transitioning from a book-educated student to a hands-on laboratory researcher.

Over the past six years, I have shared lab space with a number of exceptional graduate students and postdoctoral scholars. When I first joined the group, JT Mohr was generous (or perhaps unwitting) enough to allow me to share his hood. Not only did he accommodate an awkward and inexperienced first year student (something which significantly reduced his functional space), he also took the time out to teach me the proper basics of synthetic technique. From running asymmetric catalysis reactions to

using VNMR, JT was an exceptional mentor. Additionally, JT had an incredible tolerance for references to old movies and obscure internet culture, and never once complained when I would yell in aggravation at an exceptionally long column (or "Kahn column," as they eventually came to be known). Though I only spent a few short months cohabitating with JT in a single fume hood, he taught me much about synthesis, characterization, and surviving graduate school. He was also an excellent friend, and continued to suffer my sense of humor for years after I finally vacated his space.

While I passed my first months in the lab sharing a hood with JT, the next several years were passed sharing a bay with Kevin Allan. Whether in the basement of the Gates laboratories, the basement of the Church laboratories, or the third floor of the Schlinger building, Kevin has been one of the most motivated and inspirational chemists I've had the pleasure to know. His thoroughness, thoughtfulness, and determination in all matters of chemistry provided me with a constant example to aspire to in the lab. For example, in May of 2005 Kevin and I entered into the "Great Column Race" (which was less a race, and more an activity of curiosity). While I was able to run a total of 1,310 columns in my time as a graduate student, Kevin won the race handily with more than 1,447 columns performed. More than an accomplished and excellent experimentalist, though, Kevin was always a good sport and a great friend. From experiencing the bizarre condition of the "Thursday Night Crazies," to introducing me to new musical tastes, to suffering my bad habit of terrible puns, Kevin's presence helped me to keep my sanity throughout all of graduate school. I have no doubts whatsoever that his excellence will not diminish anytime soon, and I look forward to his continued success.

The list of positive influences and phenomenal chemists who have passed through the Stoltz group is no small list. In addition to being a top-tier scientist, Jennifer Roizen always brought a cheerful disposition and vigorous conversation to the lab, and interacting with her was consistently a positive experience. Daniel Caspi taught me not only about chemistry with highly polar materials, but he also instructed me on the fine details of computer maintenance, web design, and server upkeep. Mike Krout was an unwavering example of scientific rigor, and his dedication to reaction optimization remains an inspiration to this day. Uttam Tambar, Jenn Stockdill, Eric Ashley, Neil Garg, Eric Ferreira, David Ebner, Ryan McFadden, and Raissa Trend were and continue to be impressively talented chemists. Each and every one of them helped me to acclimate to the unfamiliar lab environment when I first joined, and never did any of them hesitate to provide me with assistance when I required it.

Douglas Behenna was instrumental in introducing me to the intricacies of the enantioselective allylation technology that he himself developed. Without his instruction and input, much of the early work of my thesis would not have been possible. He helped me considerably during my first days in the laboratory, and upon his return to Caltech, has also aided me tremendously in finishing the graduate school process. I thank him for his insightful conversations about chemistry, his willingness to edit portions of my thesis, and his direct and fantastic sense of humor.

I owe a debt of gratitude to both Chris Gilmore and Pamela Tadross for their assistance with the preparation of both my exit proposals and my thesis. Not only did they tirelessly edit even the most tedious of documents, they did so with professionalism and a keen eye, all while offering valuable advice. I also thank them both for their

entertaining and refreshing conversations, and their hospitality and generosity during gatherings of all kinds. Of course, I must thank Pam specifically for discussions (and live tests) involving all things related to baking.

Shyam Krishnan and Jun Chiba were all exemplary post-doctoral scholars, and it was a pleasure to share the basement of the Gates laboratories with them. Andrew Harned always seemed to have the perfect advice for any reaction I needed to run, and his assistance and pioneering work were fantastically helpful to me in the early days of my graduate studies. Andy McClory is one of the most organized and meticulous scientists I've ever met, and the conversations that we shared regarding any aspect of chemistry never failed to be engaging and thought provoking. Chris Henry has been a tremendous asset to the Stoltz group overall, particularly for his near super-human efforts in maintaining, moving, and repairing essential equipment. I would also like to thank Chris for his help in editing portions of my thesis. John Phillips, Christian Defieber, Nolan McDougal, Joshua Day, Kim Petersen, Toyoki Nishimata, Jan Streuff, Chris Henry, Thomas Jensen, Amanda Jones, Kousuke Tani, Zoltán Novák, Carolyn Woodroofe, Tomoko Ashizawa, Corrine Baumgartner, David White, Kristy Tran, Russell Smith, Xiaoquin Han, Charles Liu, Florian Vogt, Kotaro Kikushima, Fabian Piller, Masaki Seto, and Christian Grünanger are all model scientists. I thank them all for their freely offered assistance, as well as their camaraderie over the years. Sandy Ma, Hosea Nelson, Nathan Bennett, Alex Goldberg, Jonny Gordon, Jeff Holder, Allen Hong, Boram Hong, Narae Park, and Pradeep Bugga were also all wonderful coworkers. Though their contributions to my graduate experience are too numerous to list specifically, I thank them all for

maintaining the high level of professionalism and excellence for which the Stoltz research group is renowned.

Though science is certainly the first and foremost passion of all members of the Caltech community, it is the moments between the experiments that keep us refreshed and rejuvenated enough to revisit the lab. In this regard, Kevin and Melissa Kuhn were wonderful friends who helped to maintain my sanity. Not only did they regularly organize Friday evening gatherings, but they also shared their home with me for nearly every Thanksgiving since 2005. Conversations with Kevin regarding political or current events were always a joy, and his turkey preparation skills are unsurpassed. Nat Sherden, who is both a skilled chemist and lover of enigmatic internet culture, has also been a steadfast friend. Whether elucidating mechanistic details of the reactions I took for granted, or laughing at my references to cartoons that hardly anyone has ever seen, working with Nat has been a great experience. Matt Winston and Young In Oh have been both friendly and generous as well, and I thank them both for all they have done to help get me out of lab once and a while. Though the time we shared in lab was brief, working alongside Matt was an awesome experience, and I have few doubts that he will go far.

The Caltech chemistry department is privileged to employ an amazingly capable and warm staff, and I consider myself extremely fortunate for having the opportunity to interact with all of them. Dian Buchness was simply fantastic when I first arrived. Not only did she assist me in getting settled into a new and slightly overwhelming environment, she also helped to keep me on track during the confusing and disorienting time of my candidacy. Later, Agnes Tong provided invaluable assistance with the fine

details of completing my thesis, and I certainly thank her for all she did. Rick Gerhart is a man of both limitless patience and unquantifiable skill. His ability to repeatedly repair my clumsily broken manifolds over the years has been impressive. The good nature and speed with which he can fix any piece of damaged glassware makes a trip to the basement glass shop an awe inspiring experience. Tom Dunn is simply the linchpin of the entire department. His impressive capacity to mend any piece of broken equipment, repair any malfunctioning computer, and provide any obscure adapter has saved data, time, and heartache on multiple occasions. Paul Carroad has helped considerably with both lab upkeep and multiple relocations, and without his assistance I doubt that the department would be able to operate nearly as efficiently as it does. Joe Drew and Ron Koen have aided in the efficient ordering and shipping of numerous critical parcels, and have on many occasions assisted in locating important, but incorrectly delivered, packages. Dave VanderVelde, Chris Brandow, and Scott Ross all kept the NMR facility operating in peak condition. The mass-spectral facility run by Mona Shahgholi and Naseem Torian has always provided consistently excellent data in an expedient manner. Larry Henling and Mike Day were able to take a crystal of dubious quality and extract publication-worthy data from its nearly amorphous structure. To every one of the staff listed above, I extend my heartfelt appreciation for both their tireless contributions to the Caltech community, and their assistance with my own thesis work.

Finally, I wish to thank my family for their endless support and patience over the past six years. My mother has consistently encouraged me in my endeavors, holding confidence in my abilities even when I had none in them myself. Her reassurance, love, and care packages have helped to keep me motivated and over the years, even through the

most difficult of trials. My father has also been continually understanding and enthusiastic about my graduate studies. Weekly conversations with him always refueled my energy for the days ahead, and his advice on everything from doctors to cooking assisted me greatly. Unfortunately, a comprehensive list of all of the family members who have helped me in my graduate studies would be too large to include here. Instead, I would like to briefly offer my thanks to my stepfather Mike, my stepmother Janet, all of my grandparents, my stepbrothers Dave, Ryan, and Ben, my stepsisters Tracy, Tiffany, Christy, and Jenna, and all of their spouses and children. Their presence in my life has made me richer, and their belief in me has bolstered my resolve at times when I have needed it most.

The work contained herein would not have been possible without the contributions and help of all those listed above. To each and every one of them, I extend my deepest gratitude.

ABSTRACT

Since the initial isolation of the cyathane molecules in 1970, considerable synthetic interest has been invested into the preparation of these diterpenoid natural products. Owing to the biological activity and intriguing molecular architecture of these compounds, the members of the cyathane family of natural products have emerged as appealing targets for total synthesis. After a brief summary of the isolation and bioactivity properties of these diterpene compounds, previous synthetic efforts toward these molecules are reviewed.

A concise and versatile approach toward the preparation of the cyanthiwigin family of cyathane natural products is described. By leveraging a unique double asymmetric catalytic alkylation procedure it is possible to quickly establish two of the most critical stereocenters of the cyanthiwigin framework with high levels of selectivity and expediency. The synthesis additionally employs a tandem ring-opening and cross-metathesis reaction, and an aldehyde-olefin radical cyclization process, to rapidly arrive at the tricyclic cyathane core of the cyanthiwigin molecules. From this unifying intermediate, the preparation of cyanthiwigins B, F, and G are attained swiftly and without the need for protecting groups.

The nature of double asymmetric transformations is investigated from a historical, mathematical, and experimental perspective. The initial findings of Langenbeck and Horeau concerning the enantioenriching effects of scalemic duplication are described, with a specific focus on the impact of this phenomenon on total synthesis. A thorough mathematical examination, based on the work of Kagan, is then presented for situations involving double asymmetric transformations of prochiral starting materials. Expressions relating the final quantities of the stereoisomeric products to the intermediary selectivity of each stereoselective process are presented based on these formulae.

Finally, experiments designed to probe the selectivity of each stage of stereoselective bond construction in a double asymmetric process are presented. The compiled results are scrutinized in keeping with the previously derived equations, and these findings are analyzed to understand the nature of the double asymmetric processes in question.

TABLE OF CONTENTS

Dedication iii
Acknowledgements iv
Abstract xiii
Table of Contents xiv
List of Figures xviii
List of Schemes xxii
List of Tables xxvi
List of Abbreviations xxvii

CHAPTER 1 ***1***

Cyathane Diterpenoid Natural Products: Isolation, Activity, and Previous Synthetic Effort

1.1 Introduction 1
1.2 Overview of the Cyathane Diterpenoid Natural Products 2
1.2.1 Isolation 3
1.2.2 Bioactivity 5
1.2.3 Biosynthesis 5
1.3 Previous Synthetic Efforts 6
1.3.1 Strategy Summary 7
1.3.2 Cyanthane Core Syntheses 10
1.3.2.1 Wender's Cyathane Core Synthesis 10
1.3.2.2 Desmaële's Cyathane Core Synthesis 12
1.3.2.3 Takeda's Cyathane Core Synthesis 15
1.3.2.4 Sarpong's Cyathane Core Synthesis 16
1.3.3 Cyathane Total Syntheses 18
1.3.3.1 Snider's (±)-Allocyathin B_2 and (–)-Erinacine A Syntheses 18
1.3.3.2 Tori's (±)-Allocyathin B_2 Synthesis 20
1.3.3.3 Piers' (±)-Sarcadonin G Synthesis 21
1.3.3.4 Ward's (±)-Allocyathin B_3 Synthesis 23
1.3.3.5 Ward's (+)-Cyathin A_3 Synthesis 26
1.3.3.6 Nakada's (+)-Allocyathin B_2 Synthesis 27

1.3.3.7 Nakada's (–)-Erinacine B Synthesis 29
1.3.3.8 Nakada's (–)-Erinacine E Synthesis 31
1.3.3.9 Trost's (+)-Allocyathin B_2 Synthesis 33
1.3.3.10 Danishefsky's (–)-Scabronine G Synthesis 35
1.3.3.11 Phillip's Syntheses of (+)-Cyanthiwigin U, (+)-Cyanthiwigin W, and (–)-Cyanthiwigin Z 37
1.3.3.12 Reddy's (+)-Cyanthiwigin AC Synthesis 40
1.3.3.13 Cha's Syntheses of (±)-Cyathin A_3 and (±)-Cyathin B_2 42
1.4 Conclusions 44
1.5 Notes and References 45

CHAPTER 2 ***52***

Enantioselective Total Synthesis of Cyanthiwigin Diterpenoids

2.1 Introduction 52
2.1.1 Structure and Synthetic Challenges 52
2.1.2 Biological Activity 54
2.1.3 Retrosynthetic Analysis 55
2.2 Forward Synthetic Efforts 57
2.2.1 Double Asymmetric Decarboxylative Allylation 57
2.2.2 Diketone Desymmetrization and Elaboration 63
2.2.3 Tricycle Formation via Radical Cyclization 70
2.2.4 Completion of the Cyanthiwigin Natural Products 74
2.3 Concluding Remarks 78
2.4 Experimental Section 80
2.4.1 Materials and Methods 80
2.4.2 Preparative Procedures 82
2.5 Notes and References 116

APPENDIX 1 ***124***

Synthetic Summary for Cyanthiwigins B, F, and G

APPENDIX 2 ***126***

Spectra Relevant to Chapter 2

APPENDIX 3 ***179***

X-Ray Crystallography Reports Relevant to Chapter 2

CHAPTER 3 ***188***

A Mathematical Examination of Multiple Asymmetric Transformations: Statistical Amplification and the Horeau Principle

3.1 Introduction 188
3.1.1 Preliminary Results and Initial Interest....189
3.2 Duplication and Multiple Asymmetric Processes 191
3.2.1 The History of Statistical Amplification 192
3.2.2 Mathematical Representation of Horeau Duplication 196
3.2.3 Synthetic Applications of the Horeau Duplication 201
3.2.4 Multiple Asymmetric Transformations 205
3.2.5 Synthetic Applications of Multiple Asymmetric Transformations 220
3.3 Experimental Investigation of Multiple Asymmetric Transformations 223
3.4 Conclusion 235
3.5 Experimental Section…….. 237
3.5.1 Materials and Methods. 237
3.5.2 Preparative Procedures 239
3.6 Notes and References 253

APPENDIX 4 ***260***

Spectra Relevant to Chapter 3

APPENDIX 5 ***275***

Notebook Cross-Reference

Comprehensive Bibliography....278

Index 291

About the Author 296

LIST OF FIGURES

CHAPTER 1

Figure 1.1 Representative cyathane diterpenoid natural products 2

Figure 1.2 Transition metal and Lewis acid–catalyzed retrosynthetic disconnections toward the cyathane diterpenoid tricyclic core 8

Figure 1.3 (A) Alkylation and aldol retrosynthetic disconnections of the cyathane diterpenoid core
(B) Reddy's retrosynthetic disconnection of the cyanthiwigin AC core 9

CHAPTER 2

Figure 2.1 The cyanthiwigin diterpenoid molecules 54

Figure 2.2 X-ray crystal structure of tricycle **214** 74

APPENDIX 2

Figure A2.1 ^{1}H NMR (300 MHz, $CDCl_3$) of diallyl succinate (**187**) 127

Figure A2.2 Infrared spectrum (thin film/NaCl) of diallyl succinate (**187**) 128

Figure A2.3 ^{13}C NMR (75 MHz, $CDCl_3$) of diallyl succinate (**187**) 128

Figure A2.4 ^{1}H NMR (300 MHz, $CDCl_3$) of diallyl succinyl succinate (**189**) 129

Figure A2.5 Infrared spectrum (thin film/NaCl) of diallyl succinate (**189**) 130

Figure A2.6 ^{13}C NMR (75 MHz, $CDCl_3$) of diallyl succinate (**189**) 130

Figure A2.7 ^{1}H NMR (300 MHz, $CDCl_3$) of bis(β-ketoester) **186** 131

Figure A2.8 Infrared spectrum (thin film/NaCl) of bis(β-ketoester) **186** 132

Figure A2.9 ^{13}C NMR (75 MHz, $CDCl_3$) of bis(β-ketoester) **186** 132

Figure A2.10 ^{1}H NMR (300 MHz, $CDCl_3$) of diketone **185** 133

Figure A2.11 Infrared spectrum (thin film/NaCl) of diketone **185** 134

Figure A2.12 ^{13}C NMR (125 MHz, $CDCl_3$) of diketone **185** 134

Figure A2.13 ^{1}H NMR (300 MHz, $CDCl_3$) of triflate **194** 135

Figure A2.14 Infrared spectrum (thin film/NaCl) of triflate **194** 136

Figure A2.15 ^{13}C NMR (125 MHz, $CDCl_3$) of triflate **194** 136

Figure A2.16 ^{1}H NMR (500 MHz, $CDCl_3$) of enoate **195** 137

Figure A2.17 Infrared spectrum (thin film/NaCl) of enoate **195** 138
Figure A2.18 ^{13}C NMR (125 MHz, $CDCl_3$) of enoate **195** 138
Figure A2.19 ^{1}H NMR (500 MHz, $CDCl_3$) of cyclopentadienone **196** 139
Figure A2.20 Infrared spectrum (thin film/NaCl) of cyclopentadienone **196**.....140
Figure A2.21 ^{13}C NMR (125 MHz, $CDCl_3$) of cyclopentadienone **196** 140
Figure A2.22 ^{1}H NMR (500 MHz, $CDCl_3$) of spirocycle **197**.....141
Figure A2.23 Infrared spectrum (thin film/NaCl) of spirocycle **197**.....142
Figure A2.24 ^{13}C NMR (125 MHz, $CDCl_3$) of spirocycle **197**.....142
Figure A2.25 ^{1}H NMR (500 MHz, $CDCl_3$) of alkyne **198** 143
Figure A2.26 Infrared spectrum (thin film/NaCl) of alkyne **198**.....144
Figure A2.27 ^{13}C NMR (125 MHz, $CDCl_3$) of alkyne **198**.....144
Figure A2.28 ^{1}H NMR (500 MHz, $CDCl_3$) of ketone **200** 145
Figure A2.29 Infrared spectrum (thin film/NaCl) of ketone **200** 146
Figure A2.30 ^{13}C NMR (125 MHz, $CDCl_3$) of ketone **200** 146
Figure A2.31 ^{1}H NMR (500 MHz, $CDCl_3$) of bicyclic enone **204(A)** 147
Figure A2.32 Infrared spectrum (thin film/NaCl) of bicyclic enone **204(A)**.....148
Figure A2.33 ^{13}C NMR (125 MHz, $CDCl_3$) of bicyclic enone **204(A)**.....148
Figure A2.34 ^{1}H NMR (500 MHz, $CDCl_3$) of bicyclic enone **204(B)**.....149
Figure A2.35 Infrared spectrum (thin film/NaCl) of bicyclic enone **204(B)**.....150
Figure A2.36 ^{13}C NMR (125 MHz, $CDCl_3$) of bicyclic enone **204(B)**.....150
Figure A2.37 ^{1}H NMR (300 MHz, $CDCl_3$) of tetraolefin **183**.....151
Figure A2.38 Infrared spectrum (thin film/NaCl) of tetraolefin **183** 152
Figure A2.39 ^{13}C NMR (75 MHz, $CDCl_3$) of tetraolefin **183** 152
Figure A2.40 ^{1}H NMR (500 MHz, $CDCl_3$) of bicyclic ketone **181**.....153
Figure A2.41 Infrared spectrum (thin film/NaCl) of bicyclic ketone **181** 154
Figure A2.42 ^{13}C NMR (125 MHz, $CDCl_3$) of bicyclic ketone **181**.....154
Figure A2.43 ^{1}H NMR (300 MHz, $CDCl_3$) of bicyclic aldehyde **208**.....155
Figure A2.44 Infrared spectrum (thin film/NaCl) of bicyclic aldehyde **208**.....156
Figure A2.45 ^{13}C NMR (75 MHz, $CDCl_3$) of bicyclic aldehyde **208**.....156
Figure A2.46 ^{1}H NMR (500 MHz, $CDCl_3$) of bicyclic enoate **209**.....157
Figure A2.47 Infrared spectrum (thin film/NaCl) of bicyclic enoate **209**.....158
Figure A2.48 ^{13}C NMR (125 MHz, $CDCl_3$) of bicyclic enoate **209**.....158
Figure A2.49 ^{1}H NMR (500 MHz, $CDCl_3$) of tricyclic diketone **214** 159
Figure A2.50 Infrared spectrum (thin film/NaCl) of tricyclic diketone **214** 160
Figure A2.51 ^{13}C NMR (125 MHz, $CDCl_3$) of tricyclic diketone **214** 160

Figure A2.52 ^{1}H NMR (500 MHz, C_6D_6) of tricyclic triflate **217** 161
Figure A2.53 Infrared spectrum (thin film/NaCl) of tricyclic triflate **217** 162
Figure A2.54 ^{13}C NMR (125 MHz, C_6D_6) of tricyclic triflate **217** 162
Figure A2.55 ^{1}H NMR (500 MHz, $CDCl_3$) of cyanthiwigin F (**160**) 163
Figure A2.56 Infrared spectrum (thin film/NaCl) of cyanthiwigin F (**160**).....164
Figure A2.57 ^{13}C NMR (125 MHz, $CDCl_3$) of cyanthiwigin F (**160**) 164
Figure A2.58 ^{1}H NMR (500 MHz, $CDCl_3$) of tricyclic ketone **218** 165
Figure A2.59 Infrared spectrum (thin film/NaCl) of tricyclic ketone **218**.....166
Figure A2.60 ^{13}C NMR (125 MHz, $CDCl_3$) of tricyclic ketone **218** 166
Figure A2.61 ^{1}H NMR (500 MHz, $CDCl_3$) of tricyclic enone **220** 167
Figure A2.62 Infrared spectrum (thin film/NaCl) of tricyclic enone **220** 168
Figure A2.63 ^{13}C NMR (125 MHz, $CDCl_3$) of tricyclic enone **220** 168
Figure A2.64 ^{1}H NMR (500 MHz, $CDCl_3$) of allylic alcohol **221(A)** 169
Figure A2.65 Infrared spectrum (thin film/NaCl) of allylic alcohol **221(A)** 170
Figure A2.66 ^{13}C NMR (125 MHz, $CDCl_3$) of allylic alcohol **221(A)** 170
Figure A2.67 ^{1}H NMR (500 MHz, $CDCl_3$) of allylic alcohol **221(B)** 171
Figure A2.68 Infrared spectrum (thin film/NaCl) of allylic alcohol **221(B)**.....172
Figure A2.69 ^{13}C NMR (125 MHz, $CDCl_3$) of allylic alcohol **221(B)**.....172
Figure A2.70 ^{1}H NMR (500 MHz, $CDCl_3$) of cyanthiwigin B (**156**).....173
Figure A2.71 Infrared spectrum (thin film/NaCl) of cyanthiwigin B (**156**) 174
Figure A2.72 ^{13}C NMR (125 MHz, $CDCl_3$) of cyanthiwigin B (**156**).....174
Figure A2.73 ^{1}H NMR (500 MHz, $CDCl_3$) of 8-*epi*-cyanthiwigin E (**222**).....175
Figure A2.74 Infrared spectrum (thin film/NaCl) of 8-*epi*-cyanthiwigin E (**222**) 176
Figure A2.75 ^{13}C NMR (125 MHz, $CDCl_3$) of 8-*epi*-cyanthiwigin E (**222**).....176
Figure A2.76 ^{1}H NMR (500 MHz, $CDCl_3$) of cyanthiwigin G (**161**) 177
Figure A2.77 Infrared spectrum (thin film/NaCl) of cyanthiwigin G (**161**).....178
Figure A2.78 ^{13}C NMR (125 MHz, $CDCl_3$) of cyanthiwigin G (**161**) 178

APPENDIX 3

Figure A3.1 ORTEP drawing of tricyclic diketone **214** (shown with 50% probability ellipsoids) 179
Figure A3.2 Tricyclic diketone **214** (CCDC 664430).....182

CHAPTER 3

Figure 3.1 A graphical representation of the impact of Horeau duplication.....200

Figure 3.2 (A) Product *ee* plotted as a function of r_1 and r_2 selectivity factors
(B) Product *de* plotted as a function of r_1 and r_2 selectivity factors
(C) Product *ee* and *de* plotted as a function of r_1 and r_2 selectivity factors.....216

APPENDIX 4

Figure A4.1 ^{1}H NMR (500 MHz, $CDCl_3$) of carbonate **281**.....261

Figure A4.2 Infrared spectrum (thin film/NaCl) of carbonate **281**.....262

Figure A4.3 ^{13}C NMR (125 MHz, $CDCl_3$) of carbonate **281**.....262

Figure A4.4 ^{1}H NMR (500 MHz, $CDCl_3$) of allyl ketone **282**.....263

Figure A4.5 Infrared spectrum (thin film/NaCl) of allyl ketone **282**.....264

Figure A4.6 ^{13}C NMR (125 MHz, $CDCl_3$) of allyl ketone **282**.....264

Figure A4.7 ^{1}H NMR (500 MHz, $CDCl_3$) of β-ketoester **287(A)**.....265

Figure A4.8 Infrared spectrum (thin film/NaCl) of β-ketoester **287(A)**.....266

Figure A4.9 ^{13}C NMR (125 MHz, $CDCl_3$) of β-ketoester **287(A)**.....266

Figure A4.10 ^{1}H NMR (500 MHz, $CDCl_3$) of β-ketoester **287(B)**.....267

Figure A4.11 Infrared spectrum (thin film/NaCl) of β-ketoester **287(B)**.....268

Figure A4.12 ^{13}C NMR (125 MHz, $CDCl_3$) of β-ketoester **287(B)**.....268

Figure A4.13 ^{1}H NMR (500 MHz, $CDCl_3$) of carbonate ester **288**.....269

Figure A4.14 Infrared spectrum (thin film/NaCl) of carbonate ester **288**.....270

Figure A4.15 ^{13}C NMR (125 MHz, $CDCl_3$) of carbonate ester **288**.....270

Figure A4.16 ^{1}H NMR (500 MHz, $CDCl_3$) of carbonate ester **290**.....271

Figure A4.17 Infrared spectrum (thin film/NaCl) of carbonate ester **290**.....272

Figure A4.18 ^{13}C NMR (125 MHz, $CDCl_3$) of carbonate ester **290**.....272

Figure A4.16 ^{1}H NMR (500 MHz, $CDCl_3$) of diallyl cyclohexanone **289**.....273

Figure A4.17 Infrared spectrum (thin film/NaCl) of diallyl cyclohexanone **289**.....274

Figure A4.18 ^{13}C NMR (125 MHz, $CDCl_3$) of diallyl cyclohexanone **289**.....274

LIST OF SCHEMES

CHAPTER 1

Scheme 1.1 Biosynthesis of the cyathane core tricycle from geranylgeranyl phosphate.....6

Scheme 1.2 Preparation of the critical [5 + 2] cycloaddition precursor.....11

Scheme 1.3 Wender's [5 + 2] cycloaddition reaction to construct the cyathane core tricycle.....12

Scheme 1.4 Synthesis of Desmaële's alkyl iodide coupling partner.....13

Scheme 1.5 Preparation of the crucial Heck cyclization precursor.....13

Scheme 1.6 Heck cyclization and aluminum-promoted ring-expansion reactions to target the cyathane tricycle.....14

Scheme 1.7 Takada's key [4 + 3] annulation to target the C-ring of the cyathane core.....15

Scheme 1.8 Advancement of Takeda's cyathane core structure.....16

Scheme 1.9 Sarpong's parallel kinetic resolution method for divergent cyathane tricycle construction.....17

Scheme 1.10 Snider's carbonyl-ene strategy toward the cyathane tricycle.....19

Scheme 1.11 Completion of (±)-allocyathin B_2 and glycosylation to achieve (–)-erinacine A.....20

Scheme 1.12 Tori's strategy toward allocyathin B_2.....21

Scheme 1.13 Tori's ring-closing strategy toward construction of the seven-membered C-ring and completion of the cyathane core.....21

Scheme 1.14 Vinyl iodide construction in Pier's sarcodonin synthesis.....22

Scheme 1.15 Still–Mitra [2,3] sigmatropic rearrangement to construct the A-ring of sarcodonin G.....22

Scheme 1.16 Ring expansion and endgame for sarcodonin G.....23

Scheme 1.17 Ward's cycloaddition strategy toward tricycle formation.....24

Scheme 1.18 Ring expansion via ozonolysis and aldol reaction to target the cyathane core.....24

Scheme 1.19 Ward's allocyathin endgame strategy.....25

Scheme 1.20 Catalytic enantioselective Diels–Alder approach to intermediates **29** and **87**.....26

Scheme 1.21 Endgame synthesis for cyathin A_3 (TTBP = 2,6-di(*tert*-butyl)-4-methypyridine).....27

Scheme 1.22 Fragment coupling to prepare the aldol precursor.....28

Scheme 1.23 Intramolecular aldol reaction and ring expansion to complete the total synthesis of allocyathin B_2.....28

Scheme 1.24 Adaptation of Nakada's allocyathin B_2 route to erinacine B 30
Scheme 1.25 Estabilishing the desired stereochemistry at C(14) 30
Scheme 1.26 Completion of (–)-erinacine B 31
Scheme 1.27 Synthesis of **117** from allocyathin precursor **110** via conjugate addition-elimination 32
Scheme 1.28 Intramolecular aldol reaction for Nakada's endgame of (–)-erinacine E 32
Scheme 1.29 Asymmetric allylic alkylation to establish stereochemistry at C(9) 33
Scheme 1.30 Ru-catalyzed cycloisomerization to establish the central B-ring of allocyathin B_2 34
Scheme 1.31 Diastereoselectivity considerations in the Ru-catalyzed cycloisomerization 34
Scheme 1.32 Completion of allocyathin B_2 via hydroxylative Knoevenagel and intramolecular aldol reactions 35
Scheme 1.33 Danishefsky's Nazarov strategy for cyathane A-ring construction 36
Scheme 1.34 Advancement toward Danishefsky's ring-expansion precursor 36
Scheme 1.35 Ring expansion and endgame to complete (–)-scabronine G 37
Scheme 1.36 Auxilliary-mediated Diels–Alder reaction to establish the quanternary stereocenters of the natural product 38
Scheme 1.37 Completion of cyanthiwigin U via ring-opening ring-closing metathesis 38
Scheme 1.38 Preparation of cyanthiwigin W and cyanthiwigin Z from cyanthiwigin U 39
Scheme 1.39 Spiro-annulation of Hajos–Parrish ketone derivative **30** 40
Scheme 1.40 Further oxidation and transformation toward cyanthiwigin AC 41
Scheme 1.41 Endgame of cyanthiwigin AC 41
Scheme 1.42 Cha's spirocyclic approach to cyathin A_3 and cyathin B_2 43
Scheme 1.43 Cha's endgame for cyathin B_2 and elaboration to attain cyathin A_3 43

CHAPTER 2

Scheme 2.1 Retrosynthetic analysis of cyanthiwigin F 56
Scheme 2.2 Preparation of the bis(β-ketoester) substrate for allylation 58
Scheme 2.3 Paths of the double asymmetric decarboxylative catalytic alkylation 60
Scheme 2.4 Double asymmetric decarboxylative catalytic alkylation of **186** 62
Scheme 2.5 Attempts toward diketone functionalization 64
Scheme 2.6 (A) Triflate formation and carboxylative attempts toward diketone elaboration (B) An unanticipated carbonylative Heck reaction, and subsequent dimerization 66

Scheme 2.7 Palladium-catalyzed cross-coupling reactions of triflate **194** 66
Scheme 2.8 Ring-closing metathesis and acid hydrolysis of enol ether **202** 68
Scheme 2.9 Negishi cross-coupling for the formation of an sp^2-sp^3 carbon-carbon bond 69
Scheme 2.10 Functionalization of the C(2)-C(3) olefin via olefin cross-metathesis.....69
Scheme 2.11 Ring-closing and cross-metathesis reaction to generate bicyclic aldehyde **208** 70
Scheme 2.12 Initial attempts at radical cyclization for A-ring formation.....71
Scheme 2.13 Radical cyclization conditions developed by Tomioka and coworkers.....72
Scheme 2.14 Application of Tomioka's methodology to A-ring formation 72
Scheme 2.15 Mechanistic hypothesis and stereochemical rationale for radical cyclization of **214**.....73
Scheme 2.16 Advancement of tricycle **214** toward additional cyanthiwigin natural products.....77
Scheme 2.17 Completion of cyanthiwigins B and G 78

APPENDIX 1

Scheme A1.1 Synthesis of tricyclic diketone **214**.....125
Scheme A1.2 Synthesis of cyanthiwigin F (**160**).....125
Scheme A1.3 Synthesis of cyanthiwigins B (**156**) and G (**161**).....125

CHAPTER 3

Scheme 3.1 Double asymmetric catalytic alkylation 190
Scheme 3.2 Double asymmetric catalytic alkylation of an enol carbonate ester substrate 191
Scheme 3.3 (A) Lagenbeck's initial experiment
(B) Curves depicting the optical rotation of samples of (I) L-***225*** and (II) ***227*** vs. enantioenrichment of L-menthol starting material 193
Scheme 3.4 Product pathways for Langenbeck's duplication experiment.....194
Scheme 3.5 Duplication of *sec*-phenethyl alcohol by Horeau 196
Scheme 3.6 (A) Reaction pathways for Horeau-type dimerization
(B) Mathematical representations of relevant stereoisomeric quantities 198
Scheme 3.7 Initial steps toward Mori's synthesis of 2,8-dimethyl-1,7-dioxaspiro[5.5]undecane 201

Scheme 3.8 Horeau duplication in Mori's bee hormone synthesis 202
Scheme 3.9 Corey's total synthesis of (–)-wodeshiol via Horeau-type duplication 204
Scheme 3.10 Pathways for double asymmetric transformation, route 1 207
Scheme 3.11 Pathways for double asymmetric transformation, route 2 209
Scheme 3.12 Double asymmetric transformation via two variable simplification.....213
Scheme 3.13 Double asymmetric transformation where $r_1 = 1.0$ and $r_2 = 0$ 217
Scheme 3.14 Double asymmetric transformation where $r_1 = 0$ and $r_2 = 1.0$ 218
Scheme 3.15 Double asymmetric catalytic transformation toward quadrigemine C.....221
Scheme 3.16 Total synthesis of glabrescol by Corey 222
Scheme 3.17 Total synthesis of omaezakinol by Corey.....223
Scheme 3.18 Examples of double asymmetric catalytic alkylation 224
Scheme 3.19 (A) Schematic representation of intermediates in the double asymmetric alkylation of substrate ***186***
(B) Schematic representation of intermediates in the double asymmetric alkylation of substrate (±)-***223***.....225
Scheme 3.20 (A) Alkylation of racemic enol carbonate (±)-***281***
(B) Mathematical treatment of alkylation of ***281***.....226
Scheme 3.21 Asymmetric alkylation of an enantioenriched substrate.....229
Scheme 3.22 Substrates for double asymmetric catalytic alkylation studies 231
Scheme 3.23 Stereochemical course of double alkylation for a differentially substituted carbonate.....232
Scheme 3.24 Averaged selectivity values for double asymmetric catalytic alkylation 234
Scheme 3.25 Experiment proposed for further investigation of double asymmetric alkylation 235

LIST OF TABLES

CHAPTER 2

Table 2.1 Transition metal cross-coupling attempts toward cyanthiwigin F 76

APPENDIX 3

Table A3.1 Crystal data and structure refinement for tricyclic diketone **214** (CCDC 664430).....180

Table A3.2 Atomic coordinates (x 10^4) and equivalent isotropic displacement parameters (Å^{2}x 10^3) for diketone **214** (CCDC 664430). U(eq) is defined as the trace of the orthogonalized U^{ij} tensor 183

Table A3.3 Bond lengths [Å] and angles [°] for diketone **214** (CCDC 664430).....184

Table A3.4 Anisotropic displacement parameters (Å^{2}x 10^4) for diketone **214** (CCDC 664430). The anisotropic displacement factor exponent takes the form: $-2\pi^2[h^2a^{*2}U^{11} + ... + 2\ h\ k\ a^*\ b^*\ U^{12}]$ 186

Table A3.5 Hydrogen coordinates (x 10^4) and isotropic displacement parameters (Å^{2}x 10^3) for diketone **214** (CCDC 664430) 187

CHAPTER 3

Table 3.1 Stereochemical summary of Mori's synthetic efforts.....203

Table 3.2 Selected examples of r_1 and r_2 values, and their impact on *ee* and *de* 219

Table 3.3 Study on the effect of a pre-existing stereocenter upon asymmetric alkylation.....228

APPENDIX 5

Table A5.1 Compounds in Chapter 2 – Enantioselective Total Synthesis of Cyanthiwigin Diterpenoids.....276

Table A5.2 Compounds in Chapter 3 – A Mathematical Examination of Multiple Asymmetric Transformations: Statistical Amplification and the Horeau Principle 277

LIST OF ABBREVIATIONS

$[\alpha]_D$	angle of optical rotation of plane-polarized light
Å	angstrom(s)
Ac	acetyl
APCI	atmospheric pressure chemical ionization
app	apparent
aq	aqueous
Ar	aryl group
atm	atmosphere(s)
Bn	benzyl
Boc	*tert*-butoxycarbonyl
bp	boiling point
br	broad
Bu	butyl
i-Bu	*iso*-butyl
n-Bu	butyl or *norm*-butyl
t-Bu	*tert*-butyl
Bn	benzyl
Bz	benzoyl
c	concentration of sample for measurement of optical rotation
^{13}C	carbon-13 isotope
/C	supported on activated carbon charcoal
°C	degrees Celsius

calc'd	calculated
CAN	ceric ammonium nitrate
Cbz	benzyloxycarbonyl
CCDC	Cambridge Crystallographic Data Centre
CDI	1,1'-carbonyldiimidazole
cf.	consult or compare to (Latin: *confer*)
cm^{-1}	wavenumber(s)
cod	1,5-cyclooctadiene
comp	complex
conc.	concentrated
CSA	camphor sulfonic acid
d	doublet
D	dextrorotatory
dba	dibenzylideneacetone
pmdba	bis(4-methoxybenzylidene)acetone
dmdba	bis(3,5-dimethoxybenzylidene)acetone
DBU	1,8-diazabicyclo[5.4.0]undec-7-ene
DCE	1,2-dichloroethane
de	diastereomeric excess
DIAD	diisopropyl azodicarboxylate
DMAD	dimethyl acetylenedicarboxylate
DMAP	4-dimethylaminopyridine
DME	1,2-dimethoxyethane

DMF	*N*,*N*-dimethylformamide
DMSO	dimethylsulfoxide
dppp	1,3-bis(diphenylphosphino)propane
dr	diastereomeric ratio
ee	enantiomeric excess
E	trans (entgegen) olefin geometry
EC_{50}	median effective concentration (50%)
e.g.	for example (Latin: *exempli gratia*)
EI	electron impact
ESI	electrospray ionization
Et	ethyl
et al.	and others (Latin: *et alii*)
FAB	fast atom bombardment
g	gram(s)
h	hour(s)
^{1}H	proton
^{2}H	deuterium
^{3}H	tritium
[H]	reduction
HMDS	hexamethyldisilamide or hexamethyldisilazide
$h\nu$	light
HPLC	high performance liquid chromatography
HRMS	high resolution mass spectrometry

Hz	hertz
IC_{50}	half maximal inhibitory concentration (50%)
i.e.	that is (Latin: *id est*)
IR	infrared spectroscopy
J	coupling constant
k	rate constant
kcal	kilocalorie(s)
kg	kilogram(s)
L	liter or neutral ligand
L	levorotatory
LA	Lewis acid
LD_{50}	median lethal dose (50%)
LDA	lithium diisopropylamide
LTMP	lithium 2,2,6,6-tetramethylpiperidide
m	multiplet or meter(s)
M	molar or molecular ion
m	meta
μ	micro
m-CPBA	*meta*-chloroperbenzoic acid
Me	methyl
mg	milligram(s)
MHz	megahertz
min	minute(s)

mL	milliliter(s)
mol	mole(s)
MOM	methoxymethyl
mp	melting point
Ms	methanesulfonyl (mesyl)
MS	molecular sieves
m/*z*	mass-to-charge ratio
N	normal or molar
NBS	*N*-bromosuccinimide
nm	nanometer(s)
NMR	nuclear magnetic resonance
NOE	nuclear Overhauser effect
NOESY	nuclear Overhauser enhancement spectroscopy
o	ortho
[O]	oxidation
p	para
PCC	pyridinium chlorochromate
PDC	pyridinium dichromate
Ph	phenyl
pH	hydrogen ion concentration in aqueous solution
pK_a	acid dissociation constant
PMB	*para*-methoxybenzyl
ppm	parts per million

PPTS	pyridinium *para*-toluenesulfonate
Pr	propyl
i-Pr	isopropyl
n-Pr	propyl or *norm*-propyl
psi	pounds per square inch
py	pyridine
q	quartet
R	alkyl group
R	rectus
r	selectivity = [major stereoisomer – minor stereoisomer]/[major stereoisomer + minor stereoisomer]
ref	reference
R_f	retention factor
s	singlet or seconds
s	selectivity factor = $k_{rel(fast/slow)} = \ln[(1 - C)(1 - ee)]/\ln[(1 - C)(1 + ee)]$, where C = conversion
S	sinister
sat.	saturated
SEM	2-(trimethylsilyl)ethoxymethyl
t	triplet
TBAF	tetra-*n*-butylammonium fluoride
TBAT	tetra-*n*-butylammonium difluorotriphenylsilicate
TBDPS	*tert*-butyldiphenylsilyl
TBS	*tert*-butyldimethylsilyl

temp	temperature
TES	triethylsilyl
Tf	trifluoromethanesulfonyl
TFA	trifluoroacetic acid
THF	tetrahydrofuran
TIPS	triisopropylsilyl
TLC	thin layer chromatography
TMEDA	*N*,*N*,*N*',*N*'-tetramethylethylenediamine
TMS	trimethylsilyl
TOF	time-of-flight
tol	tolyl
t_r	retention time
Ts	*para*-toluenesulfonyl (tosyl)
UV	ultraviolet
w/v	weight per volume
v/v	volume per volume
X	anionic ligand or halide
Z	cis (zusammen) olefin geometry

CHAPTER 1[†]

Cyathane Diterpenoid Natural Products:

Isolation, Activity, and Previous Synthetic Efforts

1.1 INTRODUCTION

The following chapter is intended to present an overview of the isolation, bioactivity, and synthetic efforts published concerning the cyathane diterpenoid natural products. For the purpose of comprehensive review and comparison, all known completed total syntheses will be presented below, with a specific focus on the ring-forming and stereocenter-forming strategies employed therein.[1] The work summarized herein includes only those reports of cyathane core syntheses disclosed past 2000. All preceding work toward cyathane core preparation has been previously summarized in a review by Wright, which can be consulted for further detail.[2]

[†] Portions of this chapter have been reproduced from *Nat. Prod. Rep.* **2009**, *26*, 661–680.

1.2 OVERVIEW OF THE CYATHANE DITERPENOID NATURAL PRODUCTS

The cyathane molecules are a class of diterpene natural products, which are isolated from a diverse variety of fungi, sponges, and fruiting plants. However, despite their myriad natural sources, all cyathanes are unified by the presence of a characteristic fused 5-6-7 tricarbocyclic structure (1, Figure 1.1).

Figure 1.1 Representative cyathane diterpenoid natural products

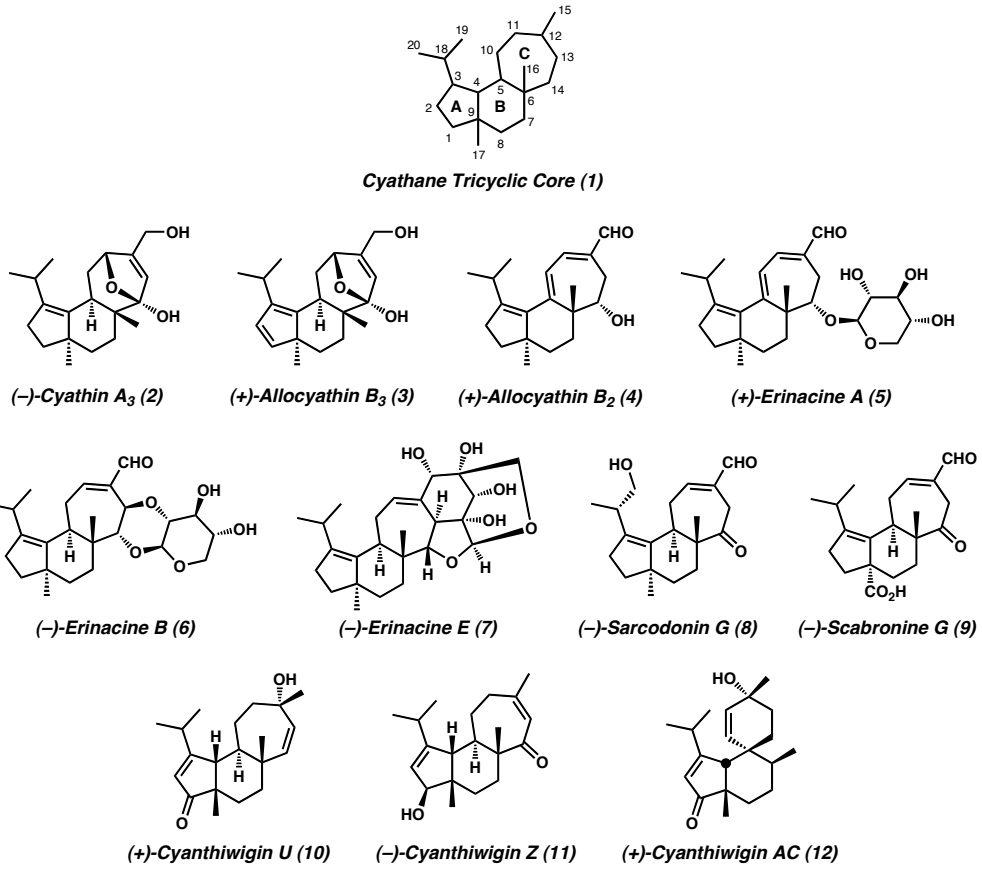

Within this class of natural products can be found the cyathins, the allocyathins, the erinacines, the sarcodonins, the scabronines, the striatals, the cyanthiwigins, and the cyafrins, all of which display the conserved carbon scaffold of the cyathane skeleton (**1**). Of the twenty carbons that comprise this cyathane framework, the C(6) and C(9) carbons

present all-carbon quaternary stereocenters that bear angular methyl groups at the points of ring fusion. Almost all of the compounds within the cyathane class display these methyl groups with an anti relative stereochemical relationship, though the cyanthiwigin natural products possess a *syn* arrangement. The cyathane core structure is additionally characterized by the presence of an isopropyl side chain at C(3) and an exocyclic carbon atom connected to C(12).

1.2.1 ISOLATION

In 1970, Ayer and Brodie published a report in which an extract from the bird's nest fungus *Cyathus helenae* was scrutinized to better understand its antimicrobial activity. Though no full structural assignment was made for any compound within the extract, the active components of the mixture were separated via chromatography. After isolation and elemental analysis, the compounds responsible for the observed antimicrobial activity were named (without structural elucidation) as cyathin A_3, A_4, B_3, B_4, C_5, and allocyathin A_4.[3] The first fully characterized cyathane diterpene natural products were subsequently reported by Ayer and coworkers in 1972, when the substance previously identified as cyathin A_3 was found to be a mixture of isomeric compounds, which they named cyathin A_3 (**2**) and allocyathin B_3 (**3**).[4] Numerous other cyathin and allocyathin natural products were discovered subsequent to this report, including allocyathin B_2 (**4**),[5] a cyathane diterpenoid that has since become the focus of numerous synthetic studies.

Following the identification of the primary cyathin diterpenoids, several structurally related compounds were isolated from additional natural sources. It was discovered that the fruiting bodies of *Hericium erinaceum* contained a number of

glycosylated allocyathin B_2 analogues, which were eventually named the erinacines. Among the compounds obtained from *Hericium erinaceum* were erinacine A (**5**), erinacine B (**6**), and the more structurally complex erinacine E (**7**).[6]

In 1989 Nakayama and coworkers published the isolation and structural assignment of eight new cyathane molecules from the fungus *Sarcodon scabrosus* that they named the sarcodonins A–H.[7] These compounds possess the conserved 5-6-7 tricyclic core found in all other cyathane natural products, but are distinct from the larger family in that they display further oxidation of the C(19) carbon, as can be observed in sarcodonin G (**8**). Beyond the sarcodonin molecules, an additional class of cyathane diterpene compounds were eventually identified from extracts of the same *Sarcodon scabrosus* fungus. In 1998, by Oshima and coworkers reported the isolation and characterization of the scabronines A–F. Six years later, Liu *et al*. disclosed the isolation of two more compounds of this type from the same source, including scabronine G (**9**).[8] Structural elucidation of the scabornine natural products revealed the presence of a carboxyl group at C(17), a feature that marks these terpenoids as distinct from the remainder of the cyathanes.

In 1992, Kashman and coworkers published a report detailing the isolation and characterization of the first cyanthiwigin molecules. Initially obtained from the marine sponge *Epipolasis reiswigi*, cyanthiwigins A–D were structurally assigned, including their absolute configurations, via NMR, X-ray, and Mosher ester analysis.[9] A decade later the laboratories of Hamann isolated an additional 23 compounds of this class from a decoction of the Jamaican sea sponge *Myrmekioderma styx*. This isolation included the products cyanthiwigin U (**10**) and cyanthiwigin Z (**11**). In the years subsequent to their

initial report, Hamann and coworkers have detailed the isolation and characterization of additional cyanthiwigin molecules AB–AG, including the structurally unique spirocyclic cyanthwigin AC (**12**).[10]

1.2.2 BIOACTIVITY

The biological activity of the cyathane natural products varies widely among the different molecules within the class. Many of these diterpene compounds possess both antibiotic and antimicrobial activity, such as the previously discussed cyathin A_3 (**2**) and allocyathin B_3 (**3**). Indeed, almost all of the subcategories of cyathane molecules display mild activity in this regard.[3,5,10] In addition to serving an antibiotic function, some members of the cyanthiwigin compounds exhibit limited cytotoxic activity against human primary tumor cells, P388 murine leukemia cells, and A549 lung tumor cells.[10,11]

However, the most significant facet of biological activity reported among these diterpenoid molecules is their powerful ability to encourage the synthesis of nerve growth factor (NGF). Both the erinacine and the scabronine natural products have displayed considerable potency in the stimulation of NGF synthesis,[6,8b] a capacity that implicates their potential use as therapeutic agents to treat neurodegenerative ailments such as Alzheimer's or Parkinson's disease.[12]

1.2.3 BIOSYNTHESIS

The details of cyathane diterpenoid biosynthesis have been covered in Wright's review, and as such will only be briefly summarized here.[2] Subsequent to his isolation of

the parent cyathins, Ayer conducted an in-depth study to scrutinize the biosynthetic origin of the cyathane diterpenoid core. By growing *Cyathus earlei* in the presence of ^{13}C-labelled sodium acetate, Ayer was able to isolate and examine isotopically enriched cyathin molecules produced by these fungal bodies. Analysis of these compounds via ^{13}C NMR allowed Ayer to conclude that the biosynthetic pathway toward the cyathane core tricycle involves cascade cyclization and subsequent rearrangement of geranylgeranyl phosphate (**13** through **16**, Scheme 1.1).[13]

Scheme 1.1 Biosynthesis of the cyathane core tricycle from geranylgeranyl phosphate

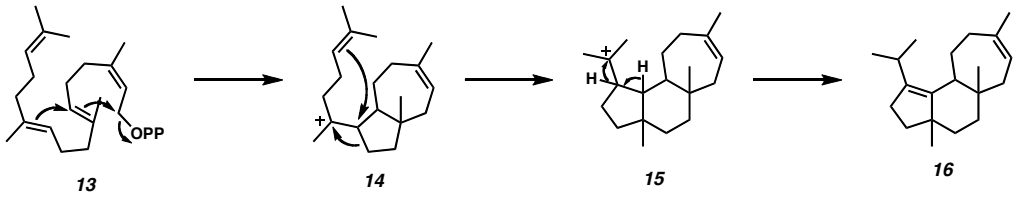

1.3 PREVIOUS SYNTHETIC EFFORTS

Since the first isolation of these diterpene natural products in the early 1970s, numerous research groups have endeavored to synthesize the cyathanes. A multitude of diverse strategies have been documented in the literature, and many of these approaches are presented below in schematic form. The synthetic efforts reported to date can be roughly categorized by their key transformations, all of which can be classified as either transition metal-mediated reactions (Scheme 1.2), or akylation/aldol reactions (Scheme 1.3).

1.3.1 STRATEGY SUMMARY

A majority of the cyathane syntheses published to date leverage various metal-catalyzed transformations to accomplish difficult or complicated ring-forming reactions. For example, the strategy employed by Trost *et al*. employs a Ru-catalyzed cycloisomerization to close the central B-ring of the cyathane core, an approach that leads back to allylic alcohol **17** (Figure 1.2). Similarly, Desmaële's route relies upon a Pd-catalyzed intramolecular Heck cyclization to construct the core B-ring, invoking diene **20** as a critical retrosynthetic precursor. Danishefsky's approach to the tricycle implements an Fe-catalyzed Nazarov cyclization for construction of the five-membered A-ring, allowing for strategic disconnection back to dienone **24**. Beyond the A- and B-rings, metal-catalyzed methodology has also been used to target the seven-membered C-ring of the cyathane core. For example, Snider's method toward these diterpene molecules utilizes an Al-catalyzed carbonyl-ene reaction for C-ring construction from bicyclic aldehyde **18**. The laboratories of Cha *et al*. have constructed the seven-membered cyathane C-ring via ring-closing metathesis, thus invoking bicycle **21** as a critical precursor. Sarpong and coworkers seal the C-ring via a novel parallel kinetic resolution, which allows for the use of racemic diene **22** in an enantiodivergent approach toward the cyathin core tricycle.

The power of transition-metal catalysis has also enabled strategies that invoke simultaneous multicyclic construction. For example, Phillips employs an efficient Ru-catalyzed ring-opening ring-closing metathesis strategy to build both the A- and C-rings of the cyathane core in tandem, thus invoking bridged bicycle **23** as a retrosynthetic precursor. Wender's [5 + 2] cycloaddition approach toward the cyathane skeleton allows

for cascade construction of both the B- and C-rings simultaneously, thus retrosynthetically disconnecting the core backward to ynone **19**.

Figure 1.2 Transition metal and Lewis acid-catalyzed retrosynthetic disconnections toward the cyathane diterpenoid tricyclic core

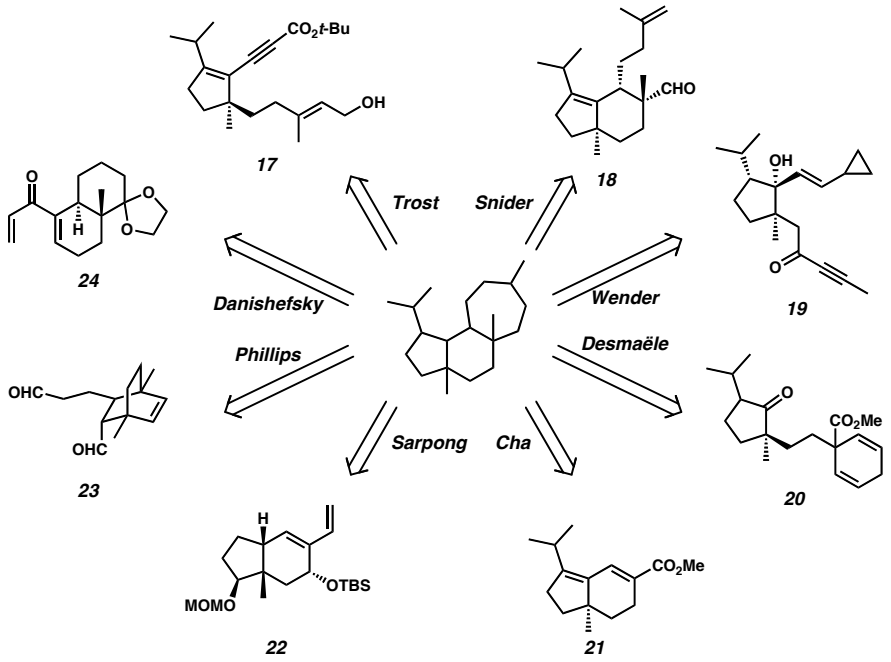

Another unifying approach by which the cyathane tricycle has been targeted is that of an aklyation strategy, often specifically in the form of an aldol reaction. In order to construct the C-ring of the tricyclic diterpene core, Ward and his group employ an ozonolysis and aldol sequence. This ring-expanding strategy invokes tricycle **29** as an important synthetic precursor (Figure 1.3A). Tori implements a similar technique to C-ring formation in his synthesis, wherein bis-aldehyde **27** is invoked via a disconnection of the cyathane core by means of an intramolecular aldol reaction.

Figure 1.3 (A) Alkylation and aldol retrosynthetic disconnections of the cyathane diterpenoid tricyclic core (B) Reddy's retrosynthetic disconnection of the cyanthiwigin AC core

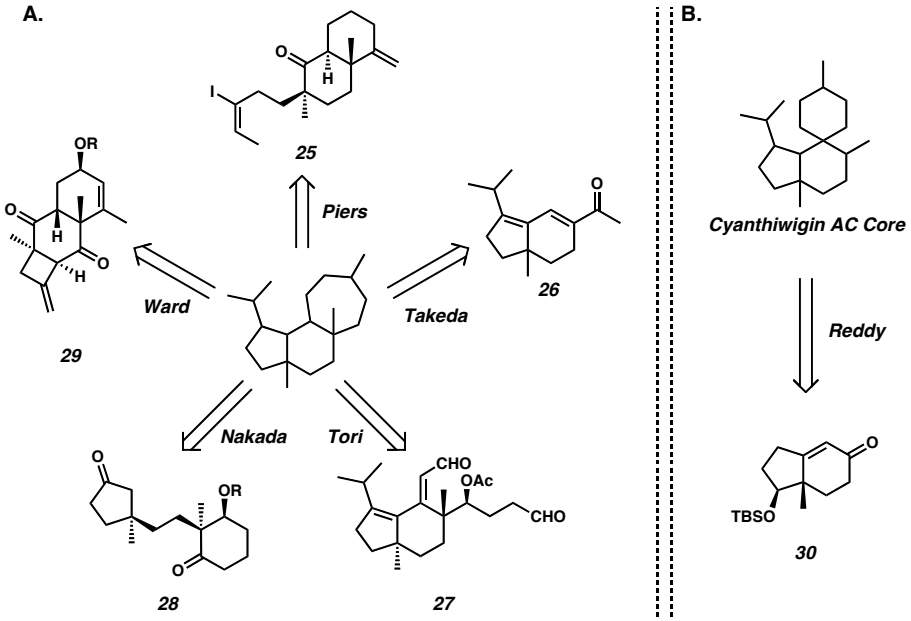

The cyathane C-ring has also been constructed via a unique [3 + 4] annulation reaction developed by Takeda, which employes **26** as a bicyclic precursor to the larger tricyclic skeleton. A convergent strategy targeting the B-ring of the cyathane core can be found in Nakada's approach toward these natural products. By disconnecting the central ring of the tricycle, Nakada invokes tethered system **28** as the critical substrate for an intramolecular aldol reaction. Non-aldol alkylation procedures have also played a role in cyathane synthetic design. Reddy disconnects the smaller six-membered C-ring of cyanthiwigin AC via an enolate spiro-alkylation strategy to invoke bicycle **30** as a precursor (Figure 1.3B). Moreover, an anionic alkylation approach has also proven fruitful for construction of the five-membered cyathane A-ring. In this regard, Piers' retrosynthetic analysis of the cyathane core opens the A-ring to vinyl iodide **25**, a

structure that, after lithium-halogen exchange and ketone trapping, closes to give a tricyclic system.

1.3.2 CYATHANE CORE SYNTHESES

Several groups have devised efficient strategies toward preparation of partial cyathane diterpenoid molecules, all of which possess potential divergent extensions to the synthesis of multiple natural products. For the purpose of this chapter, core syntheses will entail those efforts toward cyathane molecules that have successfully attained a completed tricyclic scaffold.

The section below is intended as an update to the review published in 2000.[2] As such, only cyathane core syntheses published after this date will be summarized here.

1.3.2.1 WENDER'S CYATHANE CORE SYNTHESIS

A general route toward the construction of the 5-6-7 tricyclic diterpene core was reported by the laboratories of Wender in 2001 by implementation of a [5 + 2] Rh-catalyzed cycloaddition reaction.[14] Beginning with (–)-limonene (**31**), hydrogenation, oxidative olefin cleavage, and intramolecular aldol condensation afforded enal **32** (Scheme 1.2). After reduction and vinyl ether formation, a thermal Claisen rearrangement yielded aldehyde **33** as a 10:1 mixture of inseparable diastereomers. Cyclopentane **33** was thereafter advanced along four steps, including ozonolysis of the exocyclic methylene and addition of lithium cyclopropylacetylide, to furnish cyclopentanol **34** as a mixture of diastereomers. Stereoselective reduction of cyclopropyl

alkyne **34** allowed access to diol **35**, which was oxidized, then exposed to 1-propynylmagnesium bromide to generate propargyl alcohol **36**. Attempts to execute a [5 + 2] cycloaddition reaction using alcohol **36** as the starting material were unfortunately unsuccessful, and yielded only a complicated mixture of products. Due to this difficulty, enyne **36** was oxidized to conjugated ketone **19** before executing the [5 + 2] cycloaddition reaction.

Scheme 1.2 Preparation of the critical [5 + 2] cycloaddition precursor

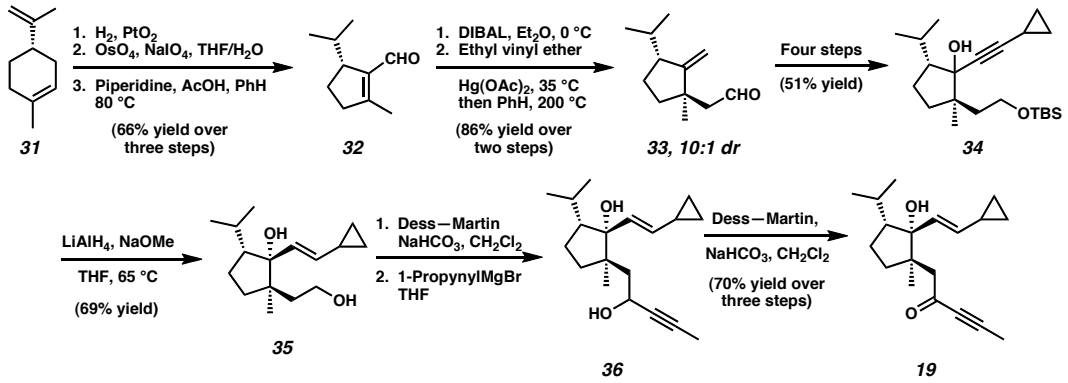

Upon exposure of vinyl cyclopropane **19** to 5 mol% of $[Rh(CO)_2Cl]_2$, the desired cycloaddition reaction proceeded in high yield to provide tricycle **39** as a single diastereomer (Scheme 1.3).[15] The critical [5 + 2] cycloaddition reaction initiates with complexation of the rhodium catalyst to both the alkyne moiety and the vinyl cyclopropane group. This is then followed by oxidative cyclometallation to form an intermediate metallocyclopentane (**37**), which in turn undergoes strain-driven cyclopropane ring-opening and ring-expansion to generate a transient metallocyclooctadiene species (**38**). Reductive elimination of rhodium from **38** thereafter yields tricyclic structure **39**, representing a completed cyathane core. The structure of

tricyclic enone **39** was verified by single-crystal X-ray crystallography. Overall, this strategy allows access to a completed 5-6-7 tricyclic structure in 14 steps and 13% overall yield.

Scheme 1.3 Wender's [5 + 2] cycloaddition reaction to construct the cyathane core tricycle

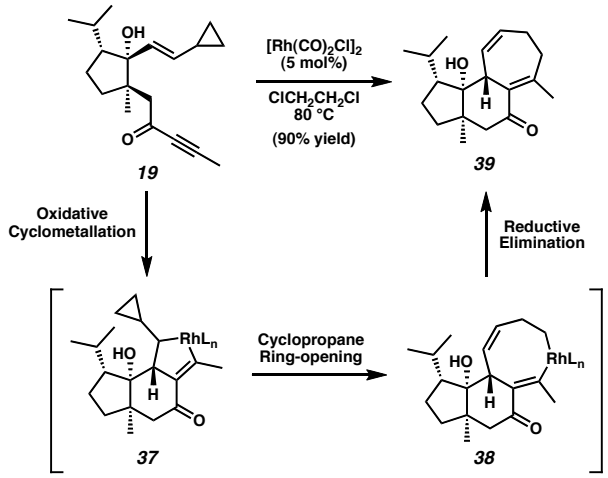

1.3.2.2 DESMAËLE'S CYATHANE CORE SYNTHESIS

A generalized synthetic route toward the tricyclic cyathane core skeleton was developed by Desmaële and coworkers in 2002, and an updated version of this strategy was later published in 2005.[16] When addressing the challenges present in constructing the tricyclic cyathane framework, Desmaële posits that establishing the anti relationship between the methyl groups of C(6) and C(9) represents the most significant obstacle. In order to solve this stereochemical issue, his envisioned strategy involves late-stage construction of the central B-ring of the tricycle via intramolecular Heck reaction between tethered A- and C-ring fragments.

Scheme 1.4 Synthesis of Desmaële's alkyl iodide coupling partner

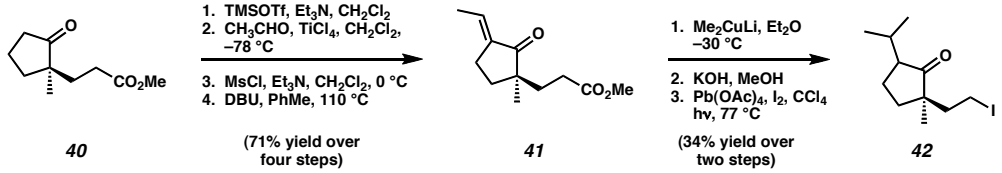

The synthesis was initated from known, enantioenriched keto-ester **40** (Scheme 1.4).[17] Mukaiyama aldol reaction with acetaldehyde, followed by dehydration and isomerization, yielded enone **41**. After cuprate addition to and saponification of ester **41**, the intermediate keto-acid obtained was then subjected to the Kochi modification of the Hunsdiecker reaction to afford primary iodide **42**. Displacement of iodide **42** with the lithium enolate of methyl ester **43** then provided tethered intermediate **20**, which was subjected to a four step sequence to access the critical Heck cyclization precursor **44** (Scheme 1.5). Notably, prior attempts at an intramolecular Heck cyclization involving a seven-membered ring dieneone proved quite difficult to advance along this synthetic path, and for this reason Desmaële opted to employ a six-membered C-ring surrogate instead.

Scheme 1.5 Preparation of the crucial Heck cyclization precursor

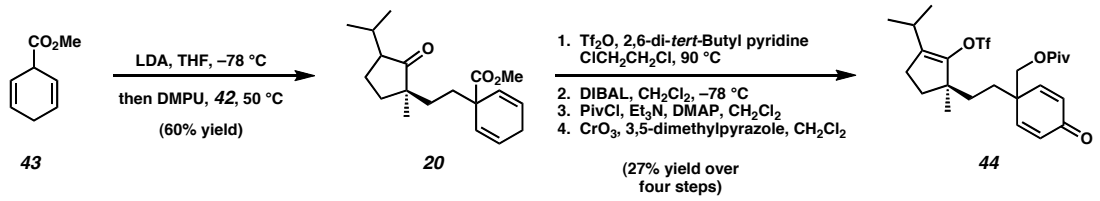

Several attempts to cyclize precursor **44** via intramolecular Heck reaction under standard conditions were complicated by either undesired acetate addition to, or incorrect

relative stereochemistry of, the resulting products.[16a] Eventually, further optimization of this reaction led Desmaële to discover that exposure of triflate **44** to 20 mol% of $Pd(OAc)_2$ in the presence of PPh_3 and *n*-Bu_4NBr could execute the desired Heck reaction to yield tricycle **45** in 73% yield and a 19:1 diastereomeric ratio (Scheme 1.6).[18] This transformation constructed the central B-ring of the cyathane core while simultaneously establishing the necessary all-carbon quaternary stereocenter at C(6) via desymmetrization of the pendent C-ring precursor.[16b,c]

Scheme 1.6 Heck cyclization and aluminum-promoted ring expansion reactions to target the cyathane tricycle

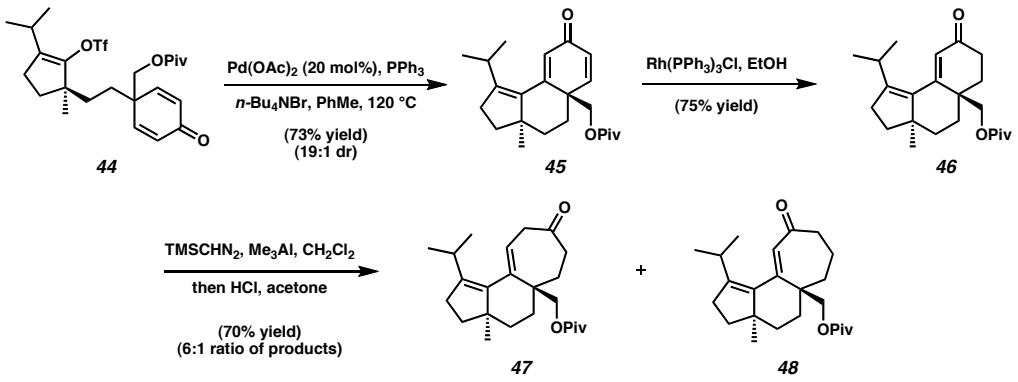

Elaboration of tricyclic dienone **45** toward the cyathane core structure proceeded via hydrogenation of the disubstituted olefin using Wilkinson's catalyst to give enone **46**. This reduction was then followed by treatment of tricycle **46** with trimethyl aluminum and trimethylsilyl diazomethane to effect an organoaluminium-promoted ring expansion.[19] This reaction afforded the completed 5-6-7 tricyclic framework as a 6:1 mixture of ketone (**47**) and enone (**48**) isomers. By obtaining these tricyclic structures, Desmaële accomplished the construction of the cyathane core tricycle over 15 steps and in an overall combined yield of 1.4% for both isomers obtained.

1.3.2.3 TAKEDA'S CYATHANE CORE SYNTHESIS

In 2000, Tekada and coworkers disclosed a synthesis of the cyathane core that leveraged a unique [4 + 3] annulation strategy for tricycle construction.[20] Starting from known racemic enone **49**, addition of ethynyl Grignard was followed by a Rupe rearrangement to give extended conjugated enone system **26** (Scheme 1.7). Formation of the lithium enolate of **26** was followed by addition to acyl silane **50**. Initial nucleophilic addition of the enolate of **26** to **50** produces intermediate alkoxide **51**, which undergoes Brook rearrangement and subsequent intramolecular nucleophilic carbonyl addition to form cyclopropane **52**. Divinyl cyclopropane species **52** thereafter undergoes spontaneous divinyl cyclopropane rearragement to form the cyathane C-ring, a process that is accelerated by the presence of an alkoxide. After this sigmatropic rearrangement occurs, the completed cyathane core structure **53** is afforded as a single diastereomer.[21]

Scheme 1.7 Takeda's key [4 + 3] annulation to target the C-ring of the cyathane core

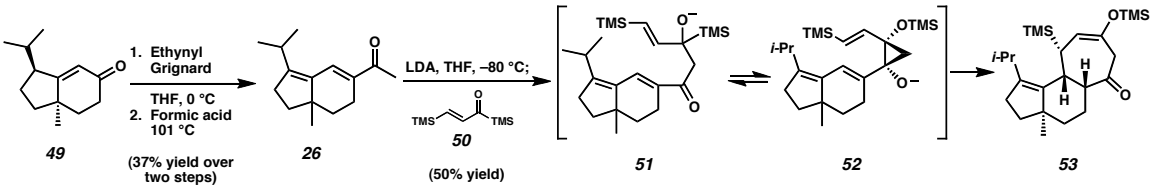

Continued functionalization of tricycle **53** was accomplished by diastereoselective DIBAL reduction, a process which provided the isomerically pure silyl enol ether **54** (Scheme 1.8). Notably, the stereochemistry yielded by this reduction at C(14) gave the alcohol epimer analogous to that of allocyathin B_2.[21] Takeda and coworkers thereafter concluded their efforts with oxidation of the enol silane present in **54** and subsequent

cleavage of the C-bound trimethylsilyl group. This furnished **55** as the final product of the synthetic sequence.

Scheme 1.8 Advancement of Takeda's cyathane core structure

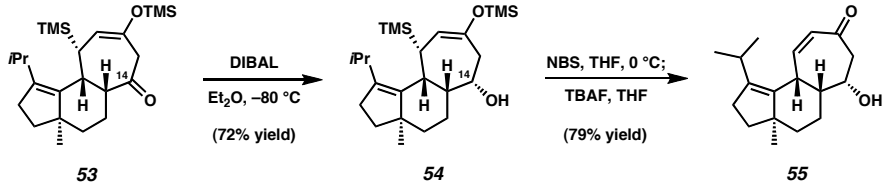

53 ***54*** ***55***

Beginning from known enone **49**, the des-methyl cyathane core was established in three steps and 19% yield, while the more elaborated cyathane analog **55** was produced in 11% yield over five steps.

1.3.2.4 SARPONG'S CYATHANE CORE SYNTHESIS

Sarpong *et al*. have described a unique parallel kinetic resolution method to target the cyathane core tricycle.[22] Bicyclic diene **22**, which was prepared from the Hajos-Parrish ketone, was subjected to a number of rhodium-catalyzed cyclopropanation reactions in order to initiate a divinylcyclopropane rearrangement for construction of the seven-membered C-ring. In the event, exposure of racemic diene **22** to vinyldiazoacetate **56** in the presence of Davies' chiral dirhodium tetraprolinate complex **57** proceeded with good catalyst control and facial selectivity (Scheme 1.9).

Scheme 1.9 Sarpong's parallel kinetic resolution method for divergent cyathane tricycle construction

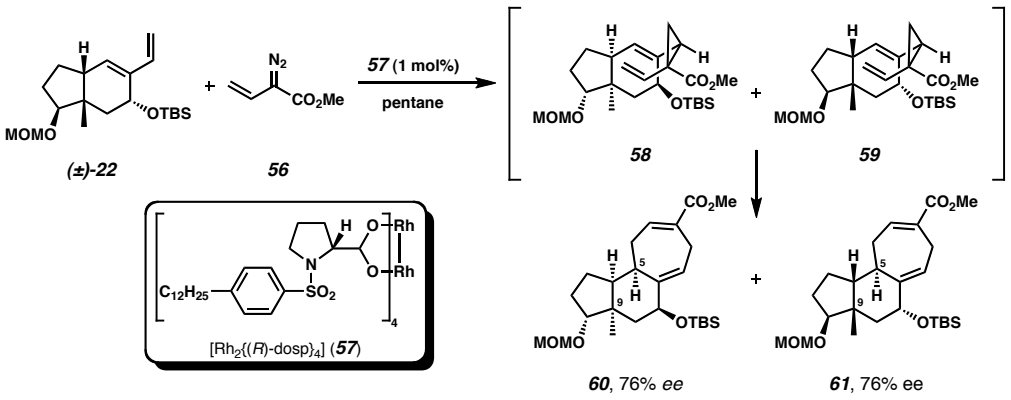

The immediate products of the cyclopropanation were presumably the diastereomeric divinylcyclopropanes **58** and **59**, structures that quickly undergo rearrangement to produce completed cyathane tricycles **60** and **61** in enantioenriched form. Notably, the use of a chiral catalyst and a racemic substrate in this parallel kinetic resolution afforded divergent products that were both well suited toward elaboration into cyathane diterpeniods. Tricycle **60** displays *syn* relative stereochemistry between the hydrogen atom of C(5) and the methyl group of C(9), which is analogous to the structure of (+)-cyathin A_3. Tricycle **61** possesses an *anti* relationship between these same groups, an arrangement that can be found in the cyanthiwigin natural products. By leveraging the exceptional catalyst selectivity of **57**, this parallel kinetic resolution allowed efficient, enantioselective access to two variants of the cyathane core structure from a single racemic starting material.

1.3.3 CYATHANE TOTAL SYNTHESES

The following section represents a comprehensive overview of all cyathane diterpenoid total syntheses published to date.

1.3.3.1 SNIDER'S (±)-ALLOCYATHIN B_2 AND (–)-ERINACINE A SYNTHESES

The first total synthesis of any cyathane diterpenoid natural product was the preparation of allocyathin B_2 by Snider in 1996.[23] Snider's synthetic plan invoked the use of a carbonyl-ene reaction to target the cyathane core, and this strategy was later extended beyond allocyathin B_2 in order to achieve the synthesis of (+)-erinacine E via glycoslyation.

Beginning with known racemic enone **62** triflate formation, palladium-catalyzed carbonylation, and oxidation state manipulation allowed access to enal **63** (Scheme 1.10).[24] Conjugate addition of a cuprate species generated from Grignard reagent **64** to the β-position of extended unsaturated system **63** provided aldehyde **65**, which was subsequently methylated at the α-position to afford bicycle **18**. At this point in the synthesis, Snider's route called for construction of the C-ring via intramolecular carbonyl-ene reaction of aldehyde **18**. In the event, treatment of **18** with Me_2AlCl initiated rearrangement to give a single isomer of alcohol **66** in excellent yield, thus completing the final ring of the tricyclic natural product.[25]

Scheme 1.10 Snider's carbonyl-ene strategy toward the cyathane tricycle

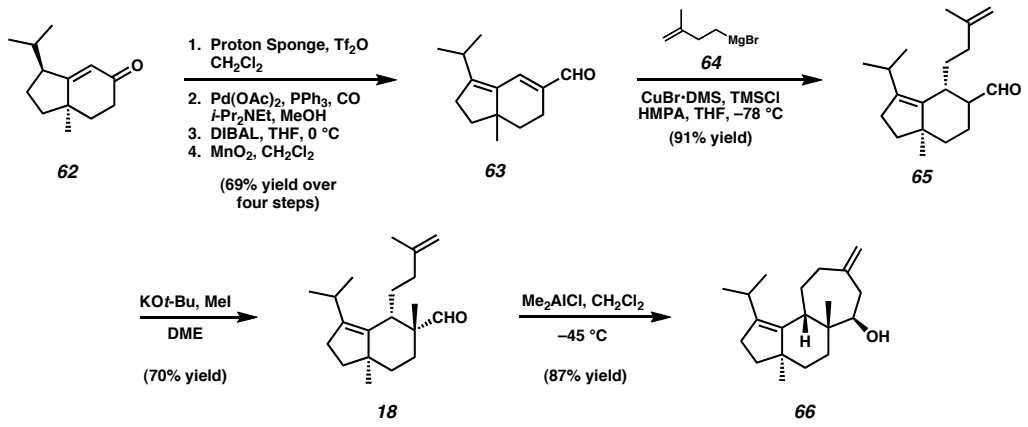

The synthesis was finalized over ten additional transformations, which involved protecting group manipulation, oxidation state modification, and palladium-catalyzed carbonylation starting from tricycle **66** (Scheme 1.11). The completed natural product (±)-allocyathin B_2 (**4**) was thus attained from precursor **62** in 17 steps and 6.4% overall yield. Because allocyathin B_2 represents an aglycone substrate for the erinacine natural products, Snider and coworkers were well equipped at this point to address the total synthesis of these more complicated compounds. As such, glycosylation of allocyathin B_2 with 2,3,4-tri-*O*-acetyl-α-D-xylopyranosyl bromide (**67**) and successive global deprotection generated the natural product (–)-erinacine A (**5**) and isomeric structure **68** as a 1:1 mixture of diastereomers.

Following Snider's route, erinacine A was prepared in 19 steps and 1.0% yield. The cyathane core framework was constructed in seven steps and 38% overall yield.

Scheme 1.11 Completion of (+)-allocyathin B_2 and glycosylation to achieve (–)-erinacine A

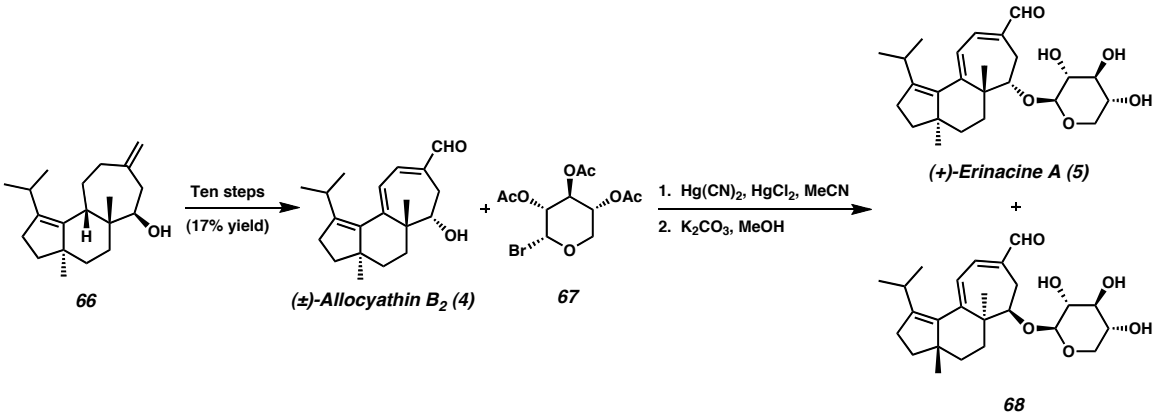

1.3.3.2 TORI'S (±)-ALLOCYATHIN B_2 SYNTHESIS

In a report published by Tori and coworkers in 1998, an intramolecular aldol strategy targeting the synthesis of the natural product allocyathin B_2 was described.[26]

Starting from 3-methyl cyclohexenone (**69**), conjugate addition, ozonloysis, and oxidation yielded diketone **70** after five steps (Scheme 1.12). Intramolecular aldol condensation of cyclohexanone **70** afforded bicyclic enone **71**, a structure containing the completed five-membered A-ring of allocyathin B_2, complete with the requisite isopropyl group. Subsequent acylation of **71** with acid chloride **72** was followed by methylation and a highly optimized diastereoselective reduction employing $Zn(BH_4)_2$ to afford keto-alcohol **73**.[27] Additional transformations over seven steps provided access to allylic alcohol **74**, which was readily oxidized under Swern conditions to give bis-aldehyde **27**. Upon exposure of **27** to methanolic KOH, a final intramolecular aldol condensation was executed to complete the cyathane C-ring and produce allyocyathin B_2 (**4**). Overall, both allocyathin B_2 and the cyathane core structure were synthesized in 19 steps and 0.5% yield, starting from **68**.

Scheme 1.12 Tori's strategy toward allocyathin B_2

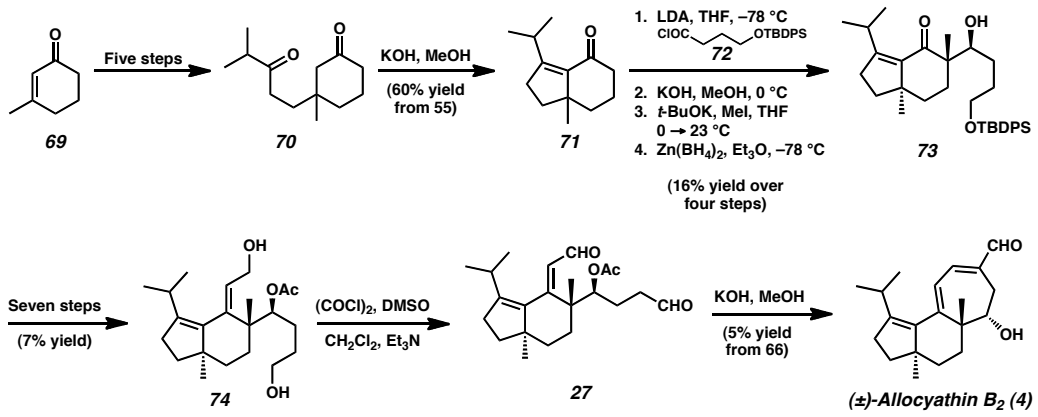

Subsequent to the preparation of allocyathin B_2, Tori also disclosed a different strategy toward the construction of the cyathane tricyclic core via ring-closing metathesis.[28] Modification of their previous synthetic route allowed access to bicyclic intermediate **75** (Scheme 1.13). Upon treatment of this material with 20 mol% of Grubbs second-generation metathesis catalyst (**76**), completed cyathane tricycle **77** was obtained as the sole product of reaction.

Scheme 1.13 Tori's ring-closing strategy toward construction of the seven-membered C-ring and completion of the cyathane core

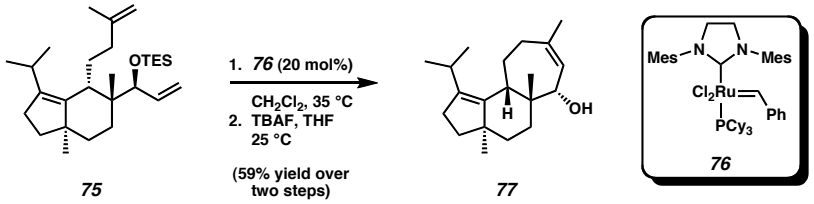

1.3.3.3 PIERS' (±)-SARCODONIN G SYNTHESIS

The first total synthesis of sarcodonin G was described by Piers *et al*. in 2000.[29] Their approach to this cyathane diterpenoid targeted the tricyclic core with an alkylation

and ring-expansion strategy, and employed late-stage installation of the peripheral functionality. Piers' synthesis began from known ketone **78** (introduced as a mixture of diastereomers),[30] which was subjected to hydrazone formation, epimerization at the ring fusion, and nucleophilic attack on alkyl iodide **79** to afford vinyl germane **80** (Scheme 1.14). Further transformation of germane **80** eventually produced the vinyl iodide species **25**.

Scheme 1.14 Vinyl iodide construction in Pier's sarcodonin synthesis

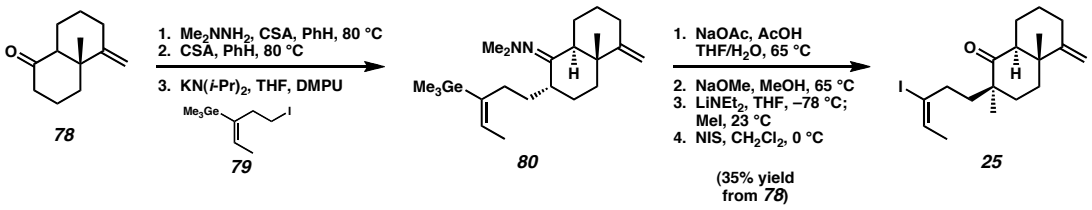

Upon treatment of **25** with *n*-BuLi, lithium-halogen exchange and intramolecular trapping of the ketone moiety constructed the five-membered A-ring of the natural product (Scheme 1.15). After deprotonation with KH and addition of Bu_3SnCH_2I, ether **81** was isolated as the major product. From this ether intermediate, a Still–Mitra [2,3]-sigmatropic rearrangement provided tricycle **82**, which contains the primary hydroxyl group at C(19) required for sarcodonin G.[31]

Scheme 1.15 Still-Mitra [2,3] sigmatropic regarrangement to construct the A-ring of sarcodonin G

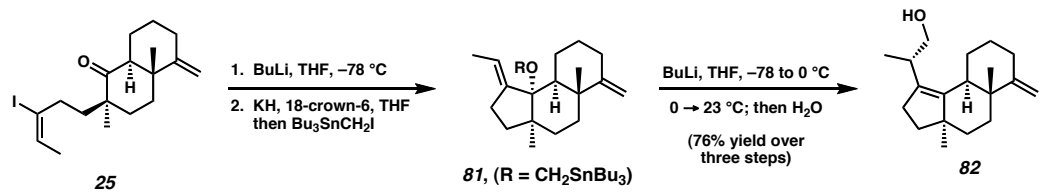

Additional synthetic transformation of **82** over four steps yielded β-ketoester **83**, which bears an α-alkyl iodide group well suited to engage in ring-expansion methodology developed by Hasegawa (Scheme 1.16).[32] Upon exposure to SmI_2 in THF, alkyl iodide **83** was converted in 71% yield to the one-carbon ring expanded product **84**. This process smoothly formed the seven-membered C-ring, and thus completed the tricyclic cyathane core. The total synthesis was thereafter concluded in six steps to yield sarcadonin G (**8**).

Scheme 1.16 Ring expansion and endgame for sarcodonin G

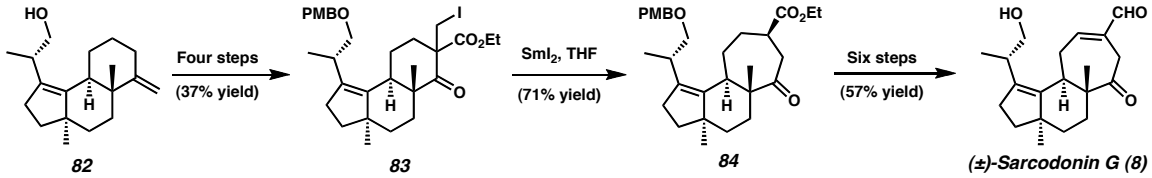

Overall the synthesis of sarcodonin G (**8**) was accomplished in a total of 21 steps and 4.0% yield. The cyathane tricyclic core was attained in 15 steps and 7.0% overall yield.

1.3.3.4 WARD'S (±)-ALLOCYATHIN B_3 SYNTHESIS

The total synthesis of allocyathin B_3 was achieved by Ward and coworkers in 2000 by leveraging an interesting cycloaddition strategy for rapid construction of the central B-ring.[33] The synthesis was initiated with a Diels–Alder cycloaddition between 2,5-dimethyl-*p*-benzoquinone (**86**) and 2,4-bis(trimethylsilyloxy)-1,3-pentadiene (**85**, Scheme 1.17). Subsequent [2 + 2] cycloaddition with allene and exposure to acidic conditions

thereafter afforded a 4-6-6 tricyclic system as a 4:1 mixture of structural isomers (**29** to **87**), wherein each was produced as a single diastereomer.[33a]

Scheme 1.17 Ward's cycloaddition stragety toward tricyclic formation

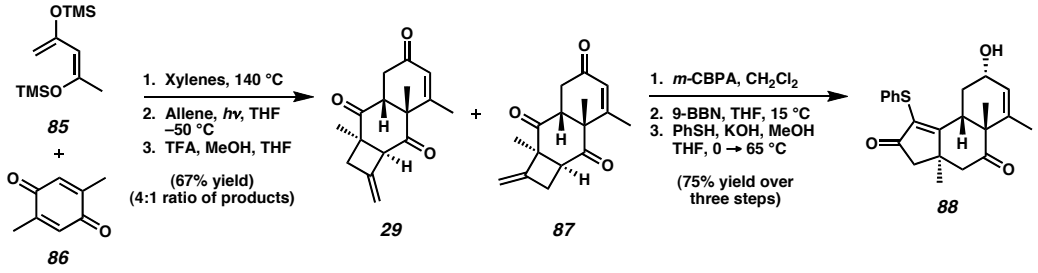

Though only isomer **29** was desired, the 4:1 mixture of **29** and **87** was epoxidized, reduced at the enone moiety, and then treated with benzenethiol at reflux under basic conditions to effect closure of the cyathane core A-ring. This furnished α-thiophenyl enone **88** in excellent yield, in a sequence that required only a single purification.[33b]

Scheme 1.18 Ring expansion via ozonolysis and aldol reaction to target the cyathane core

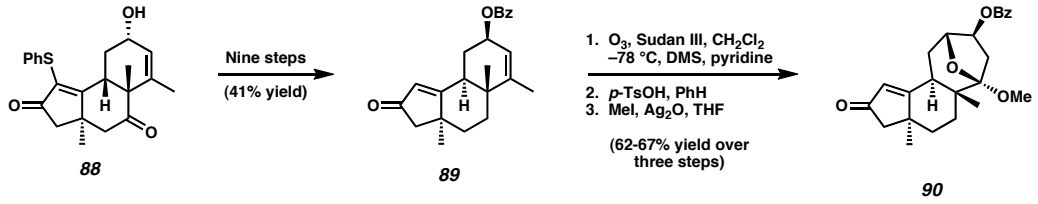

Desulfurization, deoxygenation, protection, and epimerization of **88** over nine steps then allow access to 5-6-6 allylic benzoyl ester **89** (Scheme 1.18). The six-membered ring olefin of this intermediate provided a reactive handle with which to construct the seven-membered C-ring of the natural product. Ozonolysis of enone **89** in the presence of Sudan III indicator generated a sensitive keto-aldehyde intermediate that was subjected

to aldol reaction, transacylation, and successive trapping via *O*-methylation to afford 5-6-7 tricycle **90**. This three step sequence completed the core framework and simultaneously established the trans-annular ketal bridge present in allocyathin B_3.

In order to install the necessary isopropyl side chain appended to the A-ring of the natural product, intermediate **90** was then transformed into propargyl ether **91** (Scheme 1.19). Treatment of alkyl bromide **91** with AIBN in the presence of Ph_3SnH was followed by subsequent hydrogenation to produce cyclized tetrahydrofuran **92**. After extended exposure to mild acid, tetracycle **92** was opened to tricycle **93**, a structure which contains all of the carbon atoms required for completion of the cyathane A-ring. From this point, the total synthesis was completed in 11 steps to yield allocyathin B_3 (**3**).

Scheme 1.19 Ward's allocyathin endgame strategy

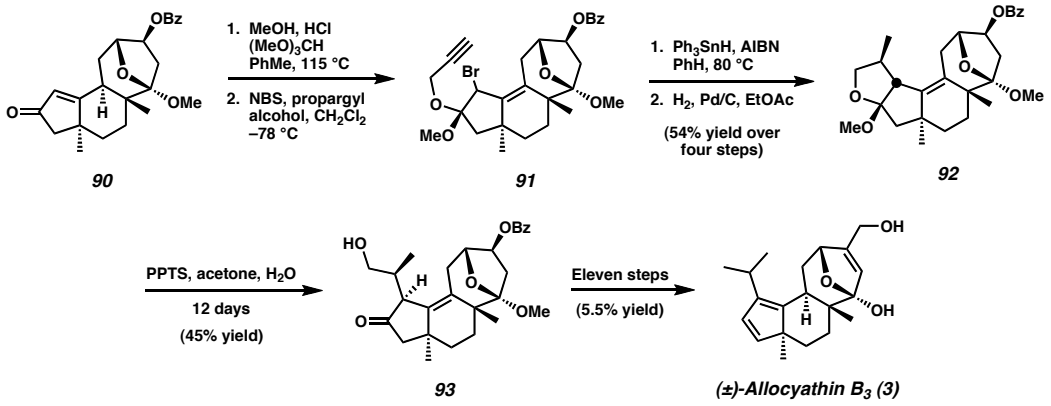

Overall, Ward's strategy toward allocyathin B_3 comprises 34 steps and is concluded in 0.1% yield. The tricyclic cyathane core was attained in 18 steps and 11% overall yield.

1.3.3.5 WARD'S (+)-CYATHIN A_3 SYNTHESIS

A variant of Ward's allocyathin A_3 strategy was later rendered enantioselective to achieve the total synthesis of the related diterpene natural product cyathin A_3.[33,34]

*Scheme 1.20 Catalytic enantioselective Diels–Alder approach to intermediates **29** and **87***

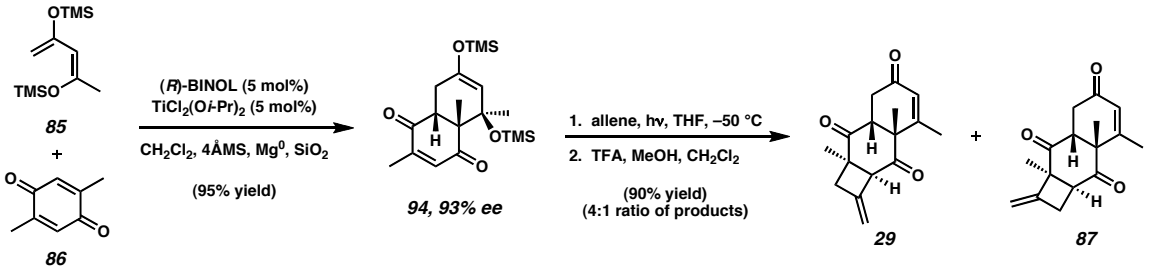

The initial Diels–Alder reaction between 2,5-dimethyl-*p*-benzoquinone (**86**) and 2,4-bis(trimethylsilyloxy)-1,3-pentadiene (**85**) was made asymmetric by employing Mikami's titanium-based BINOL catalyst (Scheme 1.20).[35] After extensive optimization of this cycloaddition, Ward and coworkers found that addition of Mg powder and silica gel afforded cycloadduct **94** in 95% yield and 93% ee. With **94** in hand, [2 + 2] cycloaddition and acidic hydrolysis proceeded as in the case of Ward's allocyathin B_3 synthesis to furnish **29** and **87** as a 4:1 mixture of structural isomers.

From the isomeric mixture of **29** and **87**, eight additional steps were taken to access enone **95** (Scheme 1.21). This then allowed Ward to follow his previously published procedure reported route. Advancement of tricycle **96** along 15 steps (including ozonolysis and aldol reaction for ring expansion) afforded the completed cyathane core in the form of acetal **96**. From this enone, oxidation, triflate formation, reductive deoxygenation, and hydrogenation produced tricycle **97** with the A-ring completed. With

this material in hand, Ward was able to conclude the synthesis with four additional reactions, thus furnishing cyathin A_3 (**2**) in 34 steps and 1.0% overall yield. The cyathane core structure was attained in 17 steps and 15% overall yield.

Scheme 1.21 Endgame synthesis for cyathin A_3 (TTBP = 2,6-di(tert-butyl)-4-methylpyridine)

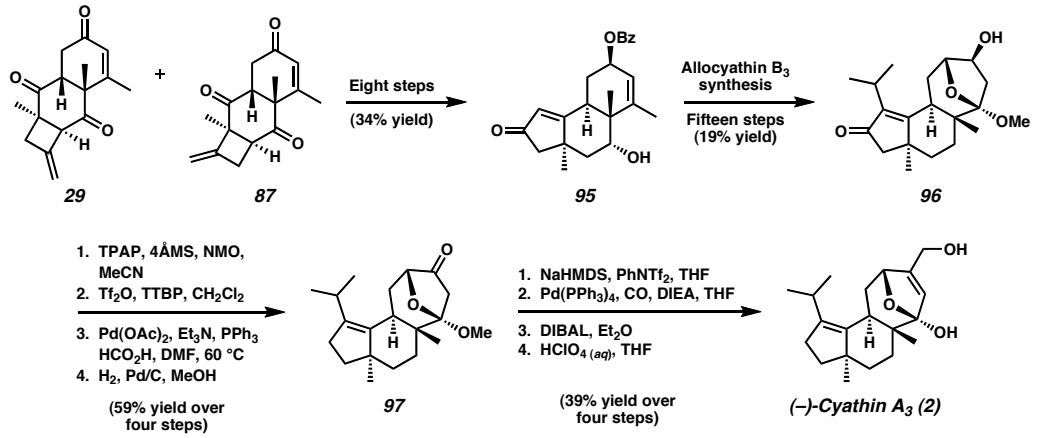

1.3.3.6 NAKADA'S (+)-ALLOCYATHIN B_2 SYNTHESIS

The first enantioselective total synthesis of allocyathin B_2 was described by the laboratories of Nakada in a report published in 2004.[36] In order to target this cyathane diterpenoid molecule, Nakada envisioned a convergent strategy starting with aldehyde **98** and alkyl iodide **99** (Scheme 1.22). Both fragment **98** and fragment **99** were prepared in enantioenriched form based on previously reported work.[37,38] After lithium-halogen exchange was performed on iodide **98**, the resulting alkyl lithium was added to a solution of aldehyde **99** to provide access to alcohol **100**. Deoxygenation, deprotection, and oxidation of this structure afforded diketone **101**.

Scheme 1.22 Fragment coupling to prepare the tethered aldol precursor

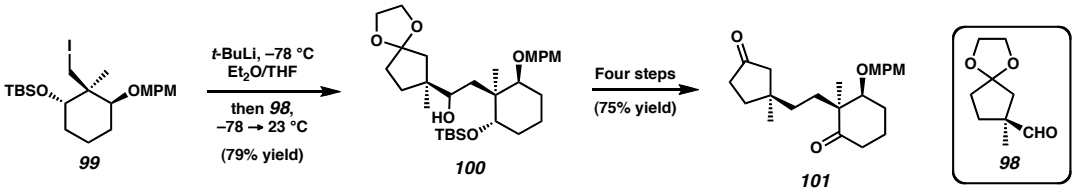

The tethered diketone **101** was subsequently cyclized via intramolecular aldol reaction upon treatment with potassium *tert*-butoxide (Scheme 1.23). This nucleophilic attack served to form the C(5)-C(4) bond, thus constructing the central B-ring of the natural product. After dehydration, tricycle **102** was isolated as the major product of the reaction sequence. In seven additional steps ketone **102** was transformed into alkyl iodide **103**, an intermediate designed to undergo the samarium-mediated one-carbon ring expansion developed by Hasegawa and employed by Piers for the synthesis of Sarcodonin G (Scheme 1.16, Section 1.3.3.3).[32] When **103** was exposed to SmI_2 in the presence of HMPA, the expected migratory ring-expansion occurred in excellent yield to generate the completed cyathane core structure in the form of γ-keto ester **104**.

Scheme 1.23 Intramolecular aldol reaction and ring expansion to complete the total synthesis of allocyathin B_2

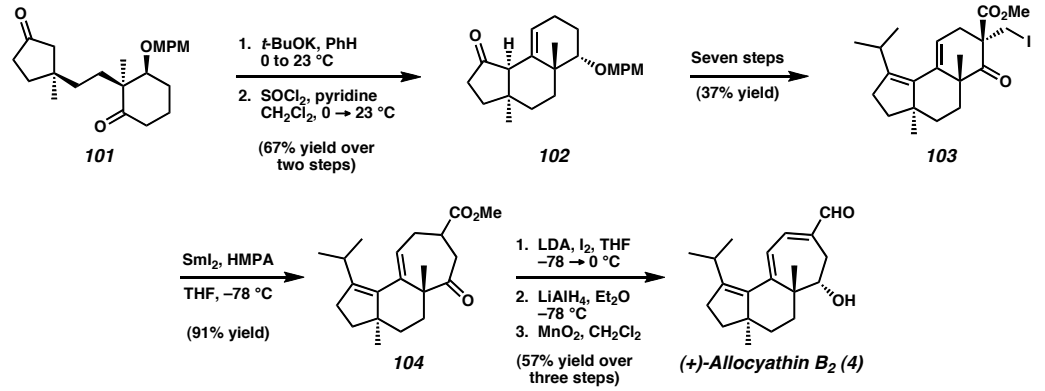

The route toward allocyathin B_2 was thereafter concluded with three additional oxidation state manipulations, affording natural product **4** in a total of 18 synthetic operations and 7.6% overall yield. The tricyclic cyathane core was attained in 15 steps and 13.4% overall yield. Notably, this synthetic approach has been adapted toward a number of other cyathane natural products.[39]

1.3.3.7 NAKADA'S (–)-ERINACINE B SYNTHESIS

In 2007 Nakada and coworkers extended their synthetic route targeting allocyathin B_2 toward the preparation of erinacine B.[40] Following their previous synthetic efforts enantioenriched alkyl iodide **99** was coupled to aldehyde **98** to furnish, after elaboration, hydroxy ketone **105** (Scheme 1.24).[38] After dehydration and deprotection to generate intermediate enone **106**, the envisioned synthetic route called for reduction of the α,β-unsaturation present across the central B-ring. Though numerous Birch reduction methods were attempted, it was discovered that such techniques provided mostly over-reduced diol products instead of the desired hydroxy ketone. Ultimately, this challenge was overcome via diastereoselective olefin reduction using SmI_2 in the presence of HMPA, which provided access to the desired tricycle **107**. These conditions were found to produce a single diastereomer of product, and established the critical C(5)α-H stereochemistry required for (–)-erinacine B. From this point Nakada was able to once again draw from his synthesis of allocyathin B_2. Over eight steps, including SmI_2-mediated ring-expansion, tricycle **108** was prepared.

Scheme 1.24 Adaptation of Nakada's allocyathin B_2 route to erinacine B

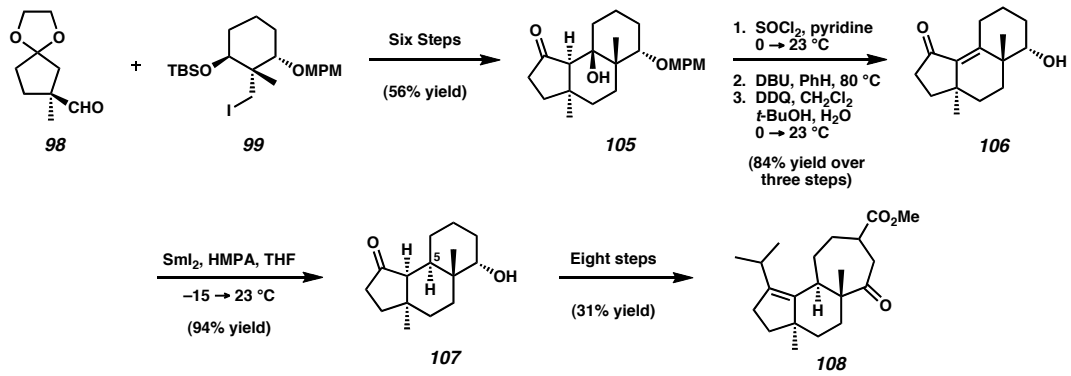

Continued synthesis from ester **108** over nine additional steps allowed access to the protected allylic alcohol **109** (Scheme 1.25). In order to proceed, reduction of the ketone moiety of **109** was required to establish the stereochemistry found in (–)-erinancine B. Unfortunately, all achiral reagents employed for the purpose of diastereoselective reduction afforded only the undesired alcohol epimer at C(14). Because of this difficulty, the ketone of **109** was reduced using the (*R*)-CBS catalyst, which set the desired relative stereochemistry with high selectivity to afford allylic alcohol **110**.

Scheme 1.25 Establishing the desired stereochemistry at C(14)

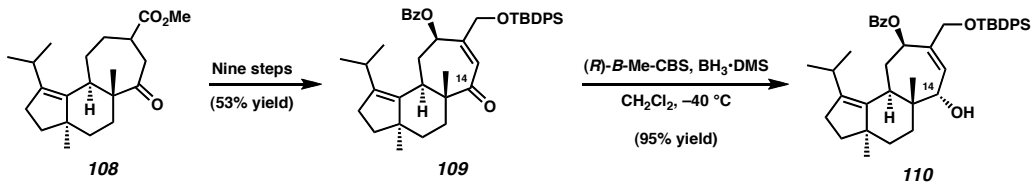

Tricyclic intermediate **110** was thereafter glycosylated with a previously prepared xylose analog **111** to furnish glycone **112** (Scheme 1.26). After full deprotection of the carbohydrate ring, this material was treated with triethylamine and lithium bromide to

effect an S_n' addition into the allylic alcohol. This provided (–)-erinacine B (**6**) as the sole product in enantioenriched form.

Scheme 1.26 Completion of (–)-erinacine B

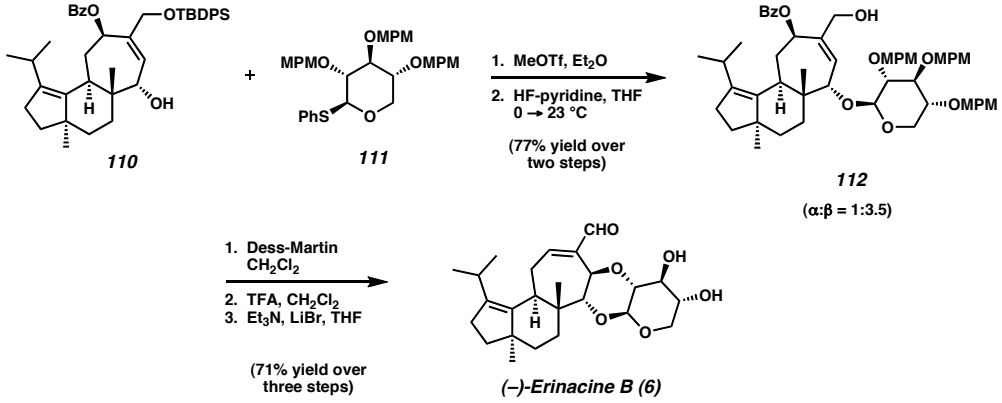

Overall, the synthesis was accomplished in 33 steps and 3.0% yield from **98** and **99**. The cyathane core structure was established in 18 steps and 14% overall yield.

1.3.3.8 NAKADA'S (–)-ERINACINE E

One year subsequent to their report of erinacine B, Nakada and coworkers disclosed a beautiful modification of their synthetic strategy to target (–)-erinacine E, which remains the most complex cyathane diterpenoid molecule isolated to date.[41] Starting from agylcone molecule **110**, glycosylation with thioglycoside **114** and deprotection provided access to intermediate **115** (Scheme 1.27). After additional protecting group manipulation, Swern oxidation generated ketone **116**, an intermediate that spontaneously undergoes conjugate addition-elimination to form pentacyclic structure **117**.

*Scheme 1.27 Synthesis of **117** from allocyathin precursor **110** via conjugate addition-elimination*

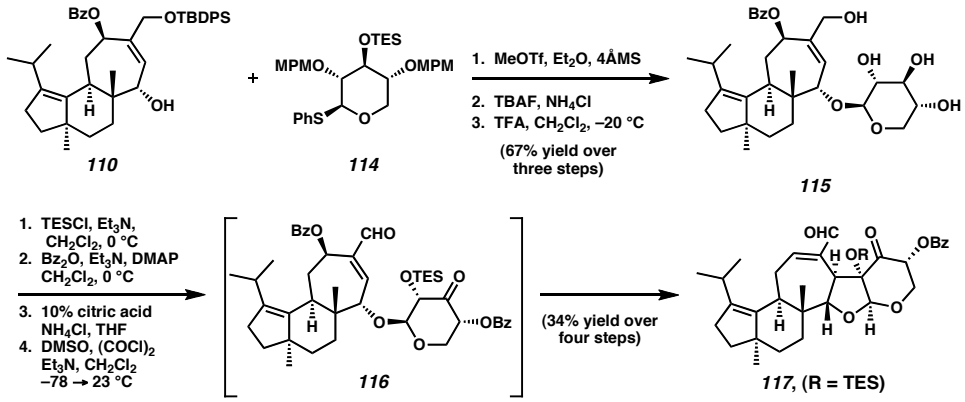

Treatment of enal **117** with DBU in benzene at room temperature initiated an intramolecular aldol reaction between the enolate generated at C(4') and the aldehyde present at C(15) (Scheme 1.28). This aldol reaction is followed by spontaneous benzoate ester migration, thus producing protected erinacine E analog **118** as the final product of the sequence. Further deprotection, oxidation, and diastereoselective carbonyl reduction thereafter completed the total synthesis of (–)-erinacine E (**7**).

Scheme 1.28 Intramolecular aldol reaction for Nakada's endgame of (–)-erinacine E

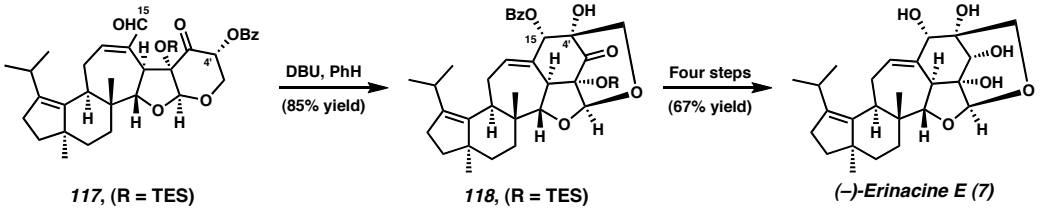

Overall, erinacine E was prepared in 39 steps from iodide **99** and aldehyde **98**, in a total yield of 0.9%.

1.3.3.9 TROST'S (+)-ALLOCYATHIN B_2 SYNTHESIS

Trost and coworkers have recently reported a unique Ru-catalyzed cycloisomerization strategy for the total synthesis of the cyathane diterpenoid molecule allocyathin B_2.[42] The synthesis was initiated with a Pd-catalyzed aysmmetric allylic alkylation. Racemic ketone **119** was alkylated in the presence of $[(\eta^3\text{-}C_3H_7)PdCl]_2$ and chiral ligand (*S,S*)-**121** to afford enantioenriched α-quaternary cyclopentanone **120** (Scheme 1.29).[43] This high-yielding allylation established an all-carbon quaternary stereocenter in 95% ee. The transformation not only served to set the configuration required at C(9) of the natural product, but also provided the stereochemical basis upon which all subsequent diastereoselective transformations were leveraged.

Scheme 1.29 Asymmetric allylic alkylation to establish stereochemistry at C(9)

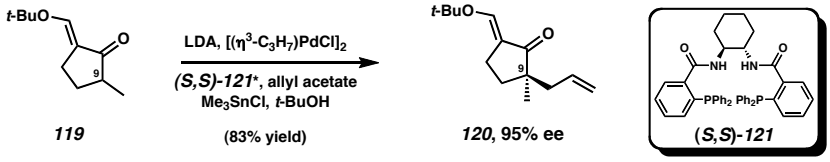

Further elaboration of the allyl side-chain of **120**, as well as manipulation of the ketone moiety, eventually produced propargyl ester **17** (Scheme 1.30). With this material, Trost and coworkers planned to seal the central B-ring of allocyathin B_2 via an intramolecular ruthenium-mediated cycloisomerization reaction. In the event, treatment of allylic alcohol **17** with $CpRu(CH_3CN)_3PF_6$ initiated cyclization of the conjugated alkyne onto the trisubstituted olefin with concomitant oxidation of the primary alcohol.[44]

Scheme 1.30 Ru-catalyzed cycloisomerization to establish the central B-ring of allocyathin B_2

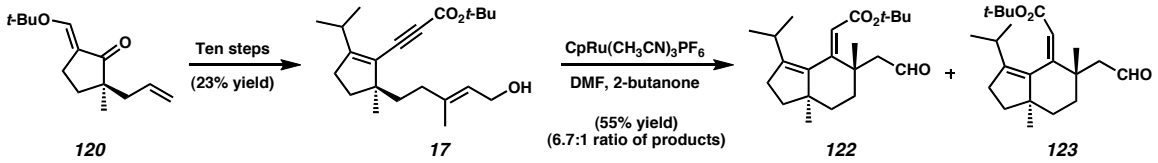

120 *17* *122* *123*

Notably, the cycloisomerization reaction proceeds with high diastereoselectivity. Both products obtained from this transformation possessed the desired anti relationship between the two all-carbon quaternary stereocenters, and no products bearing a syn arrangement were observed. Trost hypothesizes that initial ruthenium complexation to both the alkyne and alkene moieties of **17** can occur to form either a syn-coplanar orientation (**124**) or an orthogonal orientation (**126**, Scheme 1.31). Because the orbital overlap of the syn-coplanar arrangement is likely more conducive to cycloisomerization, ruthenacycle formation from intermediate **124** to give **125** is expected to be much faster than the alternative formation of **127** from **126**.

Scheme 1.31 Diastereoselectivity considerations in the Ru-catalyzed cycloisomerization

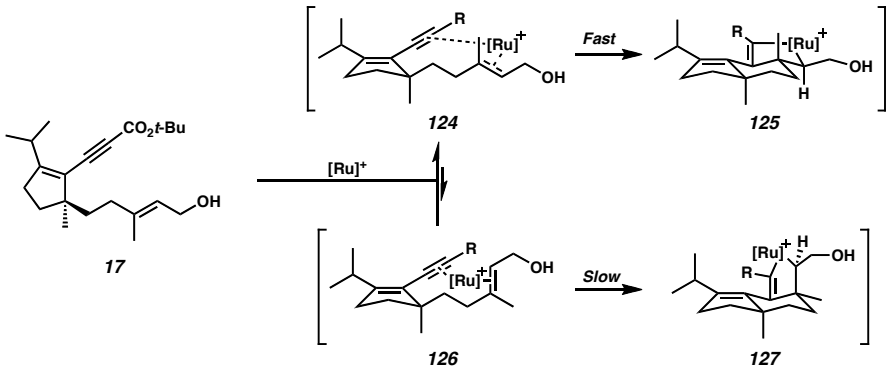

17 *124* *125* *126* *127*

After β-hydride elimination from ruthenacycle **125**, reductive elimination forms **122** and **123** as the major products of reaction. Because only **122** was desired, ultimately the

reaction was optimized by increasing the size of the alkynyl ester to a bulky *tert*-butyl group, thus preferentially forming the Z olefin isomer in a 6.7:1 ratio with isomer **123**.[42b]

From **122**, a hydroxylative Knoevenagel reaction was performed to access lactone **128** as a single diastereomer (Scheme 1.32).[45] The final stages of the synthesis involved hydrogenation and nitrile/lactone reduction, followed by an intramolecular aldol reaction to yield (+)-allocyathin B_2 (**4**). Employing this route, the natural product allocyathin B_2 (and the cyathane core) was synthesized in 16 steps and 5.2% overall yield.

Scheme 1.32 Completion of allocyathin B_2 via hydroxylative Knoevenagel and intramolecular aldol reactions

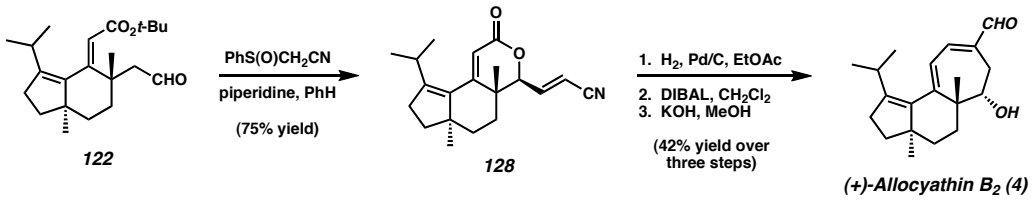

1.3.3.10 DANISHEFSKY'S (–)-SCABRONINE G SYNTHESIS

In 2005, Danishefsky and coworkers reported the first total synthesis of the cyathane diterpenoid scabronine G (**9**).[46] In order to target this bioactive compound, they approached the synthesis with "the pleasingly simple idea that scabronine G [could] be viewed as an annulated, one-carbon ring-expanded version of the (–)-Wieland–Miescher ketone." The initial transformations of the synthesis commenced from the protected ketone **129** (Scheme 1.33). Over five steps, including kinetic enolate trapping and palladium-catalyzed carbonylation, acetal **129** was converted to dieneone **24**. Construction of the five-membered A-ring of scabronine G was then accomplished via

Lewis acid-promoted Nazarov reaction. Upon treatment of dienone **24** with $FeCl_3$, cyclization proceeded smoothly to afford enone **130** in good yield. Notably, this tetracyclic product was obtained as a single tetrasubstituted olefin isomer.

Scheme 1.33 Danishefsky's Nazarov strategy for cyathane A-ring construction

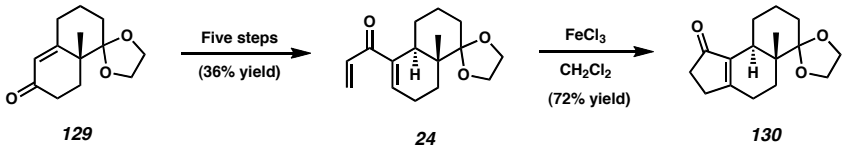

The enone of tricycle **130** was then subsequently leveraged to install the critical all-carbon quaternary stereocenter present at C(9) of scabronine G. Conjugate addition of Nagata's reagent was observed to occur with high axial diastereoselectivity, and the resulting enolate was trapped with TMSCl (Scheme 1.34).[47] The intermediate silyl enol ether obtained from this sequence was then converted to a vinyl triflate species to provide nitrile **131**. Further synthetic elaboration over seven steps allowed for the conversion of vinyl triflate **131** to thiopropylmethylidene **132**.

Scheme 1.34 Advancement toward Danishefsky's ring-expansion precursor

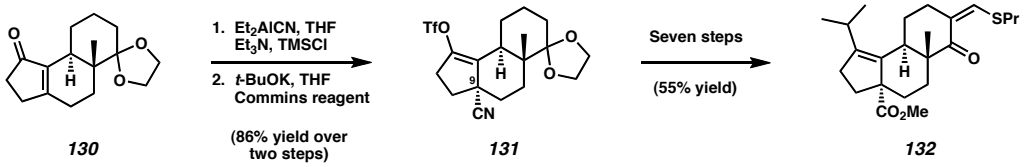

In order to access the 5-6-7 tricyclic cyathane core, vinylogous thioester **132** was first treated with the lithium anion of methoxymethyl phenyl sulfide to produce intermediate tertiary alcohol **133** as a combination of diastereomers (Scheme 1.35). Subsequent

exposure of this mixture to $HgCl_2$ effected a one-carbon ring expansion reaction to furnish tricycle **134**, forging the seven-membered C-ring and completing the cyathane framework.[48] With ring-expanded aldehyde **134** in hand Danishefsky and coworkers were able to complete (–)-scabronine G (**9**) in three additional transformations, accomplishing the total synthesis in 20 steps and 8.2% overall yield. The cyathane core framework was constructed in 17 steps and 11% yield.

Scheme 1.35 Ring expansion and endgame to complete (–)-scabronine G

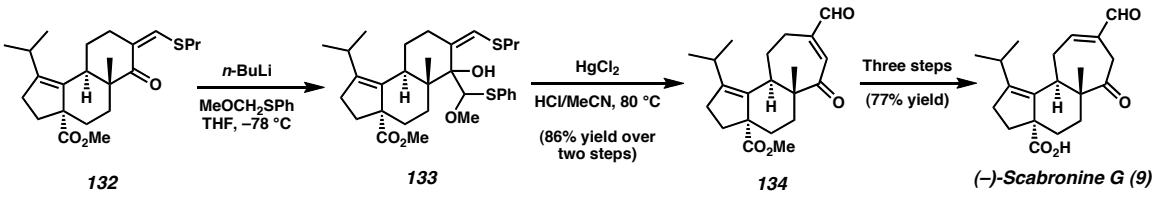

1.3.3.11 PHILLIP'S SYNTHESES OF (+)-CYANTHIWIGIN U, (+)-CYANTHIWIGIN W, AND (–)-CYANTHIWIGIN Z

The first report of the total synthesis of any member of the cyanthiwigin subclass of natural products was published by Phillips and coworkers in 2005.[49] Phillips' strategy for targeting cyanthwigin U focused upon construction of the tricyclic cyathane core via simultaneous construction of both the A- and C-rings, with late-stage installation of the peripheral functionality.

Scheme 1.36 Auxiliary-mediated Diels–Alder reaction to establish the quaternary stereocenters of the natural product

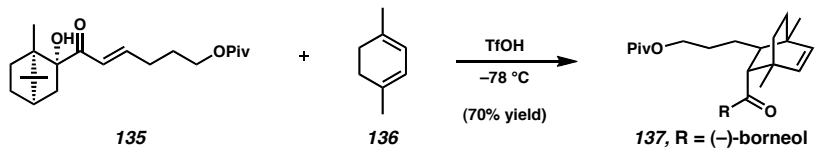

The synthesis began with an asymmetric Diels–Alder reaction between 1,4-dimethyl cyclohexadiene (**136**) and (–)-borneol-appended enone **135** (Scheme 1.36).[50] This cycloaddition reaction proceeded smoothly to give a single diastereomer of **137**, thus establishing both quaternary stereocenters of the natural product in a single synthetic operation. After cleavage of the chiral controller, deprotection, and further functional group manipulation, this sequence provided access to bridged bicyclic bis-aldehyde **23** (Scheme 1.37).

Scheme 1.37 Completion of cyanthiwigin U via ring-opening ring-closing metathesis

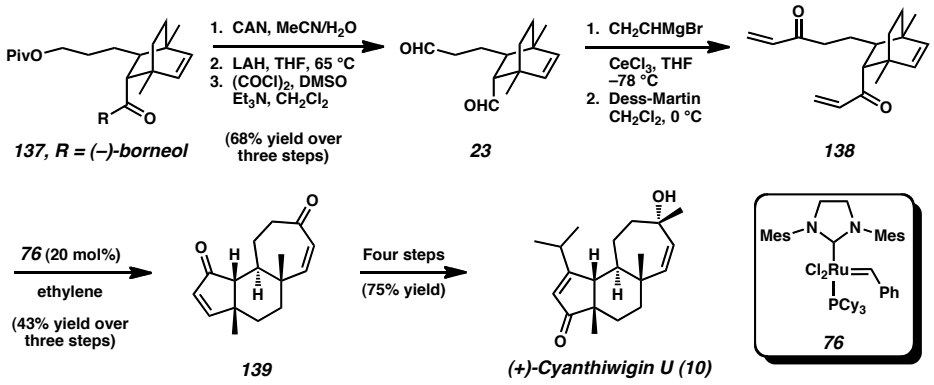

Addition of vinyl Grignard to bis-aldehyde **23** was followed by oxidiation to bis-enone **138**. The bicyclo[2.2.2]octene system of **138** was designed to be well suited to the planned synthetic strategy of "two-directional" tandem ring-opening, ring-closing

metathesis developed by Phillips in prior reports.[51] By treating this bis-enone with 20 mol% of Grubbs' second-generation metathesis catalyst (**76**) under an atmosphere of ethylene, ring-opening metathesis of the strained bridging olefin was rapidly followed by two sequental ring-closing events. This reaction established both the five- and seven-membered rings of the cyathane core, providing tricycle **139** as the ultimate product of the cascade. From this point, the synthesis of (+)-cyanthwigin U (**10**) was completed in four steps involving oxidation state manipulation, as well as addition of the isopropyl and methyl groups. Phillip's route produced the cyathane core in eight synthetic operations and 19% yield, and in total, while the synthesis in total involved only 12 steps in 17% overall yield.

Very recently, the laboratories of Phillips have reported the synthesis of additional cyanthiwigin natural products based on an extension of their route toward cyanthiwigin U.[52] Treatment of cyanthiwigin U (**10**) under Luche reduction conditions afforded the natural product cyanthwigin W in 9:1 dr (**140**, Scheme 1.38). Protection of the resulting secondary hydroxyl group was then followed by allylic transposition and alcohol oxidation via PCC. After deprotection, this sequence furnished cyanthiwigin Z (**11**).

Scheme 1.38 Preparation of cyanthiwigin W and cyanthiwigin Z from cyanthiwigin U

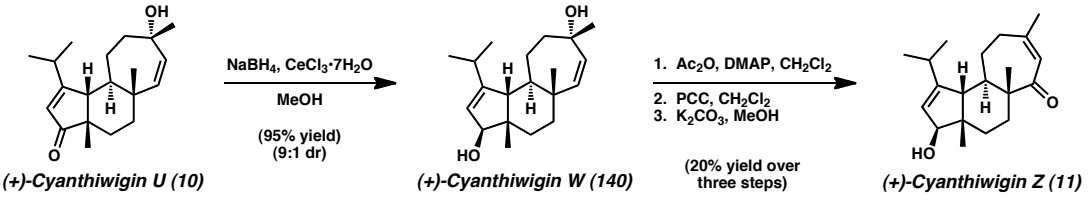

1.3.3.12 REDDY'S (+)-CYANTHIWIGIN AC SYNTHESIS

The structure of cyathane diterpenoid cyanthiwigin AC is unique in comparison to other cyathane molecules in that it does not possess a 5-6-7 fused tricyclic core. Instead, the natural product contains both a 5-6 fused bicycle and a 6-6 spirocyclic junction. The first total synthesis of this natural product was reported in 2006 by Reddy and coworkers.[53]

Starting from the (+)-Hajos–Parrish ketone derivative **30**, double alkylation with bis-mesylate **141** was effective to install the spiro-annulation of the natural product (Scheme 1.39). After methylenation of the resulting compound, spirocyclic intermediate **142** was isolated as the major product of this two step sequence. Deprotection, oxidation, and isomerization then furnished enone **143** in preparation for installation of the isopropyl sidechain to the five-membered A-ring.

*Scheme 1.39 Spiro-annulation of Hajos–Parrish ketone derivative **30***

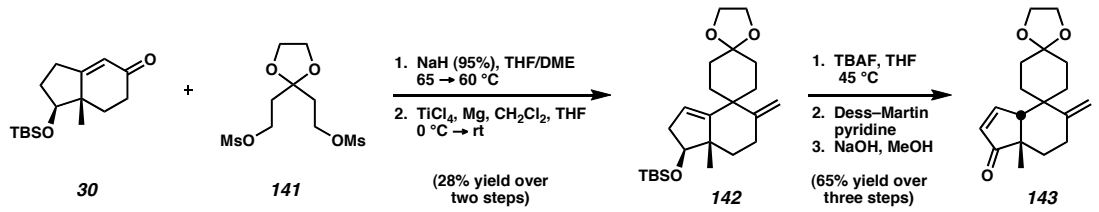

Conjugate addition of isopropenyl cyanocuprate to tetracycle **143** was followed by diastereoselective reduction of the exocyclic methylene to set the tertiary methyl stereocenter of the natural product (Scheme 1.40). This process yielded ketone **144** as a 2:1 mixture of epimers at C(6). Further elaboration of this material provided access to thioether **145**, which upon exposure to IBX in toluene underwent oxidation to generate a

mixture of six-membered ring enones.[54] After sulfoxide formation and dehydrosulfenylation of this intermediate mixture, enones **146** and **147** were obtained in a 1:1.2 ratio of isomers.

Scheme 1.40 Further oxidation and transformation toward cyanthiwigin AC

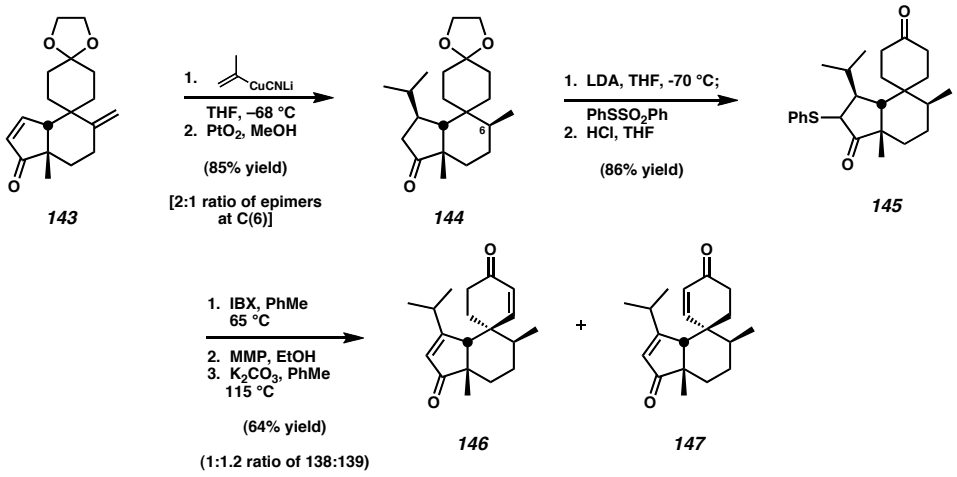

From this point, the addition of methyl lithium to dienone **147** produced the natural product as a 1:2 mixture of epimers at C(12), favoring the generation of (+)-cyanthiwigin AC (**12**, Scheme 1.41) over isomer **148**. The total synthesis of the natural product was concluded in 13 steps and 2.0% overall yield.

Scheme 1.41 Endgame of cyanthiwigin AC

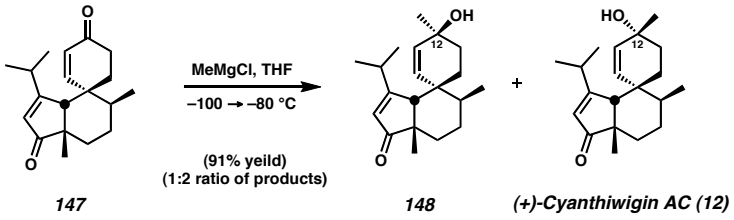

1.3.3.13 CHA'S SYNTHESIS OF (±)-CYATHIN A_3 AND (±)-CYATHIN B_2

In 2009, the laboratories of Cha disclosed the total syntheses of both cyathin A_3 and cyathin B_2.[55] Starting from racemic conjugated ester **21**, Kulinkovich cyclopropanation afforded access to tricyclic structure **149** (Scheme 1.42). After protection of this tertiary alcohol, treatment with bromoacetaldehyde dimethyl acetal in the presence of titantium(IV) chloride furnished spirocycle **150** as a 1:1 mixture of diastereomers with regard to the methoxy group stereochemistry. Notably, this ring expansion served to set the quaternary sterocenter of the spirocyclic ring fusion, establishing the necessary C(6) stereochemistry required for completion of the natural product. Cyclobutanone **150** was further advanced through three chemical transformations, including aldol addition of a cyclobutene enolate to anisaldehyde, addition to the cyclobutanone carbonyl, and elimination to yield elaborated tricyclic compound **151**. Thereafter, ring-closing metathesis of tetraolefin **151** with Grubbs' catalyst **76** installed the seven-membered C-ring, thus generating the completed cyathane core in the form of tetracyclic diol **152**. Addition of thiophenol to the diene moiety of **152** was then followed by Grob fragmentation of the cyclobutane ring, arriving at tricycle **153**. Excision of the C(6) appended side arm over three steps furnished access to a methyl group at this position, yielding **154** as the final product of the sequence.

Scheme 1.42 Cha's spirocyclic approach to cyathin A_3 and cyathin B_2

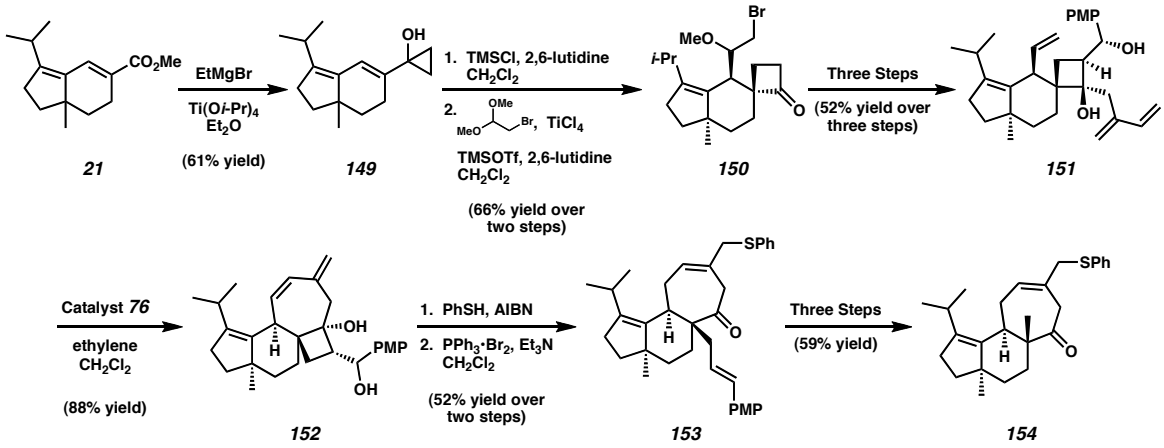

Allylic tricyclic ketone **154** was advanced toward the natural product cyathin B_2 via oxidation of the allylic thioether to a sulfoxide moiety (Scheme 1.43). After treatment with trifluoroacetic anhydride and subsequent Pummerer rearrangement, the resulting mixture of isomeric products were exposed to the conditions of acetylation and hydrolysis, yielding the tricyclic natural product cyathin B_2 (**155**) the sole product of reaction. Diterpenoid **155** was further transformed over seven steps to yield cyathin A_3 (**2**). By leveraging this novel ring-expanding technology, Cha and coworkers were able to access the cyathane tricyclic core in seven steps and18% yield. The completed total synthesis of cyathin B_2 was accomplished in 15 steps and 4.7% yield, while cyathin A_3 was afforded over 22 steps and 1.4% overall yield.

Scheme 1.43 Cha's endgame for cyathin B_2 and elaboration to attain cyathin A_3

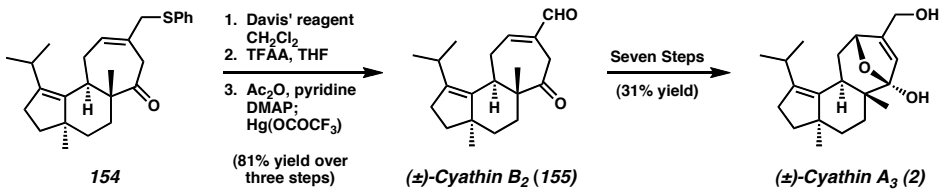

1.4 CONCLUSIONS

The cyathane diterpenoid natural products have been the focus of numerous total synthetic efforts. Seventeen completed total syntheses of these compounds have been reported, fourteen of which have emerged in the last eight years alone. Because the cyathane natural products have been implicated as important biologically active molecules, particularly in regard to the stimulation of NGF synthesis, continued investigation into and refinement of their laboratory preparation is undoubtedly forthcoming.

1.5 NOTES AND REFERENCES

(1) For a detailed account of synthetic efforts toward cyathane diterepenoids from our group, please see chapter 2.

(2) Wright, D. L.; Whitehead, C. R. *Org. Prep. Proced. Int.* **2000**, *32*, 309–330.

(3) Allbutt, A. D.; Ayer, W. A.; Brodie, H. J.; Johri, B. N.; Taube, H. *Can. J. Microbiol.* **1971**, *17*, 1401–1407.

(4) (a) Ayer, W. A.; Taube, H. *Tetrahedron Lett.* **1972**, 1917–1920. (b) Ayer, W. A.; Taube, H. *Can. J. Chem.* **1973**, *51*, 3842–3854.

(5) Ayer, W. A.; Ling, S. P. *Can. J. Chem.* **1979**, *57*, 3332–3337.

(6) (a) Kawagishi, H.; Shimada, A.; Shirai, R.; Okamoto, K.; Ojima, F.; Sakamoto, H.; Ishiguro, Y.; Furukawa, S. *Tetrahedron Lett.* **1994**, *35*, 1569–1572. (b) Kawagishi, H.; Shimada, A.; Hosokawa, S.; Mori, H.; Sakamoto, H.; Ishiguro, Y.; Sakemi, S.; Bordner, J.; Kojima, N.; Furukawa, S. *Tetrahedron Lett.* **1996**, *37*, 7399–7402.

(7) Shibata, H.; Tokunaga, T.; Karasawa, D.; Hirota, A.; Nakayama, M.; Nozaki, H.; Taka, T. *Agric. Biol. Chem.* **1989**, *53*, 3373–3375.

(8) (a) Ohta, T.; Kita, T.; Kobayashi, N.; Obara, Y.; Nakahata, N.; Ohizumi, Y.; Takaya, Y.; Oshima, Y. *Tetrahedron Lett.* **1998**, *39*, 6229–6232. (b) Kita, T.;

Takaya, Y.; Oshima, Y.; Ohta, T. *Tetrahedron* **1998**, *54*, 11877–11886. (c) Ma, B.-J.; Zhu, H.-J.; Liu, J.-K. *Helv. Chim. Acta* **2004**, *87*, 2877–2881.

(9) Green, D.; Goldberg, I.; Stein, Z.; Ilan, M.; Kashman, Y. *Nat. Prod. Lett.* **1992**, *1*, 193–199.

(10) (a) Peng, J.; Walsh, K.; Weedman, V.; Bergthold, J. D.; Lynch, J.; Lieu, K. L.; Braude, I. A.; Kelly, M.; Hamann, M. T. *Tetrahedron* **2002**, *58*, 7809–7819. (b) Peng, J.; Avery, M. A.; Hamann, M. T. *Org. Lett.* **2003**, *5*, 4575–4578. (c) Peng, J.; Kasanah, N.; Stanley, C. E.; Chadwick, J.; Fronczek, M.; Hamann, M. T. *J. Nat. Prod.* **2006**, *69*, 727–730.

(11) Sennett, S. H.; Pomponi, S. A.; Wright, A. E. *J. Nat. Prod.* **1992**, *55*, 1421–1429.

(12) Conner, B.; Dragunow, M. *Brain Res. Rev.* **1998**, *27*, 1–39.

(13) Ayer, W. A.; Ling, S. P.; Nakashima, T. T. *Can. J. Chem.* **1979**, *57*, 3338–3343.

(14) Wender, P. A.; Bi, F. C.; Brodney, M. A.; Gosseln, F. *Org. Lett.* **2001**, *3*, 2105–2108.

(15) For previous examples of [5 + 2] cycloadditions, see: (a) Wender, P. A.; Takahashi, H.; Witulski, B. *J. Am. Chem. Soc.* **1995**, *117*, 4720–4721. (b) Wender, P. A.; Husfeld, C. O.; Langkopf, E.; Love, J. A. *J. Am. Chem. Soc.*

1998, *120*, 1940–1941. (c) Wender, P. A.; Dyckman, A. J.; Husfeld, C. O.; Kadereit, D.; Love, J. A.; Rieck, H. *J. Am. Chem. Soc.* **1999**, *121*, 10442–10443.

(16) (a) Thominiaux, C.; Chiarnoi, A.; Desmaële, D. *Tetrahedron Lett.* **2002**, *43*, 4107–4110. (b) Drège, E.; Morgant, G.; Desmaële, D. *Tetrahedron Lett.* **2005**, *46*, 7263–7266. (c) Drège, E.; Tominiaux, C.; Morgant, G.; Desmaële, D. *Eur. J. Org. Chem.* **2006**, 4825–4840.

(17) The ketoester **40** can be prepared via Michael addition to the imine obtained after treatment of 1-methylcyclopentanone with (*S*)-1-phenylethylamine. See: (a) Pfau, M.; Revial, G.; d'Angelo, J.; Guingant, A. *J. Am. Chem. Soc.* **1985**, *107*, 273–274. (b) d'Angelo, J.; Desmaële, D.; Dumas, F.; Guingant, A. *Tetrahedron: Asymm.* **1992**, *3*, 459–505.

(18) The diastereomeric ration reported for this reaction is based upon the newly formed stereocenter present at C(6).

(19) (a) Maruoka, K.; Concepcion, A. B.; Yamamoto, H. *J. Org. Chem.* **1994**, *59*, 4725–4726. (b) Maruoka, K.; Concepcion, A. B.; Yamamoto, H. *Synthesis* **1994**, 1283–1290. (c) Yang, S.; Hungerhoff, B.; Metz, P. *Tetrahedron Lett.* **1998**, *39*, 2097–2098.

(20) Takeda, K.; Nakane, D.; Takeda, M. *Org. Lett.* **2000**, *2*, 1903–1905.

(21) Takeda, K.; Nakajima, A.; Takeda, M.; Okamoto, Y.; Sato, T.; Yoshii, E.; Koizumi, T.; Shiro, M. *J. Am. Chem. Soc.* **1998**, *120*, 4947–4959.

(22) Miller, L. C.; Ndungu, J. M.; Sarpong, R. *Angew. Chem., Int. Ed.* **2009**, *48*, 2398–2402.

(23) (a) Snider, B. B.; Vo, N. H.; O'Neil, S. V.; Foxman, B. M. *J. Am. Chem. Soc.* **1996**, *118*, 7644–7645; (b) Snider, B. B.; Vo, N. H.; O'Neil, S. V. *J. Org. Chem.* **1998**, *63*, 4732–4740.

(24) Snider, B. B.; Rodini, D. J.; van Straten, J. *J. Am. Chem. Soc.* **1980**, *102*, 5872–5880.

(25) (a) Snider, B. B. *Comprehensive Organic Synthesis*; Pergamon: Oxford, 1991; Vol. 2, p 527. (b) Snider, B. B.; Yang, K. J. *J. Org. Chem.* **1990**, *55*, 4392–4399.

(26) Tori, M.; Toyoda, N.; Sono, M. *J. Org. Chem.* **1998**, *63*, 306–313.

(27) (a) Gensler, W. J.; Johnson, F.; Sloan, A. D. B. *J. Am. Chem. Soc.* **1960**, *82*, 6074–6081. (b) Crabbé, P.; Garcia, G. A.; Rius, C. *J. Chem. Soc., Perkin Trans. 1* **1973**, 810–816.

(28) Nakashima, K.; Fujisaki, N.; Inoue, K.; Minami, A.; Nagaya, C.; Sono, M.; Tori, M. *Bull. Chem. Soc. Jpn.* **2006**, *79*, 1955–1962.

(29) Piers, E.; Gilbert, M.; Cook, K. L. *Org. Lett.* **2000**, *2*, 1407–1410.

(30) Piers, E.; Yeung, B. K. A.; Fleming, F. F. *Can. J. Chem.* **1993**, *71*, 280–286.

(31) Still, W. C.; Mitra, A. *J. Am. Chem. Soc.* **1978**, *100*, 1927–1928.

(32) Hasegawa, E.; Kitazume, T.; Suzuki, K.; Tosaka, E. *Tetrahedron Lett.* **1998**, *39*, 4059–4062.

(33) (a) Ayer, W. A.; Ward, D. E.; Browne, L. M.; Delbaere, L. T. J.; Hoyano, Y. *Can. J. Chem.* **1981**, *59*, 2665–2672. (b) Ward, D. E. *Can. J. Chem.* **1987**, *65*, 2380–2384. (c) Ward, D. E.; Gai, Y.; Qiao, Q. *Org. Lett.* **2000**, *2*, 2125–2127.

(34) Ward, D. E.; Shen, J. *Org. Lett.* **2007**, *9*, 2843–2846.

(35) Mikami, K.; Motoyama, Y.; Terada, M. *J. Am. Chem. Soc.* **1994**, *116*, 2812–2820.

(36) Takano, M.; Umino, A.; Nakada, M. *Org. Lett.* **2004**, *6*, 4897–4900.

(37) Honma, M.; Sawada, T.; Fujisawa, Y.; Utsugi, M.; Watanabe, H.; Umino, A.; Matsumura, T.; Hagihara, T.; Takano, M.; Nakada, M. *J. Am. Chem. Soc.* **2003**, *125*, 2860–2861.

(38) Iwamoto, M.; Kawada, H.; Tanaka, T.; Nakada, M. *Tetrahedron Lett*. **2003**, *44*, 7239–7243.

(39) An analogous synthetic approach was reported by Nakada for progress toward the synthesis of (–)-scabronine A. See: Watanabe, H.; Nakada, M. *Tetrahedron Lett*. **2008**, *49*, 1518–1522.

(40) Watanabe, H.; Takano, M.; Umino, A.; Ito, T.; Ishikawa, H.; Nakada, M. *Org*. *Lett*. **2007**, *9*, 359–362.

(41) Watanabe, H.; Nakada, M. *J. Am. Chem. Soc*. **2008**, *130*, 1150–1151.

(42) (a) Trost, B. M.; Dong, L.; Schroeder, G. M. *J. Am. Chem. Soc*. **2005**, *127*, 2844–2845. (b) Trost, B. M.; Dong, L.; Schroeder, G. M. *J. Am. Chem. Soc*. **2005**, *127*, 10259–10268.

(43) (a) Trost, B. M.; Schroeder, G. M. *J. Am. Chem. Soc*. **1999**, *121*, 6759–6760. (b) Trost, B. M.; Schroeder, G. M.; Kristensen, J. *Angew. Chem., Int. Ed*. **2002**, *41*, 3492–3495.

(44) Trost, B. M.; Toste, F. D.; Pinkerton, A. B. *Chem. Rev*. **2001**, *101*, 2067–2096.

(45) Trost, B. M.; Mallert, S. *Tetrahedron Lett*. **1993**, *34*, 8025–8028.

(46) Waters, S. P.; Tian, Y.; Li, Y.-M.; Danishefsky, S. J. *J. Am. Chem. Soc.* **2005**, *127*, 13514–13515.

(47) Nagata, W.; Mitsuru, Y.; Masayuk, M. *J. Am. Chem. Soc.* **1972**, *94*, 4644–4653.

(48) Guerrero, A.; Parrilla, A.; Camps, F. *Tetrahedron Lett.* **1990**, *31*, 1873–1876.

(49) Pfeiffer, M. W. B.; Phillips, A. J. *J. Am. Chem. Soc.* **2005**, *127*, 5334–5335.

(50) Palomo, C.; Oiarbide, M.; García, J. M.; González, A.; Lecumberri, A.; Linden, A. *J. Am. Chem. Soc.* **2002**, *124*, 10288–10289.

(51) Minger, T. L.; Phillips, A. J. *Tetrahedron Lett.* **2002**, *43*, 5357–5359.

(52) Pfeiffer, M. W. B.; Phillips, A. J. *Tetrahedron Lett.* **2008**, *49*, 6860–6861.

(53) Reddy, T. J.; Bordeau, G.; Trimble, L. *Org. Lett.* **2006**, *8*, 5585–5588.

(54) Nicolaou, K. C.; Zhong, Y.-L.; Baran, P. S. *J. Am. Chem. Soc.* **2000**, *122*, 7596–7597.

(55) Kim, K.; Cha, J. K. *Angew. Chem., Int. Ed.* **2009**, *48*, 5334–5336.

CHAPTER 2[†]

Enantioselective Total Synthesis of

Cyanthiwigin Diterpenoids

2.1 INTRODUCTION

The following sections describe the structure, biological activity, and synthetic challenges associated with the cyanthiwigin family of cyathane diterpenoid molecules. This section additionally details the retrosynthetic analysis of cyanthiwigins B, F, and G.

2.1.1 STRUCTURE AND SYNTHETIC CHALLENGES

The cyanthiwigin diterpenoid natural products were originally isolated from the marine sponge *Epipolasis reiswigi*.[1] Ten years later, additional, novel cyanthiwigin molecules were found in extracts of the Jamaican sea sponge *Mermekioderma styx*.[2] To date, over 30 different examples of cyanthiwigin diterpenoids have been isolated and characterized from these two sources. The vast majority of these compounds are

[†] Portions of this chapter have been reproduced from *Nature* **2008**, *453*, 1228–1230 and the supporting information found therein.

structurally similar, and are unified through the presence of a highly conserved tricyclic carbon scaffold (Figure 2.1). The cyanthiwigin molecules belong to a larger class of diterpene natural products known as the cyathanes. In keeping with the vast majority of other cyathane compounds, the 20 carbon atoms of the cyanthiwigins are arranged into a fused [5-6-7] tricyclic core skeleton (**155**–**180**).[3] However, in contrast to the remainder of the cyathanes, the dual all-carbon quaternary stereocenters found in the cyanthiwigin molecules at C(6) and C(9) are arranged with a *syn* relative stereochemical relationship, rather than an *anti* configuration. Furthermore, these diterpene natural products boast two additional points of stereogenicity at ring fusion carbons C(4) and C(5), structural features that establish a total of four contiguous stereocenters across the innermost bonds of the carbon scaffold. Indeed, the central ring of the cyanthiwigin [5-6-7] carbocyclic core imparts formidable challenge to the synthetic preparation of any of these natural products, due to the steric crowding surrounding and nested location of these critical stereocenters.

Structural differentiation among the members of the cyanthiwigin family is primarily manifest in variable oxidation of the peripheral carbocyclic skeleton. Oxidative diversity in the cyanthiwigins provides sparingly oxidized structures such as cyanthiwigin G (**161**), as well as more heavily oxidized examples as can be found in cyanthiwigin O (**169**). For many of the less-oxidized cyanthiwigin compounds (e.g., cyanthiwigin F (**160**)) preparative approaches toward these molecules can prove difficult owing to their sparse functionality. These minimally elaborated structures possess very few reactive handles upon which to leverage retrosynthetic planning. Because of this, synthetic routes toward the construction of less-oxygenated cyanthiwigins typically involve the installation and

subsequent removal of superfluous moieties, an often cumbersome and inefficient method due to the introduction of nonessential functionality.

Figure 2.1 The cyanthiwigin diterpenoid molecules

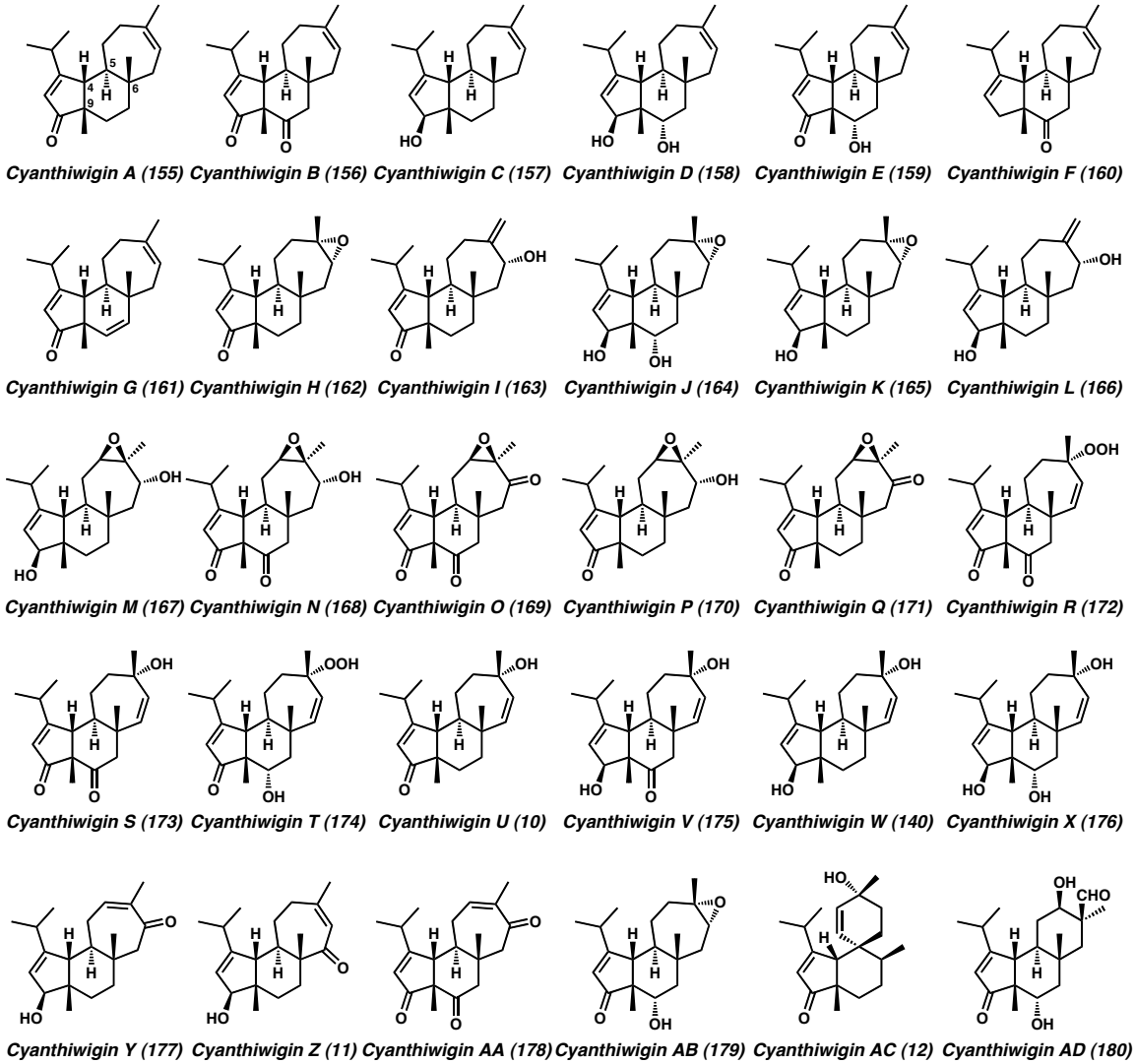

2.1.2 BIOLOGICAL ACTIVITY

The cyanthiwigin natural products boast a wide range of biological activities. The larger class of cyathanes in general possess a diverse set of bioactive properties, including

antimicrobial and antineoplastic activity, as well as κ-opioid receptor agonism.[4] Most notably, some members of the cyathane natural products possess the capacity to stimulate the synthesis of nerve growth factor (NGF), a quality that implicates their potential application as therapeutic agents for neurodegenerative diseases and spinal injuries.[5] In addition, cyanthiwigin C has shown cytotoxic activity against both A549 human lung cancer cells (IC_{50} = 4.0 μg/mL) and P-388 human leukemia cells (IC_{50} = 11.2 μg/mL).[6] Cyanthiwigin F (**160**) has displayed cytotoxic activity against human primary tumor cells (IC_{50} = 3.1 μg/mL).[2] Unfortunately, exhaustive investigation of the entire family of cyanthiwigin molecules has been impeded by a lack of sufficient material with which to perform the required biological assays. As such, synthetic preparation of these natural products has become an appealing goal.

2.1.3 RETROSYNTHETIC ANALYSIS

Because the members of the cyanthiwigin family of molecules differ from one another primarily in terms of oxygenation, we hypothesized that a synthetic route capable of rapidly preparing the carbocyclic core would provide simultaneous access to many of these marine natural products. Thus, our approach to the cyathane molecule cyanthiwigin F (**160**) was developed with a specific focus upon quickly constructing the tricyclic cyathane skeleton. In keeping with this goal, our initial retrosynthetic maneuver envisioned disconnection of either the five-membered A-ring or the seven-membered C-ring to lead back to either bicycle **181** or diketone **182**, respectively (Scheme 2.1). In either case, further simplification was anticipated via retrosynthetic opening of the remaining peripheral ring, an operation that would be addressed in the forward sense via

ring-closing metathesis. If the seven-membered C-ring were to be closed first, this strategy would lead to tetraolefin **183**. Initial closure of the five-membered A-ring would invoke triolefin precursor **184**. Regardless of the route employed, we expected that either intermediate **183** or **184** would be accessible via enantioenriched diketone **185**.

Scheme 2.1 Retrosynthetic analysis of cyanthiwigin F

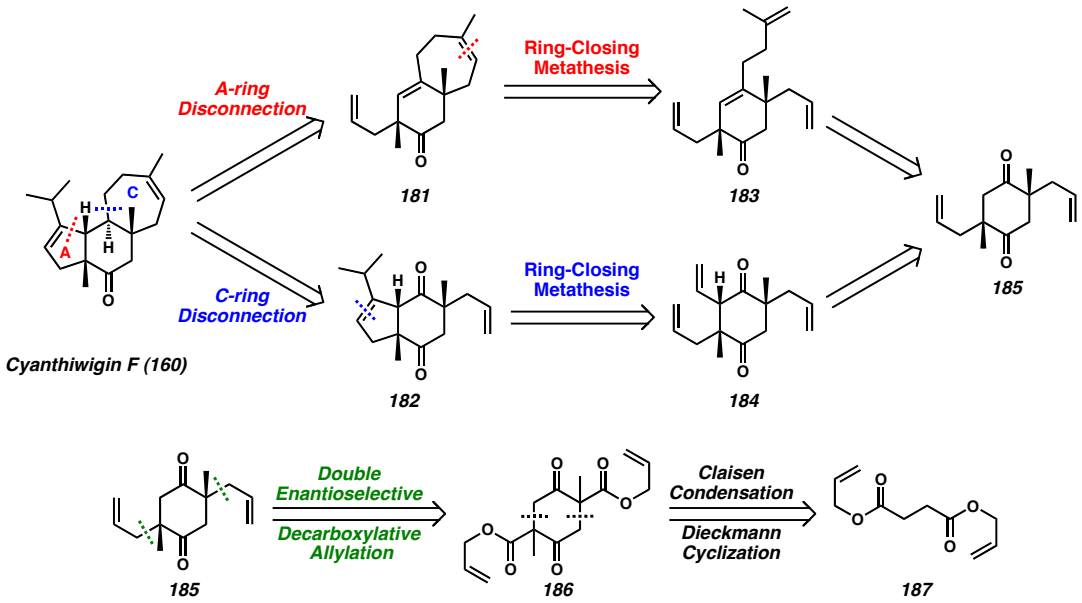

In order to target diketone **185**, we envisioned the use of enantioselective alkylation technology that had been previously developed in our lab.[7] At the outset of our synthetic efforts toward the cyanthiwigin natural products, this stereoselective methodology had already proven quite reliable for the formation of α-quaternary cyclohexanone products. We predicted that by implementing this reaction on an appropriately designed substrate, that it would be possible to forge two carbon-carbon bonds with enantiocontrol, thus providing rapid access to the critical diketone **185** in a single synthetic procedure. This double stereoselective decarboxylative alkylation reaction was anticipated to employ

bis(β-ketoester) **186** as the crucial substrate, and in a forward sense, was expected to set both of the necessary all-carbon quaternary stereocenters of the natural product. Fortuitously, compounds similar to bis(β-ketoester) **186** have been known in the literature for nearly a century. As such we were confident that this material could be prepared from diallyl succinate (**187**) via an initial Claisen condensation and a subsequent Dieckmann cyclization.[8]

2.2 FORWARD SYNTHETIC EFFORTS

The following section describes the various reactions, routes, and experiments explored in order to synthetically prepare the cyanthiwigin marine diterpene compounds.[9]

2.2.1 DOUBLE ASYMMETRIC DECARBOXYLATIVE ALKYLATION

Studies toward the total synthesis of cyanthiwigin F commenced with the Fischer esterification of succinic acid (**188**) with allyl alcohol to afford diallylsucciniate (**187**, Scheme 2.2A). Exposure of diallyl succinate to a solution of allyl alkoxide in refluxing toluene initiated the desired Claisen condensation, a transformation immediately followed by subsequent Dieckmann cyclization to generate cyclohexadione product **189** exclusively as its bis-enol tautomer.[8] Thereafter, double methylation of bis-ester **189** under standard conditions provided access to bis(β-ketoester) **186** as a 1 : 1 mixture of racemic and *meso* diastereomers. Combination and optimization of the steps in this reaction sequence eventually facilitated the direct preparation of bis(β-ketoester) **186** from diallyl succinate (**187**). In the event, addition of diallyl succinate (**187**) to a

suspension of sodium hydride in THF at room temperature, followed by subsequent quenching with methyl iodide, allowed for the generation of bis(β-ketoester) **186** under lower temperature conditions in a single step (Scheme 2.2B).[10] While the yield of the one step procedure is nominally lower than that of the two step process, the ease of operation and facile scalability of the more direct route outweigh these minimal losses. Interestingly, the diastereomers of bis(β-ketoester) **186** were found to be separable, with each possessing distinct physical properties. While the more polar of the two diastereomers of bis(β-ketoester) **186** was always observed to be a viscous oil, the less polar diastereomer was isolated as a fluffy white solid. With cyclohexadione **186** in hand, we were poised to address the double stereoselective decarboxylative alkylation reaction.

Scheme 2.2 Preparation of the bis(β-ketoester) substrate for double allylation

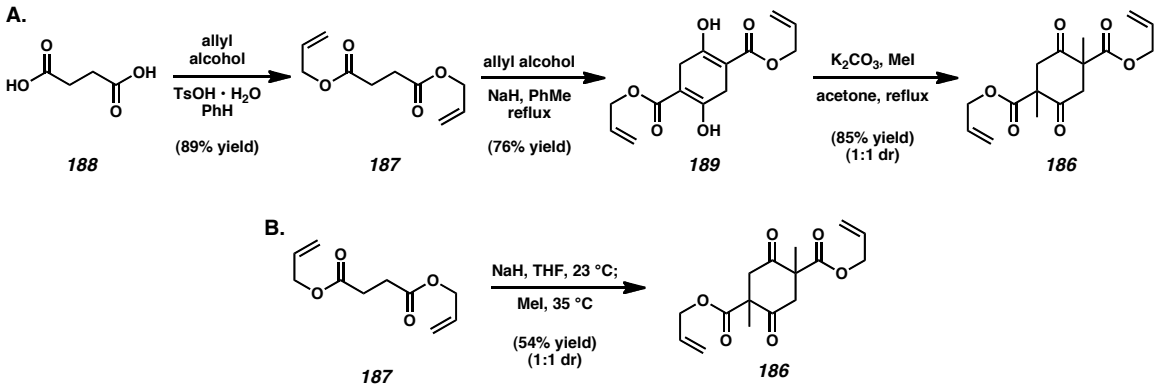

Previous to these efforts, our group had developed a powerful suite of enantioselective decarboxylative catalytic alkylation reactions. Using this technology, it is possible to access enantioenriched cyclohexanone products bearing all-carbon quaternary stereocenters at the ketone α-position, starting from substrates containing an

allyl enol carbonate, silyl enol ether, or β-ketoester moiety.[7] Having attained bis(β-ketoester) **186**, we anticipated that exposure of this material to the conditions of our palladium-catalyzed alkylation would result in the formation of two independent C–C bonds, thus forging the all-carbon quaternary stereocenters corresponding to positions C(6) and C(9) of the cyanthiwigin core.

While stereoselective transformations to set more than one stereocenter have been reported in the literature prior to our efforts, the implementation of a double catalytic, stereoselective, C–C bond-forming reaction in the context of complex total synthesis has gone relatively unexplored.[11] Nevertheless, these types of transformations are both efficient and direct, as they set multiple stereocenters with a single catalytic species, and are therefore increasingly desirable for the rapid synthetic preparation of complex natural products.

Despite the potential benefits of double asymmetric transformations, it should be emphasized that the starting material (**186**) for our envisioned reaction was attained as a 1 : 1 blend of racemic and *meso* diastereomers. Exposing such a stereoisomeric mixture to an enantiopure catalyst is typically ill-advised, as the presence of pre-existing stereocenters in the substrate could interfere with inherent catalyst selectivity and afford reduced quantities of the desired product.[12] Indeed, the potential development of mismatched catalyst-substrate interactions, which would deleteriously impact yield and selectivity of the reaction, was a major concern. We were additionally mindful of the possibility for the reaction to proceed via an undesired kinetic resolution.[13]

Subjecting a diastereomeric mixture of bis(β-ketoesters) to the conditions of the stereoselective decarboxylative alkylation was a maneuver with many prospective

outcomes. In the event of diastereomeric interference between the substrate and catalyst, the potential existed for incomplete allylation or impeded decarboxylation. Even in the case of complete transformation of bis(β-ketoester) **186** into the desired diketone (**185**), the stereochemical course of the reaction was difficult to predict. The diastereomeric mixture containing three stereoisomers of starting material could possibly traverse any of 16 distinct stereodefined pathways to give any of three potential product stereoisomers (Scheme 2.3).

Scheme 2.3 Paths of the double asymmetric decarboxylative catalytic alkylation

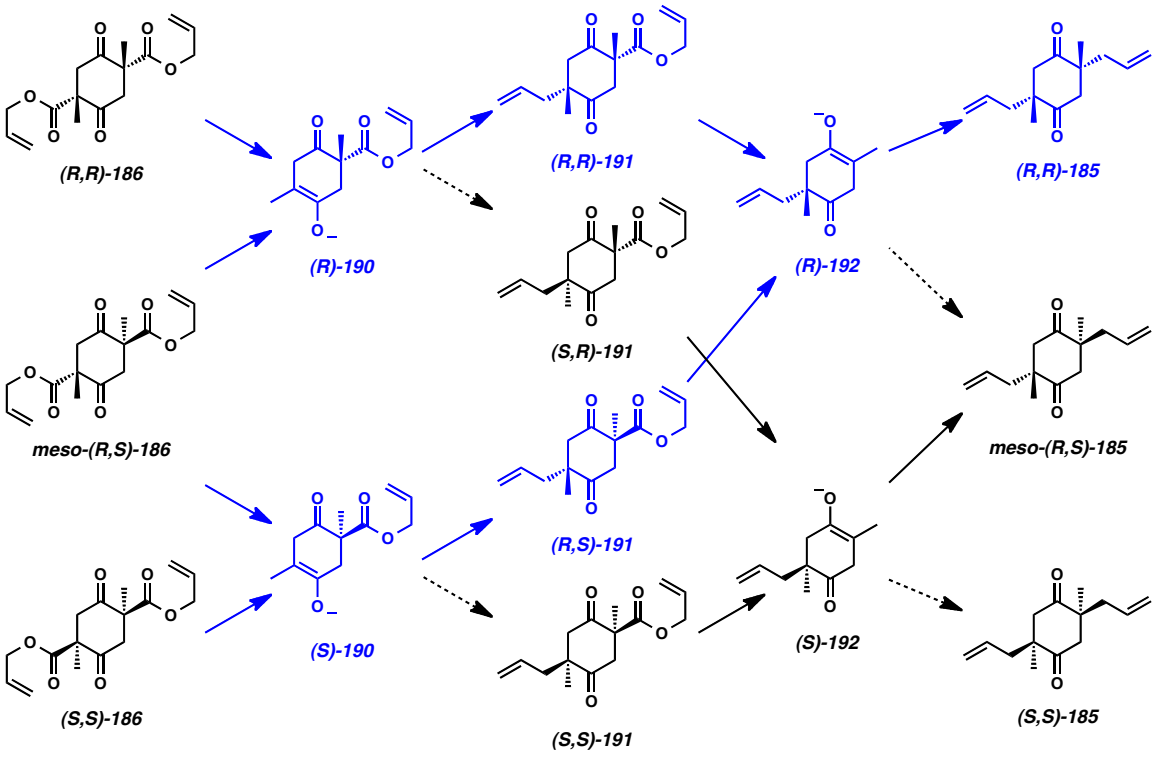

In order for the reaction to afford the desired diketone product with acceptable yield and selectivity, the catalyst employed had to meet several stringent requirements. First, initial decarboxylation of each stereoisomer of starting material ((*R*,*R*)-, *meso*-(*R*,*S*)-, or

(*S*,*S*)-**186**) to give either intermediate ketone enolate ((*R*)- or (*S*)-**190**) would need to proceed at roughly equivalent rates regardless of configuration. If a large disparity in the rate of decarboxylation existed between different stereoisomers of starting bis(β-ketoester) **186**, undesired kinetic resolution would influence the downstream stereoselective bond formation. The same requirement would be necessary for the subsequent decarboxylation of intermediates **191** to yield the transient enolates (*R*)- and (*S*)-**192**, and as such, all stereoisomers of **191** would need to react at equal rates. The second requirement envisioned was that all bond-forming reactions would occur under complete catalyst stereocontrol. This would dictate that any pre-existing or intermediately formed stereocenters present in any isomer of bis(β-ketoester) **186** or intermediate **191** should have no impact upon the selectivity of the allylation event. Third, the catalyst control in these situations would be required to be highly selective, so as to preferentially guide all of the possible ketone enolate stereoisomers ((*S*)- and (*R*)-**190**, (*S*)- and (*R*)-**192)** toward the single desired, enantioenriched product (**185**).

Despite initial uncertainty concerning the course of this reaction, we reasoned that the stereoablative nature of the stereoselective decarboxylative alkylation methodology would minimize any undesired mismatched interactions.[14] This fact, combined with the relatively distal relationship between the two reactive centers in **186**, gave us confidence in the success of our double alkylation approach. Therefore, we subjected a 1 : 1 diastereomeric mixture of racemic and *meso*-**186** to a solution of $Pd(dmdba)_2$ palladium(0) and (*S*)-*tert*-butyl phosphinooxazoline (*t*-BuPHOX, **193**) in diethyl ether (Scheme 2.4).[15] To our delight, this reaction proceeded smoothly at 25 °C to give the desired, enantioenriched diketone (*R*,*R*)-**185** in 78% yield, 99% *ee*, and a 4.4 : 1

diastereomeric ratio. This critical reaction established both of the all-carbon quaternary stereocenters necessary for completion of the cyanthiwigin molecules at an early stage of the synthesis. Creating these nested and difficult points of chirality well in advance was important to the versatility and flexibility of our route.

Scheme 2.4 Double asymmetric decarboxylative catalytic alkylation of ***186***

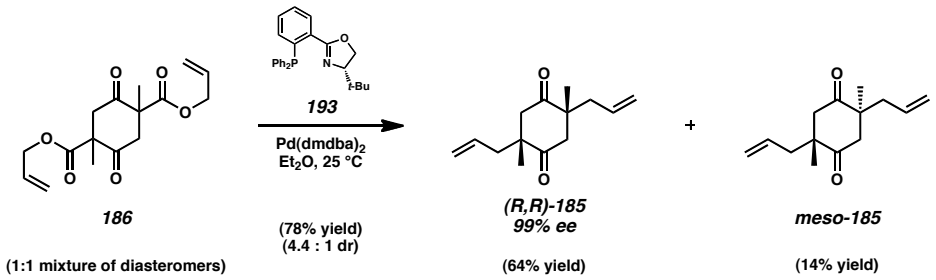

When considering the excellent enantioselectivity observed in the double alkylation reaction, the modest diastereoselectivity attained from this transformation was initially perplexing. Investigation of literature pertinent to double stereoselective transformations eventually revealed that the high levels of *ee* observed in diketone product (*R*,*R*)-**185** come at the expense of a reduced diastereomeric ratio.[16,17] When only a single undesired allylation event occurs while traversing the possible mechanistic pathways detailed in Scheme 2.3, an additional molecule of the undesired *meso* diastereomer is produced (*meso*-(*R*,*S*)-**185**) regardless of which alkylation occurs against preference. While this unwanted material negatively impacts the diastereomeric ratio of the isolated diketone, it nevertheless has no influence upon the *ee* of the desired product. In order to adversely affect the *ee* of cyclohexadione (*R*,*R*)-**185**, an individual molecule of bis(β-ketoester) (*R*,*R*)-**186**, *meso*-(*R*,*S*)-**186**, or (*S*,*S*)-**186** must undergo two disfavored allylation events in sequence to afford product (*S*,*S*)-**185**. Because the likelihood of two allylation errors

impacting a single substrate is very low in the presence of reasonable catalyst control, the total yield of the unwanted (*S*,*S*)-**185** stereoisomer is negligible, and thus the product *ee* is excellent. However, due to the much higher likelihood of a single alkylation event yielding the undesired configuration, the amount of diketone *meso*-(*R*,*S*)-**185** afforded through this reaction is larger than anticipated. In effect, generation of the *meso* diastereomer serves as a buffer against accumulation of undesired stereoisomer (*S*,*S*)-**185**, allowing this reaction to sacrifice some small measure of diastereomeric ratio in favor of exceptionally high levels of enantioselectivity.[18] This phenomenon (sometimes referred to as the "Horeau Principle"), was first observed and rationalized by Langenbeck in 1936, and was later elaborated into more thorough mathematical representations by Horeau, Kagan, and Rautenstrauch.[16,17]

2.2.2 DIKETONE DESYMMETRIZATION AND ELABORATION

With the successful generation of enantioenriched diketone (*R*,*R*)-**185** attained, our efforts were thereafter focused on elaboration of this material via construction of the peripheral A- and C-rings of the cyathane tricycle.

At this juncture of the synthesis, advancement of diketone **185** required differentiation between the functional groups of this C_2 symmetric substrate.[19] Initial desymmetrizing efforts were attempted via careful addition of various Grignard reagents to cyclohexadione **185** in the hopes of executing a single nucleophilic addition to either ketone moiety. Disappointingly, these experiments ultimately proved unsuccessful (Scheme 2.5). The steric encumbrance imposed by the α-quaternary stereocenters of diketone **185** very likely impede approach of any incoming nucleophile toward either of

the carbonyl carbons, and thus renders this cyclohexadione intransigent to 1,2-addition conditions. An alternative desymmetrization strategy we investigated involved the attempted mono-functionalization of the pendent allyl side chains of substrate **185**. Regrettably, this approach also proved ineffective. In cases where dihydroxylation or epoxidation conditions were employed, only low yields were ever obtained, and in every case the sparing material isolated was a mixture of mono- and di-functionalized products.

Scheme 2.5 Attempts toward diketone functionalization

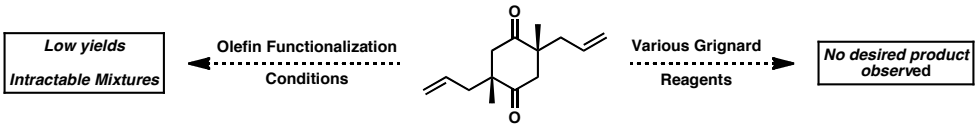

(*R,R*)-*185*

Greater selectivity and reactivity was ultimately achieved when diketone **185** was subjected to the conditions of enol triflate formation (Scheme 2.6A). Slow addition of diketone **185** to a solution of potassium bis(trimethylsilyl)amide in tetrahydrofuran allowed generation of a monoanionic ketone enolate. This intermediate was thereafter trapped via exposure to a solution of phenyl bis(trifluoromethane)sulfonimide to afford cyclohexanone **194** in reasonable yield. With this newly desymmetrized material in hand, we attempted to leverage the installed triflate to introduce functionality that would enable construction of a bicyclic structure.

By submitting enol triflate **194** to the conditions of a palladium-catalyzed carboxylation reaction in the presence of methanol, conjugated ester **195** was obtained as the major product. Unfortunately, purification of this material proved difficult, and isolates of enoate **195** were regularly contaminated with trace amounts of a strongly UV-

active impurity. Thorough and careful investigation of this contaminant eventually revealed its identity as dienone **196**, an unexpected yet intriguing byproduct of this carbonylative methodology. We suspected bicycle **196** to be the result of an intramolecular Heck-type reaction, wherein initial oxidative addition of palladium into the enol triflate bond was followed by subsequent carbon monoxide insertion and eventual olefin insertion into the pendant arm of **194**. This hypothesis was later strengthened when the methoxycarbonylation reaction was repeated in the absence of the nucleophilic cosolvent (Scheme 2.6B). Without methanol, these conditions afforded exclusively the carbonylative Heck product **196**.[20] In an additionally fascinating development, prolonged storage of neat **196** eventually generated pentacyclic spirocycle **197**, a product presumably resulting from a hetero Diels–Alder dimerization.

Interestingly, the structure of dienone product **196** suggests that oxidative addition and carbon monoxide incorporation occur before olefin complexation and insertion. While this phenomenon is known, typically in these reactions carbonylation occurs as the final step of the transformation, taking place only after olefin insertion.[20] This observed reversal in expected reactivity is likely due to the difficulty of olefin insertion directly following oxidative addition, a process that would require cyclobutane formation. The relatively greater ease of cyclopentanone formation provides a reasonable explanation for pre-emptive carbon monoxide incorporation. Regrettably, further elaboration of either enoate **195** or dienone **196** proved unproductive in our hands, and so alternative methods of functionalizing triflate **194** were sought.

Scheme 2.6 (A) Triflate formation and carboxylative attempts toward diketone elaboration (B) An unanticipated carbonylative Heck reaction, and subsequent dimerization

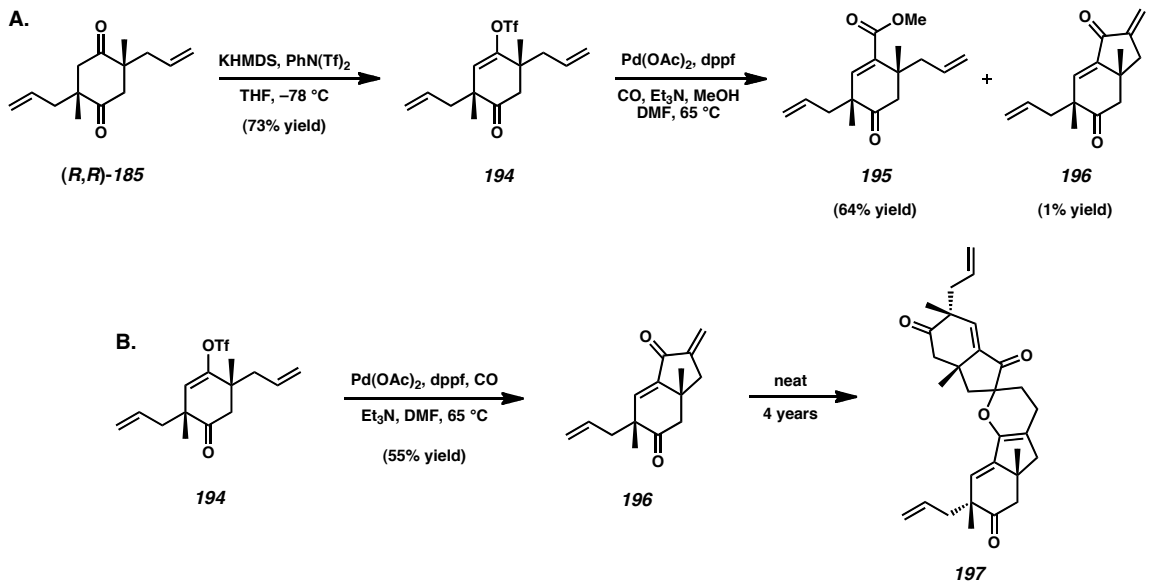

In order to better gauge the reactivity of enol triflate **194**, we executed a number of cross-coupling reactions to test the viability of sp^2-sp, sp^2-sp^2, and sp^2-sp^3 hybridized carbon-carbon bond construction. Attempts at Sonogashira coupling of ketone **194** and trimethylsilyl acetylene smoothly provided access to enyne **198** in high yield (Scheme 2.7).[21] Similarly, copper-accelerated Stille reaction of triflate **194** with enol stannane **199** proved to be very effective.[22] After acidic workup of this sp^2-sp^2 coupling reaction, enone **200** was obtained in reasonable yield.

*Scheme 2.7 Palladium-catalyzed cross-coupling reactions of triflate **194***

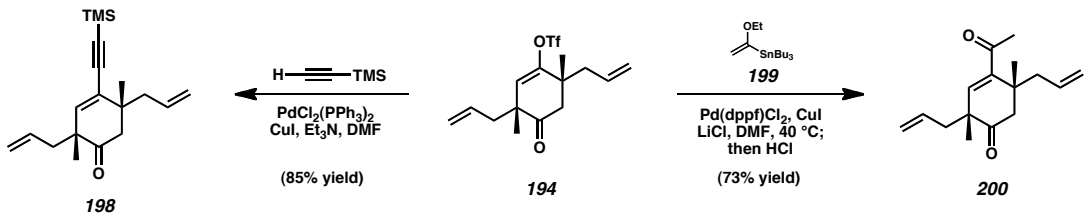

Encouraged by the successes of the preliminary Stille coupling, we repeated this reaction while employing the more complicated enol stannane **201** in place of coupling partner **199** (Scheme 2.8).[23] This transformation progressed easily to generate cyclohexanone **202**. However, purification and manipulation of this material was difficult, due to the rapid decomposition of the enol ether upon contact with silica gel or prolonged exposure to atmospheric conditions, both of which resulted in hydrolysis to reveal the latent ketone moiety. In order to circumvent issues of instability experienced with this intermediate, enol ether **202** was immediately exposed to the Grubbs/Hoveyda generation II catalyst (**203**) in order to execute ring-closing metathesis, and this process was subsequently followed by acidic workup. This synthetic procedure successfully closed the seven-membered C-ring of the cyathane tricycle, ultimately generating bicyclic ketone **204**. While our efforts were bolstered by the successful formation of a [6,7]-bicyclic intermediate, this material nevertheless provided us with unanticipated difficulty. Formation of bicycle **204** was always accompanied by an undesired shift of the anticipated C(12)–C(13) olefin into conjugation with the newly revealed C(10) ketone.[24] If enone **204** were to be used to pursue the synthesis of the cyanthiwigin molecules, this new development would necessitate isomerization of the C(11)–C(12) olefin back into the C(12)–C(13) position, a task we regarded to be nontrivial. Furthermore, while the oxygenation present at C(10) was the result of functionality necessary for the stability of stannane **201**, this newly formed ketone was superfluous to the structure of completed natural product. Thus, removal of this moiety would be required at some later stage if enone **204** were to serve as a viable synthetic intermediate. Because of these difficulties, we opted not to pursue the further elaboration of dienone

204. Instead, we chose to investigate alternative cross coupling-conditions for triflate **194**.

*Scheme 2.8 Formation, ring-closing metathesis, and acidic hydrolysis of enol ether **202***

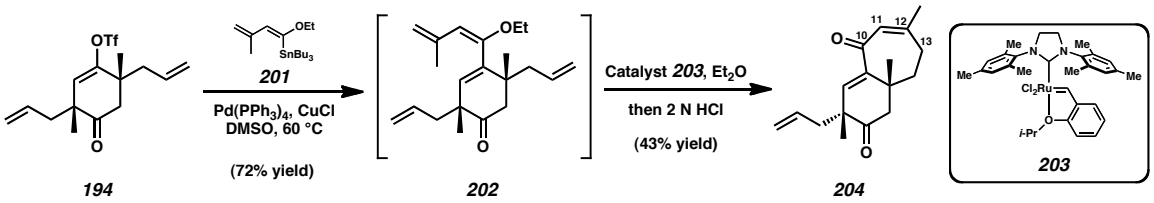

A reinvestigation of triflate **194** revealed the viability of a direct sp^2-sp^3 bond formation via a Negishi cross-coupling procedure. Zinc dust was first treated with 1,2-dibromoethane and trimethylsilyl chloride, and to this activated metal was added alkyl iodide **205**. After generation of the alkyl zinc species, a THF solution containing a palladium(0) catalyst and triflate **194** was introduced to the mixture, thus initiating Negishi cross coupling of the two fragments (Scheme 2.9).[25] After appropriate workup and purification, tetraolefin **183** was isolated as the sole product of this reaction. We were excited to find that ring-closing metathesis of cyclohexanone **183** to form the seven-membered C-ring furnished bicyclic product **181**, a structure containing two of the three rings of the cyathane skeleton. Notably, we found that this ring-forming process was both faster and higher-yielding when modified Grubbs–Hoveyda catalyst **206** was employed in place of the Grubbs/Hoveyda second-generation catalyst **203**.[26]

Scheme 2.9 Negishi cross coupling for the formation of an sp^2-sp^3 carbon-carbon bond

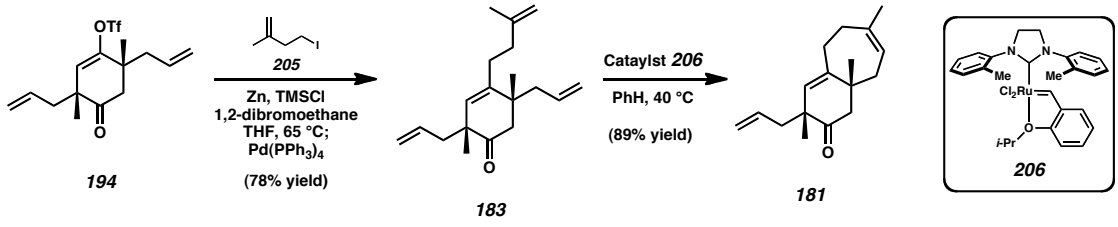

We anticipated that further advancement of this material toward the cyanthiwigin natural products would undoubtedly require selective functionalization of the remaining allyl side chain in the presence of the C(12)–C(13) olefin. For this reason, we turned our attention toward the possibility of using metathesis reactivity for the elaboration of the remaining terminal olefin. Cross-metathesis of vinyl boronate species **207** with newly attained bicycle **181** proved fruitful, and upon exposure to an oxidative workup involving aqueous sodium perborate, this process generated aldehyde **208** as the major product (Scheme 2.10A).[27] With the success of the ring-closing and cross-metathesis processes confirmed as independent reactions, we hypothesized that both transformations might be accomplished concurrently via the use of the same catalyst.

Scheme 2.10 Functionalization of the C(2)–C(3) olefin via olefin cross-metathesis

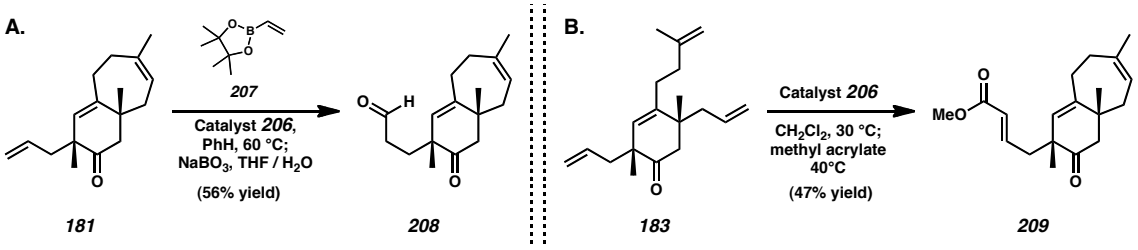

In the event, the addition of methyl acrylate to the conditions used for the ring-closing metathesis of tetraolefin **183** executed both formation of the seven-membered cyathane

C-ring and functionalization of the terminal allyl moiety (Scheme 2.10B). By employing this reaction, monocyclic starting material **183** was smoothly transformed into bicyclic enoate **209** in a single synthetic operation. Though ester **209** was not amenable to further desired transformation, the technique elucidated by its formation nevertheless aided considerably in our synthetic efforts. By subjecting tetraolefin **183** to the conditions of concurrent ring-closing and cross-metathesis in the presence of vinyl boronate **206**, and executing a subsequent oxidative workup with sodium perborate, it was possible to rapidly prepare bicyclic aldehyde **208** (Scheme 2.11).

Scheme 2.11 Ring-closing and cross-metathesis reaction to generate the bicyclic aldehyde ***208***

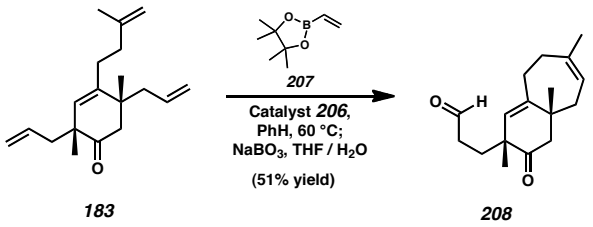

2.2.3 TRICYCLE FORMATION VIA RADICAL CYCLIZATION

At this stage in the synthesis, the synthetic challenges remaining to be addressed included the finalization of the tricyclic cyathane core via installation of the five-membered A-ring, as well as the establishment of both the C(4) and C(5) stereocenters. We hypothesized that all of these pending goals might be accomplished in tandem through the use of a radical cyclization reaction. It was envisioned that the formation of a high-energy acyl radical species via hydrogen atom abstraction from aldehyde **208** would encourage thermodynamically-controlled carbon-carbon bond formation with the C(4)–

C(5) olefin. To test this hypothesis, we turned our attention toward methods for the reliable production of acyl radical intermediates from aldehydes.[28]

Preliminary attempts to generate an acyl radical for the purpose of intramolecular cyclization were unfortunately unsuccessful. Subjecting bicyclic aldehyde **208** to tributylstannane or triphenylstannane did not yield the desired product. Both radical propagators were employed in combination with either azobisisobutyronitrile (AIBN) or 2,2'-azobis(4-methoxy-2,4-dimethyl valeronitrile) (V-70) initiators, yet in each case only unreacted substrate **208** or nonspecific decomposition were observed (Scheme 2.12).[29,30]

Scheme 2.12 Initial attempts at radical cyclization for A-ring formation

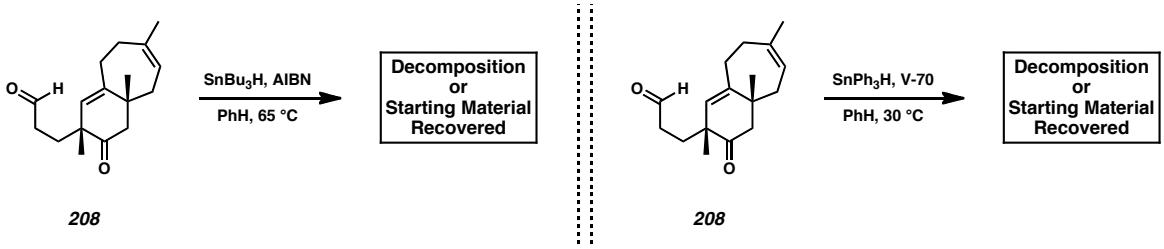

In light of the failure of stannane reagents to furnish the targeted tricyclic product, we sought alternative conditions for the reliable formation of acyl radical species. After a thorough investigation of the literature, we became familiarized with aldehyde-olefin cyclization methodology developed by Tomioka *et al*. in 2005.[31] By implementing a bulky thiol radical propagator and an appropriate initiator, Tomioka was able to achieve the cyclization of aldehyde functional groups onto olefins to form cyclic ketone products. By employing this reaction, it was demonstrated that in the presence of *tert*-dodecanethiol and AIBN, linear aldehyde **210** could be cyclized onto an isolated olefin moiety to be smoothly converted into cyclopentanone **211** (Scheme 2.13). Similarly,

tert-dodecanethiol and 1,1'-azobis(cyclohexane-1-carbonitrile) (V-40 initiator) enabled the conversion of aldehyde **212** into cyclohexanone **213**.

Scheme 2.13 Radical cyclization conditions developed by Tomioka and coworkers[31]

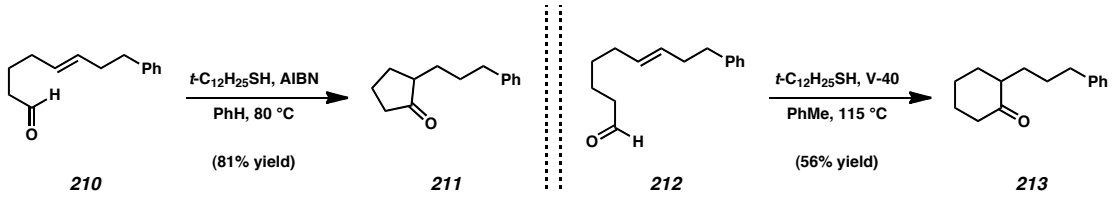

Because our work required the cyclization of an aldehyde onto an unconjugated olefin, we attempted to subject bicyclic aldehyde **208** to Tomioka's methodology with the intention of forming the required cyathane A-ring. Fortuitously, employing *tert*-dodecanethiol and V-40 initiator in the radical cyclization of **208** forged the desired cyclopentanone and provided access to fully formed cyathane tricycle **214** (Scheme 2.14A). Minor optimization of this reaction was possible under lower temperature conditions, wherein using *tert*-butylthiol as propagator and AIBN as initiator afforded slightly increased yield of the desired product (Scheme 2.14B). Regardless of the exact reagents used, both reactions afforded **214** as a single diastereomer.

Scheme 2.14 Application of Tomioka's methodology to A-ring formation

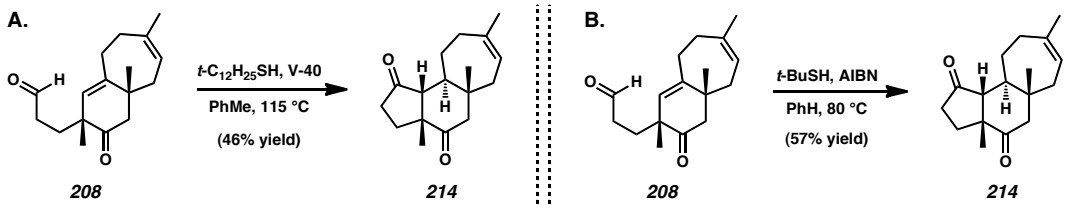

It is possible that the diastereoselectivity observed in this cyclopentanone-forming reaction is a consequence of thermodynamic control. After initial hydrogen atom abstraction from aldehyde **208**, acyl radical species **215** is formed (Scheme 2.15). Due to steric and conformational constraints, this radical species has limited access to the C(4)–C(5) olefin. Indeed, acyl radical approach and carbon-carbon bond formation may only occur from the bottom face of the bicyclic system as drawn in Scheme 2.15. Construction of this bond in line with such a trajectory establishes the desired stereochemistry at C(4), and additionally generates a rapidly equilibrating tertiary radical at C(5) (**216**). Further hydrogen atom abstraction from *tert*-butyl thiol to quench the radical found in intermediate **216** proceeds under thermodynamic control, and this affords the more stable trans-oriented [6,7] ring fusion in preference to the cis-fused alternative. Ultimately, these factors ensure that tricycle **214** is furnished as the sole stereoisomeric product of the reaction. The formation of the five-membered A-ring to construct tricyclic diketone **214** marked the completion of the cyathane core skeleton.

Scheme 2.15 Mechanistic hypothesis and stereochemical rationale for radical cyclization of ***214***

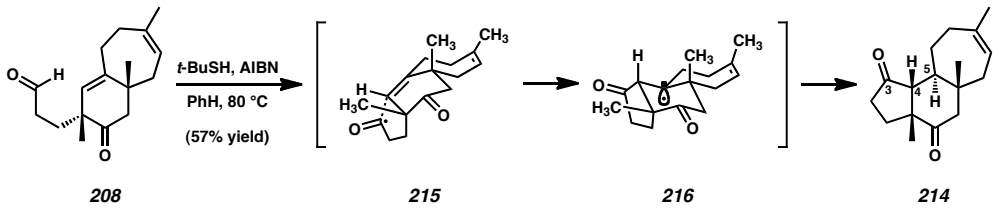

Attaining this material was of considerable significance to our synthetic efforts, not only because of its proximity to cyanthiwigin F (**160**), but also because we envisioned that this tricyclic diketone **214** could serve as a platform from which to access other cyanthiwigin natural products. Fortunately, solid crystals of this critical intermediate

were amenable to X-ray analysis (Figure 2.2). The data collected from X-ray crystallography on diketone **214** revealed not only the stereochemistry set by the radical cyclization reaction, but also confirmed the relative stereochemistry established by the initial double alkylation reaction as well.

*Figure 2.2 X-ray crystal structure of tricycle **214***

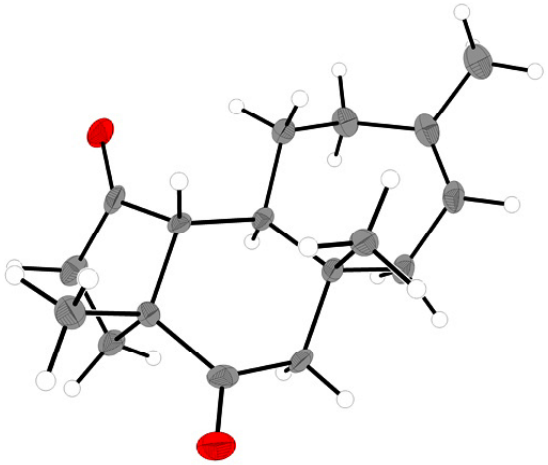

2.2.4 COMPLETION OF THE CYANTHIWIGIN NATURAL PRODUCTS

With tricyclic diketone **214** in hand, the final challenges remaining in the total synthesis of cyanthiwigin F were the installation of the C(3) isopropyl group and introduction of the C(2)–C(3) olefin. In order to address these requirements, we envisioned harnessing the reactivity of the newly installed C(3) ketone to establish a vinyl triflate suitable for transition metal-catalyzed cross-coupling reactions. In the event, selective deprotonation of diketone **214** with KHMDS and trapping with *N*-phenyl bis(trifluoromethane)sulfonimide produced vinyl triflate **217** in reasonable yield (Table 2.1). Having achieved the synthesis of tricycle **217**, we predicted that isopropyl group installation could be accomplished via a Negishi cross-coupling process similar to the one

used previously.[25] Regrettably, when these coupling conditions were employed with triflate **217** and 2-iodopropane, the only isolated material was reductive deoxygenation product **218** (Table 2.1, entry 1).

Because palladium-catalyzed cross-coupling of **217** and 2-iodopropane was met with difficulty, alternative copper-catalyzed methods to install the required three-carbon fragment were investigated. Preliminary experiments involved direct addition of isopropyl magnesium chloride to suspensions of triflate **217** and catalytic amounts of either copper iodide or copper cyanide. Disappointingly, these reactions were similarly ineffective, affording mostly the reduced tricycle **218** (Entries 2–4).[32] Use of copper bromide dimethyl sulfide complex for this direct-addition technique did yield small quantities of the natural product, but these sparing amounts of the desired compound were contaminated with larger amounts of the reduction product **218**. To rectify this issue, we endeavored to approach the coupling via the use of stoichiometric quantities of pre-generated isopropyl-cuprate reagents, using a variety of different copper sources (Entries 5–8). In all cases, we observed either low reactivity or a preference for reductive deoxygenation.

Table 2.1 Transition metal cross-coupling attempts toward cyanthiwigin F

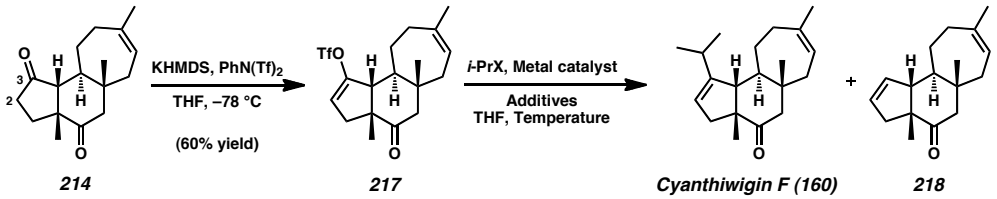

Entry	Stoichometric *i*-PrX Reagent	Metal Catalyst	Additives	Temperature (°C)	Yield ***160*** (%)	Yield ***218*** (%)	Yield ***217*** (%)
1	*i*-PrZnI [a]	$Pd(PPh_3)_4$	1,2-dibromoethane TMSCl	65 °C	-	ND	-
2[b]	*i*-PrMgCl	CuI	-	-10 °C	-	65%	-
3[b]	*i*-PrLi	CuCN	-	–20 °C	-	-	73%
4[b]	*i*-PrMgCl	CuBr•DMS	-	–20 °C	26%	ND	57%
5[c, d]	*i*-PrMgCl + CuCN	-	-	–78 → 0 °C	-	-	99%
6[c]	*i*-PrMgCl + CuBr•DMS	-	-	–78 → –20 °C	15%, 20%	ND	-
7[c, e]	*i*-PrLi + CuCN	-	-	–78 → –20 °C	11	ND	27%
8[c, e]	*i*-PrLi + CuCN	-	BF_3•OEt_2	–20 °C	-	-	99%
9[f]	*i*-PrMgCl	$Ni(dppp)Cl_2$	-	35 °C	-	-	99%
10	*i*-PrMgCl	$Pd(PPh_3)_4$	-	–78 → 23 °C	-	ND	19%
11	*i*-PrMgCl	$Pd(dppf)Cl_2$	-	35 °C	-	ND	-
12[c,e]	*i*-PrMgCl + CuCN	$Pd(dppf)Cl_2$	-	–78 → 0 °C	41%	23%	-

All reactions with yields listed as 'not determined' gave predominantly tricycle ***218*** as product. [a] Reagent formed via addition of *i*-PrI to activated Zn^0 metal. [b] Reaction performed via direct addition of *i*-PrX species to a suspension of the metal catalyst and ***217***. [c] Reaction involved the use of a pre-formed cuprate species. [d] A lower-order cyanocuprate was employed (1 : 1 ratio of *i*-PrX to Cu). [e] A higher-order cyanocuprate was employed (2 : 1 ratio of *i*-PrX to Cu). [f] Et_2O was employed as solvent.

Additional experiments into isopropyl cross-coupling involved employing a number of nickel and palladium catalysts in a series of Kumada-type reactions (Entries 9–11),[33] but the results overwhelmingly favored reduced product **218** in those instances where reactivity was observed. Finally, we discovered that introduction of a pre-generated, higher-order isopropyl cyanocuprate to a solution of triflate **217** and dichloro(1,1'-bis(diphenylphosphino)ferrocene)palladium(II) gave a combined 65% yield of the natural

product (**160**) and tricycle **218**, in a 1.8 : 1 mixture favoring cyanthiwigin F (Entry 12).[34,35]

In addition to being instrumental in the total synthesis of cyanthiwigin F, it was our hope that the completed cyathane core represented by tricycle **214** would prove useful in the synthesis of other diterpenes of this natural product family. Starting from diketone **214**, deprotonation at the α-position of the C(3) ketone and trapping of the incipient enolate with allyl chloroformate provided access to enol carbonate **219**. Thereafter, treatment of this material with a catalytic quantity of palladium(0) in acetonitrile provided enone **220** in high yield (Scheme 2.16).[36] Unsaturated ketone **220** afforded an excellent opportunity for direct introduction of the C(3) isopropyl group via 1,2-addition, and so was exposed to isopropyl lithium under Luche-type activation conditions. Cerium-mediated alkyl lithium reactivity proceeded with exclusive addition to C(3), generating tertiary alcohol **221** as a mixture of inconsequential diastereomers.

*Scheme 2.16 Advancement of tricycle **214** toward additional cyanthiwigin natural products*

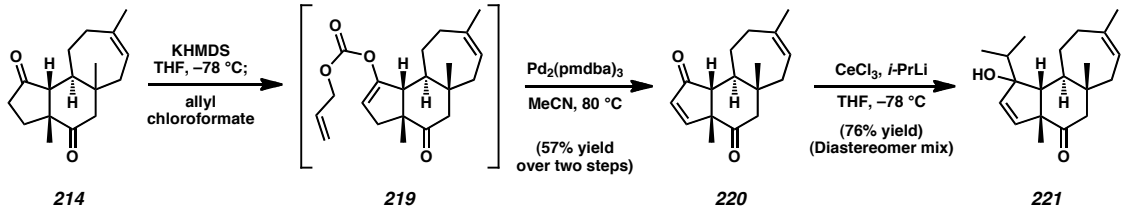

The mixture of alcohols, **221**, was then subjected to PCC in dichloromethane, conditions anticipated to execute allylic oxidation with concomitant oxygen transposition. In the event, **221** was smoothly transformed into natural product **156**, thus completing the total synthesis of cyanthiwigin B (Scheme 2.17).[37] We further envisioned that cyanthiwigin B (**156**) might be additionally advanced toward other members of this

natural product family via selective carbonyl reduction at C(8).[38] Conditions reported to selectively reduce ketones in the presence of enones unfortunately provided exclusively over-reduction of both carbonyl moieties, but this difficulty was mitigated by immediate and selective reoxidation of the resulting material with manganese(IV) dioxide. This allylic oxidation process generated enone **222** as the sole product of reaction. Notably, tricycle **222** was found to be structurally identical to cyanthiwigin E, with the single exception of the configuration of the stereogenic alcohol present at C(8), which was determined to be epimeric to that found in the natural product. Nevertheless, 8-*epi*-cyanthiwigin E (**222**) served as an invaluable intermediate in the preparation of another cyanthiwigin compound. Treatment of enone **222** with Martin's sulfurane in deuterated chloroform successfully eliminated the C(8) secondary alcohol to install the C(7)–C(8) olefin, thus finalizing the total synthesis of cyanthiwigin G (**161**).[39,40]

Scheme 2.17 Completion of cyanthiwigins B and G

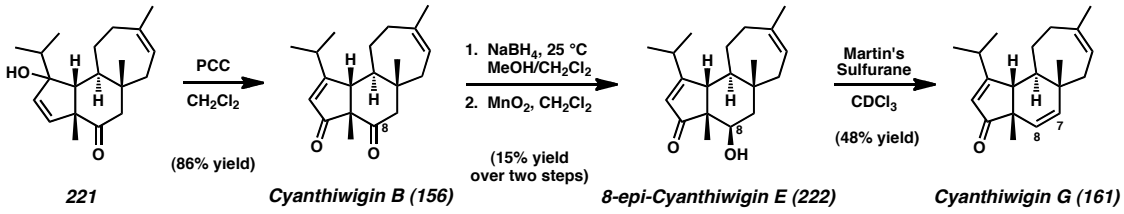

221 ***Cyanthiwigin B (156)*** ***8-epi-Cyanthiwigin E (222)*** ***Cyanthiwigin G (161)***

2.3 CONCLUDING REMARKS

In summary, we have developed an efficient, versatile, and enantioselective route to the cyanthiwigin natural products. Our approach toward these molecules involves a rapid synthesis of the central six-membered B-ring, with a specific focus on early installation of both the C(6) and C(9) all-carbon quaternary stereocenters. The use of a double

asymmetric decarboxylative catalytic alkylation reaction not only enables access to the critical enantioenriched cyclohexadione **185**, but this methodology has additionally proven tolerant of a diastereomeric mixture of racemic and *meso* starting materials in the same catalytic transformation. Because of the ease with which stereoisomeric mixtures of precursor bis(β-ketoester) **186** can be prepared, this stereoablative approach expedites the early phases of our synthesis considerably. Our strategy also involves an efficient, single operation ring-closing and cross-metathesis reaction to generate a bicyclic aldehyde from a monocyclic tetraolefin. Combined with a powerful radical cyclization, these techniques furnish ready and rapid access to a versatile tricyclic intermediate representing the completed cyathane core (**214**). By leveraging this core compound as a branching point toward marine natural products, our group was able to expediently prepare multiple cyanthiwigin molecules. In particular, the total synthesis of cyanthiwigin F (**160**) was accomplished in nine total steps, seven of which form carbon-carbon bonds. Of the seven carbon-carbon bond-forming transformations in our synthetic sequence, four construct more than one carbon-carbon bond simultaneously. Additionally, the synthesis is highly efficient in terms of its use of redox reactions, as only minimal oxidative or reductive processes are employed. The flexibility and modularity of our synthetic route later accommodated further extrapolation of tricyclic intermediate **214** toward additional members of the cyanthiwigin family, thus facilitating the preparation of cyanthiwigins B (**156**) and G (**161**).

2.4 EXPERIMENTAL SECTION

2.4.1 MATERIALS AND METHODS

All reactions were performed at ambient temperature (22 °C) unless otherwise noted. Reactions requiring external heat were modulated to the specified temperatures indicated by using an IKAmag temperature controller. All reactions were performed in glassware flame dried under vacuum and allowed to cool under nitrogen or argon. Solvents were dried by passage over a column of activated alumina with an overpressure of argon gas. Tetrahydrofuran was distilled directly over benzophenone and sodium, or else was dried by passage over a column of activated alumina with an overpressure of argon gas. Grubbs' ruthenium catalysts **203** and **206** were donated by Materia Inc. and used without further purification. (*S*)-*t*-BuPHOX (**193**),[15,41] enol stannane **201**,[23] 4-iodo-2-methyl-1-butene (**205**),[42] and vinyl boronate ester **207**[27] were prepared according to known methods. All other chemicals and reagents were used as received. Compounds purified by flash chromatography utilized ICN silica gel (particle size 0.032–0.063 mm) or SiliCycle® Silia*Flash*® P60 Academic Silica Gel (particle size 40–63 μm; pore diameter 60 Å). Thin-layer chromatography (TLC) was performed using E. Merck silica gel 60 F254 pre-coated plates (0.25 mm) and visualized by UV, *p*-anisaldehyde, or alkaline permanganate staining. NMR spectra were recorded on a Varian Mercury 300 (at 300 MHz for ^{1}H NMR and 75 MHz for ^{13}C NMR), Varian Inova 500 (at 500 MHz for ^{1}H NMR and 125 MHz for ^{13}C NMR), or Varian Inova 600 (at 600 MHz for ^{1}H NMR only) instrument, and are reported relative to residual $CHCl_3$ (δ 7.26 for ^{1}H NMR, δ 77.16 for ^{13}C NMR) or C_6H_6 (δ 7.16 for ^{1}H NMR, δ 128.06 for ^{13}C NMR). The following format is

used for the reporting of ^{1}H NMR data: chemical shift (δ ppm), multiplicity, coupling constant (Hz), and integration. Data for ^{13}C NMR spectra are reported in terms of chemical shift. IR spectra were recorded on a Perkin Elmer Spectrum Paragon 1000 spectrometer, and data are reported in frequency of absorption (cm^{-1}). High-resolution mass spectra were obtained from the Caltech Mass Spectral Facility, or else were acquired using an Agilent 6200 Series TOF mass spectrometer with an Agilent G1978A Multimode source in ESI, APCI, or MM (ESI/APCI) ionization mode. Analytical chiral gas chromatography was performed with an Agilent 6850 GC using a G-TA (30 m x 0.25 mm) column (1.0 mL/min carrier gas flow). Analytical achiral gas chromatography was performed with an Agilent 6850 GC using a DB-WAX (30 x 0.25 mm) column (1.0 mL/min carrier gas flow). Preparatory reverse-phase HPLC was performed on a Waters HPLC with Waters Delta-Pak 2 x 100 mm, 15 μm column equipped with a guard, employing a flow rate of 1 mL/min and a variable gradient of acetonitrile and water as eluent. HPLC visualization was performed by collecting 1 mL fractions after initial injection and analyzing each fraction via TLC. Optical rotations were measured with a Jasco P-1010 polarimeter at 589 nm using a 100 mm path-length cell.

2.4.2 PREPARATIVE PROCEDURES

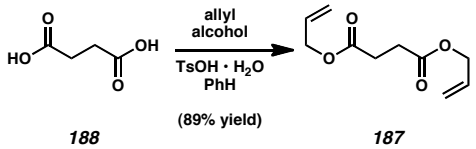

Diallyl succinate (187). To a solution of succinic acid (**188**, 40.0 g, 338.7 mmol) in benzene (300 mL) was added TsOH • H_2O (0.21 g, 1.2 mmol, 0.003 equiv). After brief mixing, allyl alcohol (70 mL, 1.01 mol, 3.00 equiv) was added to the reaction, and the flask was fitted with a Dean–Stark trap and reflux condenser under nitrogen. The reaction was heated to 105 °C and allowed to reflux over 12 h. After collection of 13 mL H_2O from the Dean–Stark trap, the reaction was allowed to cool to room temperature and was quenched by slow treatment with saturated $NaHCO_{3(aq)}$ until gas evolution halted. The phases were separated, and the organic layer was washed with saturated $NaHCO_{3(aq)}$ (2 x 40 mL) and brine (2 x 30 mL). The combined organic layers were dried over $MgSO_4$, filtered, and solvent was removed in vacuo. The resulting colorless oil was dried under high vacuum to afford diallyl succinate (**187**, 59.8 g, 89% yield). This material was carried into the next step without further purification: R_f = 0.35 (10:90 Et_2O/pentane); ^{1}H NMR (300 MHz, $CDCl_3$) δ 5.90 (ddt, *J* = 17.3, 10.5, 5.6 Hz, 2H), 5.31 (ddt, *J* = 17.0, 1.6, 1.3 Hz, 2H), 5.23 (ddt, *J* = 10.4, 1.3, 1.1 Hz, 2H), 4.60 (ddd, *J* = 5.9, 1.3, 1.3 Hz, 4H), 2.67 (s, 4H); ^{13}C NMR (75 MHz, $CDCl_3$) δ 172.0, 132.1, 118.5, 65.5, 29.2; IR (Neat film, NaCl) 3086, 2942, 1738, 1649, 1413, 1377, 1271, 1157, 990, 932 cm^{-1}; HRMS (EI) *m/z* calc'd for $C_{10}H_{14}O_4$ $[M]^+$: 198.0892, found 198.0888.

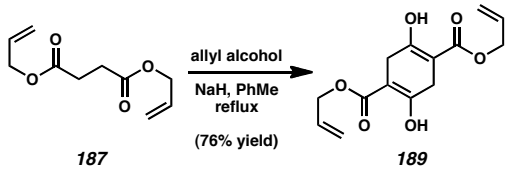

187 ***189***

Diallyl succinylsuccinate (189).[8] To a flame dried flask under argon was added NaH (60% in mineral oil, 25.0 g, 630.6 mmol, 2.50 equiv) and toluene (125 mL). To this was added, dropwise, neat allyl alcohol (4.14 mL, 70.6 mmol, 0.28 equiv) with vigorous stirring. After gas evolution had ceased, neat diallyl succinate (**187**, 50.0 g, 252.2 mmol, 1.00 equiv) was added dropwise, and the reaction was heated to 95 °C. The reaction flask was fitted with a reflux condenser, and reaction was allowed to proceed over 10 h. After ca. 15 min, an additional portion of toluene (125.0 mL) was added to the reaction to ensure fluidity of the mixture. Once the reaction had completed by TLC, the flask was cooled to room temperature, and the solvent was removed in vacuo. The crude solid was immediately suspended in CH_2Cl_2, and then acidified by addition of 2 N $HCl_{(aq)}$ (350 mL). The biphasic mixture was allowed to stir over 2 h, after which time all solids had dissolved. The phases were separated, and the aqueous layer was extracted with CH_2Cl_2 (2 x 50 mL). The combined organic layers were dried over $MgSO_4$, filtered, and solvent was removed in vacuo to yield a crude orange solid. The crude residue was recrystallized twice from a mixture of petroleum ether and acetone to afford diallyl succinylsuccinate (**189**) as a flaky white solid (26.9 g, 76% yield): R_f = 0.6 (15:85 ethyl acetate/hexane) ^{1}H NMR (300 MHz, $CDCl_3$) δ 12.11 (s, 2H), 5.95 (dddd, *J* = 17.1, 10.7, 5.7, 5.7 Hz, 2H), 5.35 (ddt, *J* = 17.3, 1.6, 1.3 Hz, 2H), 5.27 (ddt, *J* = 10.4, 1.3, 1.3 Hz, 2H), 4.69 (ddd, *J* = 5.3, 1.3, 1.3 Hz, 4H), 3.22 (s, 4H); ^{13}C NMR (75 MHz, $CDCl_3$) δ 170.8, 168.8, 131.7, 118.4, 93.1, 65.2, 28.5; IR (Neat film, NaCl) 1666, 1647, 1684, 1451, 1389, 1329, 1219,

1204, 1133, 1061, 961, 843, 783 cm^{-1}; HRMS (EI) *m/z* calc'd for $C_{14}H_{16}O_6$ $[M]^+$: 280.0947, found 280.0948.

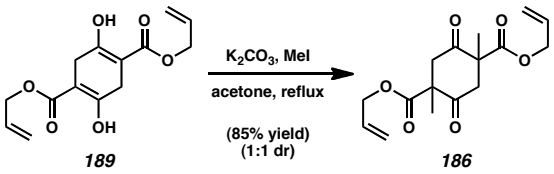

Bis(β-ketoester) 186. Prior to use in the reaction, acetone was dried by stirring it over anhydrous calcium sulfate, and then was passing the solvent over a short plug of silica. Potassium carbonate (5.80 g, 43.9 mmol, 4.10 equiv) and diallyl succinylsuccinate (**189**, 3.00 g, 10.7 mmol, 1.00 equiv) were suspended in acetone (21.3 mL). After addition of solvent to the solids, the reaction mixture was fitted with a reflux condenser and then was heated to 50 °C. To this mixture was added methyl iodide (3.40 mL, 54.5 mmol, 5.10 equiv). The reaction was stirred vigorously to ensure completion. (Note: If reaction is not stirred, or if stirring is not efficient, potassium carbonate will collect into a solid aggregate and the reaction will halt. Breaking up these solid collections with a spatula is typically enough to reinitiate reaction, though in some cases additional methyl iodide may be required.) After 6 h, the reaction was allowed to cool and then was passed through filter paper. The remaining solids were washed with additional CH_2Cl_2 to ensure complete solvation of any precipitated product trapped within the potassium carbonate. The collected organic layers were combined and concentrated to yield an amorphous semi-solid, which was purified over silica gel using 15% → 20% ethyl acetate in hexanes as eluent. Compound **186** was afforded as two diastereomers in a 1 : 1 ratio. The less polar diastereomer (by TLC analysis with 20% ethyl acetate in hexane) was obtained as a white, fluffy solid, and the more polar diastereomer was obtained as a thick, yellow oil

(1.4 g for each diastereomer, 2.8 g for combined diastereomers, 85% yield). **Diastereomer A**: R_f = 0.30 (20:80 ethyl acetate/hexane); ^{1}H NMR (300 MHz, $CDCl_3$) δ 5.84 (dddd, *J* = 17.3, 10.4, 5.8, 5.8 Hz, 2H), 5.30 (app dq, *J* = 17.3, 1.3 Hz, 2H), δ 5.26 (app dq, *J* = 10.4, 1.3 Hz, 2H), δ 4.60 (app ddd, *J* = 5.9, 1.3, 1.3 Hz, 4H), δ 3.14 (d, *J* = 15.2 Hz, 2H), δ 2.80 (d, *J* = 15.2 Hz, 2H), δ 1.43 (s, 6H); ^{13}C NMR (75 MHz, $CDCl_3$) δ 201.8, 170.6, 131.0, 119.7, 66.8, 57.6, 48.1, 20.8; IR (Neat film, NaCl) 2988, 2940, 1749, 1708, 1420, 1375, 1281, 1227, 1132, 1076, 911, 809, 744 cm^{-1}; HRMS (EI) *m/z* calc'd for $C_{16}H_{20}O_6$ [M^+]: 308.1260, found 308.1263. **Diastereomer B**: R_f = 0.20 (20:80 ethyl acetate/hexane); ^{1}H NMR (300 MHz, $CDCl_3$) δ 5.88 (dddd, *J* = 17.1, 10.4, 5.7, 5.7 Hz, 2H), δ 5.31 (app dq, *J* = 17.2, 1.5 Hz, 2H), δ 5.27 (app dq, *J* = 10.3, 1.5, 2H), δ 4.62 (app ddd, *J* = 5.4, 1.5, 1.5 Hz, 4H), δ 3.47 (d, *J* = 15.6 Hz, 2H), δ 2.63 (d, *J* = 15.9 Hz, 2H), δ 1.46 (s, 6H); ^{13}C NMR (75 MHz, $CDCl_3$) δ 202.5, 169.9, 131.1, 119.1, 66.7, 56.6, 47.1, 21.5; IR (Neat film, NaCl) 3088, 2984, 2940, 1747, 1722, 1649, 1454, 1422, 1381, 1275, 1233, 1196, 1110, 984, 934 cm^{-1}. HRMS (EI) *m/z* calc'd for $C_{16}H_{20}O_6$ [M^+]: 308.1260, found 308.1263.

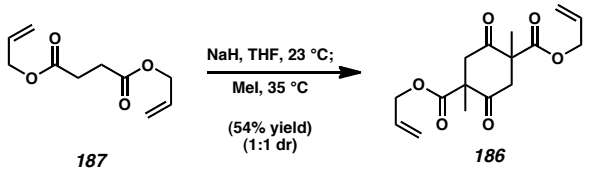

187 ***186***

Alternative preparation of bis(β-ketoester) 186.[10] A flame dried round bottom flask was charged with NaH (60% in mineral oil, 4.44 g, 111.0 mmol, 2.2 equiv). The flask was briefly vacuum purged, and then was backfilled with argon. The solid NaH was then suspended in freshly distilled (or freshly dispensed) THF (40 mL). The

resulting suspension was cooled to 0 °C in an ice water bath. After cooling, the NaH slurry was treated with a THF solution (20 mL) of diallyl succinate (**187**, 10.0 g, 50.4 mmol) added via cannula. The reaction was allowed to gradually warm to room temperature overnight (12 h). The next morning the reaction was heated to 40 °C to encourage completion of the Claisen condensation/Dieckmann cyclization process. After 24 h at this temperature, TLC analysis revealed total consumption of diallyl succinate (**187**). The reaction was cooled to 35 °C, and then a single portion of MeI (8.16 mL, 131.2 mmol, 2.6 equiv) was introduced via syringe. After an additional 12 h at 35 °C, the reaction was quenched with saturated $NH_4Cl_{(aq)}$ (40 mL). The organic layer was separated from the aqueous layer, and the aqueous layer was extracted with CH_2Cl_2 (3 x 40 mL). The combined organic layers were washed with brine (40 mL), dried over $MgSO_4$, and filtered. The crude material obtained upon removal of solvent in vacuo was further purified via column chromatography over silica using 15% → 20% ethyl acetate in hexanes as eluent. Compound **186** was afforded as two diastereomers in a 1 : 1 ratio, again as both a white solid and a clear oil (2.1 g for each diastereomer, 4.2 g for combined diastereomers, 54% yield). All spectroscopic data was identical to that reported above.

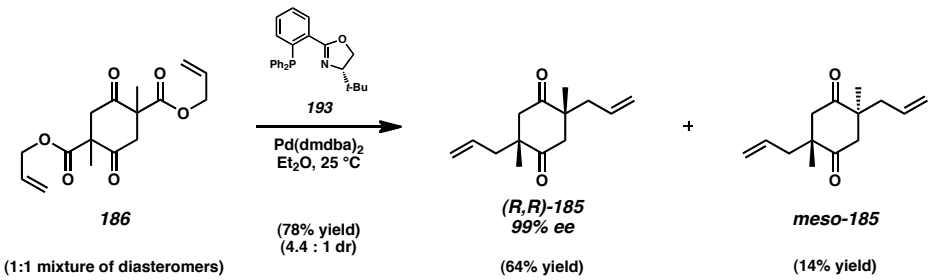

Diketone 185. A flame dried round bottom flask cooled under argon was charged with bis(3,5-dimethoxydibenzylideneacetone)palladium(0) ($Pd(dmdba)_2$, 0.268 g, 0.330 mmol, 0.05 equiv) and (*S*)-*t*-BuPHOX (**193**) (0.140 g, 0.362 mmol, 0.055 equiv). The flask was purged under vacuum briefly, and then backfilled with argon. The solids were dissolved in Et_2O (500 mL), and the resulting solution was stirred at 25 °C for 30 min. After precomplexation, neat **186** (2.00 g, 6.59 mmol, 1.00 equiv) was added to the reaction. The solution was stirred vigorously at 25 °C for 10 h (Note: continual stirring is necessary due to the apparent low solubility of $Pd(dmdba)_2$ in Et_2O.), after which time the solvent was removed in vacuo. The crude oil was purified over silica gel using 3% ethyl acetate in hexanes as eluent to afford **185** as a colorless oil (1.07 g, 78% yield, 4.4 : 1 dr, 99% *ee*): R_f = 0.7 (15:85 ethyl acetate/hexane); ^{1}H NMR (300 MHz, $CDCl_3$) δ 5.68 (dddd, *J* = 18.3, 10.2, 6.9, 6.9 Hz, 2H), 5.17–5.09 (comp. m, 3H), 5.07–5.04 (m, 1H), 2.82 (d, *J* = 14.7 Hz, 2H), 2.38 (d, *J* = 15 Hz, 2H), 2.34 (app ddt, *J* = 13.2, 6.9, 1.0 Hz, 2H), 2.09 (app ddt, *J* = 13.5, 7.8, 0.9 Hz, 2H), 1.10 (s, 6H); ^{13}C NMR (125 MHz, $CDCl_3$) δ 212.8, 132.4, 120.0, 49.4, 48.4, 43.8, 24.3; IR (Neat film, NaCl) 3078, 2978, 1712, 1640, 1458, 1378, 1252, 1129, 1101, 998, 921 cm^{-1}; HRMS (EI) *m/z* calc'd for $C_{14}H_{20}O_2$ $[M]^+$: 220.1463, found 220.1466; $[\alpha]^{25}_D$ –163.1 (*c* 0.52, CH_2Cl_2). Chiral GC assay (GTA column): 100 °C isothermal method over 90 min. Retention times: 67.7 min (Major enantiomer, C_2 diastereomer, 81.7%), 74.1 min (Minor enantiomer, C_2

diastereomer, 0.6%), 77.4 min (*meso* diastereomer, 17.6%). Achiral GC assay (DB-Wax column): 100 °C isotherm over 2.0 min, ramp 5 °C/min to 190 °C, then 190 °C isotherm for 10.0 min. Retention times: 18.5 min (C_2 diastereomer, 81.0%), 18.7 min (*meso* diastereomer, 19.0%).

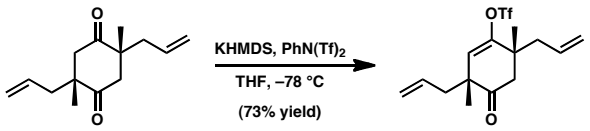

185 ***194***

Triflate 194. A flask was charged with potassium bis(trimethylsilyl)amide (1.49 g, 7.49 mmol, 1.10 equiv) in the glovebox, and then was transferred to a manifold line outside of the glovebox under argon. The solids were dissolved in THF (180 mL), and the resulting solution was stirred while being cooled to –78 °C. To this alkaline solution was added, dropwise, neat diketone **185** (1.50 g, 6.80 mmol, 1.00 equiv). The solution immediately turned yellow, and viscosity increased. Deprotonation was allowed over 30 min, after which time the anionic solution was transferred by cannula into a solution of *N*-phenyl bis(trifluoromethane)sulfonimide (2.91 g, 8.17 mmol, 1.20 equiv) in THF (60 mL) at –78 °C. Reaction was allowed to proceed at this temperature over 6 h, after which time the mixture was brought to room temperature. The anionic reaction was quenched with brine (100 mL). The phases were separated, and the aqueous layer was extracted with diethyl ether (3 x 100 mL) and ethyl acetate (1 x 100 mL). The combined organic layers were washed with brine (2 x 50 mL), dried over $MgSO_4$, filtered, and the solvent was removed in vacuo. The crude oil obtained was loaded onto a silica gel column and eluted with 2% Et_2O in pentane. This afforded triflate **194** as a colorless oil (1.75 g, 73%

yield). R_f = 0.40 (5:95 ethyl acetate/hexane); ^{1}H NMR (500 MHz, $CDCl_3$) δ 5.77–5.58 (comp. m, 2H), 5.63 (s, 1H), 5.22–5.03 (comp. m, 4H), 2.71 (d, *J* = 14.3 Hz, 1H), 2.40 (d, *J* = 14.4 Hz, 1H), 2.49–2.30 (comp. m, 2H), 2.24 (app ddt, *J* = 13.5, 6.9, 1.3 Hz, 1H), 2.09 (app ddt, *J* = 13.8, 8.24, 1.2 Hz, 1H), 1.22 (s, 3H), 1.19 (s, 3H); ^{13}C NMR (125 MHz, $CDCl_3$) δ 209.6, 152.0, 132.6, 132.1, 122.9, 120.6, 119.7, 49.2, 48.9, 43.8, 43.0, 42.1, 25.2, 24.6; IR (Neat film, NaCl) 3081, 2980, 2934, 1721, 1673, 1641, 1457, 1416, 1214, 1141, 1010, 923.6, 895.2, 836.2 cm^{-1}; HRMS *m/z* calc'd for $C_{15}H_{19}O_4SF_3$ [M^+]: 352.0956, found 352.0949; $[\alpha]^{25}_D$ –6.5 (*c* 1.15, CH_2Cl_2).

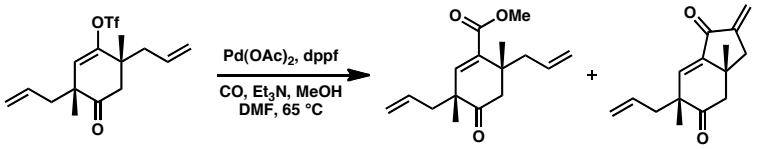

194 ***195*** (64% yield) ***196*** (1% yield)

Enoate 195. A flame dried round bottom flask was charged with $Pd(OAc)_2$ (0.089 g, 0.397 mmol, 0.07 equiv) and dppf (0.315 g, 0.568 mmol, 0.10 equiv). The solids were briefly vacuum purged, and then the flask was backfilled with nitrogen. To the palladium and ligand were added, in sequence, DMF (67 ml), MeOH (4.6 mL), triflate **194** (2.01 g, 5.68 mmol, 1.00 equiv), and triethyl amine (2.37 mL, 17.0 mmol, 3.00 equiv). The resulting solution was sparged for 10 min with an overpressure of carbon monoxide. After this time had elapsed, the reaction was fitted with a double-walled balloon of carbon monoxide to preserve gas overpressure, and then was heated to 65 °C for 10 h. Once the reaction had completed by TLC analysis, a majority of the DMF solvent was removed in vacuo. The crude residue obtained was dissolved in CH_2Cl_2 (50 mL) and was washed with brine (30 mL). The layers were separated, and the aqueous layer was

thereafter extracted with CH_2Cl_2 (4 x 30 mL). Combined organics were washed with brine (50 mL), then were dried over $MgSO_4$ and filtered. The crude product was purified via chromatography over silica gel, using 2% → 3% → 4% → 5% ethyl acetate in hexanes, followed by 100% diethyl ether, as eluent. This afforded enoate **195** (848 mg, 54% yield) and dienone **196** (17.0 mg, 1% yield), both as clear oils: Data for enoate **195** was observed as follows: R_f = 0.30 (5:95 ethyl acetate/hexane); ^{1}H NMR (500 MHz, $CDCl_3$) δ 6.57 (s, 1H), 5.70–5.58 (m, 2H), 5.09–4.99 (m, 4H), 3.75 (s, 3H), 2.69 (dd, *J* = 13.9, 6.3 Hz, 2H), 2.36 (app ddt, *J* = 13.6, 8.1, 0.9 Hz, 1H), 2.26 (app ddt, *J* = 13.7, 6.9, 1.2 Hz, 1H), 2.15 (dd, *J* = 13.9, 7.3 Hz, 2H), 1.23 (s, 3H), 1.16, (s, 3H); ^{13}C NMR (125 MHz, $CDCl_3$) δ 212.5, 167.1, 144.8, 136.4, 134.1, 132.9, 119.1, 119.0, 51.8, 50.1, 49.0, 44.2, 43.9, 41.9, 27.5, 23.3; IR (Neat film, NaCl) 3077, 29.54, 2871, 1717, 1639, 1436, 1326, 1244, 1063, 995, 920 cm^{-1}; HRMS *m/z* calc'd for $C_{16}H_{22}O_3$ [M+H]: 263.1642, found 263.1649; $[\alpha]^{25}_D$ –85.9 (*c* 0.62, CH_2Cl_2).

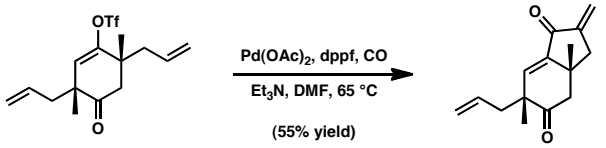

194 *196*

Dieneone 196. A flame dried round bottom flask was charged with $Pd(OAc)_2$ (10.0 mg, 45.0 μmol, 0.07 equiv) and dppf (31.0 mg, 56.0 μmol, 0.10 equiv). The solids were briefly vacuum purged, and then the flask was backfilled with nitrogen. To the palladium and ligand were added, in sequence, DMF (5.5 ml), triflate **194** (200 mg, 0.568 mmol, 1.0 equiv), and triethyl amine (237 μL, 1.70 mmol, 3.0 equiv). The resulting solution was sparged for 15 min with an overpressure of carbon monoxide. After this time had

elapsed, the reaction was fitted with a double-walled balloon of carbon monoxide to preserve gas overpressure, and then was heated to 65 °C for 3 h. Once the reaction had completed by TLC analysis, a majority of the DMF solvent was removed in vacuo. The crude residue obtained was dissolved in ethyl acetate (50 mL) and was washed with brine (30 mL). The layers were separated, and the aqueous layer was thereafter extracted with ethyl acetate (4 x 30 mL). The combined organics were washed with brine (30 mL), then were dried over $MgSO_4$ and filtered. The crude product was purified via chromatography over silica gel, using 2% → 3% ethyl acetate in hexanes, followed by 100% diethyl ether, as eluent. This afforded dieneone **196** as a clear oil (67 mg, 55% yield): R_f = 0.30 (5:95 ethyl acetate/hexane); ^{1}H NMR (500 MHz, $CDCl_3$) δ 6.66 (s, 1H), 6.19 (ddd, *J* = 3.4, 1.6, 0.9 Hz, 1H), 5.62 (dddd, *J* = 16.8, 10.1, 8.5, 6.6 Hz, 1H), 5.52–5.49 (m, 1H), 5.05 (dddd, *J* = 16.9, 4.5, 2.3, 1.2 Hz, 2H), 2.69 (app dt, *J* = 15.8, 1.6 Hz, 1H), 2.64 (d, *J* = 13.8 Hz, 1H), 2.57 (app dt, *J* = 15.9, 3.1 Hz, 1H), 2.46 (dd, *J* = 13.8, 0.6 Hz, 1H), 2.37 (app ddt, *J* = 13.5, 8.5, 1.0 Hz, 1H), 2.27 (app ddt, *J* = 13.5, 6.5, 1.5 Hz, 1H), 1.24 (s, 3H), 1.06 (s, 3H); ^{13}C NMR (125 MHz, $CDCl_3$) δ 212.2, 192.9, 144.9, 144.3, 137.9, 132.7, 120.3, 119.4, 52.4, 48.8, 45.6, 43.1, 39.7, 27.9, 23.2; IR (Neat film, NaCl) 2958, 2929, 1711, 1657, 1639, 1454, 1437, 1399, 1378, 1259, 1156, 1131, 929 cm^{-1}; HRMS *m/z* calc'd for $C_{15}H_{18}O_2$ [M^+]: 230.1307, found 230.1313; $[\alpha]^{25}_D$ –130.8 (*c* 0.50, CH_2Cl_2).

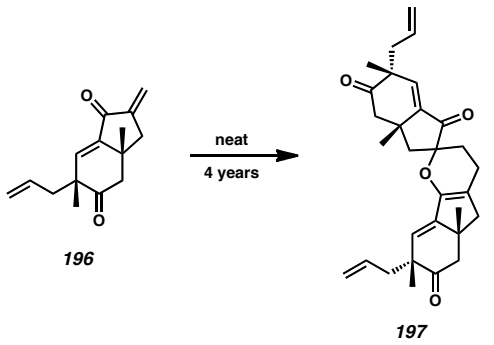

196 *197*

Spirocyclic dimer 197. Upon allowing dienone **196** to stand neat for ca. four years, repurification over silica using 2% ethyl acetate in hexanes as eluent afforded spirocyclic dimer **197** as a clear oil. ^{1}H NMR (500 MHz, $CDCl_3$) δ 6.87 (s, 1H), 5.76–5.59 (m, 2H), 5.39 (s, 1H), 5.12–4.96 (comp. m, 4H), 2.62 (d, *J* = 13.6 Hz, 2H), 2.56–2.05 (comp. m, 6H), 2.48 (d, *J* = 10.6 Hz, 2H), 2.31 (d, *J* = 13.6 Hz, 2H), 2.10 (d, *J* = 12.3 Hz, 2H), 2.00–1.90 (m, 2H), 1.33–1.04 (m, 2H), 1.26 (s, 3H), 1.19 (s, 6H), 1.06 (s, 3H); ^{13}C NMR (125 MHz, $CDCl_3$) δ 214.9, 211.9, 201.5, 147.2, 144.8, 142.4, 140.8, 133.9, 132.4, 119.7, 118.2, 117.6, 114.4, 81.5, 53.9, 52.0, 49.0, 48.2, 47.8, 46.5, 45.4, 45.2, 41.2, 37.5, 29.3, 29.0, 28.8, 24.8, 23.1, 20.2; IR (Neat film, NaCl) 2960, 2928, 1711, 1651, 1451, 1395, 1280, 1157, 1124, 917 cm^{-1}; HRMS (EI) *m/z* calc'd for $C_{30}H_{38}O_4$ [M+H]: 461.2686, found 461.2701; $[\alpha]^{25}_{D}$ –98.6 (*c* 0.39, CH_2Cl_2).

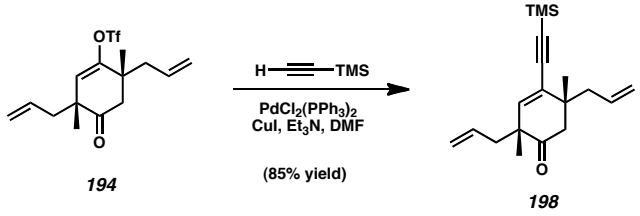

194 *198*

Enyne 198. To a flame dried flask was added $PdCl_2(PPh_3)_2$ (59 mg, 85.0 μmol, 0.1 equiv) and CuI (10 mg, 52.0 μmol, 0.05 equiv). These solids were briefly vacuum purged, and then the flask was backfilled with nitrogen. The metal salts were thereafter

dissolved in DMF (5.1 mL), and treated with triethyl amine (356 μL, 2.55 mmol, 3.00 equiv), triflate **194** (300 mg, 0.851 mmol, 1.00 equiv), and (trimethylsilyl)acetylene (241 μL, 1.70 mmol, 2.0 equiv). The resulting solution was stirred at room temperature for 4 h, after which time the reaction had completed. The reaction was quenched by the addition of brine (10 mL), followed by extraction with diethyl ether (4 x 20 mL). The combined organics were washed with brine (10 mL), then were dried over $MgSO_4$ and filtered. The crude material isolated was purified silica gel chromatography using 2% ethyl acetate in hexanes as eluent. Enyne **198** was isolated as a clear oil (218 mg, 85% yield): R_f = 0.50 (5:95 ethyl acetate/hexane); ^{1}H NMR (500 MHz, $CDCl_3$) δ 5.94 (s, 1H), 5.80 (dddd, *J* = 16.6, 10.1, 8.4, 6.3 Hz, 1H), 5.66 (dddd, *J* = 17.0, 10.2, 8.1, 6.9 Hz, 1H), 5.14–5.01 (comp. m, 4H), 2.60 (d, *J* = 13.9 Hz, 1H), 2.43 (app ddt, *J* = 13.7, 6.3, 1.3 Hz, 1H), 2.31 (app ddt, *J* = 13.7, 8.1, 1.0 Hz, 1H), 2.20 (app ddt, *J* = 13.6, 6.9, 1.3 Hz, 1H), 2.19 (d, *J* = 13.9 Hz, 1H), 2.03 (app ddt, *J* = 13.7, 8.4, 1.0 Hz, 1H), 1.12 (s, 3H), 1.10 (s, 3H), 0.21 (s, 9H); ^{13}C NMR (125 MHz, $CDCl_3$) δ 212.7, 141.2, 134.3, 133.3, 128.5, 118.9, 118.8, 103.2, 95.8, 49.3, 48.5, 45.3, 44.5, 42.5, 27.5, 23.6, 0.1; IR (Neat film, NaCl) 3077, 2962, 2144, 1717, 1638, 1457, 1375, 1250, 1147, 996, 843 cm^{-1}; HRMS *m/z* calc'd for $C_{19}H_{28}OSi$ [M+H]: 301.1982, found 301.1980; $[\alpha]^{25}_D$ –88.3 (*c* 0.33, CH_2Cl_2).

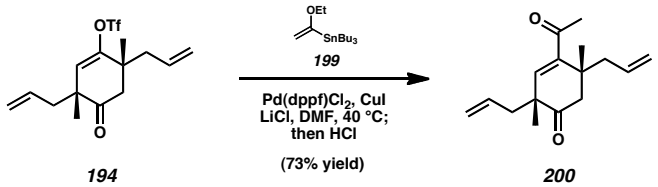

Enone 200. To a flame dried round bottom flask under argon was added Pd(dppf)Cl_2 (116 mg, 0.142 mmol, 0.10 equiv), CuI (27 mg, 0.142 mmol, 0.10 equiv), and LiCl (319

mg, 7.52 mmol, 5.3 equiv). These solids were briefly vacuum purged before being backfilled with argon, and then were dissolved in DMF (20 mL). The resulting solution was then treated with triflate **194** (500 mg, 1.42 mmol, 1.0 equiv) and tributylethoxyvinyl stannane (**199**, 623 μL, 1.84 mmol, 1.3 equiv). Subsequent to the addition of all reagents, the reaction was freeze-pump-thawed, and then was heated to 40 °C. After 9 h at 40 °C, the reaction was cooled to room temperature and diluted with brine (40 mL). The resulting solution was extracted with diethyl ether (3 x 40 mL), and the combined organic layers were washed with additional brine (2 x 30 mL). The combined aqueous layers were thereafter back-extracted with CH_2Cl_2 (2 x 20 mL). The combined organic layers from all extractions were dried over $MgSO_4$, filtered, and solvent was removed in vacuo. The crude material obtained after removal of solvent was then redissolved in CH_2Cl_2 (40 mL) and stirred with 2 N $HCl_{(aq)}$ (20 mL) for 2 h. The phases were separated, and the aqueous layer was extracted with CH_2Cl_2 (2 x 15 mL). The combined organic layers were dried over $MgSO_4$, filtered, and concentrated in vacuo. The crude material obtained was purified via silica gel chromatography using 2% → 3% ethyl acetate in hexanes as eluent. This afforded enone **200** as a clear oil (255 mg, 73%): R_f = 0.50 (5:95 ethyl acetate/hexane); ^{1}H NMR (500 MHz, $CDCl_3$) δ 6.40 (s, 1H), 5.68 (dddd, *J* = 16.9, 10.1, 8.2, 6.9 Hz, 1H), 5.57 (app dt, *J* = 17.5, 10.2, 7.5 Hz, 1H), 5.13–4.96 (m, 4H), 2.75 (app ddt, *J* = 13.5, 7.0, 1.0 Hz, 1H), 2.69 (d, *J* = 13.8 Hz, 1H), 2.39 (app ddt, *J* = 13.6, 8.2, 0.8 Hz, 1H), 2.32 (s, 3H), 2.29 (app ddt, *J* = 13.5, 6.8, 1.3 Hz, 1H), 2.12 (d, *J* = 13.9 Hz, 1H), 2.03 (app ddt, *J* = 13.8, 7.6, 1.2 Hz, 1H), 1.22 (s, 3H), 1.19 (s, 3H); ^{13}C NMR (125 MHz, $CDCl_3$) δ 212.4, 199.8, 145.1, 145.0, 134.3, 132.8, 119.3, 118.9, 50.5, 49.1, 44.5, 43.4, 42.7, 28.1, 27.7, 23.2; IR (Neat film, NaCl) 3077, 2977, 2930, 2869, 1717, 1676, 1637,

1540, 1457, 1365, 1235, 995, 919 cm^{-1}; HRMS *m/z* calc'd for $C_{16}H_{22}O_2$ [M+H]: 247.1693, found 247.1699; $[\alpha]^{25}_D$ –60.4 (*c* 0.33, CH_2Cl_2).

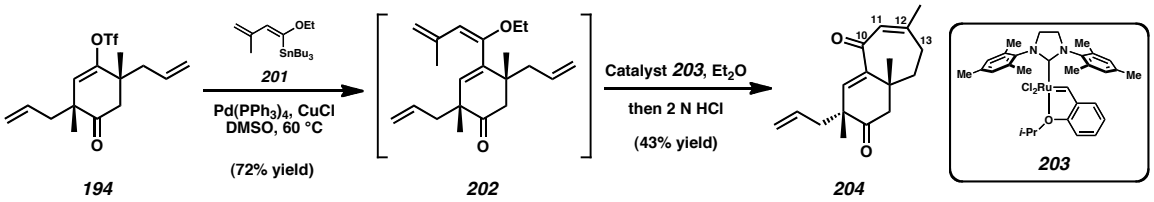

Enol ether 204. To a round bottom flask was added LiCl (64 mg, 1.50 mmol, 6.0 equiv). This flask was flame dried, backfilled with argon, and then was transferred to the glovebox. Once inside the glovebox, $Pd(PPh_3)_4$ (29 mg, 25.0 μmol, 0.1 equiv) and CuCl (124 mg, 1.25 mmol, 5.0 equiv) were added to the flask. The flask was removed from the glovebox and was transferred to a manifold line. The solids were briefly purged under vacuum, then were backfilled with argon. Afterwards, the solids were dissolved in DMSO (2.0 mL), resulting in an immediate black solution. The flask was wrapped with aluminium foil to shield from light, and then triflate **194** (88 mg, 0.250 mmol, 1.0 equiv) and enol stannane **201** (120 mg, 0.300 mmol, 1.2 equiv) were added. The solution was freeze-pump-thawed thrice, and then was heated to 60 °C. After 24 h, the reaction was cooled to room temperature and diluted with brine (4 mL). To this mixture was added ethyl acetate (5 mL), and the phases were separated. The ethyl acetate layer was separated, then was washed with brine (5 mL) and saturated $NH_4Cl_{(aq)}$ (2 x 20 mL). Combined aqueous layers were extracted with ethyl acetate (3 x 30 mL), and the resulting combined organic layers were washed with brine (40 mL). After washing, the organic layer was dried over Na_2SO_4, filtered, and concentrated in vacuo. The crude material obtained was purified via chromatography over silica gel, using 1% → 2% → 5% diethyl

ether in pentane. This afforded crude enol ether **202** as a clear oil. This material was carried directly into the next reaction without further purification or characterization, due to tautomeric instability.

To a flame dried flask under argon was added crude **202** from the previous reaction sequence. This oil was dissolved in acetonitrile and azeotroped three times, and then was dried briefly under vacuum to remove residual solvent. The residue obtained was dissolved in diethyl ether (24 mL, **Note:** Diethyl ether was mistakenly added in this reaction, as CH_2Cl_2 was the intended solvent), and then was treated with the Grubbs–Hoveyda second-generation catalyst (**203**, 18 mg, 21.0 μmol, 0.05 equiv). The reaction was heated to 30 °C for 30 min, and then was cooled to room temperature and quenched with saturated $NaHCO_{3(aq)}$. The phases were separated, and the aqueous layer was extracted with diethyl ether (3 x 30 mL). The combined organic layers were washed with brine (30 mL), then were dried over $MgSO_4$ and filtered. In order to prevent purification difficulties resulting from partial decomposition of the enol ether moiety on silica, the enol ether was pre-emptively cleaved to reveal the ketone. The crude product oil was redissolved in diethyl ether (25 mL) and was stirred with 2 N $HCl_{(aq)}$ (25 mL) for 30 min. The phases were separated, and the aqueous layer was extracted with diethyl ether (3 x 30 mL). The combined organic layers were washed with brine (30 mL), then were dried over $MgSO_4$ and filtered. After concentrating in vacuo, the crude residue obtained was purified via chromatography over silica gel using 50% benzene in hexanes as eluent. This afforded bicyclic enone **204** as a clear oil, and as a mixture of diastereomers (19.7 mg, 30% yield). **Diastereomer A**: R_f = 0.30 (5:95 ethyl acetate/hexane); ^{1}H NMR (500 MHz, $CDCl_3$) δ 6.31 (s, 1H), 6.06 (dd, *J* = 2.3, 1.2 Hz, 1H), 5.66 (dddd, *J* = 17.0, 10.2,

8.2, 6.8 Hz, 1H), 5.08–5.00 (comp. m, 2H), 2.57 (dd, *J* = 13.7, 0.6 Hz, 1H), 2.49 (dddd, *J* = 7.1, 3.3, 1.3, 0.8 Hz, 1H), 2.45 (dddd, *J* = 7.0, 3.2, 1.2, 0.8 Hz, 1H), 2.39 (app ddt, *J* = 13.6, 8.2, 0.9 Hz, 1H), 2.25 (d, 13.7 Hz, 1H), 2.24 (app ddt, *J* = 13.5, 6.8, 1.2 Hz, 1H), 1.97 (app t, *J* = 0.5 Hz, 3H), 1.89 (ddd, *J* = 14.4, 9.5, 3.4 Hz, 1H), 1.69 (ddd, *J* = 14.4, 7.1, 3.7 Hz, 1H), 1.21 (s, 3H), 1.12 (app d, *J* = 0.6 Hz. 3H); ^{13}C NMR (125 MHz, $CDCl_3$) δ 212.9, 193.1, 157.9, 146.5, 140.3, 133.2, 129.9, 119.0, 52.9, 49.1, 44.9, 39.2, 38.6, 32.8, 27.2, 26.4, 23.4; IR (Neat film, NaCl) 2964, 2929, 1716, 1648, 1593, 1456, 1436, 1418, 1375, 1266 cm^{-1}. HRMS *m/z* calc'd for $C_{17}H_{22}O_2$ [M+H]: 259.1693, found 259.1694; $[\alpha]^{25}_D$ –112.6 (*c* 0.28, CH_2Cl_2). **Diastereomer B**: R_f = 0.25 (5:95 ethyl acetate/hexane); ^{1}H NMR (500 MHz, $CDCl_3$) δ 6.35 (s, 3H), 6.06 (dd, *J* = 2.4, 1.2, Hz, 1H), 5.66 (dddd, *J* = 17.2, 10.1, 7.8, 7.2 Hz, 1H), 5.08–5.02 (comp. m, 2H), 2.67 (dd, *J* = 13.5, 0.6 Hz, 1H), 2.54 (app ddt, 13.6, 7.9, 1.0 Hz, 1H), 2.47–2.34 (comp. m, 2H), 2.26 (app ddt, *J* = 13.6, 7.1, 1.2 Hz, 1H), 2.20 (d, *J* = 13.5 Hz, 1H), 1.96 (d, *J* = 1.1 Hz, 2H), 1.91 (ddd, *J* = 14.3, 9.5, 3.9 Hz, 1H), 1.68 (ddd, *J* = 14.4, 6.5, 4.1 Hz, 1H), 1.21 (s, 3H), 1.11 (s, 3H); ^{13}C NMR (125 MHz, $CDCl_3$) δ 212.6, 192.8, 157.2, 146.2, 140.3, 133.5, 129.9, 119.0, 51.9, 49.2, 41.9, 39.4, 38.5, 33.1, 27.1, 25.9, 25.5; IR (Neat film, NaCl) 2927, 1715, 1647, 1591, 1451, 1378, 1270, 1034, 919 cm^{-1}; HRMS *m/z* calc'd for $C_{17}H_{22}O_2$ [M+H]: 259.1693, found 259.1700; $[\alpha]^{25}_D$ –35.6 (*c* 0.28, CH_2Cl_2).

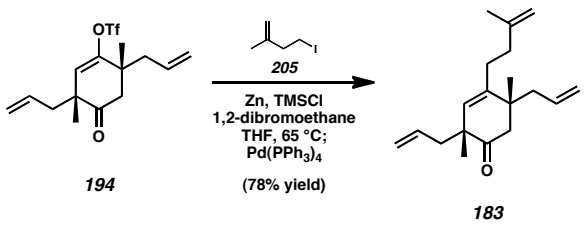

Tetraene 183. To a flame dried Schlenk flask backfilled with argon was added powdered Zn metal (3.20 g, 48.9 mmol, 7.5 equiv). After a brief vacuum purge and argon backfill, the metal was suspended in THF (45 mL). To this suspension was cannula transferred a prepared solution of 1,2-dibromoethane (0.675 mL, 7.83 mmol, 1.2 equiv) and trimethylsilyl chloride (0.271 mL, 2.13 mmol, 0.33 equiv) in THF (22.5 mL). The reaction vessel was sealed, then heated to 65 °C for 15 min. After this time had elapsed, the reaction was cooled to room temperature, and a solution of 4-iodo-2-methyl-1-butene (**205**, 1.92 g, 9.79 mmol, 1.5 equiv) in THF (22.5 mL) was cannula transferred into the suspension of activated Zn metal. The reaction vessel was sealed once again, and then was heated to 65 °C for 2 h. After this time had elapsed, the reaction was cooled to room temperature, and a prepared solution of triflate **194** (2.3 g, 6.53 mmol, 1.0 equiv) and $Pd(PPh_3)_4$ (0.377g, 0.33 mmol, 0.05 equiv) in THF (45 mL) was added to the alkyl zinc solution via cannula. The reaction was sealed and heated to 65 °C for 3 h. After reaction had completed by TLC, it was cooled to room temperature and filtered over a Celite pad with copious washing with Et_2O. The filtrate then was diluted with brine and extracted with Et_2O (4 x 100 mL). The combined organic layers were washed with brine (40 mL), followed by saturated $Na_2S_2O_{3(aq)}$ (40 mL) to removed colored impurities. The washed organic layers were dried over $MgSO_4$, filtered, and then solvent was removed in vacuo. The crude material obtained was then purified over silica gel using 0.5% → 1.0% → 1.5% → 3.0% Et_2O in petroleum ether as eluent. This afforded tetraene **183** as a

colorless oil (1.40 g, 78%): R_f = 0.50 (5:95 ethyl acetate/hexane); ^{1}H NMR (500 MHz, $CDCl_3$) δ 5.77–5.61 (comp. m, 2H), 5.20 (s, 1H), 5.10–4.97 (comp. m, 4H), 4.74 (d, *J* = 8.8 Hz, 2H), 2.56 (d, *J* = 13.5 Hz, 1H), 2.40–2.13 (comp. m, 8H), 2.05–1.98 (m, 1H), 1.77 (s, 3H), 1.09 (s, 3H), 1.04 (s, 3H); ^{13}C NMR (125 MHz, $CDCl_3$) d 214.4, 145.5, 142.5, 134.1, 134.0, 128.6, 118.6, 117.9, 110.1, 49.5, 48.7, 44.4, 44.3, 43.2, 36.5, 28.6, 26.5, 24.7, 22.7; IR (Neat film, NaCl) 3076, 2996, 2928, 2360, 1715, 1639, 1455, 1376, 1320, 1298, 1261, 1229, 1138, 1093, 996, 916, 887 cm^{-1}; HRMS (EI) *m/z* calc'd for $C_{19}H_{28}O$ [M^+]: 272.2140, found 272.2138; $[\alpha]^{25}_D$ –72.4 (*c* 0.22, CH_2Cl_2).

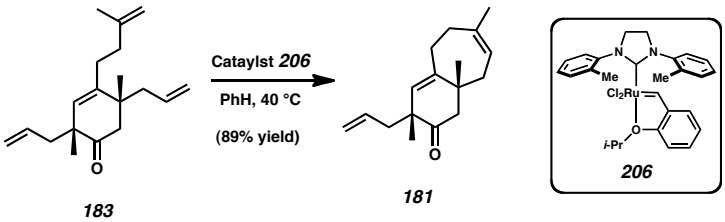

Bicyclic triolefin 181. To a flame dried flask was added tetraolefin **183** (160 mg, 588 mmol, 1.00 equiv). This oil was dissolved in benzene (5 mL), and then azeotroped from this solvent. This process was repeated three times, and then the resulting residue was dissolved in benzene (28 mL) and sparged with argon for 30 min. After the sparge time had elapsed, a single portion of Grubbs–Hoveyda catalyst **206** (34.0 mg, 59.0 μmol, 0.10 equiv) was added to the solution. The reaction was then heated to 40 °C. (Note: tetraolefin **183** and bicyclic triolefin **181** are difficult to separate by TLC in a wide variety of solvent systems, and frequently are seen to co-spot. In order to afford more efficient separation via TLC, the use of silver nitrate treated silica gel TLC plates is very effective.) After 20 min at 40 °C, the reaction had completed by TLC, and so was quenched via the addition of ethyl vinyl ether (20 mL). The solvents were removed in

vacuo, and the resulting crude mixture was purified via chromatography over silica gel using 0.5% → 1.0% → 1.5% → 3.0% Et_2O in petroleum ether as eluent. This afforded bicyclic triene **121** as a colorless oil (128 mg, 89% yield): R_f = 0.50 (5:95 ethyl acetate/hexane); ^{1}H NMR (500 MHz, $CDCl_3$) δ 5.64 (dddd, *J* = 16.8, 10.2, 8.4, 6.5 Hz, 1H), 5.33 (dddd, *J* = 6.9, 5.4, 2.9, 1.5 Hz, 1H), 5.19 (s, 1H), 5.01–4.93 (comp. m, 2H), 2.73 (dd, *J* = 13.4, 0.6 Hz, 1H), 2.53 (dddd, *J* = 13.2, 11.7, 5.3, 0.6 Hz, 1H), 2.45–2.39 (m, 2H), 2.22–2.17 (m, 1H), 2.22 (app ddt, *J* = 13.5, 8.4, 0.9 Hz, 1H), 2.11–2.03 (m, 2H), 2.11 (app ddt, *J* = 13.5, 6.5, 1.4 Hz, 1H), 2.03 (d, *J* = 13.5 Hz, 1H), 1.65 (s, 3H), 1.10 (s, 3H), 0.95 (s, 3H); ^{13}C NMR (125 MHz, $CDCl_3$) δ 216.6, 145.3, 138.5, 134.0, 129.2, 120.2, 117.8, 51.7, 49.0, 46.3, 44.9, 37.4, 29.5, 28.1, 25.8, 23.7; IR (Neat film, NaCl) 3076, 2961, 2927, 1711, 1639, 1452, 1372, 1225, 1163, 997, 916 cm^{-1}; HRMS (EI) *m/z* calc'd for $C_{17}H_{24}O$ [M^+]: 244.1827, found 244.1821; $[\alpha]^{25}_D$ –96.7 (*c* 1.33, CH_2Cl_2).

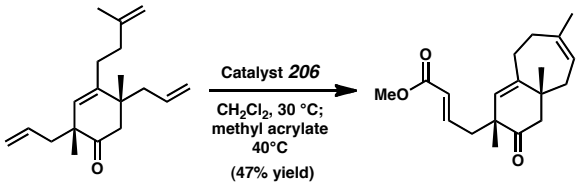

183 *209*

Enoate 209. To a flame dried flask under argon was added tetraolefin **183** (49.0 mg, 0.180 mmol, 1.00 equiv). This material was dissolved in benzene and azeotroped thrice, then briefly dried under high vacuum to remove residual solvent. The flask was then charged with Grubbs–Hoveyda catalyst **206** (7.0 mg, 9.0 μmol, 0.05 equiv) and CH_2Cl_2 (12 mL) and was heated to 30 °C. The reaction was allowed to stir at this temperature for 20 min, after which time TLC analysis showed complete conversion of the starting material to the ring-closed product. After 20 min had elapsed the reaction was treated

with methyl acrylate (243 μL, 2.70 mmol, 15 equiv) in a single portion, and the heat was increased to 40 °C. After 4 h, the reaction was quenched via the addition of water (20 mL). The phases were separated, and the aqueous layer was extracted with CH_2Cl_2 (3 x 30 mL). The combined organic layers were washed with brine (40 mL), dried over $MgSO_4$, filtered, and concentrated in vacuo. The crude material obtained was purified via chromatography over silica gel using 3% → 5% ethyl acetate in hexanes as eluent. This afforded enoate **209** as a colorless oil (25.0 mg, 47% yield): R_f = 0.10 (5:95 ethyl acetate/hexane); ^{1}H NMR (500 MHz, $CDCl_3$) δ 6.77 (ddd, *J* = 15.7, 8.7, 7.1 Hz, 1H), 5.75 (app dt, *J* = 15.7, 1.3 Hz, 1H), 5.33 (dddd, *J* = 7.1, 5.6, 3.0, 1.5 Hz, 1H), 3.70 (s, 3H), 2.65 (dd, *J* = 13.6, 0.7 Hz, 1H), (2.58–2.51 (m, 1H), 2.47–2.41 (comp. m, 2H), 2.39 (dd, *J* = 8.7, 1.2 Hz, 1H), 2.37 (dd, *J* = 8.7, 1.2 Hz, 1H), 2.22 (ddd, *J* = 13.6, 7.1, 1.6 Hz, 2H), 2.12–2.02 (m, 2H), 1.68–1.62 (m, 2H), 1.66 (s, 3H), 1.15 (s, 3H), 0.96 (s, 3H); ^{13}C NMR (125 MHz, $CDCl_3$) δ 214.9, 166.5, 146.6, 144.3, 138.6, 128.2, 123.9, 119.9, 51.4, 49.6, 48.8, 44.8, 44.3, 37.5, 37.4, 29.5, 28.0, 25.8, 24.2; IR (Neat film, NaCl) 2954, 2879, 1725, 1657, 1436, 1374, 1332, 1271, 1200, 1151, 1039, 987, 851, 825 cm^{-1}; HRMS (EI) *m/z* calc'd for $C_{19}H_{26}O_3$ [M^+]: 302.1882, found 302.1881; $[\alpha]^{25}_D$ –106.4 (*c* 1.09, CH_2Cl_2).

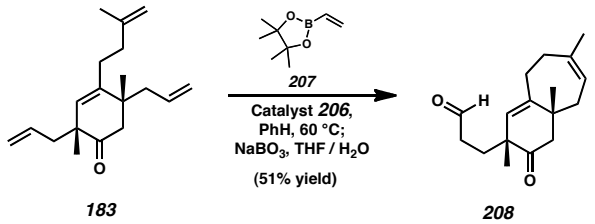

Bicyclic aldehyde 208. The following reaction was preformed in a glovebox under an atmosphere of nitrogen. To a flame dried flask was added tetraene **183** (100 mg, 0.37 mmol, 1.00 equiv) and PhH (10 mL). The solution was treated with Grubbs–Hoveyda

catalyst **206** (23.0 mg, 37.0 μmol, 0.10 equiv) and was heated to 40 °C for 30 min. After this time had elapsed vinyl boronate ester **207**[27] (283 mg, 1.84 mmol, 5.0 equiv) was added via syringe and the temperature was maintained at 40 °C for 20 h. The reaction was then cooled to –20 °C briefly and treated with ethyl vinyl ether (ca. 200 μL) to quench the remaining catalyst. At this stage, the reaction was removed from the glovebox. Solvent was removed in vacuo, and the crude mixture was passed over a short plug of silica gel using 20% ethyl acetate in hexanes as eluent to remove all remaining catalyst and various ruthenium byproducts. The oil obtained was then redissolved in THF (10 mL) and treated with water (10 mL). A single portion of $NaBO_3 \bullet H_2O$ (220 mg, 2.20 mmol, 6.00 equiv) was added, and the reaction was allowed to stir for 1 h. After complete consumption of the boronate was observed via TLC, the phases were separated, and the aqueous phase was extracted with ethyl acetate (4 x 20 mL). The combined organics were washed with brine, dried over $MgSO_4$, filtered, and concentrated in vacuo. The crude material was purified over silica gel using 5.0% → 7.5% ethyl acetate in hexanes as eluent to afford bicyclic aldehyde **208** as a colorless oil (48.0 mg, 51% yield): R_f = 0.20 (10:90 ethyl acetate/hexane); ^{1}H NMR (500 MHz, $CDCl_3$) δ 9.71 (app t, *J* = 1.3 Hz, 1H), 5.38–5.31 (m, 1H), 5.15 (s, 1H), 2.70 (d, *J* = 13.6 Hz, 1H), 2.59–2.32 (comp. m, 5H), 2.12 (d, *J* = 13.8 Hz, 1H), 2.24–2.04 (comp. m, 2 H), 1.89–1.64 (comp. m, 3 H), 1.67 (s, 3H), 1.12 (s, 3H), 0.97 (s, 3H); ^{13}C NMR (125 MHz, $CDCl_3$) δ 215.5, 201.6, 146.4, 138.7, 129.0, 120.1, 51.6, 47.7, 39.9, 37.6, 37.2, 33.1, 29.6, 27.8, 25.9, 23.9; IR (Neat film, NaCl) 2960, 2927, 2360, 2341, 1711–1710 (overlapping peaks), 1452, 1374, 1296, 1163 cm^{-1}; HRMS (EI) *m/z* calc'd for $C_{17}H_{24}O_2$ [M^+]: 260.1776, found 260.1784; $[\alpha]^{25}_D$ –83.5 (*c* 1.09, CH_2Cl_2).

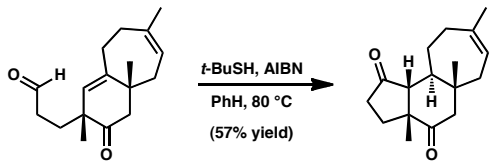

208 *214*

Tricyclic diketone 214. To a flame dried Schlenk flask was added bicyclic aldehyde **208** (600 mg, 2.32 mmol, 1.0 equiv). Dry PhH (5 mL) was added, then evaporated under vacuum. This azeotropic drying procedure was repeated two additional times, and the resulting material was then dried under high vacuum and backfilled with argon. To this was added *t*-butyl thiol (0.78 mL, 6.91 mmol, 3.0 equiv), AIBN (568 mg, 3.46 mmol, 1.5 equiv), and PhH (20 mL). The reaction was freeze-pump-thawed thrice, and afterward was backfilled with argon. The reaction vessel was sealed and the reaction was heated to 80 °C and allowed to react over 22 h. After this time, the reaction was cooled to room temperature and solvent was removed in vacuo. The crude material was purified over silica gel using a gradient of 5.0% → 7.5% → 10.0% ethyl acetate in hexanes as eluent to afford tricyclic diketone **214** as an amorphous solid (342 mg, 57% yield). An analytically pure sample was prepared via reverse-phase HPLC purification using 30% acetonitrile in water. X-ray diffraction samples were grown via diffusion crystallization of the amorphous solid from acetonitrile and water. R_f = 0.40 (10:90 ethyl acetate/hexane); ^{1}H NMR (500 MHz, $CDCl_3$) δ 5.33 (ddq, *J* = 5.13, 5.13, 1.71 Hz, 1 H), 2.65 (d, *J* = 14.5 Hz, 1H), 2.55–2.49 (m, 1H), 2.41–2.28 (m, 2H), 2.27–2.21 (m, 1H), 2.20–2.12 (m, 1H), 2.02 (d, *J* = 14.5 Hz, 1H), 2.01–1.93 (m, 2H), 1.89 (dd, *J* = 12.2, 1.2 Hz, 1H), 1.83–1.72 (m, 3H), 1.74 (s, 3H), 1.09 (s, 3H), 0.70 (s, 3H); ^{13}C NMR (125 MHz, $CDCl_3$) δ 218.0, 212.8, 142.6, 121.0, 63.2, 52.6, 51.0, 47.8, 42.3, 40.1, 34.4, 32.4, 31.4, 25.4, 24.1, 21.7, 17.3; IR (Neat film, NaCl) 2961, 2926, 2868, 1735, 1705, 1576, 1453, 1380, 1149 cm^{-1};

HRMS (EI) *m/z* calc'd for $C_{17}H_{24}O_2$ [M^+]: 260.1777, found 260.1776; $[\alpha]^{25}_D$ –158.6 (*c* 0.925, CH_2Cl_2); mp 94–96 °C.

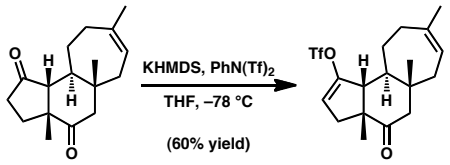

214 ***217***

Tricyclic triflate 217. To a flame dried flask under argon was added tricyclic diketone **214** (250 mg, 0.960 mmol, 1.0 equiv). Dry PhH (5 mL) was added, then evaporated under vacuum. This azeotropic drying procedure was repeated two additional times, and the resulting material was then dried under high vacuum briefly, then dissolved in THF (10 mL). A separate flame dried flask under argon was charged with potassium bis(trimethylsilyl)amide (211 mg, 1.06 mmol, 1.1 equiv) and THF (10 mL). The flask containing diketone **214** was cooled to –78 °C, and the basic solution was cannula transferred into the cooled solution containing the substrate diketone via a positive pressure of argon. Deprotonation was allowed over 30 min. After this time had elapsed, a solution of *N*-phenyl bis(trifluoromethane)sulfonimide (395 mg, 1.10 mmol, 1.15 equiv) in THF (10 mL) was cannula transferred to the anionic solution under a positive pressure of argon. After 3 h, the reaction was quenched via addition of a solution of saturated $NaHCO_{3\,(aq)}$. The phases were separated, and the aqueous layer was extracted with Et_2O (3 x 30 mL). The combined organic layers were washed, sequentially, with 2 N $NaOH_{(aq)}$ (30 mL), 2 N $HCl_{(aq)}$ (30 mL), and brine (2 x 30 mL). The organic layers were then dried over $MgSO_4$, filtered, and the solvent was removed in vacuo. The crude material was purified over silica gel using 0.5% → 1.0% ethyl acetate

in hexanes as eluent to afford triflate **217** as a white solid (226 mg, 60% yield): R_f = 0.45 (10:90 ethyl acetate/hexane); ^{1}H NMR (500 MHz, C_6D_6) δ 5.16 (ddq, *J* = 5.1, 1.7, 1.7 Hz, 1H), 5.08 (dd, *J* = 3.0, 2.0 Hz, 1H), 2.07 (dd, *J* = 10.7, 2.2 Hz, 1H), 2.02 (br. t, *J* = 13.3 Hz, 1 H), 1.94–1.86 (m, 3H), 1.90 (s, 1H), 1.85 – 1.79 (m, 1H), 1.74 (app ddt, *J* = 14.8, 6.8, 1.5 Hz, 1H), 1.59 (s, 3H), 1.57 (d, *J* = 3.4 Hz, 1H), 1.54 (d, *J* = 3.4 Hz, 1H), 1.38–1.31 (m, 1H), 1.35 (dd, *J* = 14.4, 8.5 Hz, 1H), 1.23 (s, 3H), 0.44 (s, 3H); ^{13}C NMR (125 MHz, C_6D_6) δ 209.8, 153.2, 141.9, 121.4, 116.0, 57.6, 54.1, 54.0, 51.2, 41.6, 38.1, 36.5, 32.5, 26.2, 25.0, 23.6, 16.8; IR (Neat film, NaCl) 2932, 1709, 1656, 1423, 1382, 1245, 1211, 1141, 1097, 927 cm^{-1}; HRMS (EI) *m/z* calc'd for $C_{17}H_{23}F_3O_4S$ [M^+]: 392.1269, found 392.1273; $[\alpha]^{25}_D$ –101.9 (*c* 0.63, CH_2Cl_2).

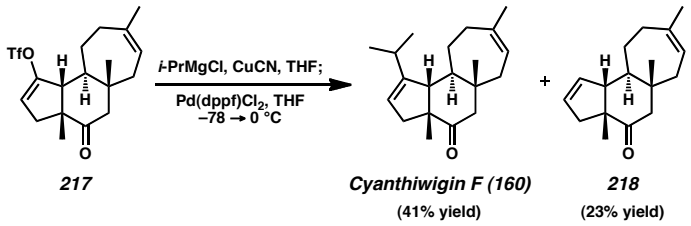

217 ***Cyanthiwigin F (160)*** (41% yield) ***218*** (23% yield)

Cyanthiwigin F (160). To a flame dried 1 dram vial under argon was added CuCN (3.8 mg, 40.0 μmol, 1.5 equiv), followed by 0.5 mL of THF. This suspension was cooled to –78 °C, and to this was dropwise added *i*-PrMgCl (40 μL, 1.91 M solution in THF, 80.0 μmol, 3.00 equiv). After complete addition, the reaction was warmed to 0 °C and allowed to remain at this temperature until a homogeneous pale pink solution was obtained (~10 min). A separate solution was then prepared, consisting of Pd(dppf)Cl_2 (3.0 mg, 5.0 μmol, 0.15 equiv) and triflate species **217** (10.0 mg, 25.0 μmol, 1.00 equiv) dissolved in 0.5 mL of THF. The solution containing **217** was treated with the organocuprate solution via dropwise cannula addition at 0 °C. This was allowed to react

at 0 °C for 3 h, after which time the reaction was quenched with a 1 : 1 mixture of saturated $NH_4Cl_{(aq)}$ and $NH_4OH_{(aq)}$ (1 mL). The phases were separated, and the aqueous layer was extracted with Et_2O (3 x 5 mL). The combined organic layers were washed with brine, dried over Na_2SO_4, filtered, and concentrated in vacuo. The crude material was purified over silica gel using 1% Et_2O in petroleum ether as eluent to afford colorless crystals (4.4 mg, 63% yield, 1.8 : 1 mixture of **160** : **218**). An analytically pure sample of **160** was prepared via reverse-phase HPLC purification using a gradient of 15% → 30% acetonitrile in water. R_f = 0.30 (5:95 ethyl acetate/hexane); ^{1}H NMR (500 MHz, $CDCl_3$) δ 5.38 (app q, *J* = 1.6 Hz, 1H), 5.34 (ddq, *J* = 5.1, 1.5, 1.5 Hz, 1H), 2.60 (d, *J* = 16.1 Hz, 1H), 2.50 (d, *J* = 13.7 Hz, 1H), 2.47 (app t, *J* = 6.4 Hz, 1H), 2.24 (app t, *J* = 13.3 Hz, 1H), 2.19–2.17 (m, 1H), 2.15 (d, *J* = 10.3 Hz, 1 H), 1.99 (app ddt, *J* = 14.6, 6.8, 1.5 Hz, 1H), 1.98 (d, *J* = 14.1 Hz, 1H), 1.89 (dd, *J* = 16.1, 2.4 Hz, 1H), 1.84 (app ddt, *J* = 14.2, 6.8, 2.5 Hz, 1H), 1.74 (s, 3H), 1.73 (app dd, *J* = 14.6, 8.3 Hz, 1H), 1.61 (dt, *J* = 11.0, 2.9 Hz, 1H), 1.25 (m, 1H), 1.15 (d, *J* = 6.3 Hz, 3H), 1.09 (s, 3H), 0.99 (d, *J* = 6.8 Hz, 3H), 0.70 (s, 3H); ^{13}C NMR (125 MHz, $CDCl_3$) δ 215.5, 156.5, 141.8, 121.4, 119.9, 59.8, 55.2, 54.7, 54.3, 42.7, 42.2, 37.8, 33.2, 30.3, 26.4, 25.1, 22.8, 22.4, 21.6, 17.3; IR (Neat film, NaCl) 2961, 2924, 1703, 1444, 1380, 1294, 1144, 912, 858, 810 cm^{-1}; HRMS (EI) *m/z* calc'd for $C_{20}H_{30}O_2$ [M^+]: 286.2297, found 286.2292; $[\alpha]^{25}_D$ –125.4 (*c* 0.025, MeOH).

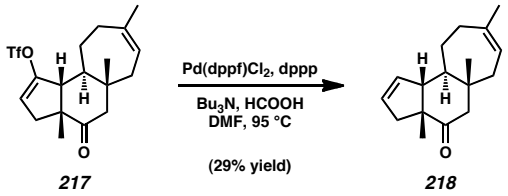

217 ***218***

Reduction byproduct 218. This material was obtained as a side product from the cross-coupling attempts to synthesize cyanthiwigin F (**160**), presumably as a result of reduction of the triflate moiety of **217**. Compound **218** was later synthesized directly by the following method: To a flame dried vial containing 22 mg of **217** (22 mg, 56.0 μmol, 1.00 equiv) was added dppp (7.0 mg, 17.0 μmol, 0.30 equiv) and $PdCl_2$(dppf) (5.0 mg, 6.83 μmol, 0.12 equiv). The solids were dissolved in DMF (0.5 mL), and the resulting solution was treated with 114 of Bu_3N (114 μL, 0.479 μmol, 0.009 equiv) and 11 of formic acid (11 μL, 0.292 μmol, 0.005 equiv) (Note: Upon addition of the formic acid, the reaction evolves white smoke). The reaction mixture was heated to 95 °C for 4 h, after which time all of the starting triflate was observed to be consumed by TLC. The reaction was quenched by the addition of brine (1 mL), followed by dilution with Et_2O (2 mL). The aqueous and organic phases were separated, and the aqueous phase was thereafter extracted with Et_2O (3 x 10 mL). The combined organic phases were washed with 2 N $HCl_{(aq)}$ (5 mL) to remove any residual amine, then washed with brine (3 mL). The collected organic phases were dried over $MgSO_4$, filtered, and then concentrated in vacuo. The resulting crude material was purified over silica gel using 2% Et_2O in petroleum ether to afford **218** as a white solid (4.0 mg, 29% yield): R_f = 0.30 (5:95 ethyl acetate/hexane); ^{1}H NMR (300 MHz, $CDCl_3$) δ 6.00–5.94 (m, 1H), 5.72–5.68 (m, 1H), 5.39–5.30 (m, 1H), 2.55 (ddd, *J* = 16.6, 4.4, 2.2 Hz, 1H), 2.39 (d, *J* = 14.9 Hz, 1H), 2.23 (t, *J* = 13.5 Hz, 1H), 2.18–2.12 (comp. m, 1H), 2.08 (dd, *J* = 2.7, 1.1 Hz, 1H), 2.03 (dd, *J*

= 2.7, 1.2 Hz, 1H), 2.02 (d, *J* = 14.7 Hz, 1H), 2.01 (dddd, *J* = 14.6, 6.9, 1.5, 1.5 Hz 1H), 1.99 (d, *J* = 14.6 Hz, 1H), 1.97–1.94 (m, 1H), 1.75 (s, 3H), 1.61 (s, 1H), 1.43–1.35 (m, 1H), 1.12 (s, 3H), 0.7 (s, 3H); ^{13}C NMR (75 MHz, $CDCl_3$) δ 215.7, 142.0, 134.9, 128.0, 121.5, 59.4, 55.8, 54.9, 51.9, 43.8, 41.9, 37.5, 33.1, 26.6, 25.3, 23.8, 16.8; IR (Neat film, NaCl) 2961, 2927, 1702, 1559, 1441, 1380, 1293, 1257, 1140, 856, 726 cm^{-1}; HRMS (EI) *m/z* calc'd for $C_{17}H_{24}O$ [M^+]: 244.1827, found 244.1821; $[\alpha]^{25}_D$ –238.4 (*c* 0.02, MeOH).

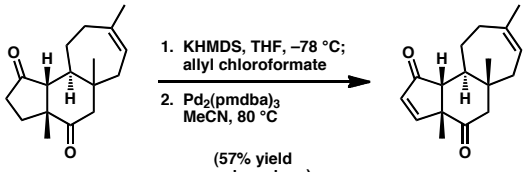

214 ***220***

Tricyclic Enone 220. A flame dried vial charged with tricyclic diketone **214** (22 mg, 77.0 μmol, 1.00 equiv), and this material was thereafter dissolved in THF (200 μL). A separate flame dried vial was backfilled with argon and cycled into a glovebox. Once inside, this vessel was charged with KHMDS (19 mg, 95.0 μmol, 1.30 equiv), and then was removed from the glovebox. Once placed on a manifold line, the KHMDS was dissolved in THF (200 μL). Both solutions were cooled to –78 °C, and then the KHMDS solution was added dropwise to the solution of diketone **214**. The mixed solutions were allowed to deprotonate at –78 °C for 30 min, after which time allyl chloroformate (10 μL, 92.0 μmol, 1.20 equiv) was added. This was allowed to react for a further 2.5 h at –78 °C. Once this time had elapsed, the reaction was warmed slowly to room temperature, and then was quenched with an excess of saturated $NH_4Cl_{(aq)}$. The phases were separated, and the aqueous layer was extracted with diethyl ether (4 x 10 mL). The combined organic layers were washed with brine (5 mL), then dried over $MgSO_4$, filtered, and

concentrated. The crude material obtained was briefly passed over a plug of silica gel using 3% ethyl acetate in hexanes as eluent. The material obtained from this rapid purification was used directly in the next reaction without further characterization.

The material obtained from the silica plug above (ca. 16.6 mg) was transferred to a flame dried vial under argon, and then was azeotroped thrice from acetonitrile. The material was briefly dried under high vacuum, and then $Pd_2(pmdba)_3$ (2.8 mg, 2.0 μmol, 0.05 equiv) and acetonitrile (250 μL) were added. The reaction vial was sealed, and then the reaction was heated to 80 °C. After 2 h, the vial was cooled to room temperature, and solvent was removed in vacuo. The crude material obtained was purified via chromatography over silica using 5% ethyl acetate in hexanes as eluent. This afforded enone **220** as a colorless oil (11 mg, 57% yield): R_f = 0.60 (10:90 ethyl acetate/hexane); ^{1}H NMR (500 MHz, $CDCl_3$) δ 7.31 (d, *J* = 5.5 Hz, 1H), 6.09 (d, *J* = 5.5 Hz, 1H), 5.33 (dddd, *J* = 8.7, 5.2, 3.6, 1.7 Hz, 1H), 2.37 (app ddt, *J* = 14.3, 6.8, 2.2 Hz, 1H), 2.27–2.14 (m, 2H) 2.21 (dd, *J* = 15.7, 0.7 Hz, 1H), 2.15 (d, *J* = 15.7 Hz, 1H), 2.04 (d, *J* = 11.0 Hz, 1H), 2.03 (app ddt, *J* = 15.0, 6.7, 1.5 Hz, 1H) 1.75 (s, 3H), 1.77–1.67 (m, 1H), 1.35 (s, 3H), 1.27 (app dtd, *J* = 13.9, 12.1, 1.7 Hz, 1H), 1.21 (d, *J* = 15.1 Hz, 1H), 0.82 (s, 3H); ^{13}C NMR (125 MHz, $CDCl_3$) δ 211.7, 210.6, 165.9, 142.7, 131.4, 120.7, 59.1, 56.8, 55.5, 51.7, 41.7, 38.4, 32.9, 26.9, 26.0, 25.3, 17.9; IR (Neat film, NaCl) 2963, 2925, 2867, 1703, 1590, 1444, 1381, 1331, 1255, 1227, 1184, 1070, 996 cm^{-1}; HRMS (MM: ESI-APCI) *m/z* calc'd for $C_{17}H_{22}O_2$ [M^+]: 258.1620, found 258.1622; $[\alpha]^{25}_D$ –210.9 (*c* 0.97, CH_2Cl_2).

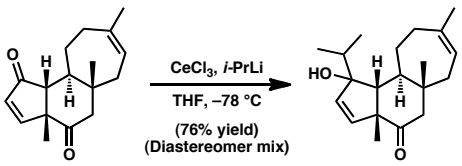

220 ***221***

Allylic alcohol 221. To a flame dried vial was added enone **220** (29 mg, 0.112 mmol, 1.00 equiv). This material was briefly vacuum purged, and then was backfilled with argon. The vial was cycled into the glovebox, where it was charged with $CeCl_3$ (31 mg, 0.118 mmol, 1.05 equiv). The vial was then removed from the glovebox, placed under a manifold line, charged with THF (1.1 mL), and cooled to –78 °C. After reaching the desired temperature, isopropyl lithium (200 μL, 0.7 M in hexanes, 0.135 mmol, 1.20 equiv) was added to the suspension dropwise at –78 °C. The reaction was allowed to reach room temperature slowly by warming in the bath overnight. The reaction looked incomplete the next morning, and so was allowed to continue for an additional 14 h (total 22 h). The reaction was thereafter quenched with saturated $NH_4Cl_{(aq)}$ (2 mL). The phases were separated, and the aqueous layer was extracted with diethyl ether (4 x 5 mL). The combined organics were washed with brine (5 mL), dried over $MgSO_4$, filtered, and concentrated in vacuo. The crude material obtained was purified via chromatography over silica gel using 7% → 8% → 9% ethyl acetate in hexanes as eluent. This afforded allylic alcohol **221** as a clear oil (26 mg, isolated as two diastereomers, 76% combined yield). **Diastereomer A**: R_f = 0.40 (20:80 ethyl acetate/hexane); ^{1}H NMR (500 MHz, $CDCl_3$) δ 5.70 (d, *J* = 5.6 Hz, 1H), 5.54 (d, *J* = 5.6 Hz, 1H), 5.33 (dddd, *J* = 8.6, 5.1, 3.4, 1.6 Hz, 1H), 2.27 (dd, *J* = 15.4, 0.9 Hz, 1H), 2.25 (m, 1H) 2.06 (d, *J* = 15.4 Hz, 1H), 2.00 (app ddt, *J* = 14.9, 6.6, 1.5 Hz, 1H), 1.99 (d, *J* = 10.6 Hz, 2H), 1.91 (app ddt, *J* = 13.6, 6.6, 2.1 Hz, 1H), 1.85 (app dt, *J* = 10.6, 2.1 Hz, 1H), 1.81–1.73 (comp. m, 3H), 1.75 (s,

3H), 1.30 (s, 3H), 1.11 (dddd, *J* = 13.6, 12.1, 10.6, 1.6 Hz, 1H), 1.04 (d, *J* = 6.9 Hz, 3H), 0.93 (d, *J* = 6.8 Hz, 3H), 0.83 (s, 3H); ^{13}C NMR (125 MHz, $CDCl_3$) δ 214.6, 142.3, 137.3, 36.2, 121.2, 90.3, 59.9, 57.2, 55.1, 49.5, 42.9, 39.0, 36.6, 33.6, 28.5, 26.9, 25.5, 18.7, 18.2, 18.0; IR (Neat film, NaCl) 3494, 2968, 2923, 1694, 1456, 1382, 1286, 1249, 1137, 1110, 979 cm^{-1}; HRMS (MM: ESI-APCI) *m/z* calc'd for $C_{20}H_{30}O_2$ [M$^+$]: 302.2246, found 302.2248; $[\alpha]^{25}_D$ –89.3 (*c* 0.72, CH_2Cl_2). **Diastereomer B**: R_f = 0.20 (20:80 ethyl acetate/hexane); ^{1}H NMR (500 MHz, $CDCl_3$) δ 5.83 (d, *J* = 5.8 Hz, 1H), 5.62 (d, *J* = 5.8 Hz, 1H), 5.38–5.33 (m, 1H), 2.30 (d, *J* = 18.1 Hz, 1H), 2.27–2.20 (m, 2H), 2.10 (dd, *J* = 18.1, 0.5 Hz, 2H), 2.01 (d, *J* = 10.7, 2H), 1.86 (dd, *J* = 14.5, 8.9 Hz, 2H), 1.81–1.75 (m, 2H), 1.77 (s, 3H), 1.47 (s, 3H) 1.41–1.34 (m, 1H), 1.06 (d, *J* = 6.9 Hz, 3H), 1.05 (s, 3H), 0.71 (d, *J* = 6.6 Hz, 3H); ^{13}C NMR (125 MHz, $CDCl_3$) δ 141.8, 138.5, 121.8, 92.5, 62.8, 59.3, 54.3, 48.9, 44.4, 36.2, 33.6, 31.5, 30.3, 29.3, 25.9, 21.0, 19.9, 18.5; IR (Neat film, NaCl) 3472, 2963, 2925, 1698, 1449, 1382, 1287, 1246, 1012, 980, 795 cm^{-1}; HRMS (MM: ESI-APCI) *m/z* calc'd for $C_{20}H_{30}O_2$ [M$^+$]: 302.2246, found 302.2249; $[\alpha]^{25}_D$ –67.3 (*c* 0.16, CH_2Cl_2).

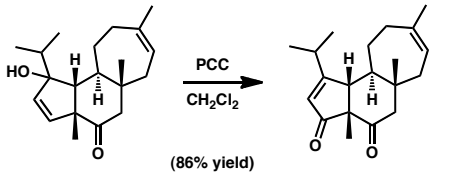

221 ***Cyanthiwigin B (156)***

Cyanthiwigin B (156). To a flame dried vial was added allylic alcohol **221** (8.2 mg, 27.0 μmol, 1.00 equiv). This was dissolved in CH_2Cl_2 (275 μL), and then was treated with PCC (23 mg, 108.0 μmol, 4.00 equiv). This reaction was allowed to stir at room temperature for 14 h, and then was diluted with diethyl ether (1 mL) and passed over a

plug of celite. The celite pad was washed with additional diethyl ether (5 mL), and the collected organic solvents were concentrated to dryness. The residue obtained was purified over silica gel using 6.5% ethyl acetate in hexanes as eluent. This afforded cyanthiwigin B (**156**) as a white solid (7.0 mg, 86% yield): ^{1}H NMR (500 MHz, $CDCl_3$) δ 5.81 (s, 1H), 5.30–5.25 (m, 1H), 2.73 (app dt, *J* = 13.5, 6.7 Hz, 1H), 2.54 (d, *J* = 9.2 Hz, 1H), 2.20–2.12 (m, 1H), 2.10 (s, 1H), 2.09 (dd, *J* = 13.6, 0.7 Hz, 1H), 2.02 (app ddt, *J* = 15.1, 6.5, 1.6 Hz, 1H), 2.00 (d, *J* = 13.7 Hz, 1H), 1.81 (app ddt, *J* = 14.2, 6.6, 2.0 Hz, 1H), 1.71 (dd, *J* = 14.8, 8.7 Hz, 1H), 1.69 (s, 3H), 1.56 (ddd, *J* = 11.4, 9.3, 2.2 Hz, 1H), 1.47–1.39 (m, 1H), 1.24 (s, 3H), 1.23 (d, *J* = 6.5 Hz, 3H), 1.10 (d, *J* = 7.0 Hz, 3H), 0.68 (s, 3H); ^{13}C NMR (125 MHz, $CDCl_3$) δ 207.2, 141.4, 123.2, 121.7, 63.7, 58.9, 56.8, 56.2, 42.6, 39.1, 33.7, 31.4, 31.2, 28.5, 25.8, 25.2, 21.9, 21.4, 18.3; IR (Neat film, NaCl) 2920, 1723, 1693, 1602, 1452, 1261, 1161, 866 cm^{-1}; HRMS (MM: ESI-APCI) *m/z* calc'd for $C_{20}H_{28}O_2$ [M^+]: 300.2089, found 300.2093. $[\alpha]^{24}_D$ –215.2 (*c* 0.84, CH_2Cl_2), $[\alpha]^{25}_D$ –195.7 (*c* 0.84, MeOH).

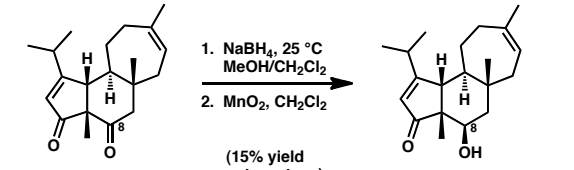

Cyanthiwigin B (156) ***8-epi-Cyanthiwigin E (222)***

8-*epi*-Cyanthiwigin E (222). To a flame dried vial was added cyanthiwigin B (**156**, 7.2 mg, 24.0 μmol, 1.00 equiv). The solids were dissolved in a 1 : 1 mixture of CH_2Cl_2 and methanol (1.0 mL). In a separate flame dried vial, $NaBH_4$ (23 mg) was dissolved in 1 : 1 mixture of CH_2Cl_2 and methanol (2.0 mL). Both solutions were cooled to –78 °C, and then a portion of the $NaBH_4$ solution (100 μL, 1.1 mg, 30.0 μmol, 1.20 equiv) was

added to the solution of cyanthiwigin B (**156**). After 1 h, no conversion was observed, and so an additional portion of the $NaBH_4$ solution was added (100 μL, 1.1 mg, 30.0 μmol, 1.2 equiv). After no conversion was observed over an additional 2.5 h period, an additional portion of the $NaBH_4$ solution was added (200 μL, 2.2 mg, 60.0 μmol, 2.40 equiv) and the temperature of reaction was warmed to –45 °C. The reaction was thereafter allowed to progress overnight. After an additional 8 h of reaction, conversion was still incomplete, and so reaction was pushed to completion by the addition of solid $NaBH_4$ (4.0 mg, 106.0 μmol, 4.40 equiv). The reaction was allowed to stir for 3 h, and then was quenched with acetone (1 mL) and 2 N $NaOH_{(aq)}$ (5 mL). The phases were separated, and the organic layer was washed immediately with brine (5 mL), and then dried over Na_2SO_4. The reaction was filtered and the solvent was removed in vacuo. The crude material obtained was purified over silica using 20% → 30% ethyl acetate in hexanes as eluent. Repurification was then executed using 7% → 10% → 20% → 50% ethyl acetate in hexanes as eluent. The material obtained as a white solid was difficult to characterize, and so was taken directly into the next reaction.

The white solid obtained above (ca. 2.2 mg) and MnO_2 (9.0 mg, 108.0 μmol, 15.0 equiv) were added to a flame dried vial. These solids were suspended in CH_2Cl_2 (0.5 mL), and were allowed to stir at room temperature for 15 h. The reaction was then passed over a plug of celite, and the plug was washed with ethyl acetate (15 mL). The solvent was removed in vacuo, and the crude material was purified via chromatography over silica using 6% ethyl acetate in hexanes as eluent. The material obtained was then repurified over silica using 4% ethyl acetate in hexanes as eluent. This afforded 8-*epi*-cyanthiwigin E (**222**) as a white solid (1.1 mg, 15% over two steps): ^{1}H NMR (500 MHz,

$CDCl_3$) δ 5.93 (s, 1H), 5.40–5.35 (m, 1H), 4.15 (ddd, *J* = 11.3, 5.0, 2.2 Hz, 1H), 2.63 (app dt, *J* = 13.6, 6.9, 1H), 2.53 (d, *J* = 2.2 Hz, 1H), 2.45 (d, *J* = 10.8 Hz, 1H), 2.29–2.20 (m, 1H), 2.12–2.04 (m, 1H), 1.98 (app ddt, *J* = 15.0, 6.3, 1.6 Hz, 1H), 1.89 (dd, *J* = 14.8, 8.8 Hz, 1H), 1.71 (s, 3H), 1.63 (dd, *J* = 13.8, 11.3 Hz, 1H), 1.57 (d, *J* = 5.1 Hz, 1H), 1.43–1.28 (comp. m, 3H), 1.24 (d, *J* = 6.8 Hz, 3H), 1.11 (d, *J* = 6.9 Hz, 3H), 1.10 (s, 3H), 0.95 (s, 3H); ^{13}C NMR (125 MHz, $CDCl_3$) δ 215.9, 193.9, 139.4, 125.4, 123.1, 77.4, 67.4, 56.6, 55.3, 55.0, 44.8, 44.4, 35.2, 34.2, 33.5, 25.7, 25.3, 23.3, 22.1, 20.4, 19.6; IR (Neat film, NaCl) 3429, 2963, 2918, 1684, 1602, 1444, 1367, 1270, 1002 cm^{-1}; HRMS (MM: ESI-APCI) *m/z* calc'd for $C_{20}H_{30}O_2$ [M^+]: 302.2246, found 302.2248; $[\alpha]^{23}_D$ –7.19 (*c* 0.16, MeOH).

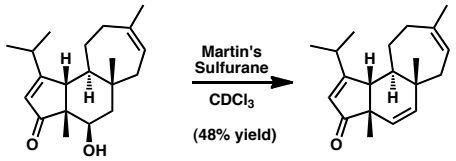

8-epi-Cyanthiwigin E (222) ***Cyanthiwigin G (161)***

Cyanthiwigin G (161). To a flame dried vial was added *epi*-8-cyanthiwigin E (**222**, 1.1 mg, 4.0 μmol, 1.00 equiv). This vial was then cycled into the glovebox directly, and then was treated with Martin's sulfurane (6.2 mg, 9.0 μmol, 2.50 equiv). The vial was removed from the glovebox and transferred to a manifold line, where it was then charged with $CDCl_3$ (250 μL) and allowed to react at room temperature for 5 h. After this time had elapsed, the reaction was directly loaded onto a silica gel column and purified via chromatography using 3% ethyl acetate in hexanes as eluent. This afforded cyanthiwigin G (**161**) as a white solid (0.5 mg, 48% yield): ^1H NMR (500 MHz, $CDCl_3$) δ 5.87 (d, *J* = 0.9 Hz, 1H), 5.69 (d, *J* = 9.9 Hz, 1H), 5.54 (d, *J* = 9.9 Hz, 1H), 5.39–5.35 (m, 1H), 2.75–

2.67 (m, 1H), 2.48 (d, *J* = 10.4, 1H), 2.22–2.12 (comp. m, 2H), 1.96 (app ddt, *J* = 14.7, 6.7, 1.4 Hz, 1H), 1.89 (dd, *J* = 14.5, 8.6 Hz, 1H), 1.74 (s, 3H), 1.77–1.67 (m, 1H), 1.36–1.29 (comp. m, 2H), 1.25 (d, *J* = 6.6 Hz, 3H), 1.15 (s, 3H), 1.13 (d, *J* = 6.9 Hz, 3H), 0.88 (s, 3H); ^{13}C NMR (125 MHz, $CDCl_3$) δ 211.5, 192.1, 141.4, 140.9, 127.3, 124.4, 122.2, 58.2, 55.3, 53.8, 41.5, 37.6, 33.7, 33.4, 30.5, 28.4, 26.1, 25.2, 23.2, 20.3, 19.8; IR (Neat film, NaCl) 2962, 2921, 1706, 1601, 1444, 1366, 1261, 1156, 1091, 863, 761 cm^{-1}; HRMS (EI) *m/z* calc'd for $C_{20}H_{29}O$ [M+H]: 285.2218, found 285.2221; $[\alpha]^{25}_{D}$ –12.35 (*c* 0.10, MeOH).

2.5 NOTES AND REFERENCES

(1) Green, D.; Goldberg, I.; Stein, Z.; Ilan, M.; Kashman, Y. *Nat. Prod. Lett.* **1992**, *1*, 193–199.

(2) (a) Peng, J.; Walsh, K.; Weedman, V.; Bergthold, J. D.; Lynch, J.; Lieu, K. L.; Braude, I. A.; Kelly, M.; Hamann, M. T. *Tetrahedron* **2002**, *58*, 7809–7819. (b) Peng, J.; Avery, M. A.; Hamann, M. T. *Org. Lett.* **2003**, *5*, 4575–4578. (c) Peng, J.; Kasanah, N.; Stanley, C. E.; Chadwick, J.; Fronczek, M.; Hamann, M. T. *J. Nat. Prod.* **2006**, *69*, 727–730.

(3) (a) Wright, D. L.; Whitehead, C. R. *Org. Prep. Proced. Int.* **2000**, *32*, 309–330.; (b) Enquist, J. A., Jr.; Stoltz, B. M. *Nat. Prod. Rep.* **2009**, *26*, 661–680.

(4) Saito, T.; Aoki, F.; Hirai, H.; Inagaki, T.; Matsunaga, Y.; Sakakibara, T.; Sakemi, S.; Suzuki, Y.; Watanabe, S.; Suga, O.; Sujaku, T.; Smogowicz, A. A.; Truesdell, S. J.; Wong, J. W.; Nagahisa, A.; Kojima, Y.; Kojima, N. *J. Antibiot. (Tokyo)* **2003**, *51*, 983–990.

(5) (a) Obara, Y.; Nakahata, N.; Kita, T.; Takaya, Y.; Kobayashi, H.; Hosoi, S.; Kiuchi, S.; Ohta, T.; Oshima, Y.; Ohizumi, Y. *Eur. J. Pharmacol.* **1999**, *370*, 79–84. (b) Obara, Y.; Kobayashi, H.; Ohta, T.; Ohizumi, Y.; Nakahata, N. *Mol. Pharmacol.* **2001**, *59*, 1287–1297.

(6) Sennett, S. H.; Pomponi, S. A.; Wright, A. E. *J. Nat. Prod.* **1992**, *55*, 1421–1429.

(7) (a) Behenna, D. C.; Stoltz, B. M. *J. Am. Chem. Soc.* **2004**, *126*, 15044–15045. (b) Mohr, J. T.; Behenna, D. C.; Harned, A. M.; Stoltz, B. M. *Angew. Chem., Int. Edn. Engl.* **2004**, *44*, 6924–6927.

(8) Ebert, H. *Liebigs Ann. Chem.* **1885**, *229*, 45–88.

(9) Enquist, J. A., Jr.; Stoltz, B. M. *Nature* **2008**, *453*, 1228–1230.

(10) Conditions for this optimized procedure were adapted from a Dieckmann reaction previously published by our group in *Organic Syntheses*. See: Mohr, J. T.; Krout, M. R.; Stoltz, B. M. *Org. Synth.* **2009**, *86*, 194–211.

(11) (a) Masamune, S.; Choy, W.; Peterson, J.; Sita, L. *Angew. Chem., Int. Ed. Engl.* **1985**, *24*, 1–30. (b) Rieck, H.; Helmchen, G. *Angew. Chem., Int. Ed. Engl.* **1995**, *34*, 2687–2689. (c) Lebsack, A. D.; Link, J. T.; Overmann, L. E.; Stearns, B. A. *J. Am. Chem. Soc.* **2002**, *124*, 9008–9009. (d) Kolodiazhnyi, O. I. *Tetrahedron* **2003**, *59*, 5953–6018. (e) Welter, C.; Dahnz, A.; Brunner, B.; Streiff, S.; Dübon, P.; Helmchen, G. *Org. Lett.* **2005**, *7*, 1239–1242.

(12) Kagan, H. *Tetrahedron* **2001**, 57, 2449–2468.

(13) Eliel, E. L.; Wilen, S. H. *Stereochemistry of Organic Compounds*; John Wiley & Sons, Inc.: New York, 1994; pp 965–971.

(14) Mohr, J. T.; Ebner, D. C.; Stoltz, B. M. *Org. Biomol. Chem.* **2007**, *5*, 3571–3576.

(15) (a) Helmchen, G.; Pfaltz, A. *Acc. Chem. Res.* **2000**, *33*, 336–345. (b) Tani, K.; Behenna, D. C.; McFadden, R. M.; Stoltz, B. M. *Org. Lett.* **2007**, *9*, 2529–2531.

(16) Langenbeck, W.; Triem, G. *Z. Phys. Chem. A* **1936**, *117*, 401–409.

(17) (a) Vigneron, J. P.; Dhaenens, M.; Horeau, A. *Tetrahedron* **1973**, *29*, 1055–1059. (b) Rautentrauch, V. *Bull. Soc. Chim. Fr.* **1994**, *131*, 515–524. (c) Baba, S. E.; Sartor, K.; Poulin, J.; Kagan, H. *Bull. Soc. Chim. Fr.* **1994**, *131*, 525–533.

(18) For a more thorough, mathematical treatment of this phenomenon, please see chapter 3.

(19) Poss, C. S.; Schreiber, S. L. *Acc. Chem. Res.* **1994**, *27*, 9–17.

(20) (a) Negishi, E.-I.; Ma, S.; Amanfu, J.; Copéret, C.; Miller, J. A.; Tour, J. M. *J. Am. Chem. Soc.* **1996**, *118*, 5919–5913. (b) Satoh, T.; Itaya, T.; Okuro, K.; Miura, M.; Nomura, M. *J. Org. Chem.* **1996**, *60*, 7267–7271. (c) Matsuura, T.; Overmann, L. E.; Poon, D. J. *J. Am. Chem. Soc.* **1998**, *120*, 6500–6503. (d) Iwasawa, N.; Satoh, H. *J. Am. Chem. Soc.* **1999**, *121*, 7951–7952. (e) Hayashi, T.; Tang, J.; Kato, K. *Org. Lett.* **1999**, *1*, 1487–1489. (f) Artman, G. D., III; Weinreb, S. M. *Org. Lett.* **2003**, *5*, 1523–1526. (g) Wu, X.; Nilsson, P.; Larhed, M. *J. Org. Chem.* **2005**, *70*, 346–349. (h) Wu, X.-F.; Neumann, H.; Beller, M.

Angew. Chem. Int. Ed. **2010**, *49*, 5284–5288. (i) Bloome, K. S.; Alexanian, E. J. *J. Am. Chem. Soc.* **2010**, *ASAP*, doi: 10.1021/ja1053913.

(21) (a) Sonogashira, K.; Tohda, Y.; Hagihara, N. *Tetrahedron Lett.* **1975**, *16*, 4467–4470. (b) Eckhardt, M.; Brückner, R.; Suffert, J. *Tetrahedron Lett.* **1995**, *36*, 5167–5170.

(22) Han, X.; Stoltz, B. M.; Corey, E. J. *J. Am. Chem. Soc.* **1999**, *121*, 7600–7605.

(23) Tivola, P. B.; Deagostino, A.; Prandi, C.; Venturello, P. *J. Chem. Soc., Perkin Trans. 1* **2001**, 437–441.

(24) All attempts to directly isolate the bicyclic enol ether resulting from ring-closing metathesis of **202** resulted in substantial decomposition to bicyclic enone **204** on silica gel.

(25) (a) King, A. O.; Okukado, N.; Negishi, E.-I. *J. Chem. Soc., Chem. Commun.* **1977**, 683–684. (b) Taishi, T.; Takechi, S.; Mori, S. *Tetrahedron Lett.* **1998**, *39*, 4347–4350.

(26) Stewart, I. C.; Ung, T.; Pletnev, A. A.; Berlin, J. M.; Grubbs, R. H.; Schrodi, Y. *Org. Lett.* **2007**, *9*, 1589–1592.

(27) For development and synthetic application of the vinyl boronate cross-metathesis, See: (a) Morrill, C.; Funk, T. W.; Grubbs, R. H. *Tetrahedron Lett.* **2004**, *45*,

7733–7736. (b) Morrill, C.; Grubbs, R. H. *J. Org. Chem.* **2003**, *68*, 6031–6034. (c) Njardarson, J. T.; Biswas, K.; Danishefsky, S. J. *Chem. Commun.* **2002**, 2759–2761.

(28) (a) Kharasch, W. H.; Urry, W. H.; Kuderna, B. M. *J. Org. Chem.* **1949**, *14*, 248–253. (b) Starker, L. N.; Cosulich, D. B.; Smith, J. M., Jr. *J. Am. Chem. Soc.* **1955**, *77*, 2534–2536. (c) Stetter, H.; Kuhlmann, H. *Tetrahedron Lett.* **1974**, *15*, 4505–4508.

(29) Faced with the difficulty of generating an appropriate acyl radical species, we postulated that formation of a ketyl radical would be more facile, as well as more reactive. See: (a) Yeh, M.-C. P.; Wang, F.-C.; Tu, J.-J.; Chang, S.-C.; Chou, C.-C.; Liao, J.-W. *Organometallics* **1998**, *17*, 5656–5662. (b) Molander, G. A.; McKie, J. A. *J. Org. Chem.* **1992**, *57*, 3132–3139. (c) Molander, G. A.; Kenny, C. *J. Org. Chem.* **1991**, *56*, 1439–1445.

Toward this end, bicyclic aldehyde **208** was treated with a solution of samarium(II) iodide in the presence of hexamethylphosphoramide (HMPA), with the expectation that these conditions would afford an appropriate ketyl radical. Unfortunately, rather than undergo the radical-olefin cyclization process we envisaged, the ketyl radical instead engaged in an undesired intramolecular Pinacol-type coupling to yield [5-6-7] tricyclic system **C2-S1**.

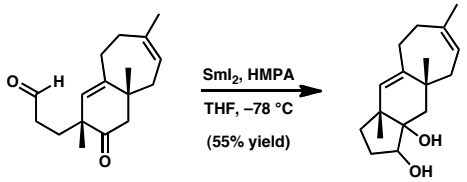

208 ***C2-S1***

Diol C2-S1. To a flame dried vial was added a THF solution of aldehyde **208** (20 mg, 0.077 mmol, 1.0 equiv, in 500 μL solvent). To this solution was added HMPA (25 μL), and the vial was cooled to –78 °C. Once this temperature had been reached, SmI_2 (921 μL, 0.1 M in THF, 0.092 mmol, 1.2 equiv) was added dropwise to the reaction. After complete addition of a single portion of SmI_2, the reaction had not reached completion. A second portion of SmI_2 (921 μL, 0.1 M in THF, 0.092 mmol, 1.2 equiv) was added, and the reaction was allowed to reach 0 °C over 30 min. After this time had elapsed, the reaction was poured into a solution of brine (20 mL) that contained citric acid (770 mg). The phases were separated, and the aqueous layer was extracted with ethyl acetate (4 x 30 mL). Combined organic layers were washed with brine (40 mL), dried over $MgSO_4$, filtered, and concentrated in vacuo. The resulting crude material was purified over silica using 10% → 12% → 15% ethyl acetate in hexanes as eluent. This afforded diol **C2-S1** as a colorless oil (11 mg, 55% yield). Incomplete characterization data is as follows: ^{1}H NMR (500 MHz, $CDCl_3$) δ 5.33 (app t, *J* = 6.8 Hz, 1H), 5.13 (s, 1H), 3.83 (app dt, *J* = 6.8, 4.3 Hz, 1H), 2.38 (d, *J* = 4.4 Hz, 1H), 2.35–2.33 (m, 1H), 2.31 (s, 1H), 2.24–2.16 (m, 1H), 2.12 (ddd, *J* = 14.5, 6.8, 0.8 Hz, 1H), 2.03 (app dt, *J* = 14.7, 5.2 Hz, 2H), 1.95 (dddd, *J* = 14.0, 8.9, 6.8, 5.3 Hz, 1H), 1.88 (dd, *J* = 14.5, 6.8 Hz, 1H), 1.74 (ddd, *J* = 12.7, 9.1, 5.3 Hz, 1H), 1.66 (s, 3H), 1.65–1.58 (m, 1H), 1.62 (d, *J* = 4.8 Hz, 1H), 1.47 (d, *J* = 14.1 Hz, 1H), 1.44 (ddd, *J* = 12.7, 8.9, 7.2 Hz, 1H), 1.15 (s, 3H), 1.06 (s, 3H); ^{13}C NMR (125 MHz, $CDCl_3$) δ 142.9, 139.3, 131.5, 121.3, 79.5, 79.0, 46.4, 44.6, 40.1, 39.7, 38.4, 35.9, 30.5, 29.8, 27.7, 25.7, 23.7. IR (Neat film, NaCl) cm^{-1}.

(30) Namy, J. L.; Souppe, J.; Kagan, H. B. *Tetrahedron Lett.* **1983**, *24*, 765–766.

(31) Yoshikai, K.; Hayama, T.; Nishimura, K.; Yamada, K.; Tomioka, K. *J. Org. Chem.* **2005**, *70*, 681–683.

(32) Rawat, D. S.; Gibbs, R. A. *Org. Lett.* **2002**, *4*, 3027–3030.

(33) Tamao, K.; Sumitani, K.; Kiso, Y.; Zembayashi, M.; Fujioka, H.; Kodama, S.-I.; Nakajima, I.; Minato, A.; Kumada, M. *Bull. Chem. Soc. Jpn.* **1976**, *49*, 1958–1969.

(34) Although, to our knowledge, there have been no reports of cuprate-mediated palladium cross-coupling reactions, there nevertheless do exist reports of copper-accelerated Negishi reactions. See: Weichert, A.; Bauer, M.; Wirsig, P. *Synlett* **1996**, 473–474.

(35) Products **160** and **218** were ultimately separated via reverse phase HPLC purification.

(36) (a) Shimizu, I.; Tsuji, J. *J. Am. Chem. Soc.* **1982**, *104*, 5844–5846. (b) Shimizu, I.; Minami, I.; Tsuji, J. *Tetrahedron Lett.* **1983**, *24*, 1797–1800. (c) Minami, I.; Takahashi, K.; Shimizu, I.; Kimura, T.; Tsuji, J. *Tetrahedron* **1986**, *42*, 2971–2977.

(37) The final two steps of our synthetic route toward cyanthiwigin B were adapted from Phillips' synthesis of cyanthiwigin U. See: Pfeiffer, M. W. B.; Phillips, A. J. *J. Am. Chem. Soc.* **2005**, *127*, 5334–5335.

(38) Ward, D. E.; Rhee, C. K. *Can. J. Chem.* **1989**, *67*, 1206–1211.

(39) (a) Arhart, R. J.; Martin, J. C. *J. Am. Chem. Soc.* **1972**, *94*, 5003–5010. (b) Martin, J. C.; Franz, J. A.; Arhart, R. J. *J. Am. Chem. Soc.* **1974**, *96*, 4604–4611.

(40) An alternative approach toward cyanthiwigin G involving formation of an enol triflate species from cyanthiwigin B (**156**) via deprotonation at C(7) and trapping with *N*-phenyl bis(trifluoromethane)sulfonimide, failed to achieve the desired product. Under these conditions, only γ-deprotonation at C(18) was observed.

(41) Peer, M.; de Jong, J. C.; Kiefer, M.; Langer, T.; Rieck, H.; Schell, H.; Sennhenn, P.; Sprinz, J.; Steinhagen, H.; Wiese, B.; Helmchen, G. *Tetrahedron* **1996**, *52*, 7547–7583.

(42) (a) Yong, K.; Lotoski, J. A.; Chong, J. M. *J. Org. Chem.* **2001**, *66*, 8248–8251. (b) Helmboldt, H.; Köhler, D.; Hiersemann, M. *Org. Lett.* **2006**, *8*, 1573–1576.

APPENDIX 1

Synthetic Summary for Cyanthiwigins B, F, and G

Scheme A1.1 Synthesis of tricyclic diketone ***214***

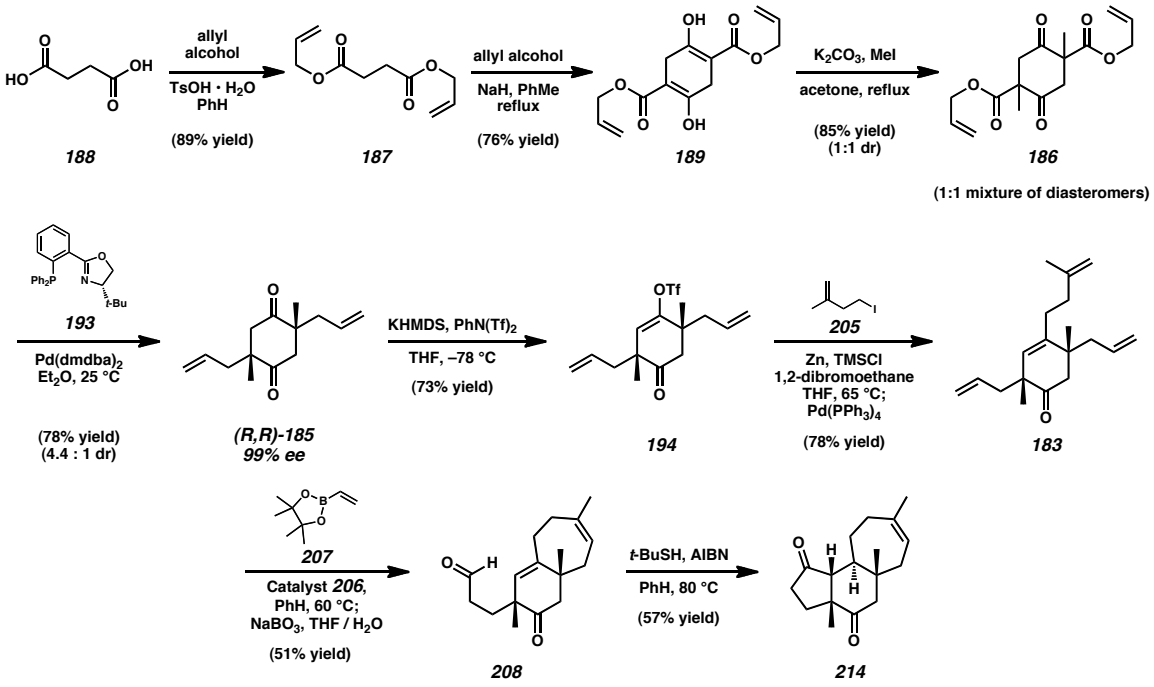

*Scheme A1.2 Synthesis of cyanthiwigin F (****160****)*

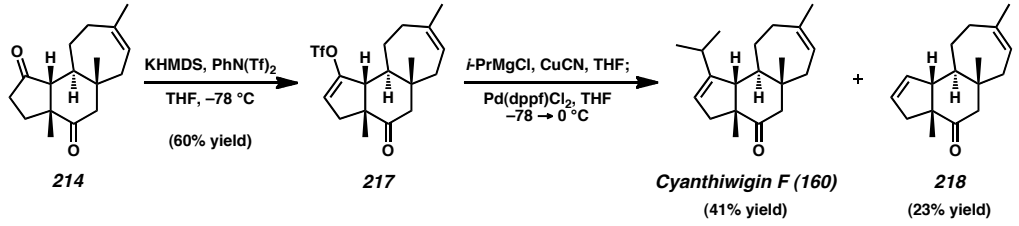

*Scheme A1.3 Synthesis of cyanthiwigins B (****156****) and G (****161****)*

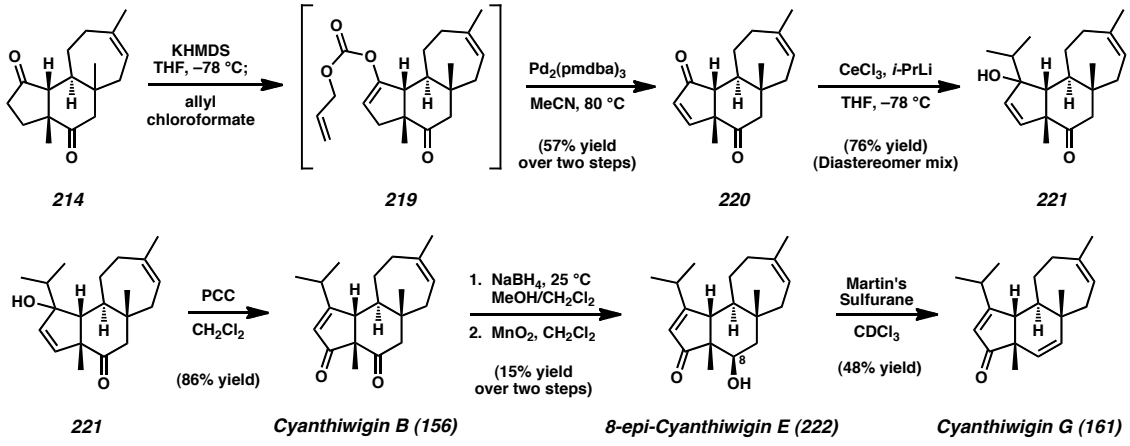

APPENDIX 2

Spectra Relevant to Chapter 2

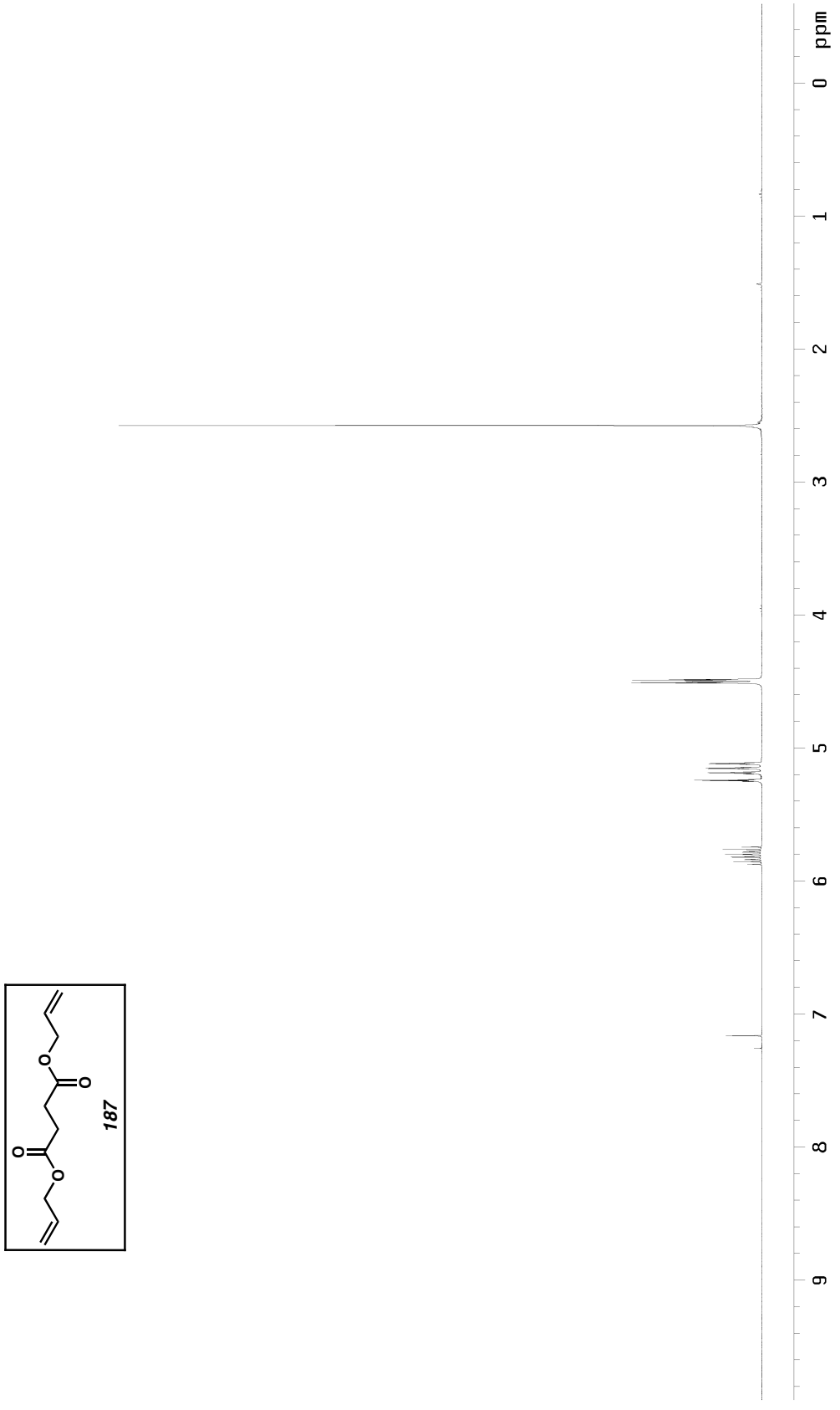

Figure A2.1 ^{1}H NMR (300 MHz, $CDCl_3$) of diallyl succinate (**187**).

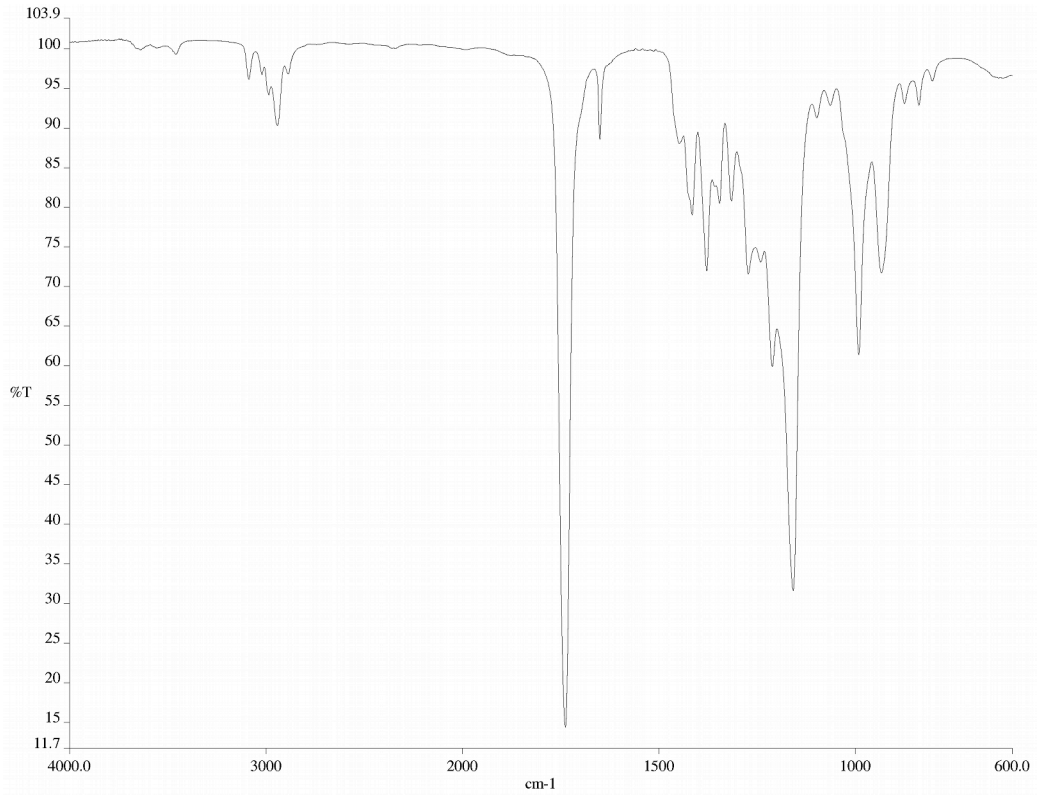

Figure A2.2 Infrared spectrum (thin film/NaCl) of diallyl succinate (**187**).

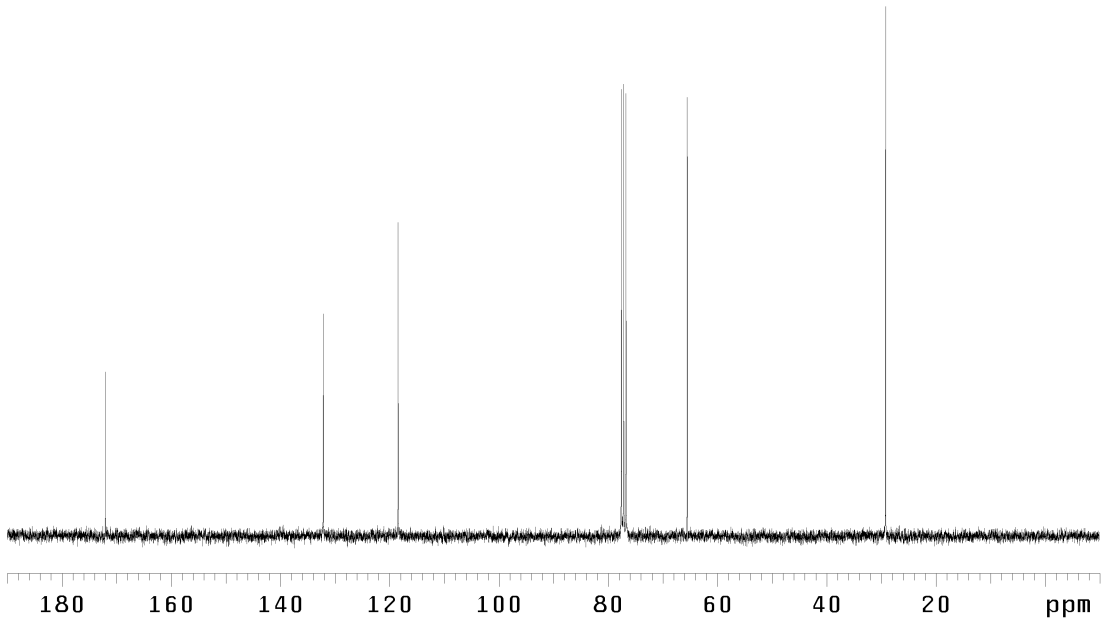

Figure A2.3 ^{13}C NMR (75 MHz, $CDCl_3$) of diallyl succinate (**187**).

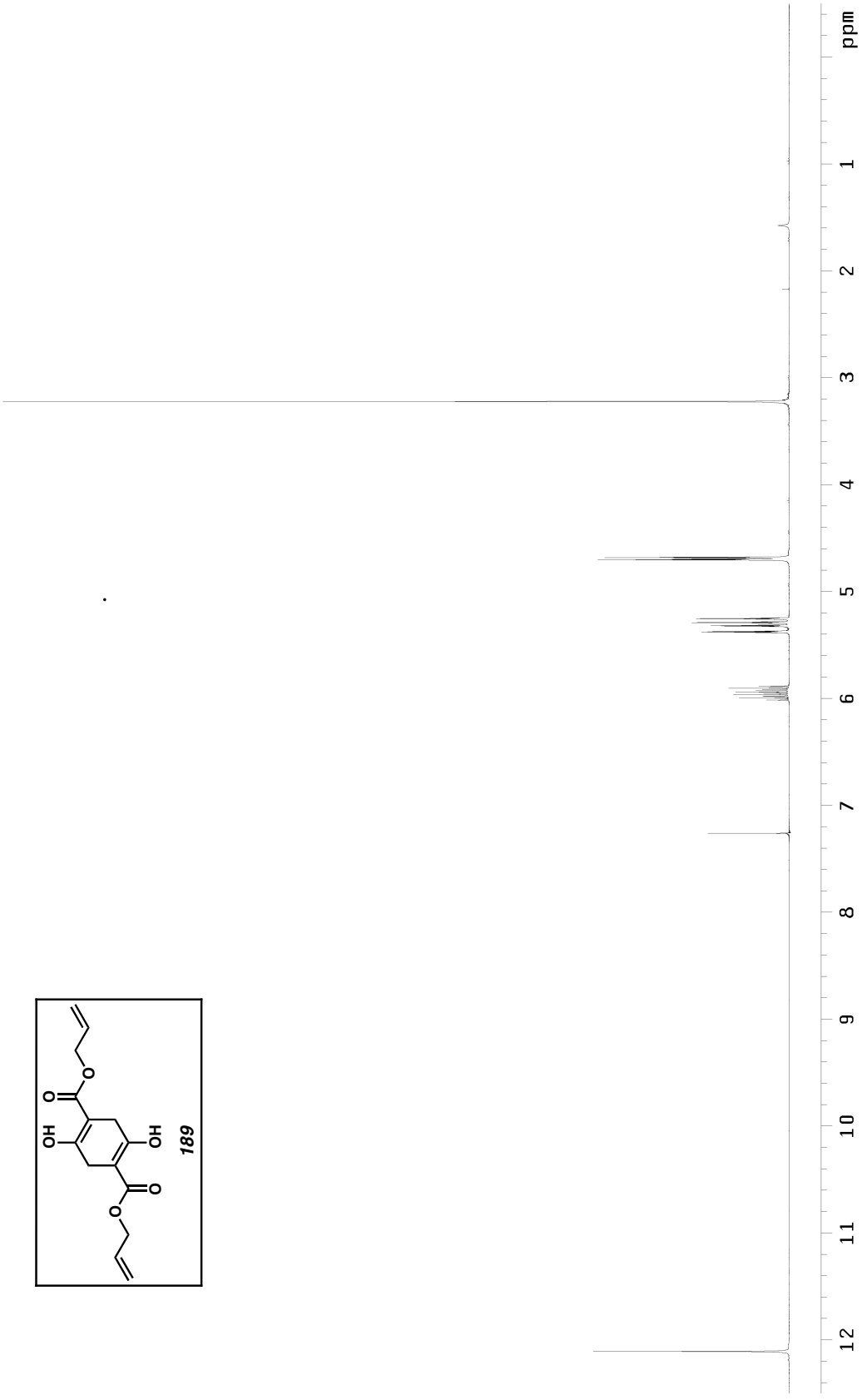

Figure A2.4 ^{1}H NMR (300 MHz, $CDCl_3$) of diallyl succinyl succinate (**189**).

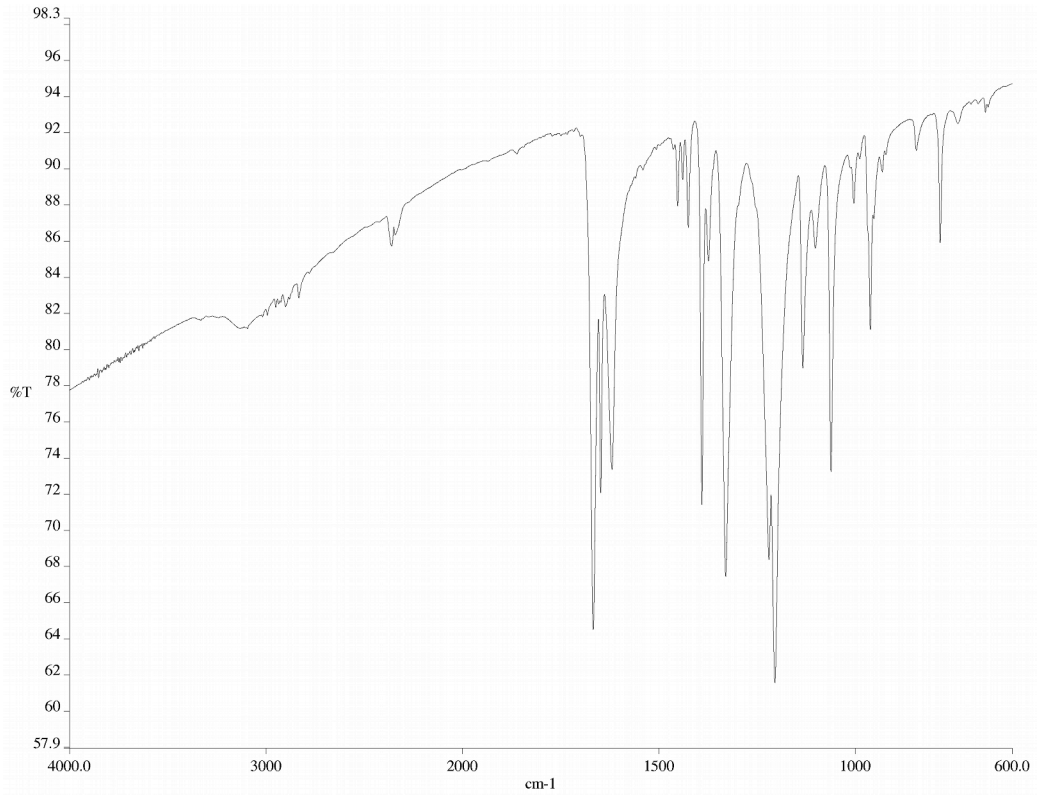

Figure A2.5 Infrared spectrum (thin film/NaCl) of diallyl succinyl succinate (**189**).

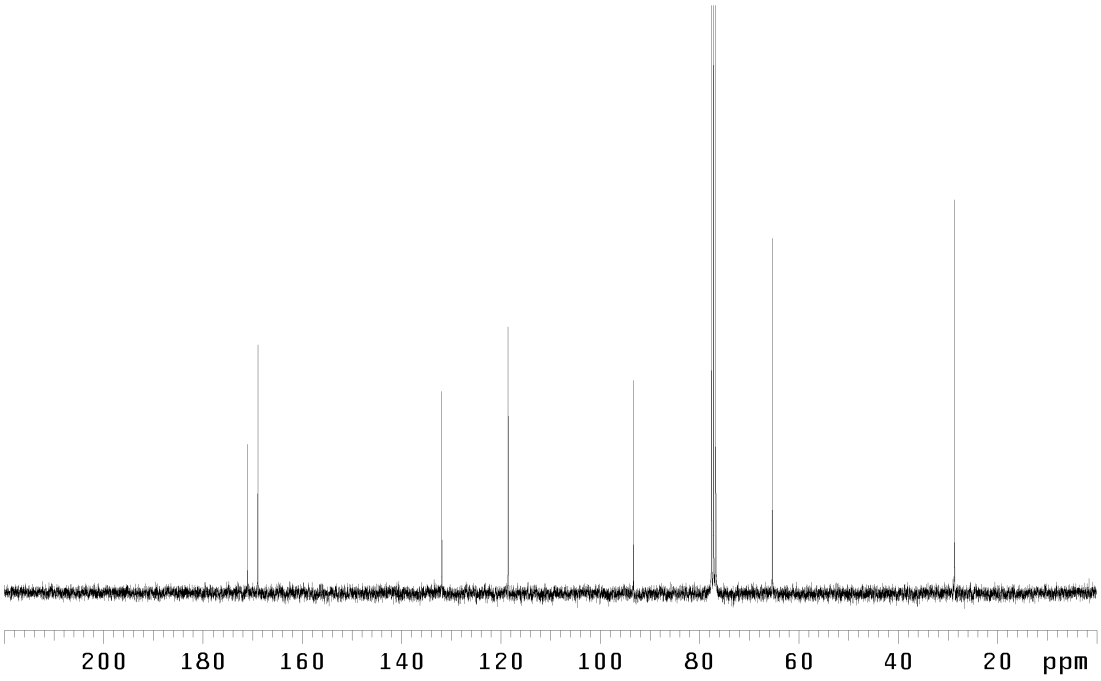

Figure A2.6 ^{13}C NMR (75 MHz, $CDCl_3$) of diallyl succinyl succinate (**189**).

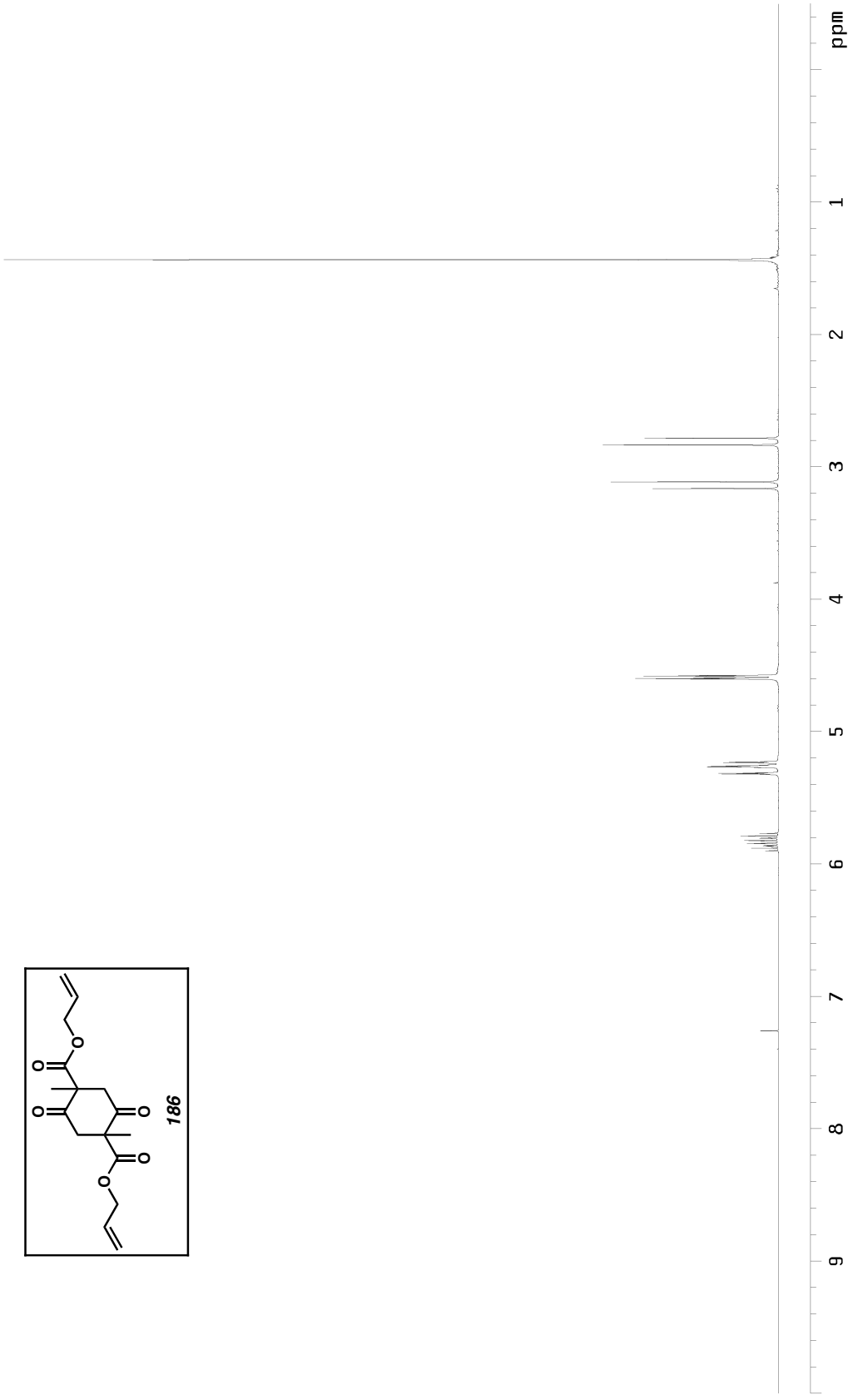

Figure A2.7 ^{1}H NMR (300 MHz, $CDCl_3$) of bis(β-ketoester) **186**.

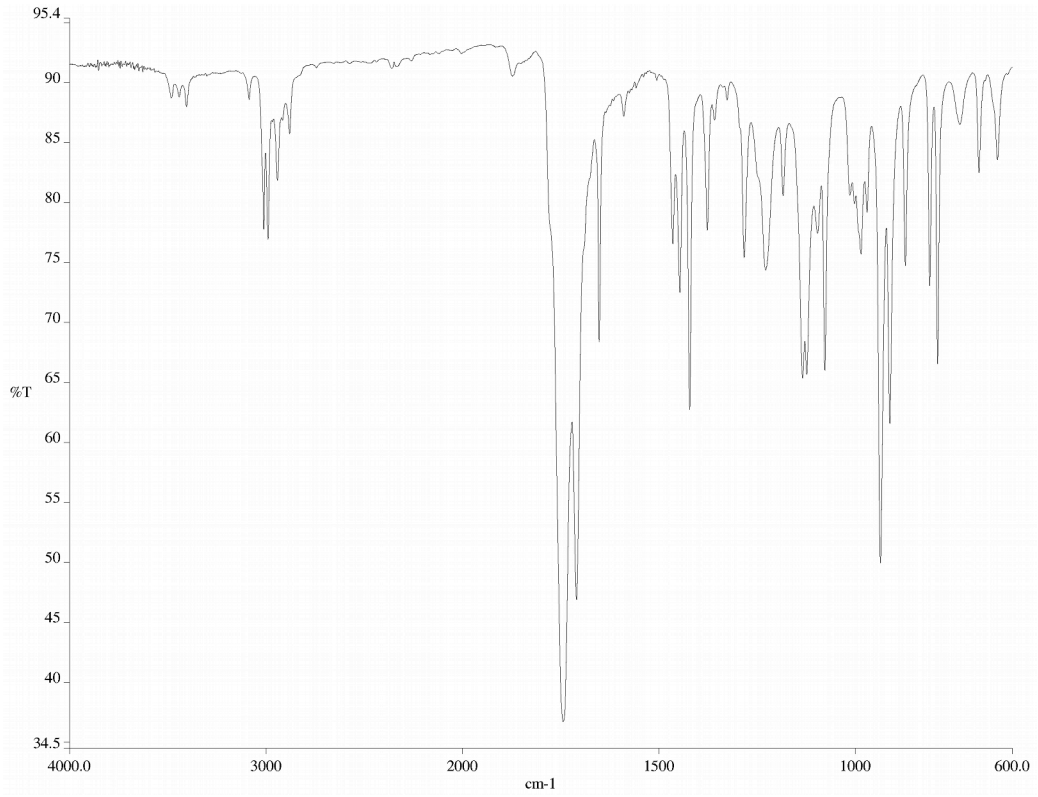

Figure A2.8 Infrared spectrum (thin film/NaCl) of bis(β-ketoester) **186**.

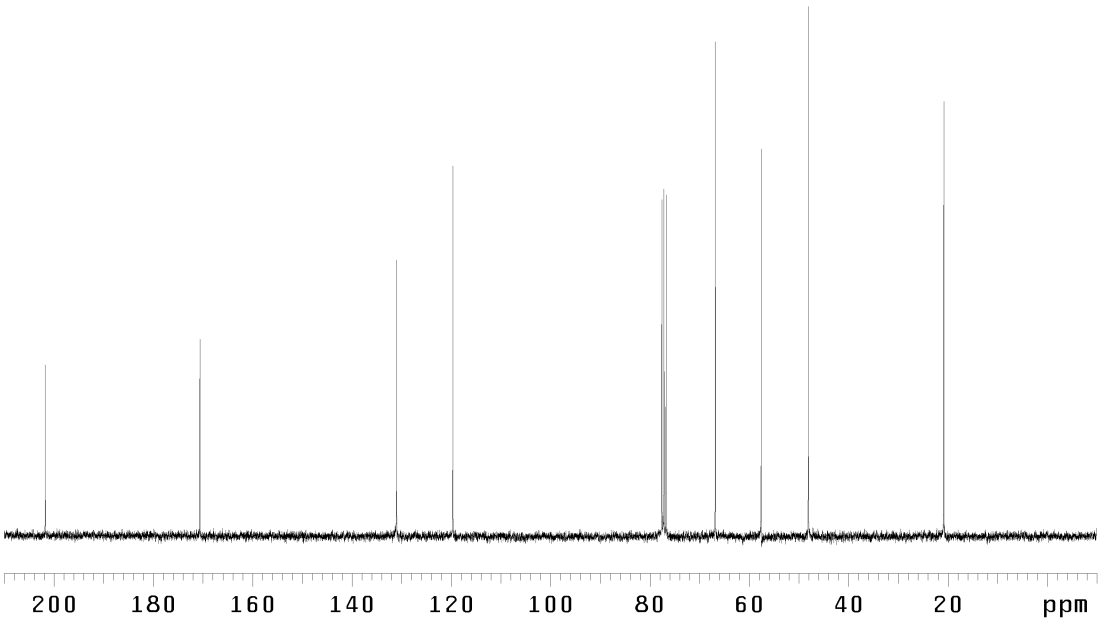

Figure A2.9 ^{13}C NMR (75 MHz, $CDCl_3$) of bis(β-ketoester) **186**.

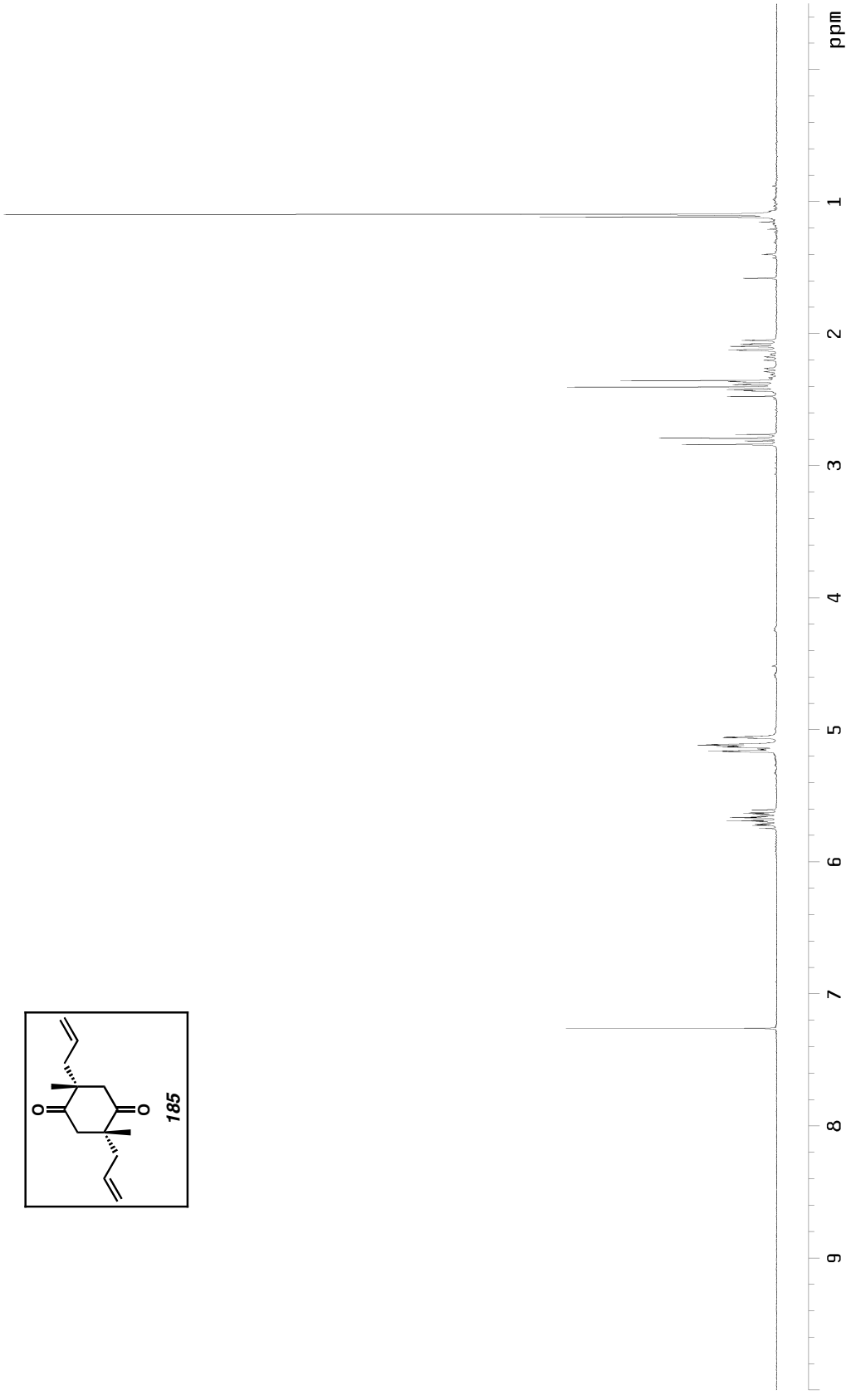

Figure A2.10 ^{1}H NMR (300 MHz, $CDCl_3$) of diketone **185**.

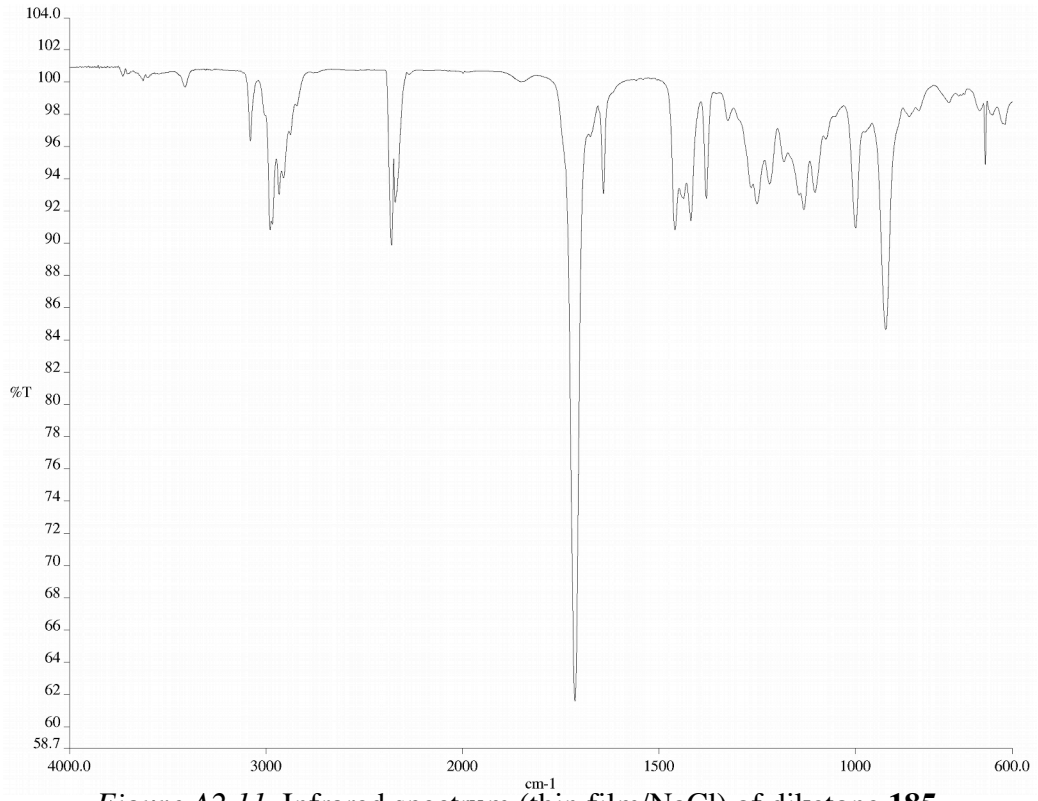

Figure A2.11 Infrared spectrum (thin film/NaCl) of diketone **185**.

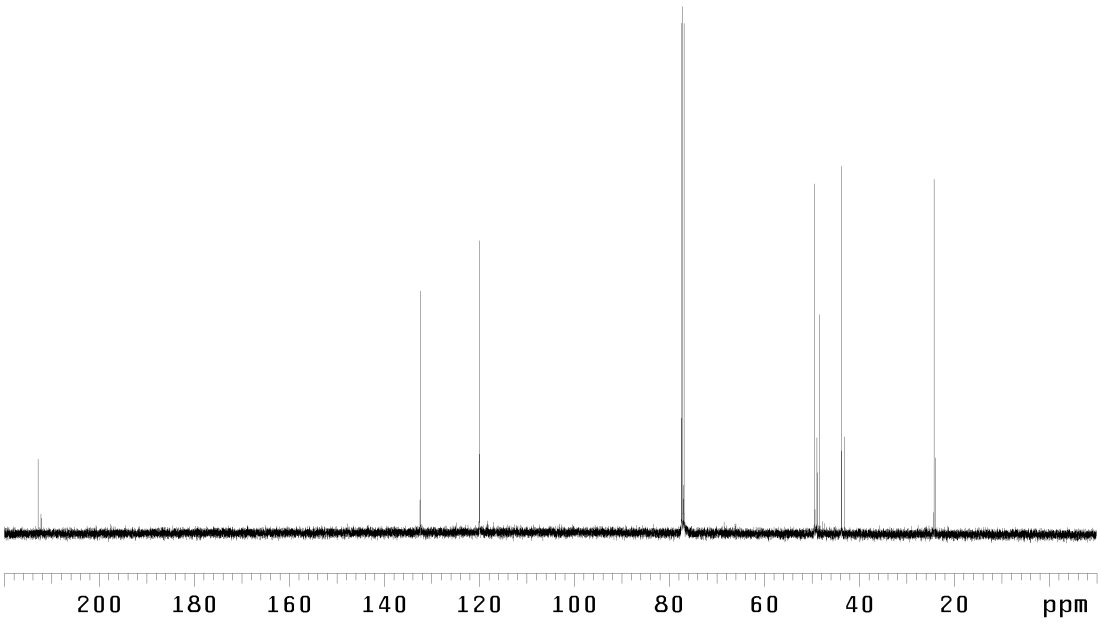

Figure A2.12 ^{13}C NMR (125 MHz, $CDCl_3$) of diketone **185**.

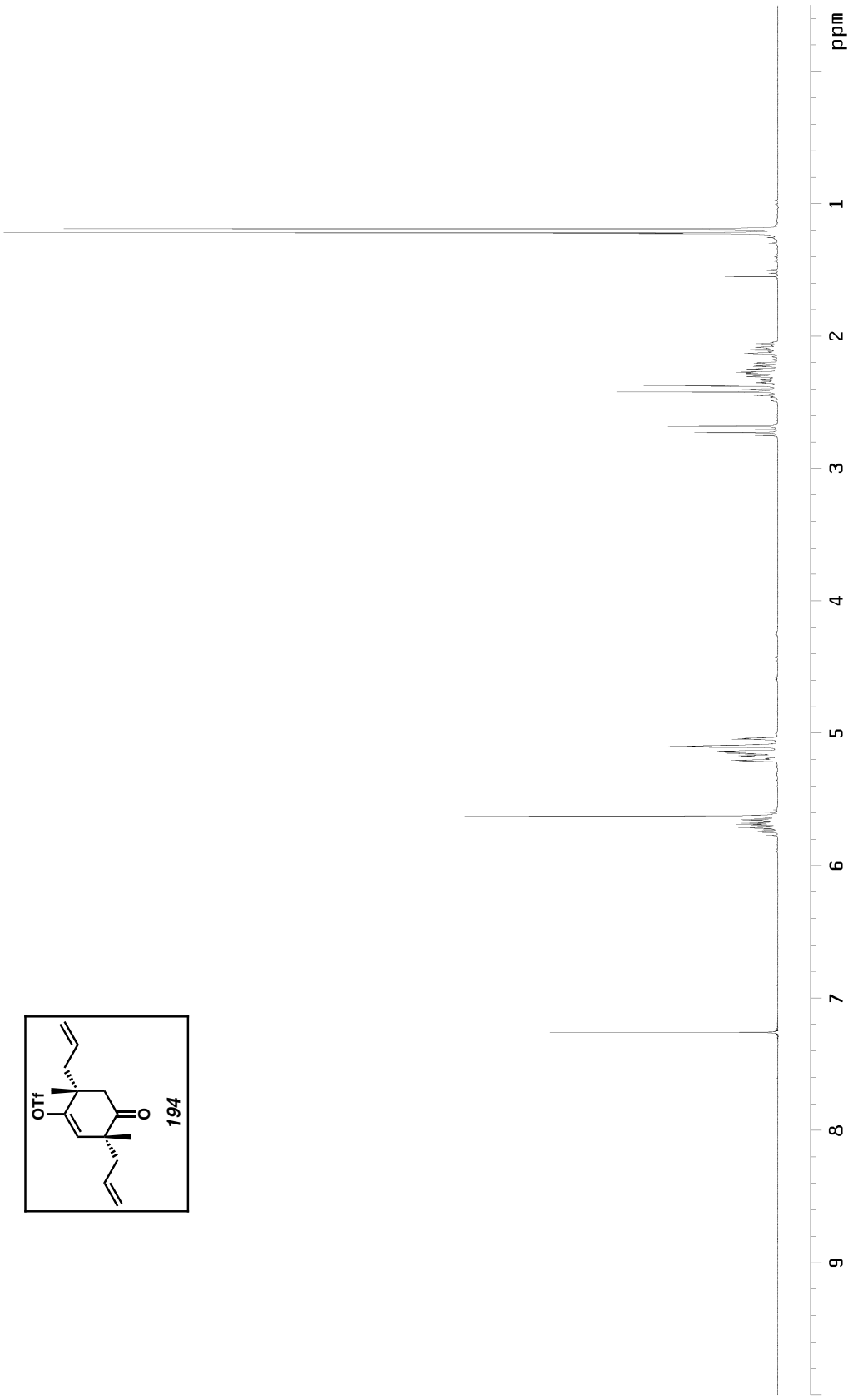

Figure A2.13 ^{1}H NMR (300 MHz, $CDCl_3$) of triflate **194**.

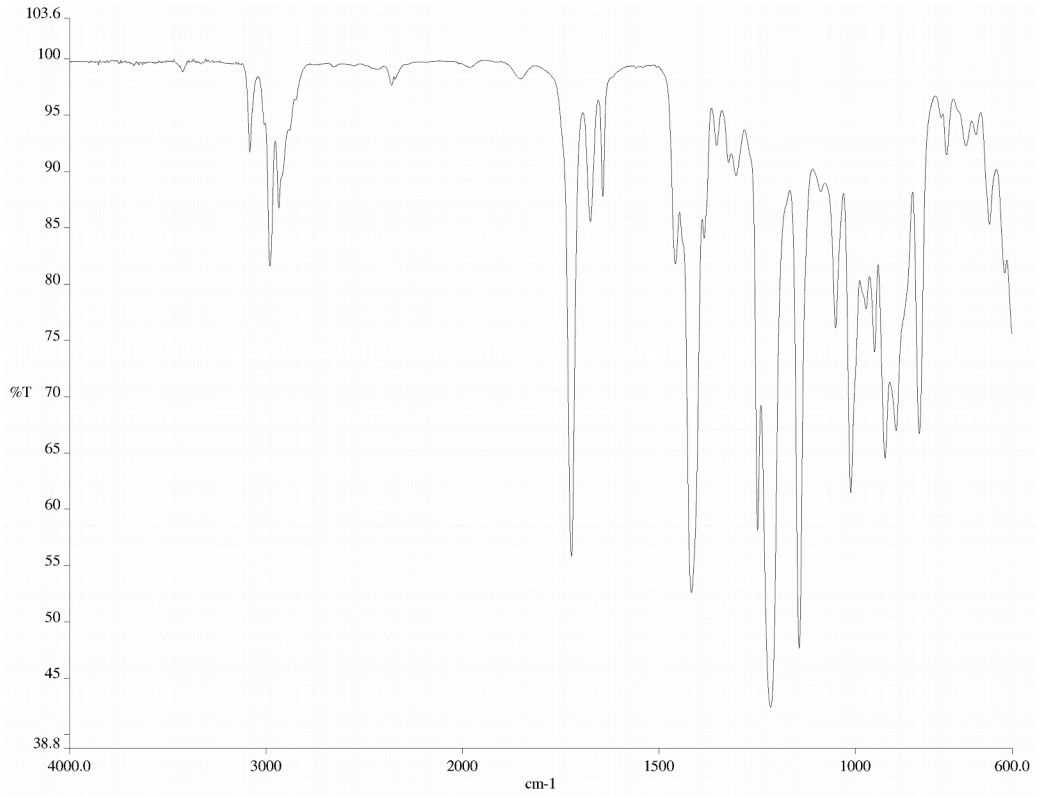

Figure A2.14 Infrared spectrum (thin film/NaCl) of trilfate **194**.

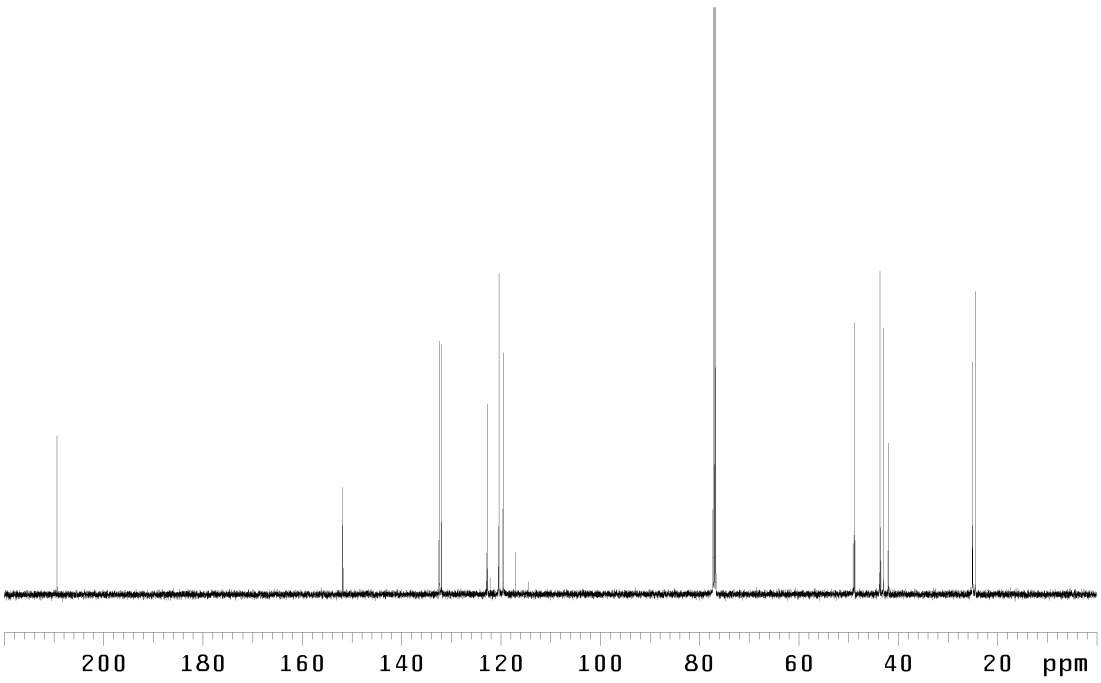

Figure A2.15 ^{13}C NMR (125 MHz, $CDCl_3$) of triflate **194**.

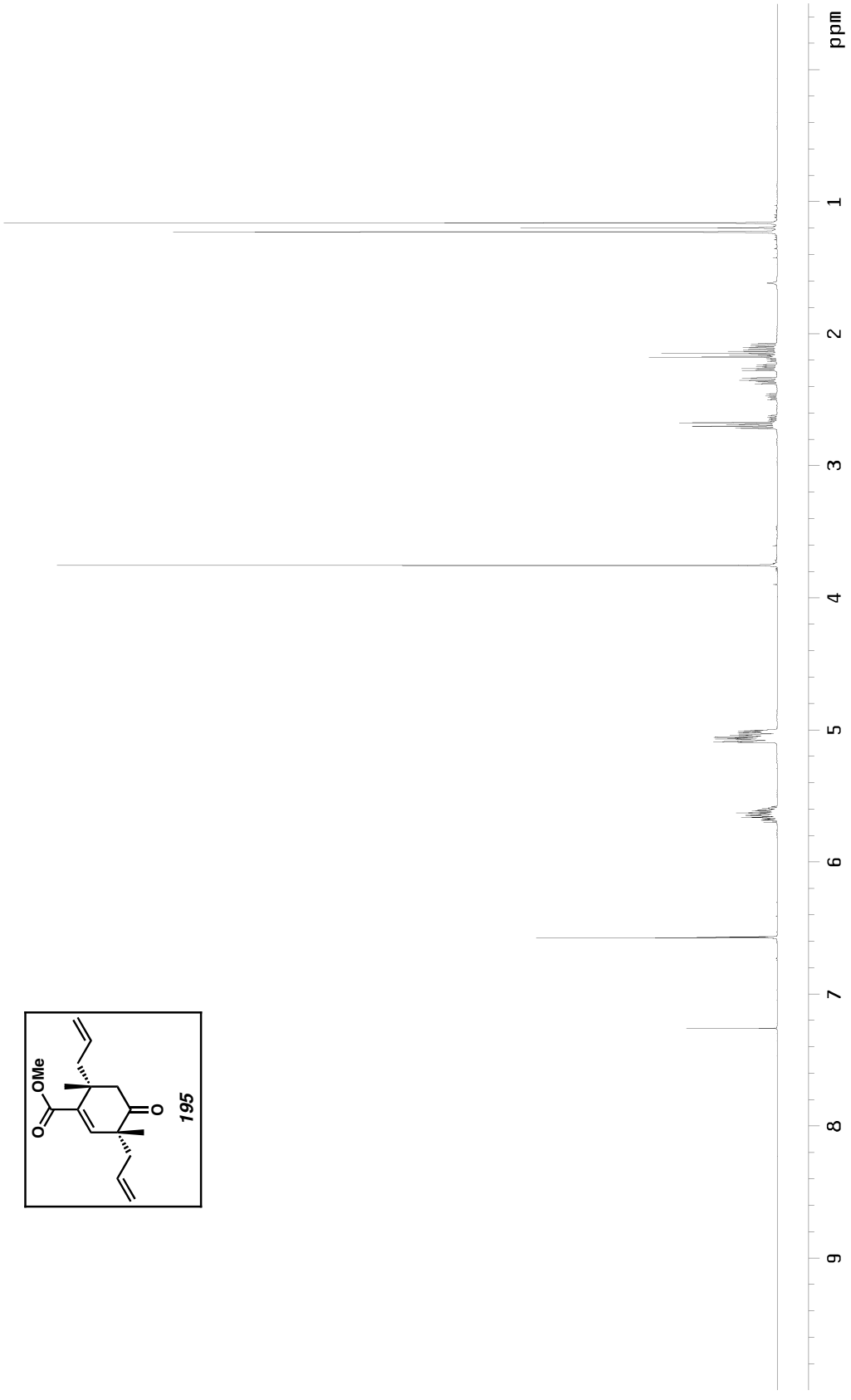

Figure A2.16 ^{1}H NMR (500 MHz, $CDCl_3$) of enoate **195**.

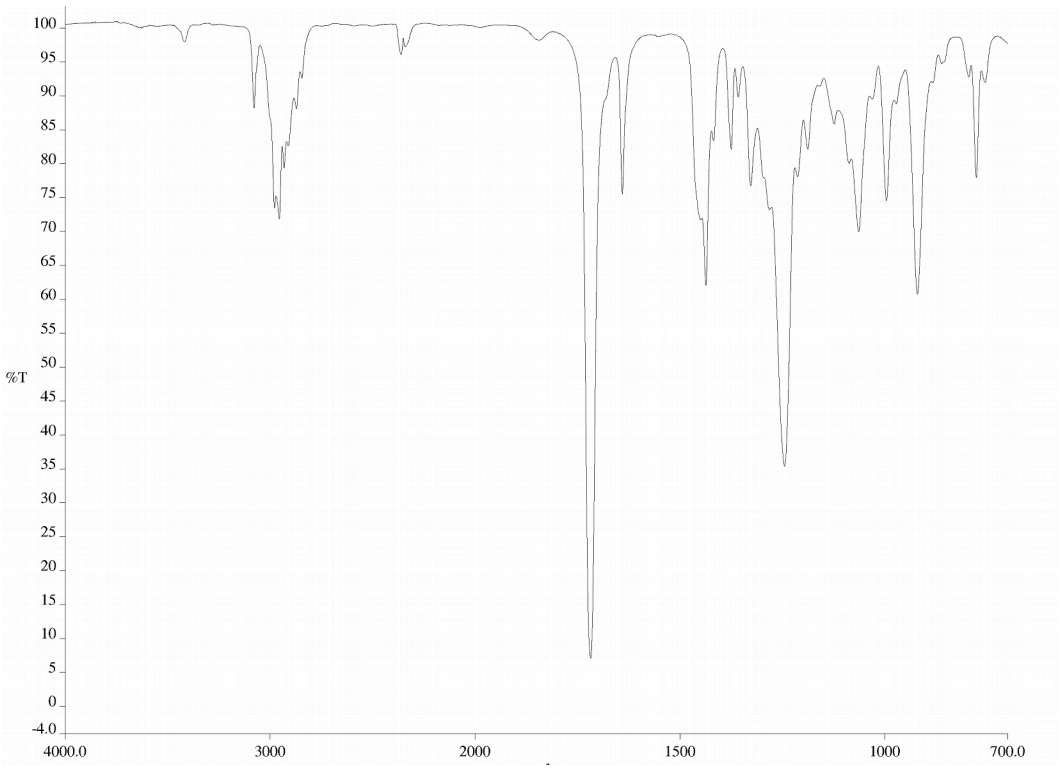

Figure A2.17 Infrared spectrum (thin film/NaCl) of enoate **195**.

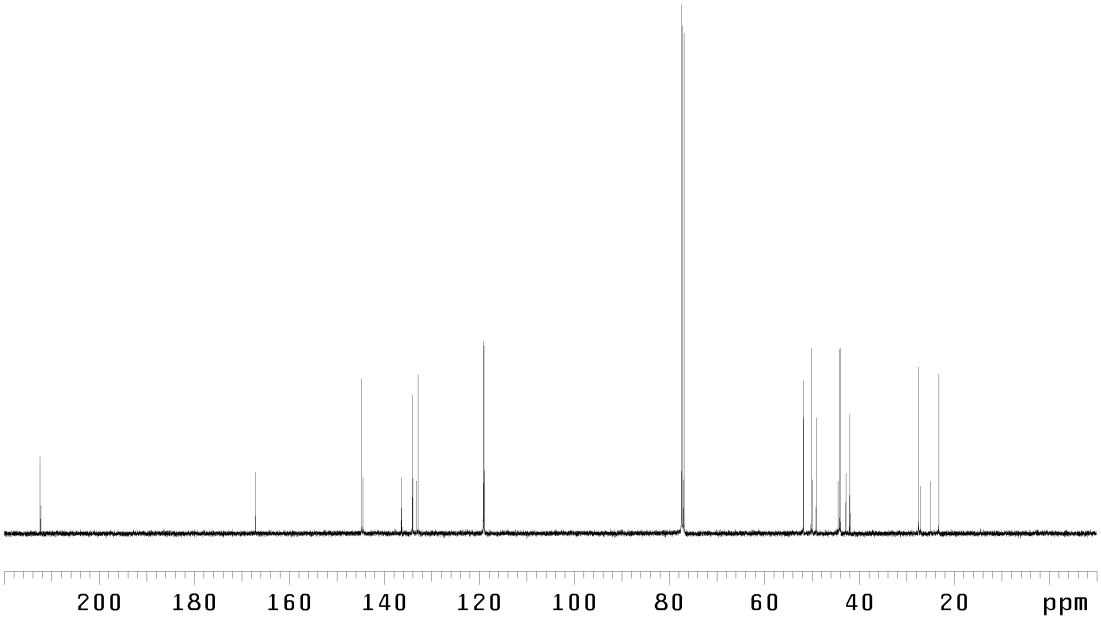

Figure A2.18 ^{13}C NMR (125 MHz, $CDCl_3$) of enoate **195**.

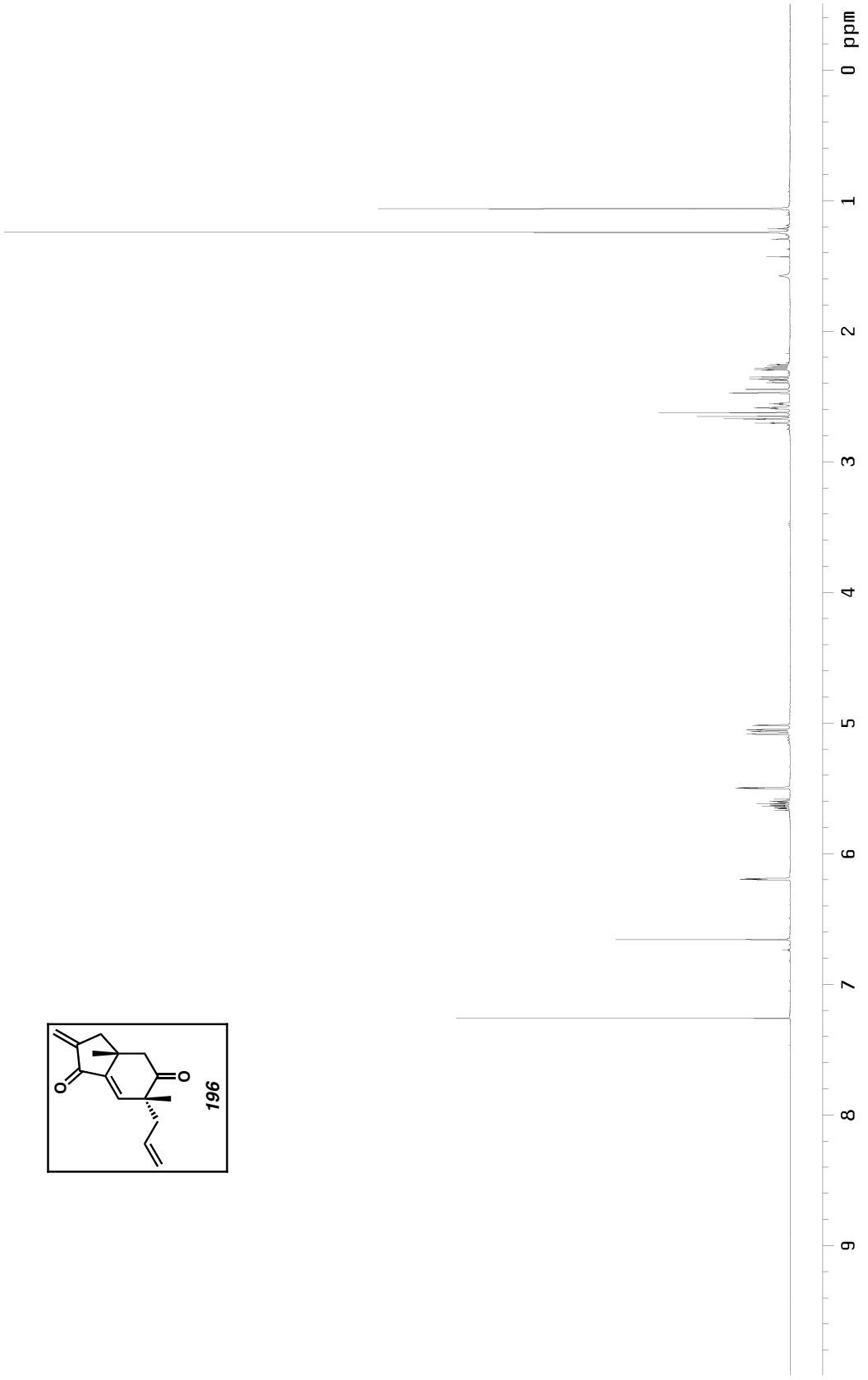

Figure A2.19 ^{1}H NMR (500 MHz, $CDCl_3$) of cyclopentadienone **196**.

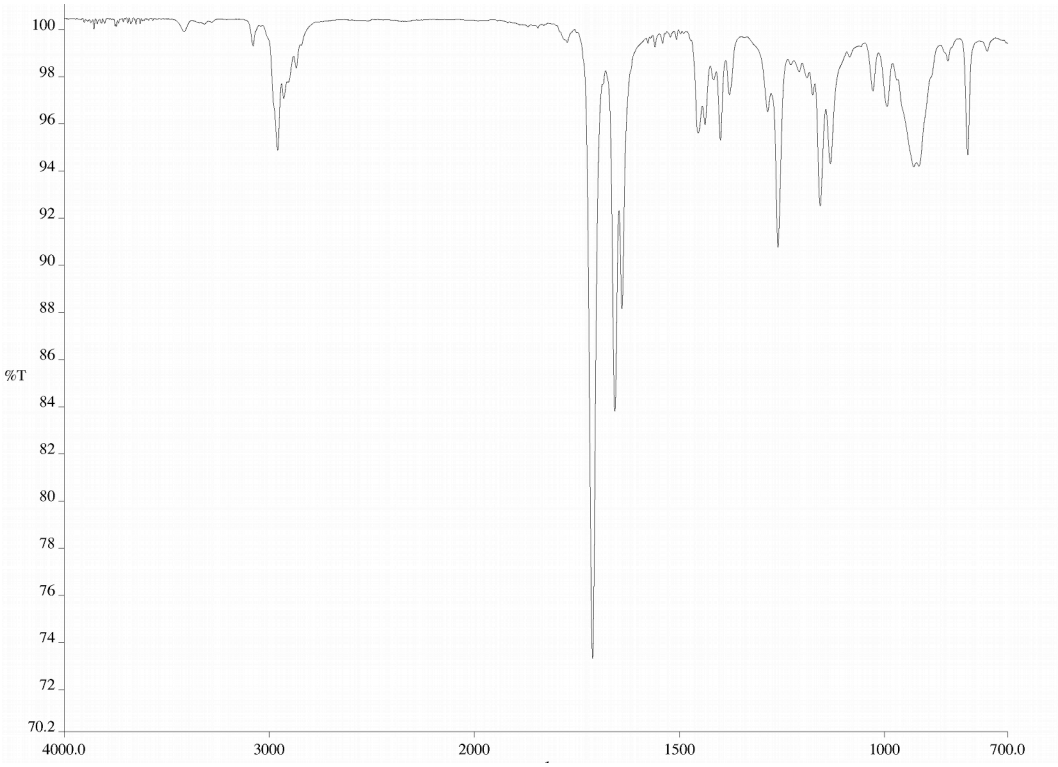

Figure A2.20 Infrared spectrum (thin film/NaCl) of cyclopentadienone **196**.

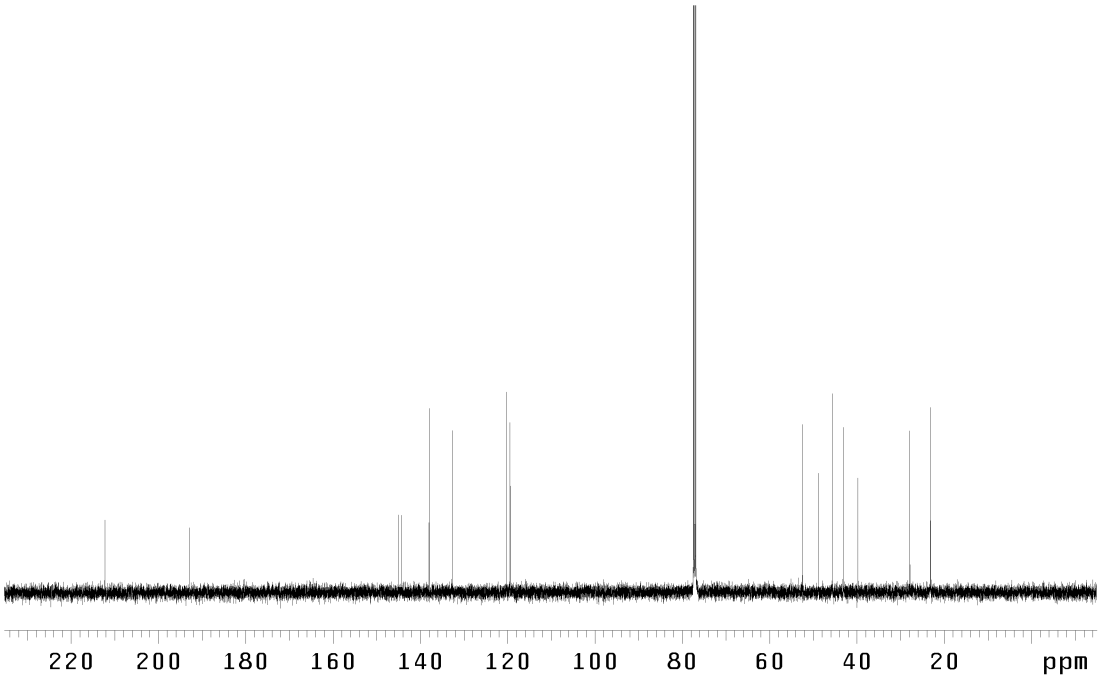

Figure A2.21 ^{13}C NMR (125 MHz, $CDCl_3$) of cyclopentadienone **196**.

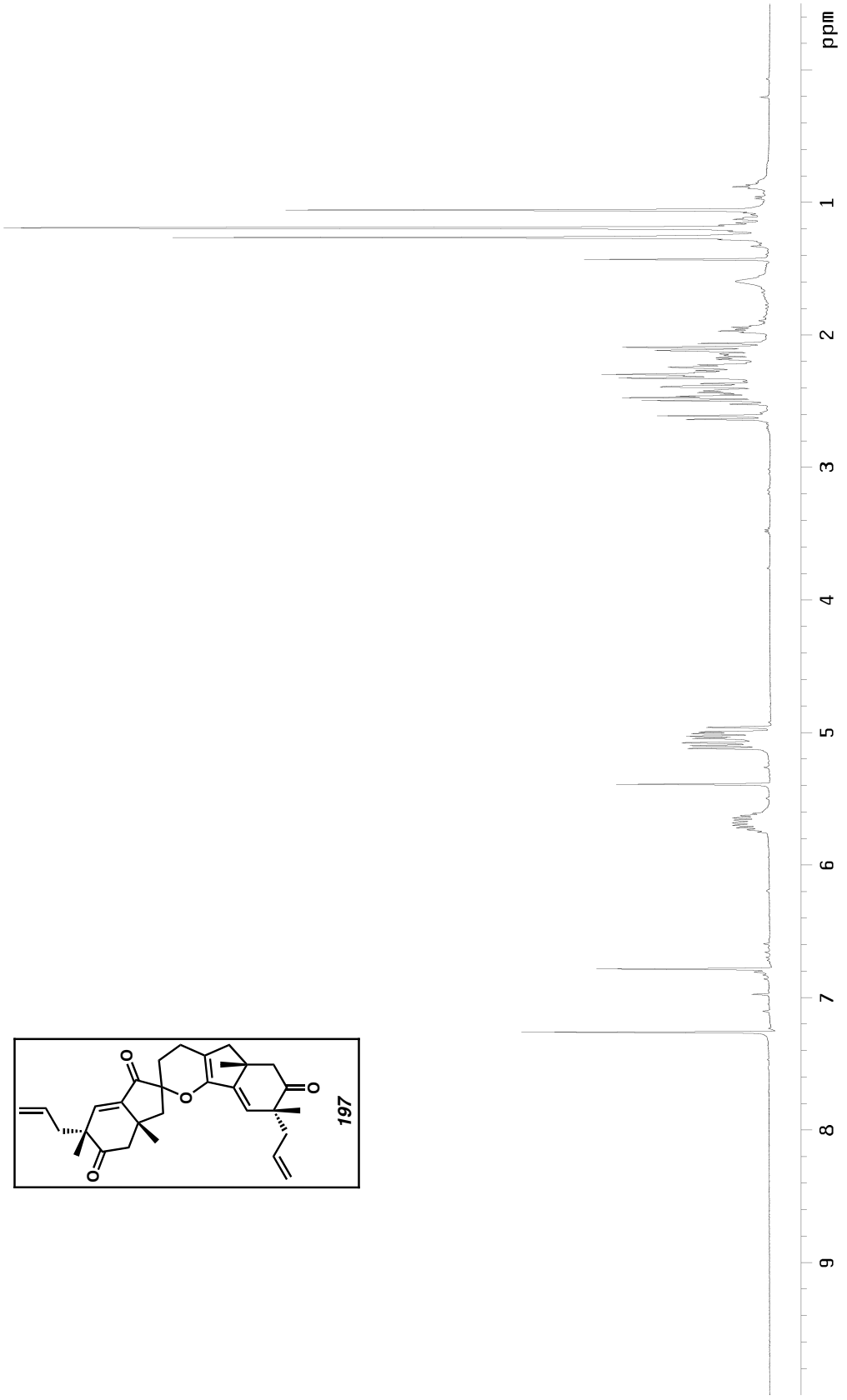

Figure A2.22 ^{1}H NMR (500 MHz, $CDCl_3$) of spirocycle **197**.

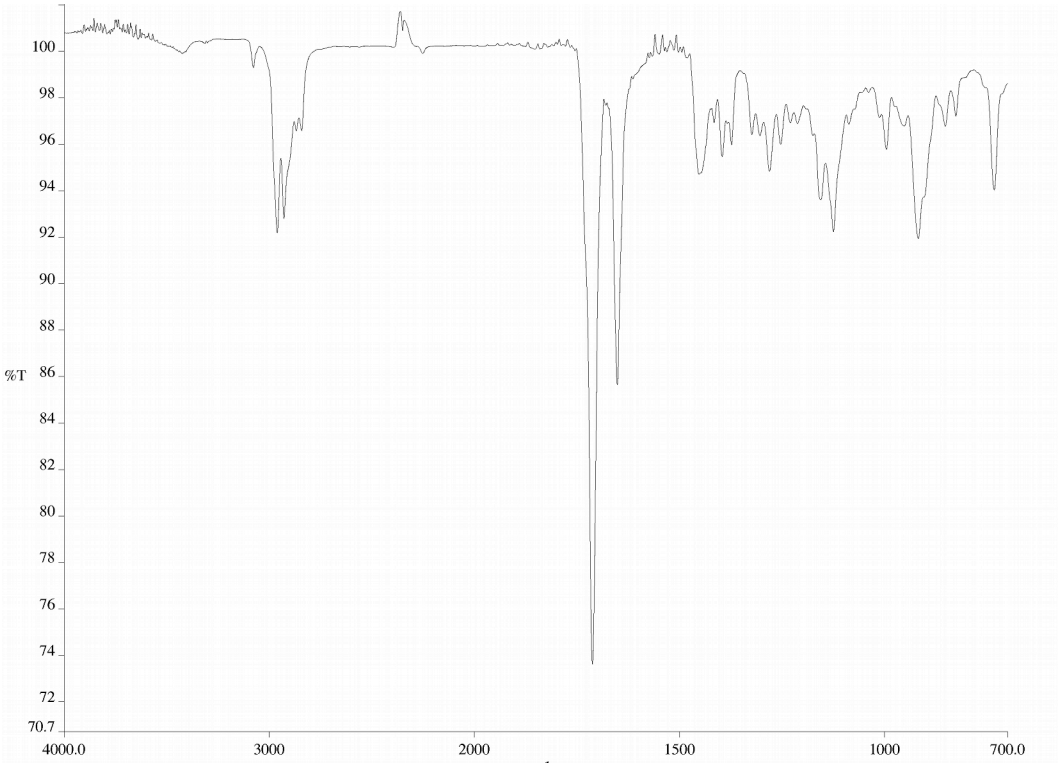

Figure A2.23 Infrared spectrum (thin film/NaCl) of spirocycle **197**.

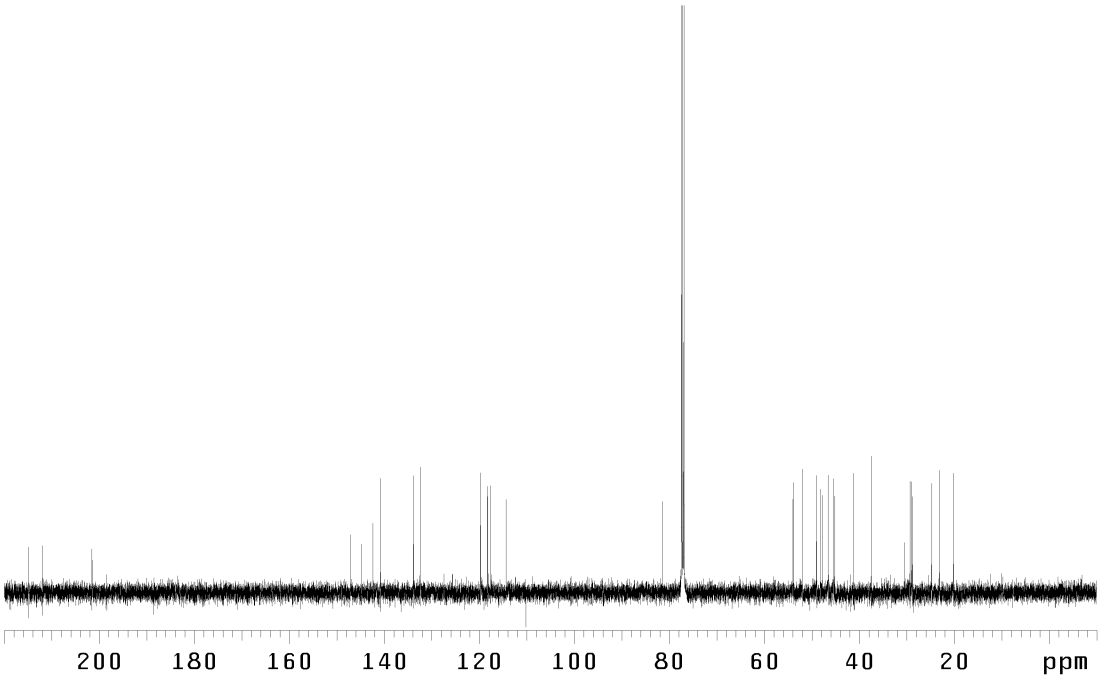

Figure A2.24 ^{13}C NMR (125 MHz, $CDCl_3$) of spirocycle **197**.

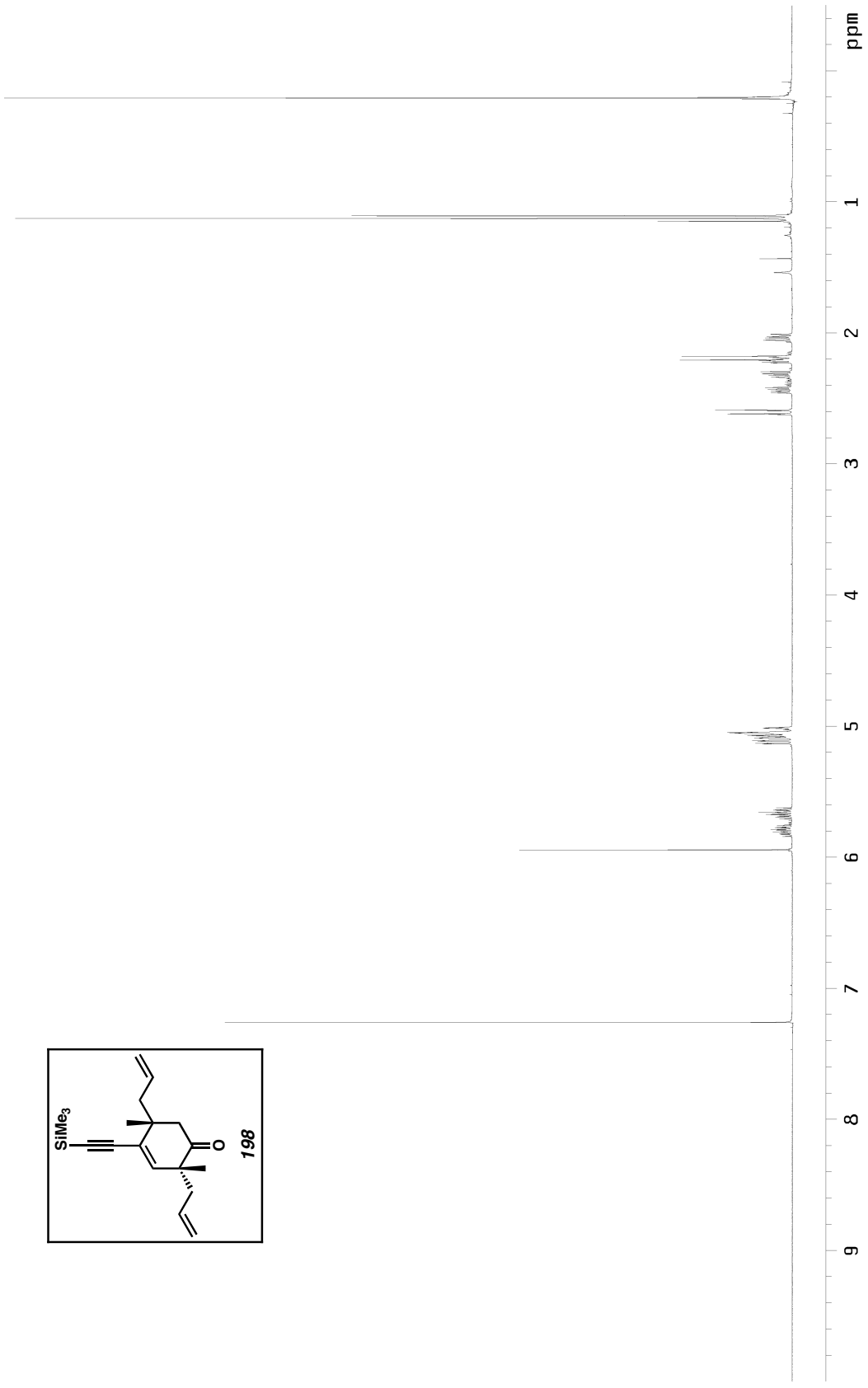

Figure A2.25 ^{1}H NMR (500 MHz, $CDCl_3$) of alkyne **198**.

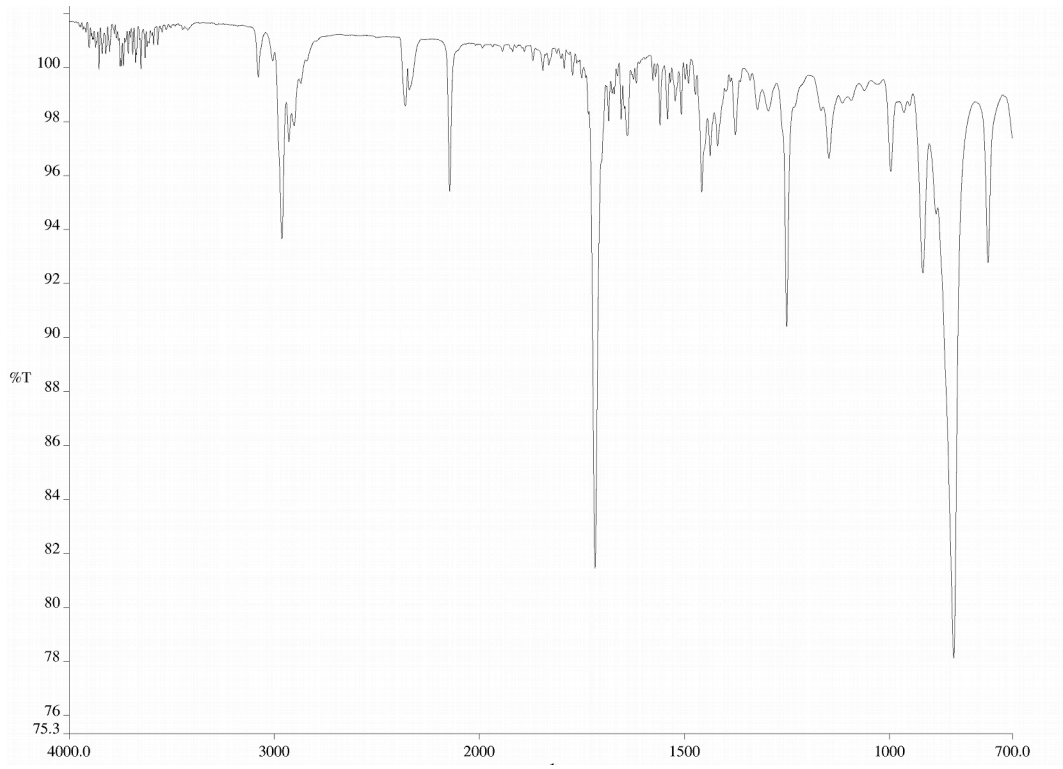

Figure A2.26 Infrared spectrum (thin film/NaCl) of alkyne **198**.

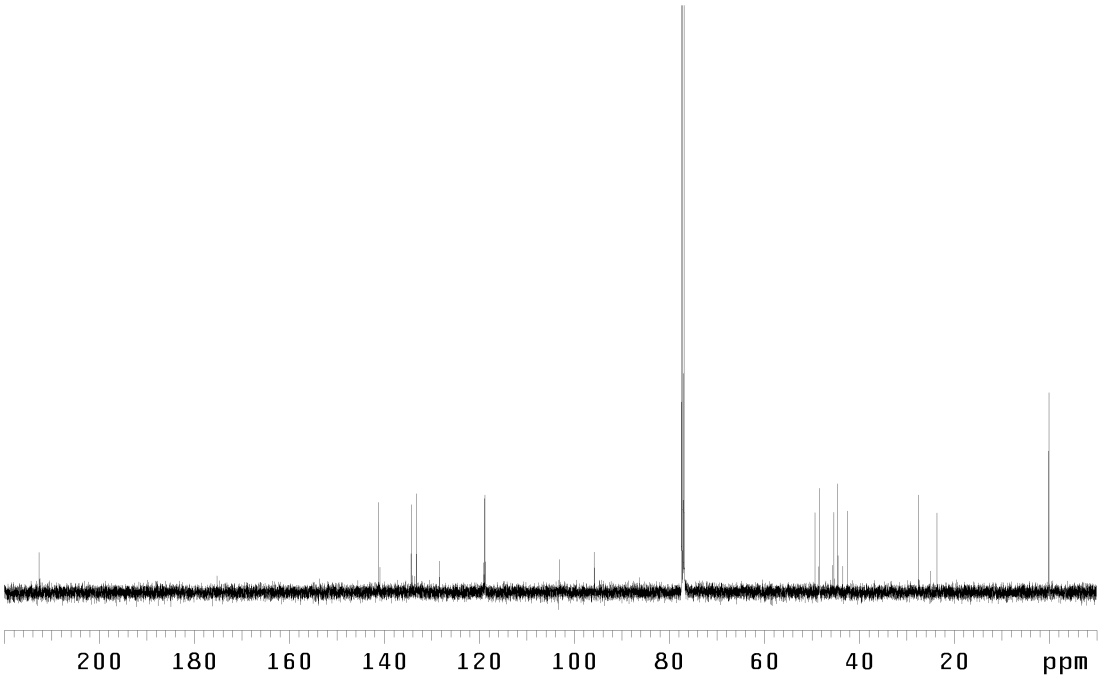

Figure A2.27 ^{13}C NMR (500 MHz, $CDCl_3$) of alkyne **198**.

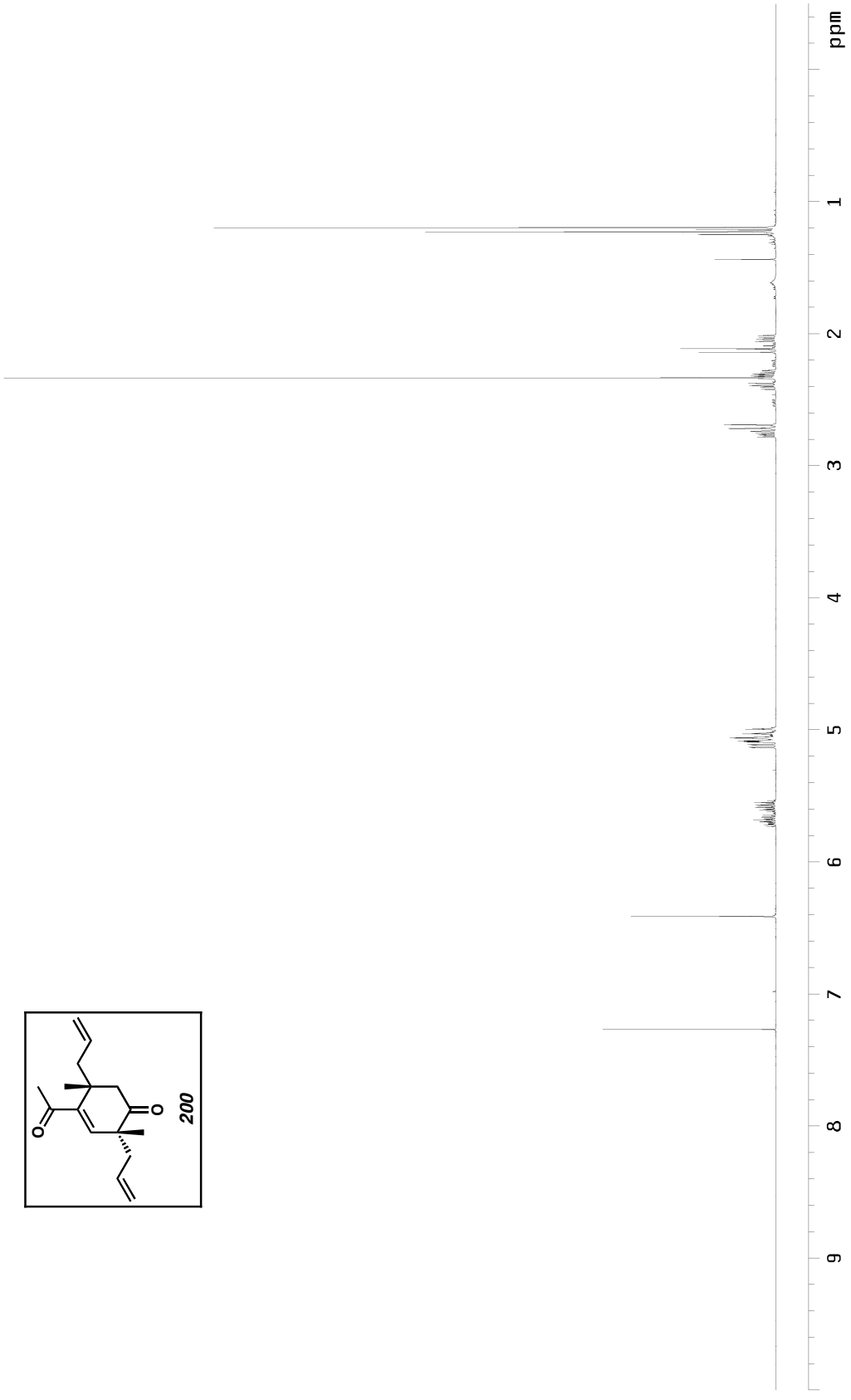

Figure A2.28 ^{1}H NMR (500 MHz, $CDCl_3$) of ketone **200**.

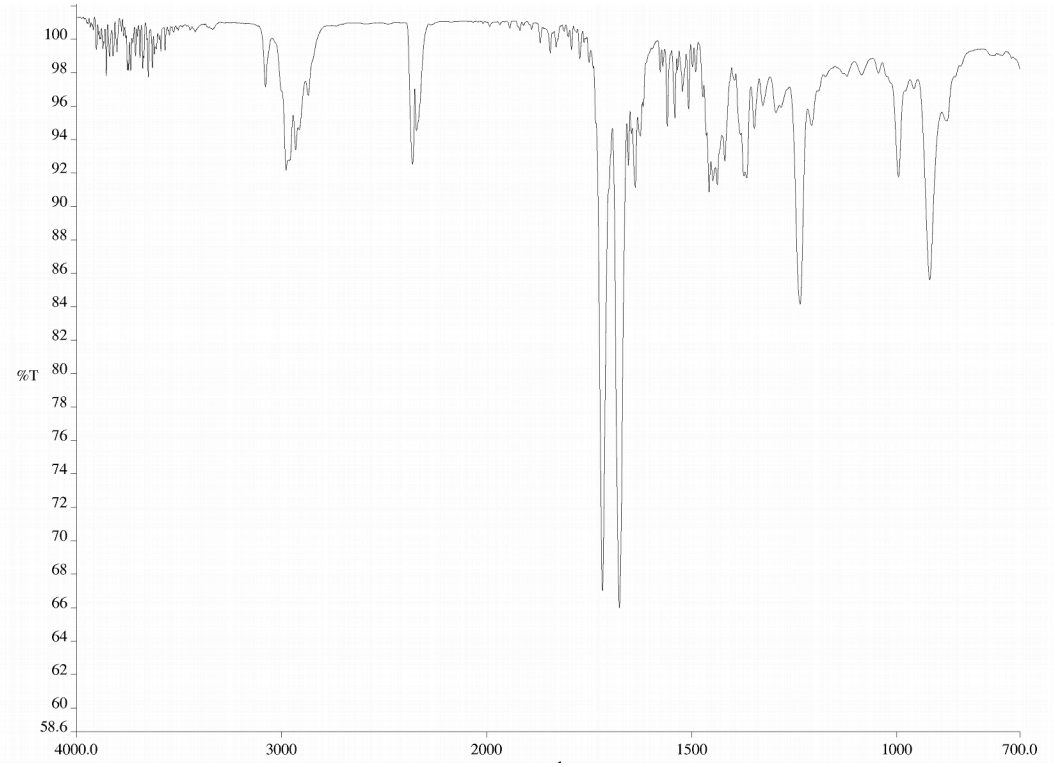

Figure A2.29 Infrared spectrum (thin film/NaCl) of ketone **200**.

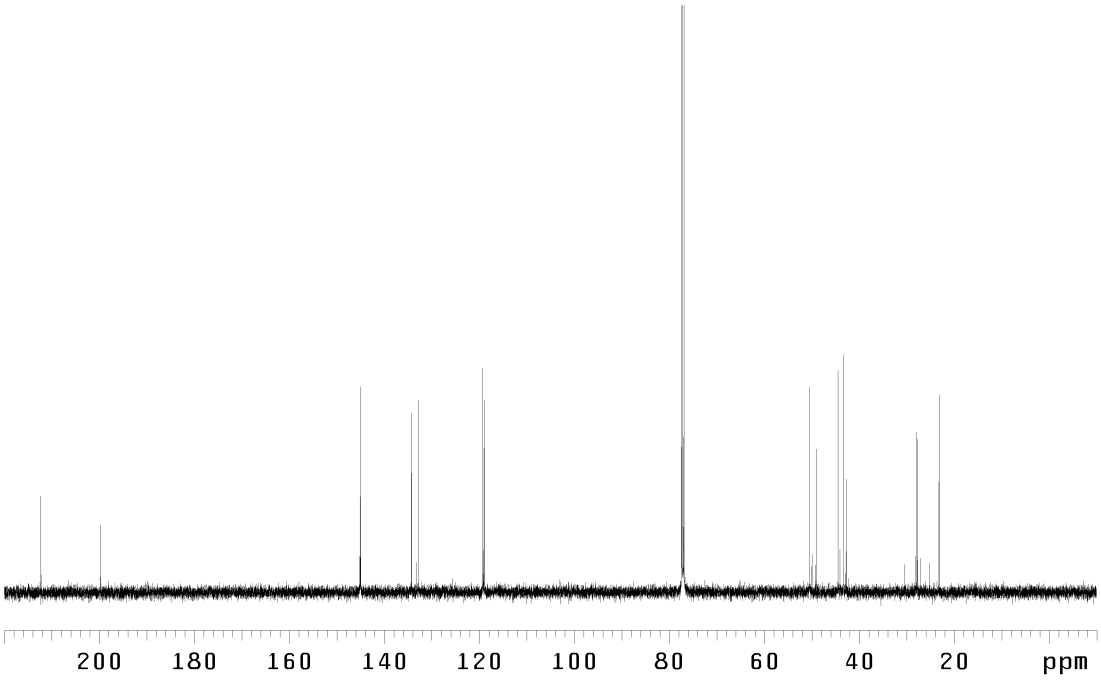

Figure A2.30 ^{13}C NMR (125 MHz, $CDCl_3$) of ketone **200**.

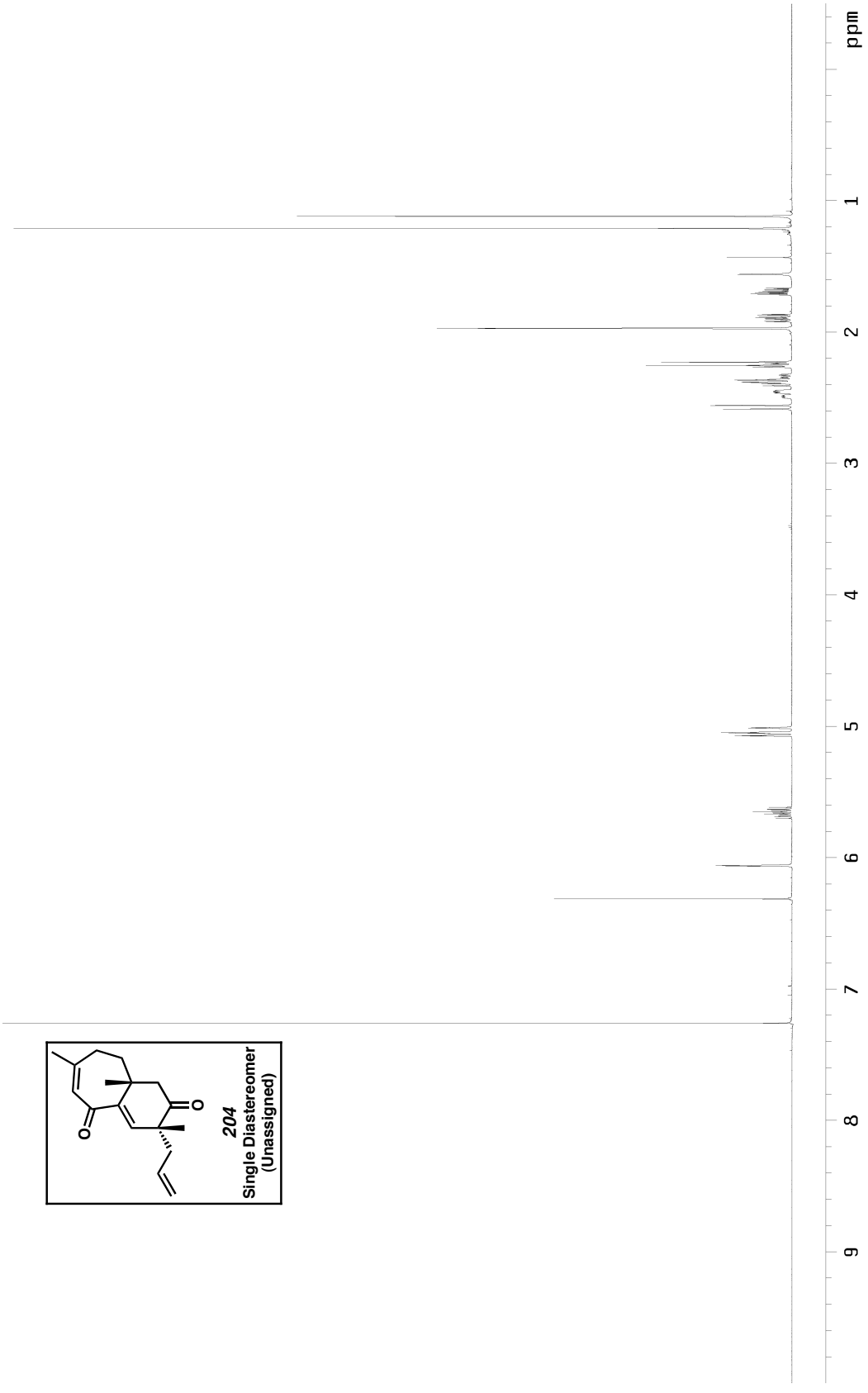

Figure A2.31 ^{1}H NMR (500 MHz, $CDCl_3$) of bicyclic enone **204(A)**.

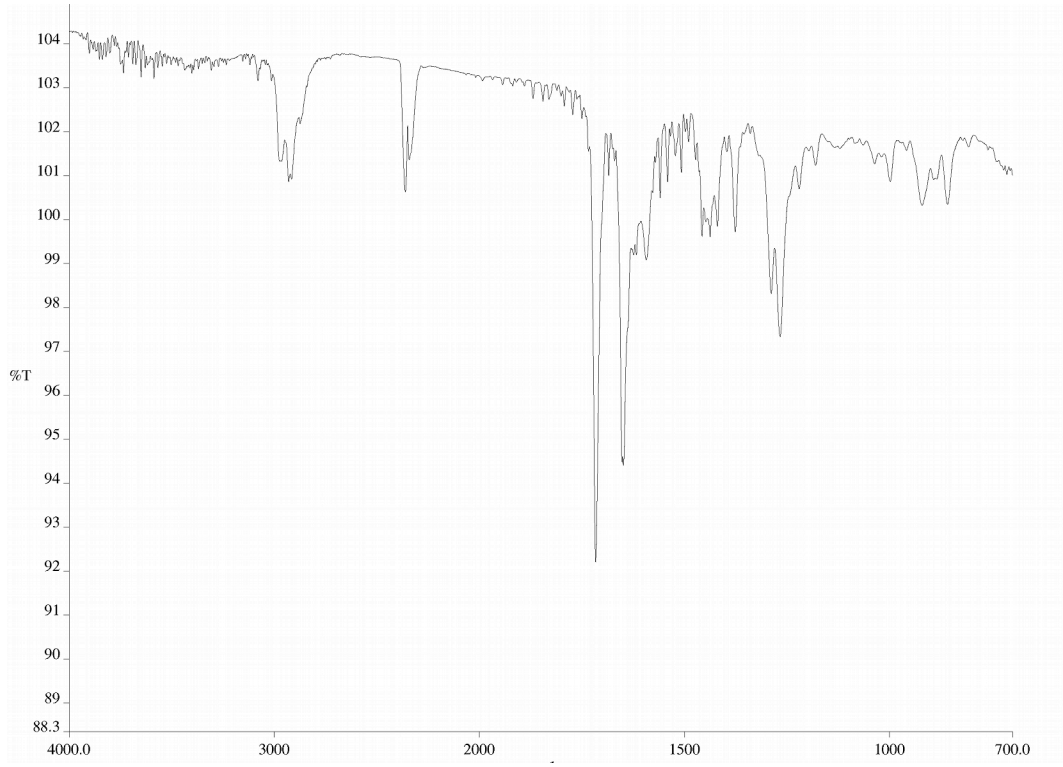

Figure A2.32 Infrared spectrum (thin film/NaCl) of bicyclic enone **204(A)**.

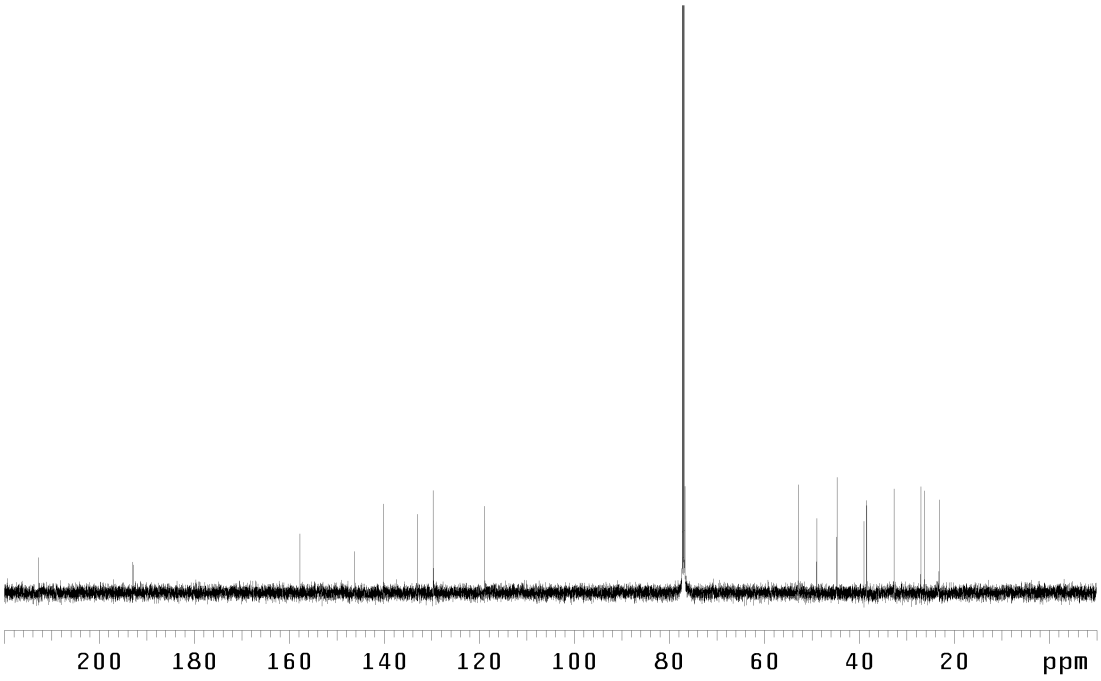

Figure A2.33 ^{13}C NMR (125 MHz, $CDCl_3$) of bicyclic enone **204(A)**.

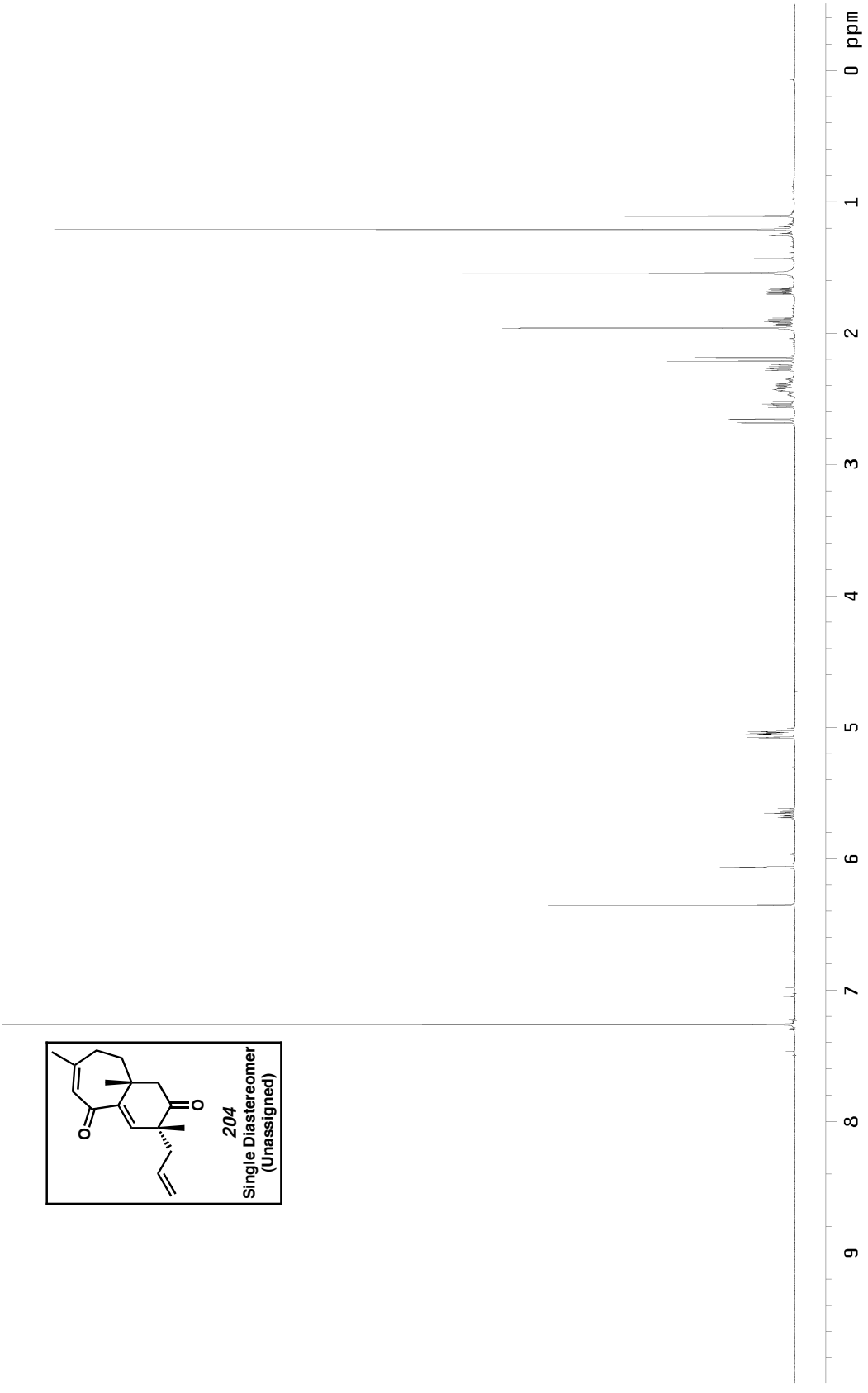

Figure A2.34 ^{1}H NMR (500 MHz, $CDCl_3$) of bicyclic enone **204(B)**.

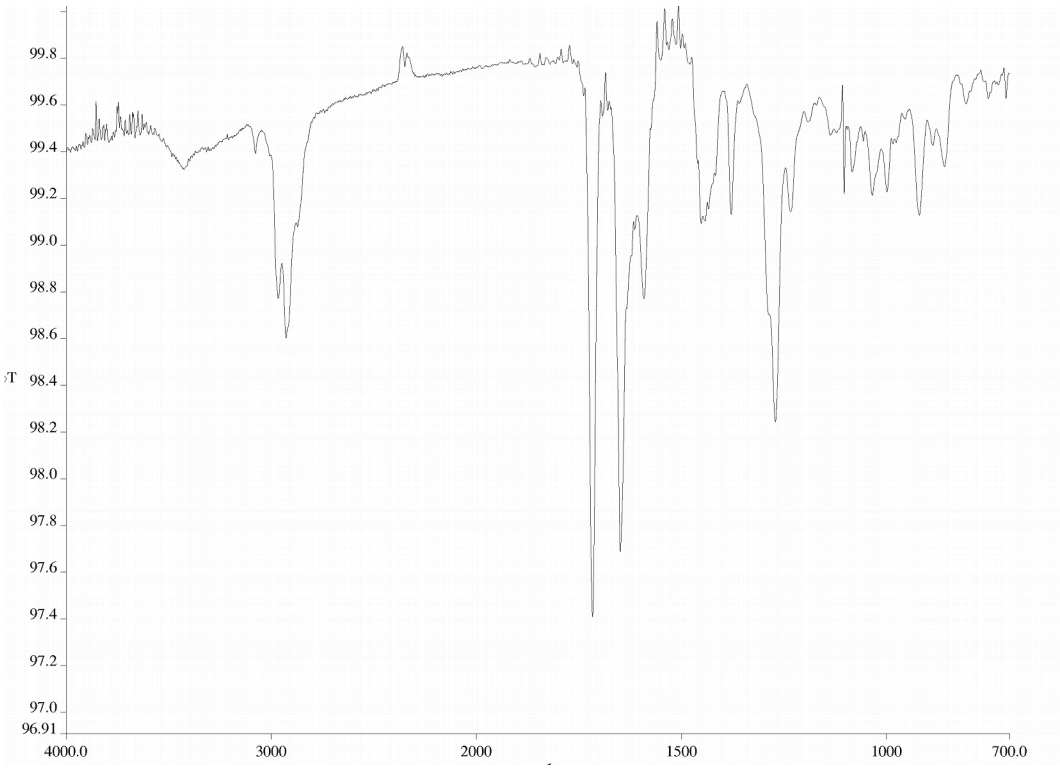

Figure A2.35 Infrared spectrum (thin film/NaCl) of bicyclic enone **204(B)**.

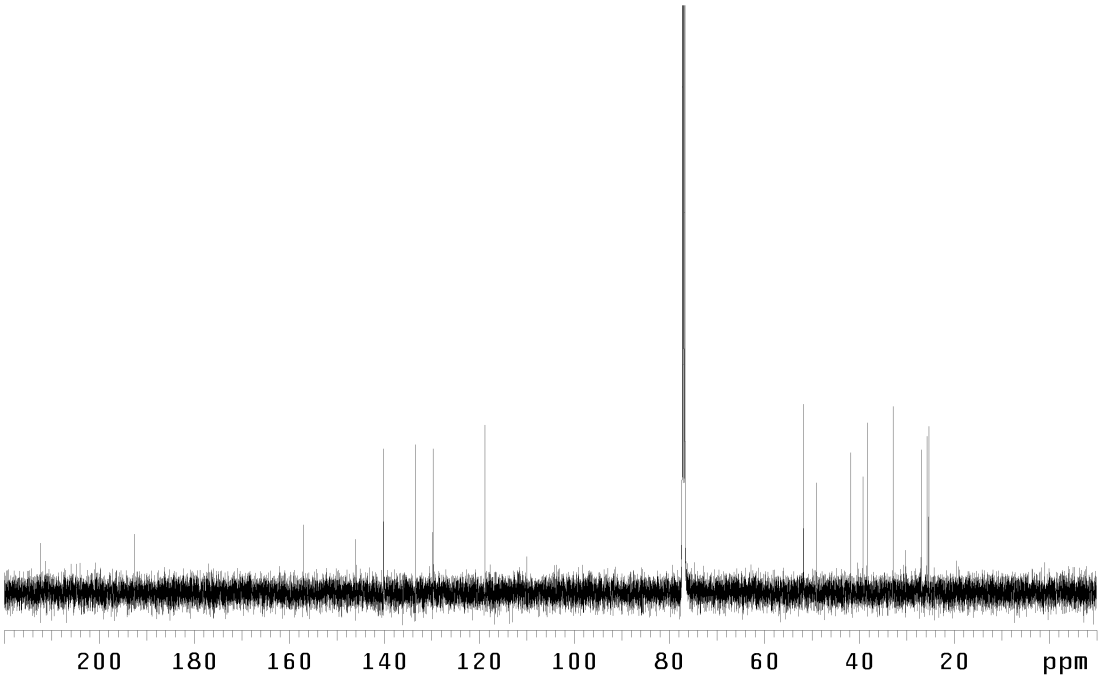

Figure A2.36 ^{13}C NMR (125 MHz, $CDCl_3$) of bicyclic enone **204(B)**.

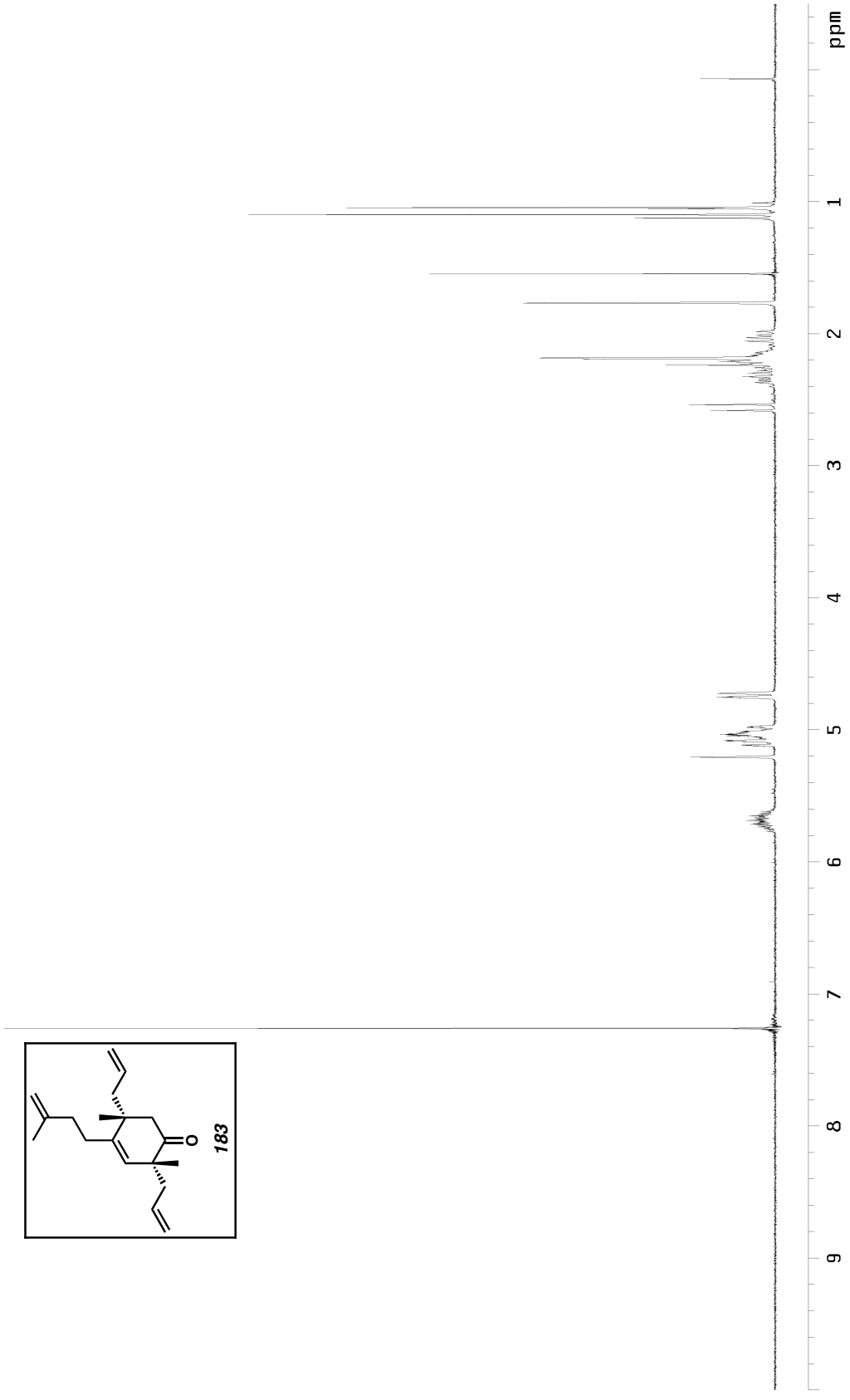

Figure A2.37 ^{1}H NMR (300 MHz, $CDCl_3$) of tetraolefin **183**.

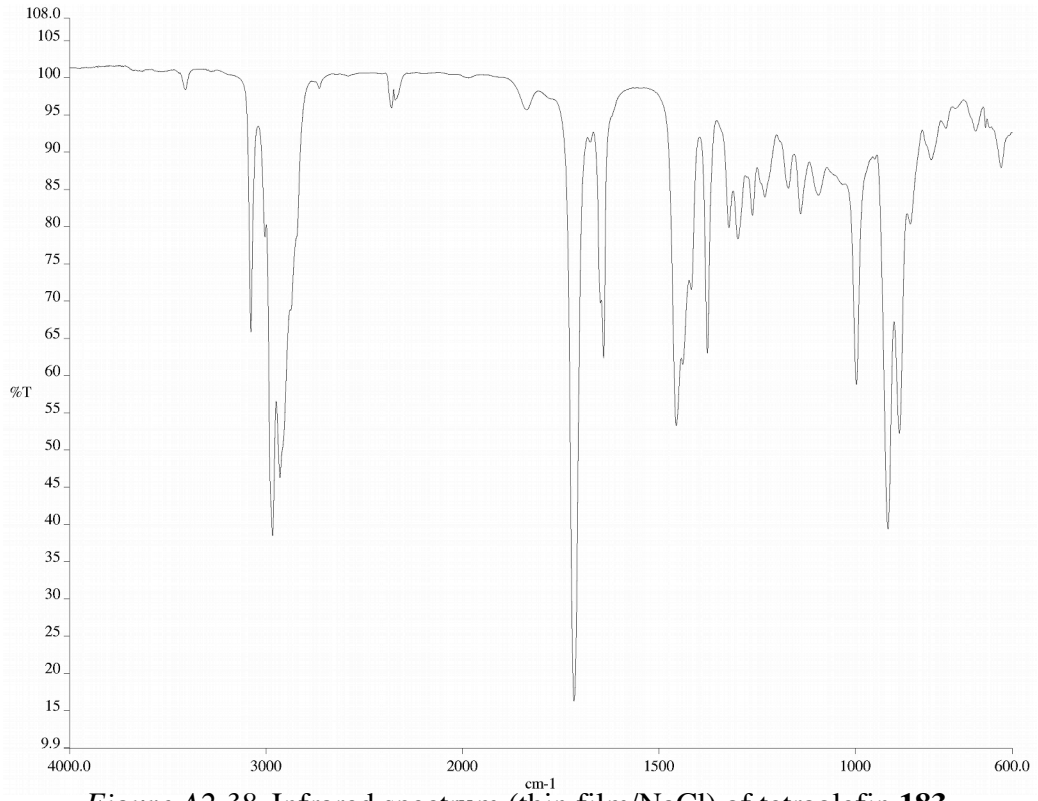

Figure A2.38 Infrared spectrum (thin film/NaCl) of tetraolefin **183**.

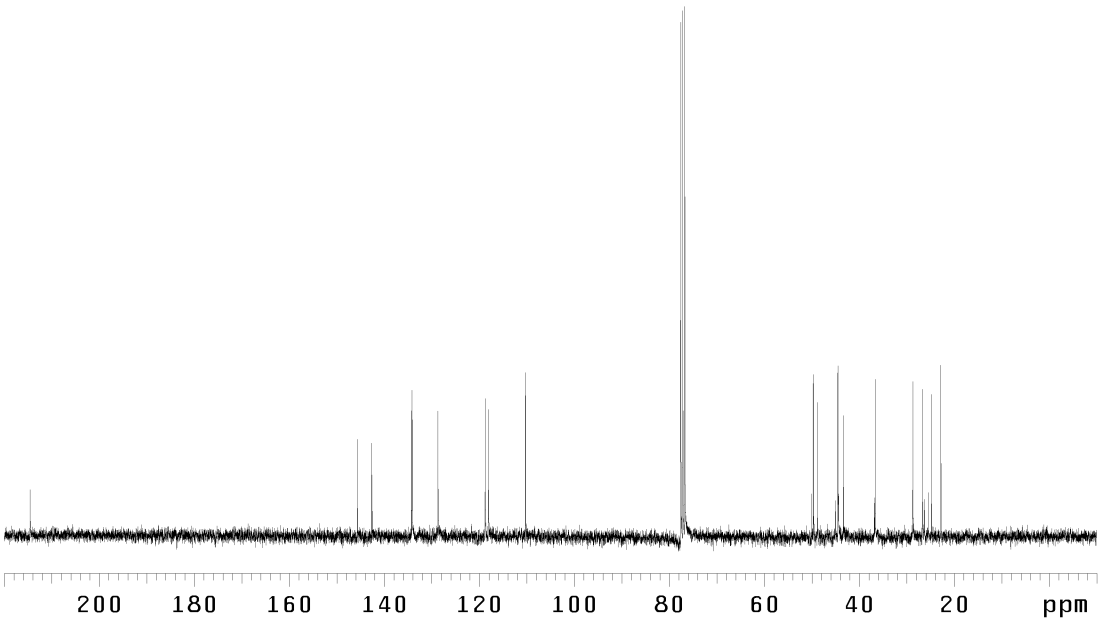

Figure A2.39 ^{13}C NMR (75 MHz, $CDCl_3$) of tetraolefin **183**.

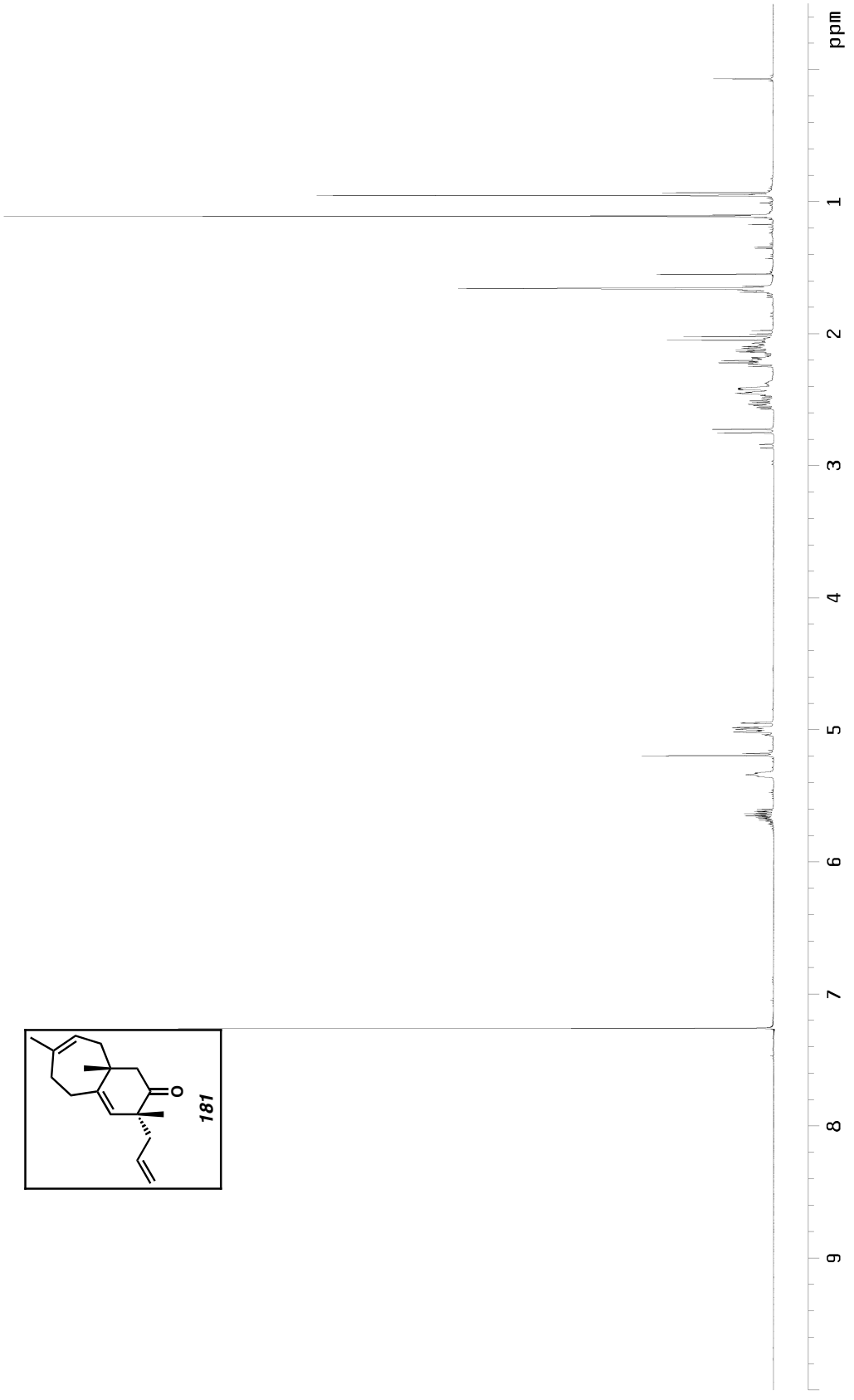

Figure A2.40 ^{1}H NMR (500 MHz, $CDCl_3$) of bicyclic ketone **181**.

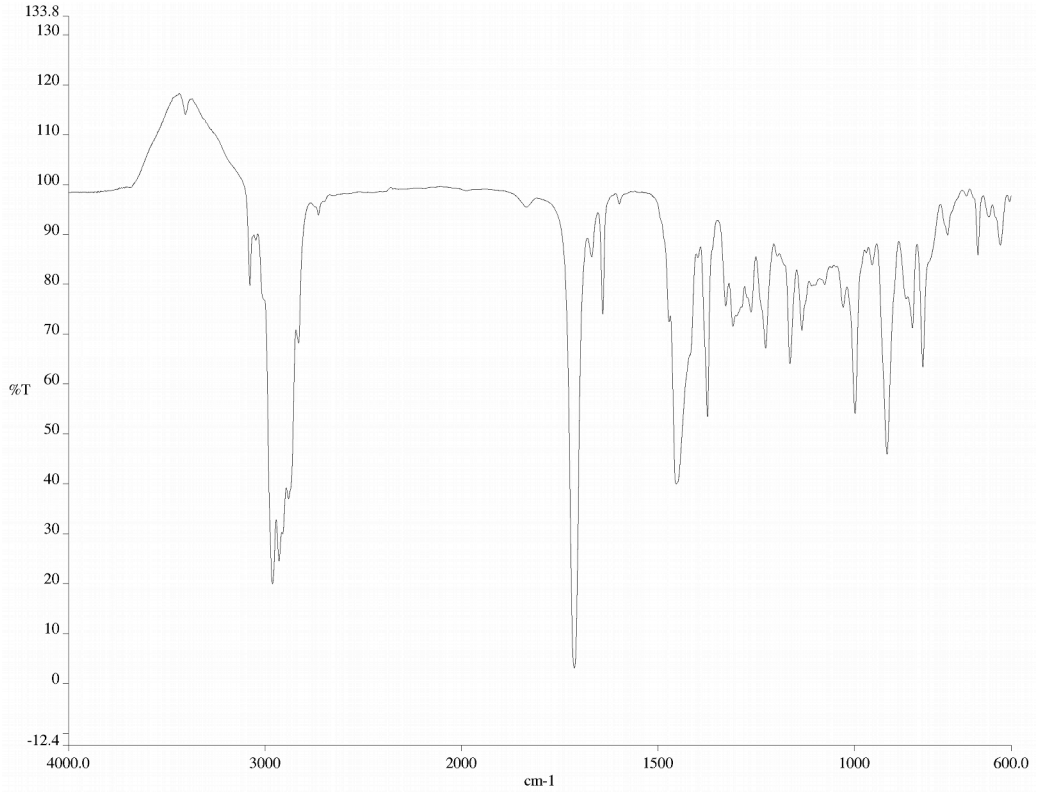

Figure A2.41 Infrared spectrum (thin film/NaCl) of bicyclic ketone **181**.

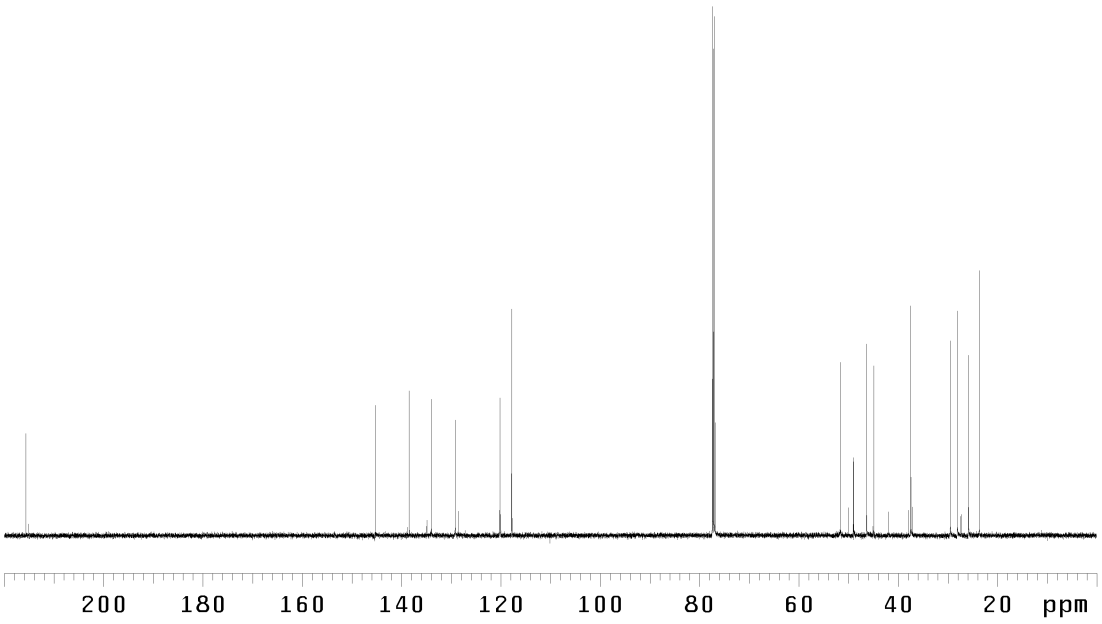

Figure A2.42 ^{13}C NMR (125 MHz, $CDCl_3$) of bicyclic ketone **181**.

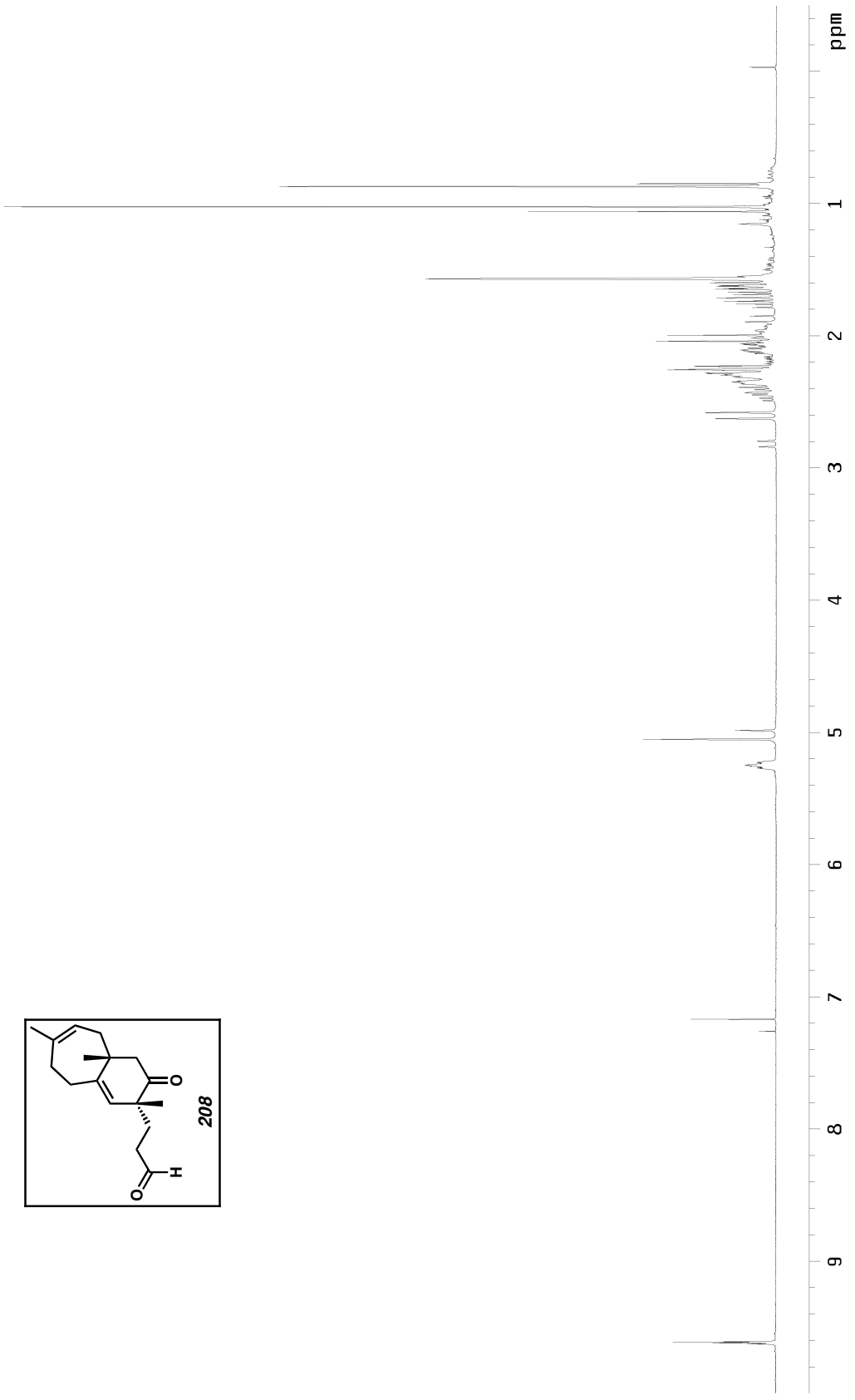

Figure A2.43 ^{1}H NMR (300 MHz, $CDCl_3$) of bicyclic aldehyde **208**.

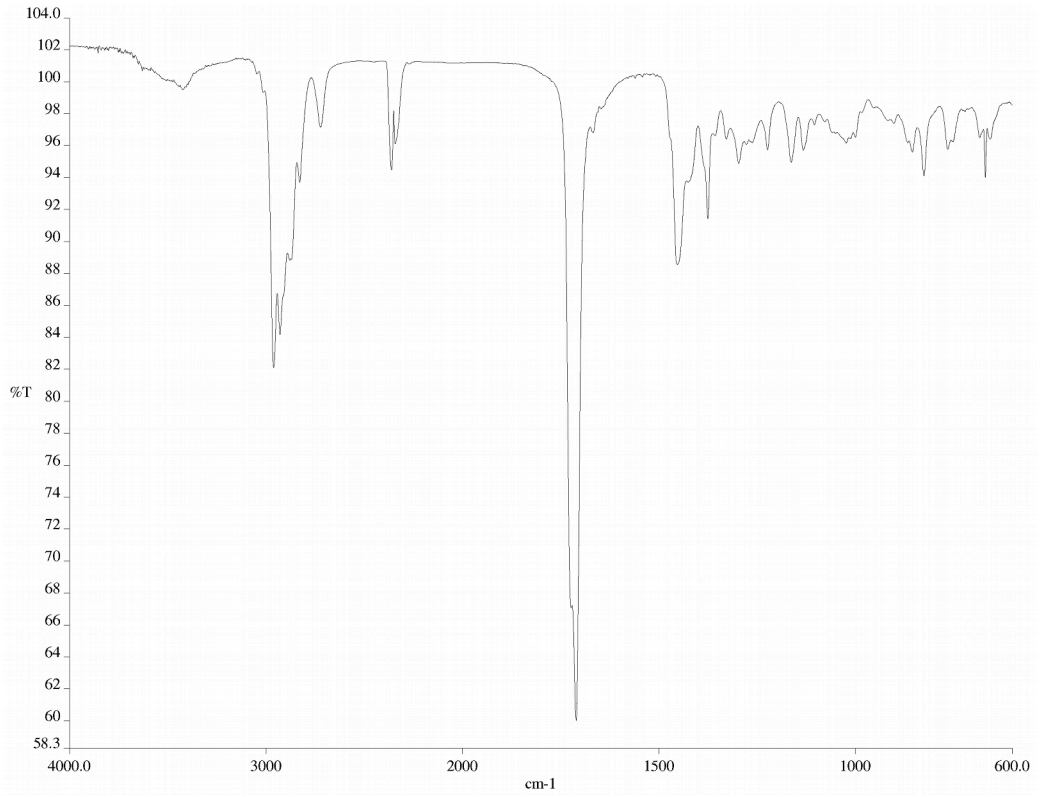

Figure A2.44 Infrared spectrum (thin film/NaCl) of bicyclic aldehyde **208**.

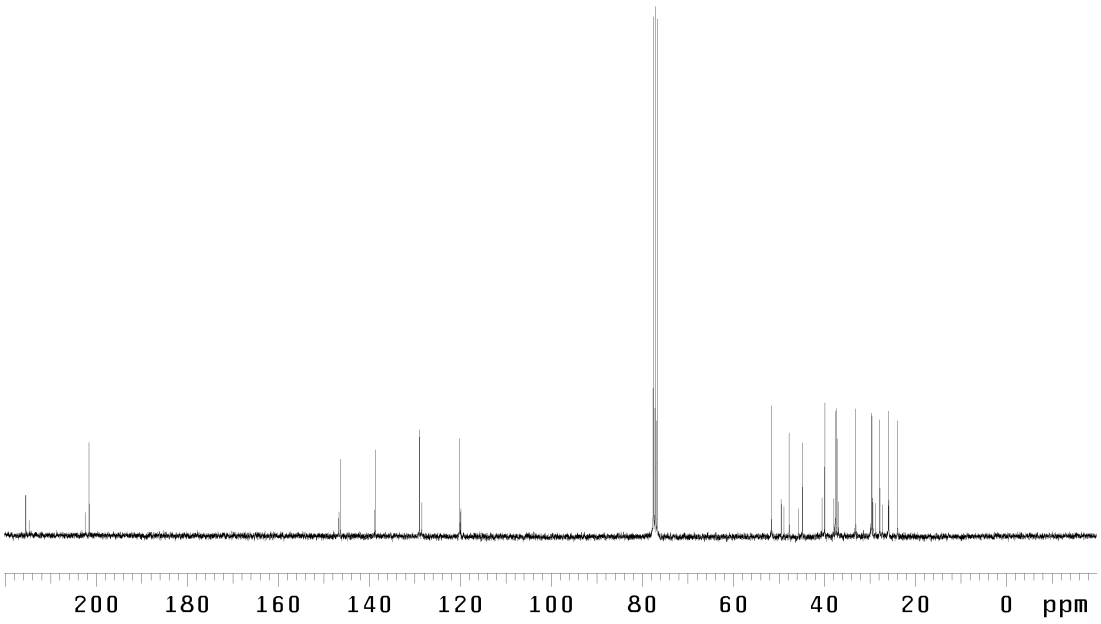

Figure A2.45 ^{13}C NMR (75 MHz, $CDCl_3$) of bicyclic aldehyde **208**.

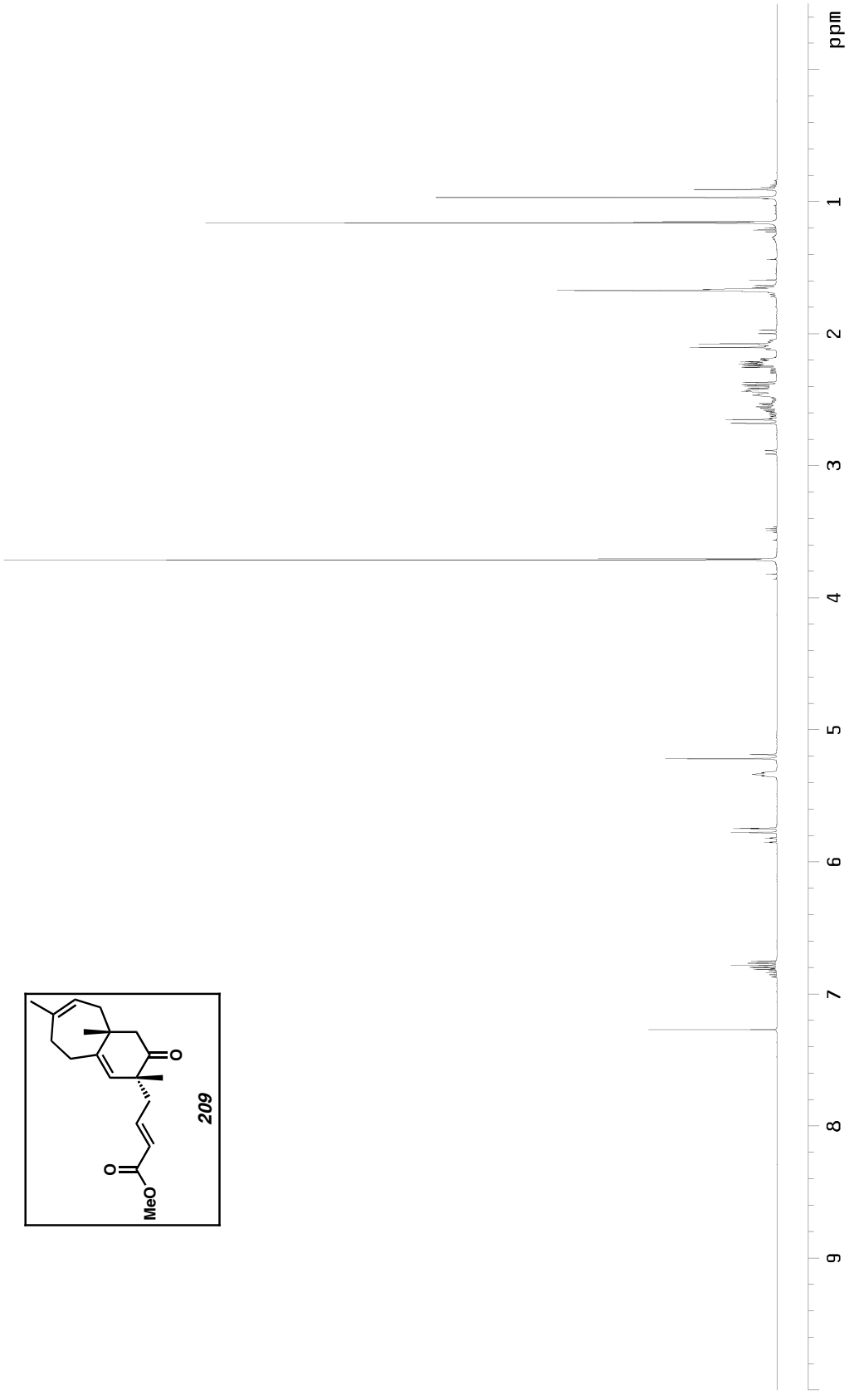

Figure A2.46 ^{1}H NMR (500 MHz, $CDCl_3$) of bicyclic enoate **209**.

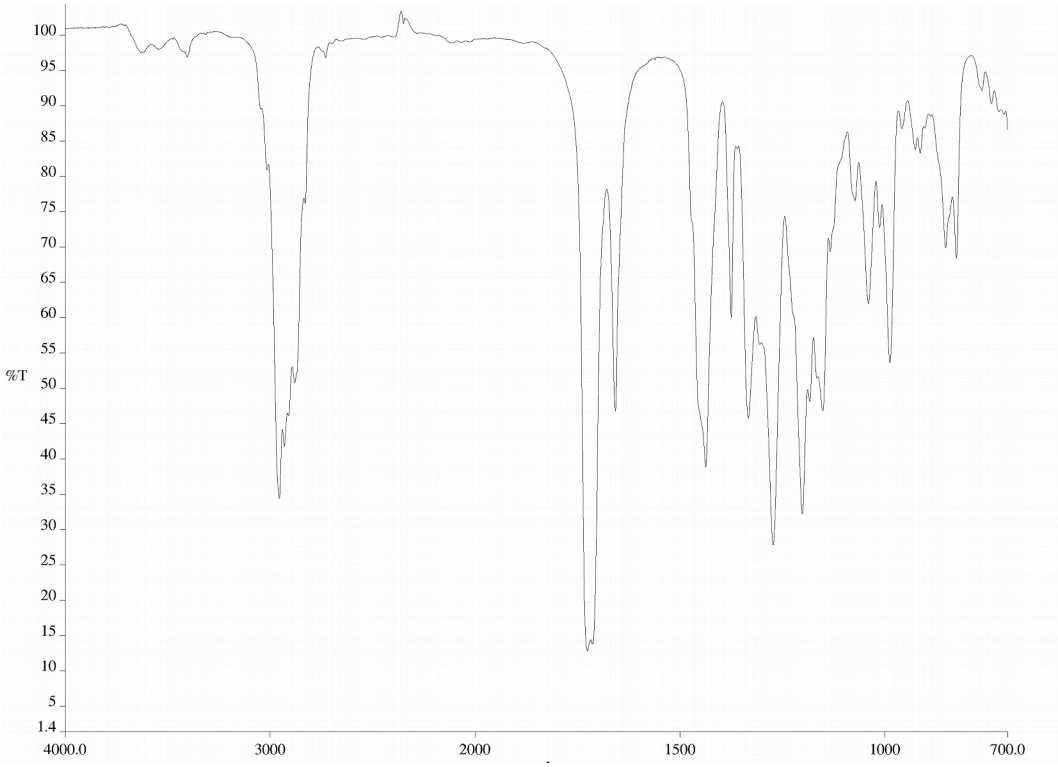

Figure A2.47 Infrared spectrum (thin film/NaCl) of bicyclic enoate **209**.

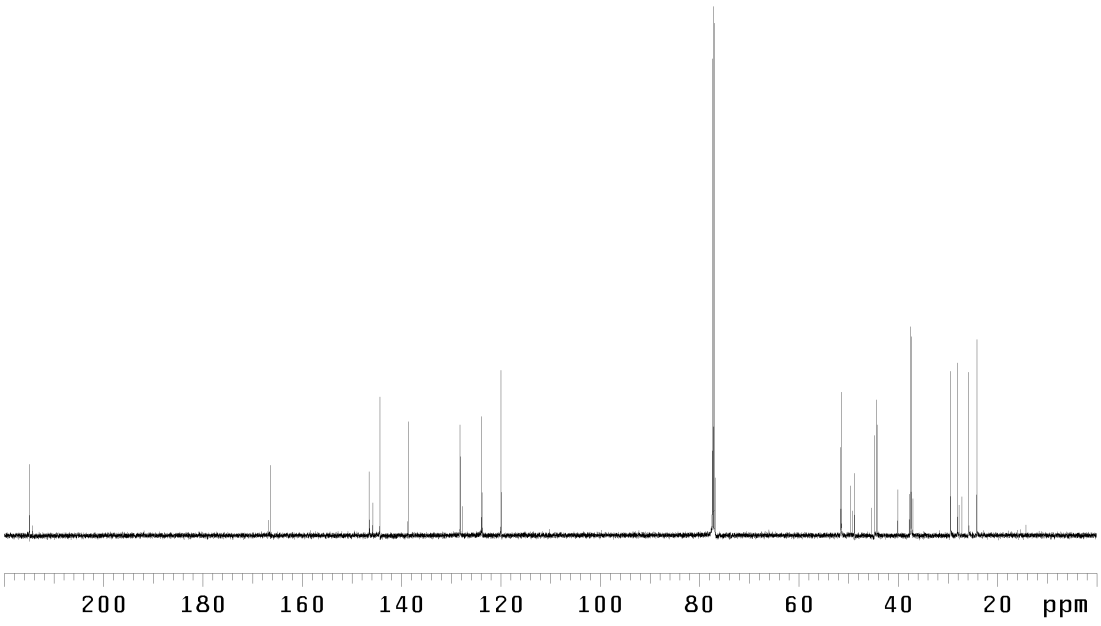

Figure A2.48 ^{13}C NMR (125 MHz, $CDCl_3$) of bicyclic enoate **209**.

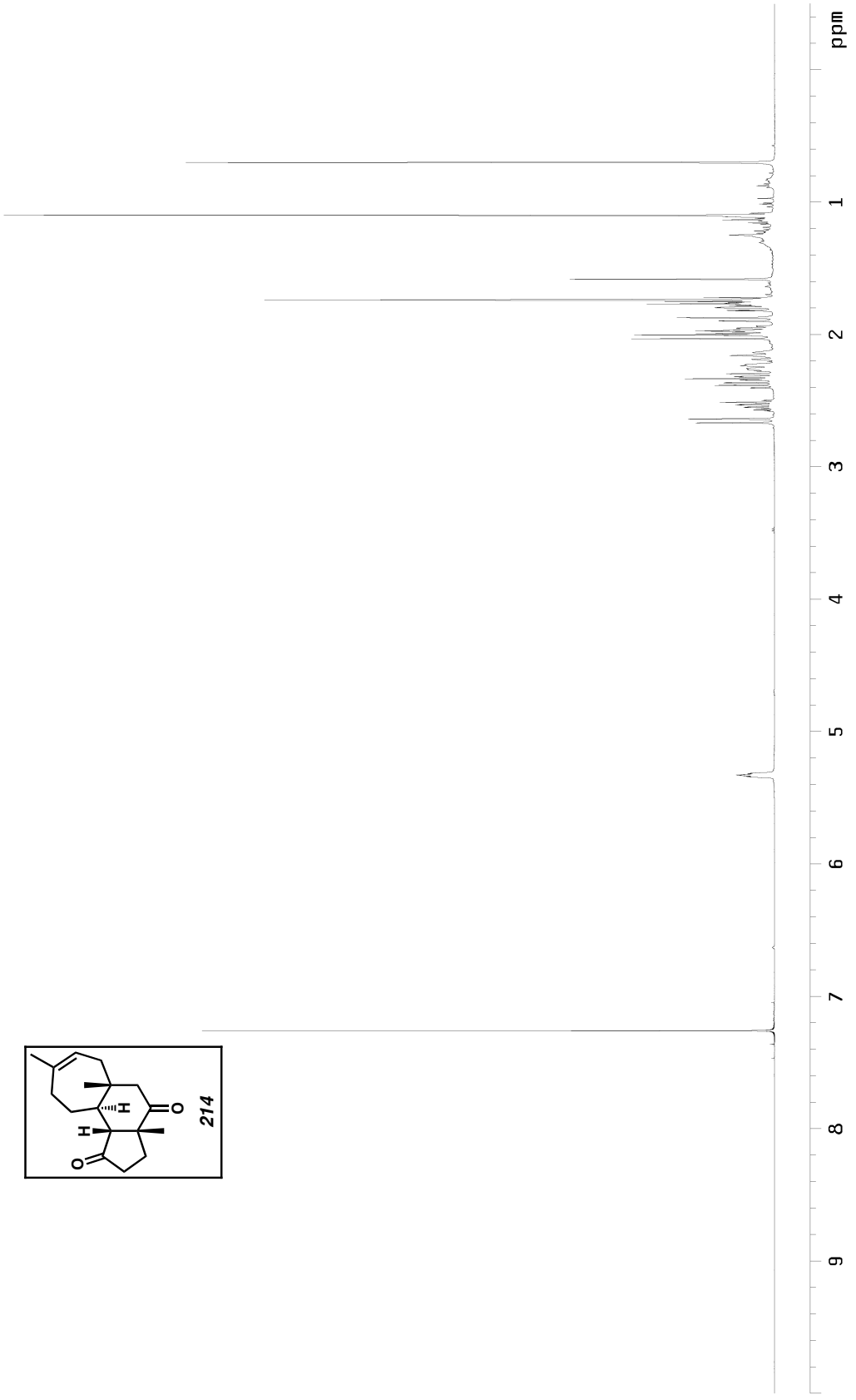

Figure A2.49 ^{1}H NMR (500 MHz, $CDCl_3$) of tricyclic diketone **214**.

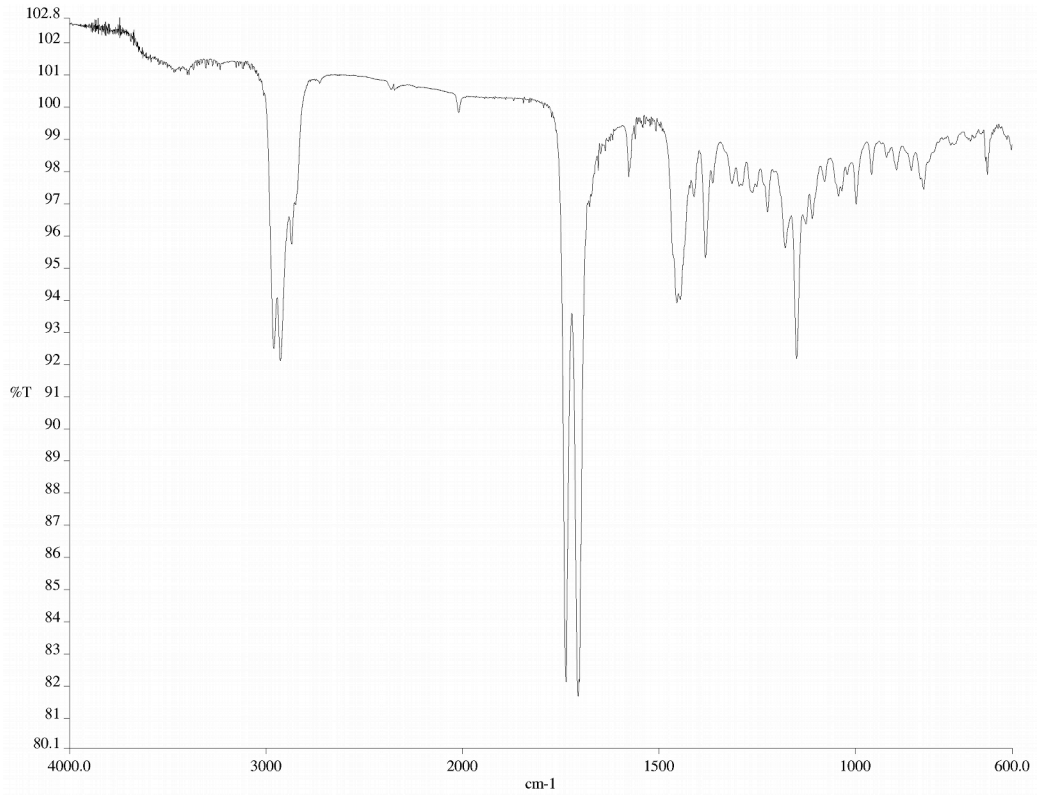

Figure A2.50 Infrared spectrum (thin film/NaCl) of tricyclic diketone **214**.

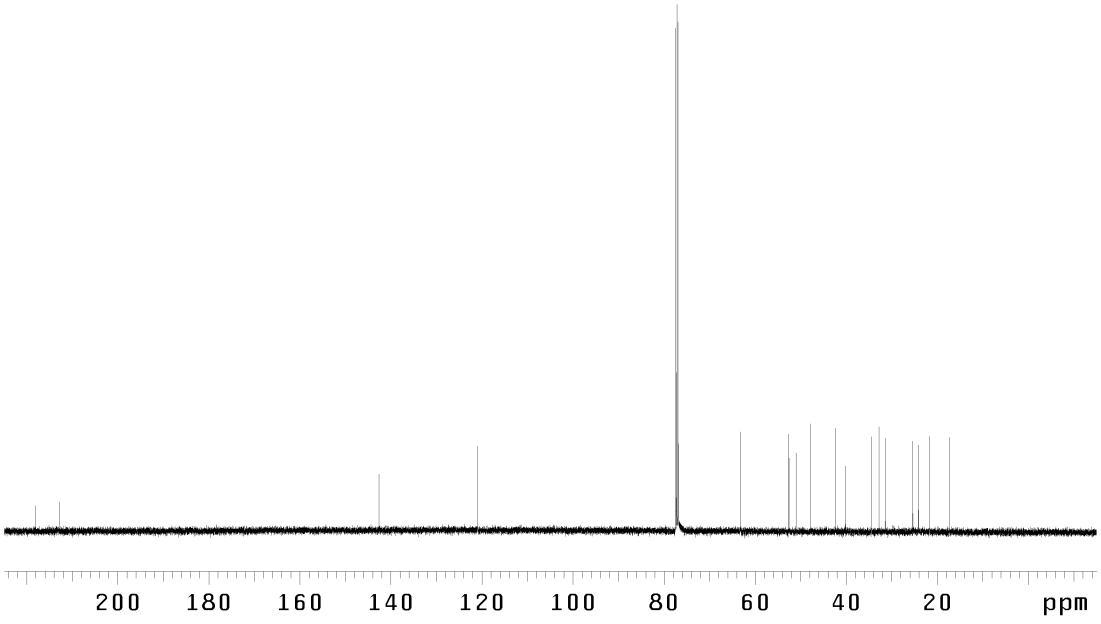

Figure A2.51 ^{13}C NMR (125 MHz, $CDCl_3$) of tricyclic diketone **214**.

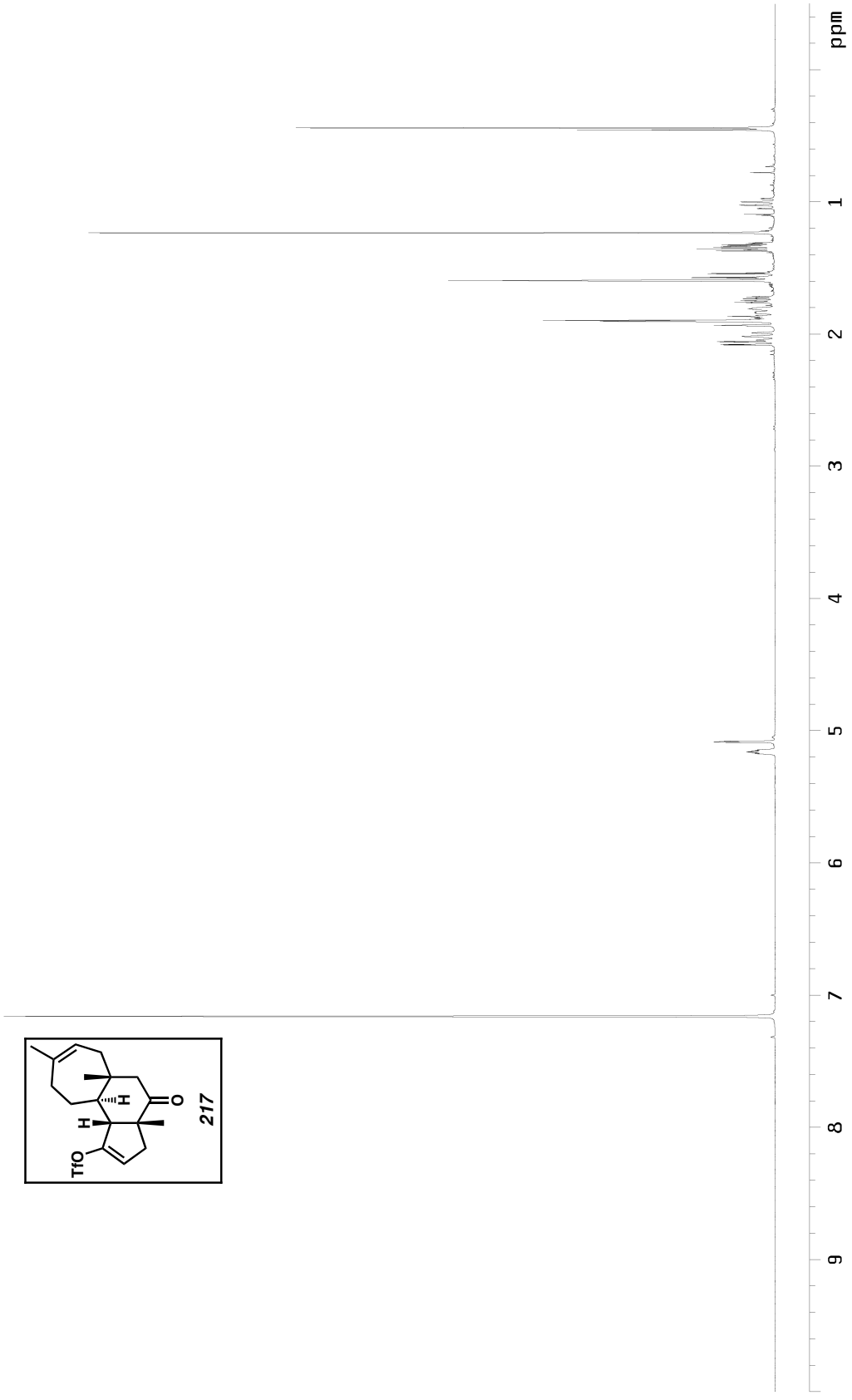

Figure A2.52 ^{1}H NMR (500 MHz, C_6D_6) of tricyclic triflate **217**.

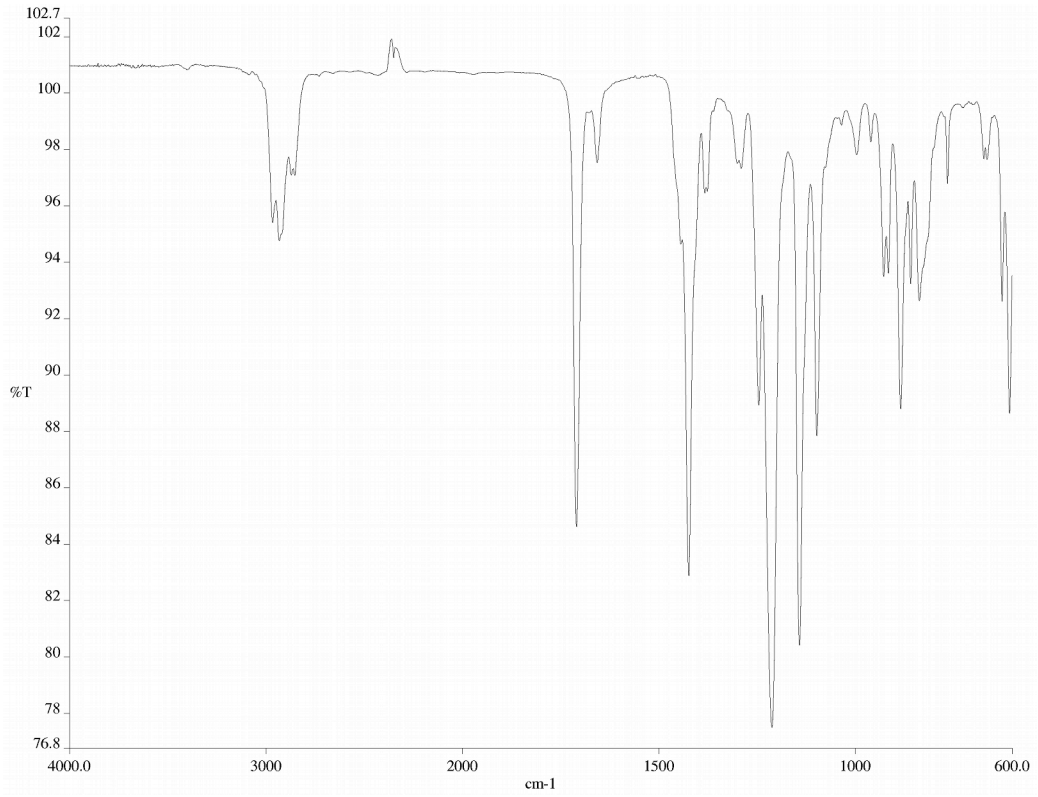

Figure A2.53 Infrared spectrum (thin film/NaCl) of tricyclic triflate **217**.

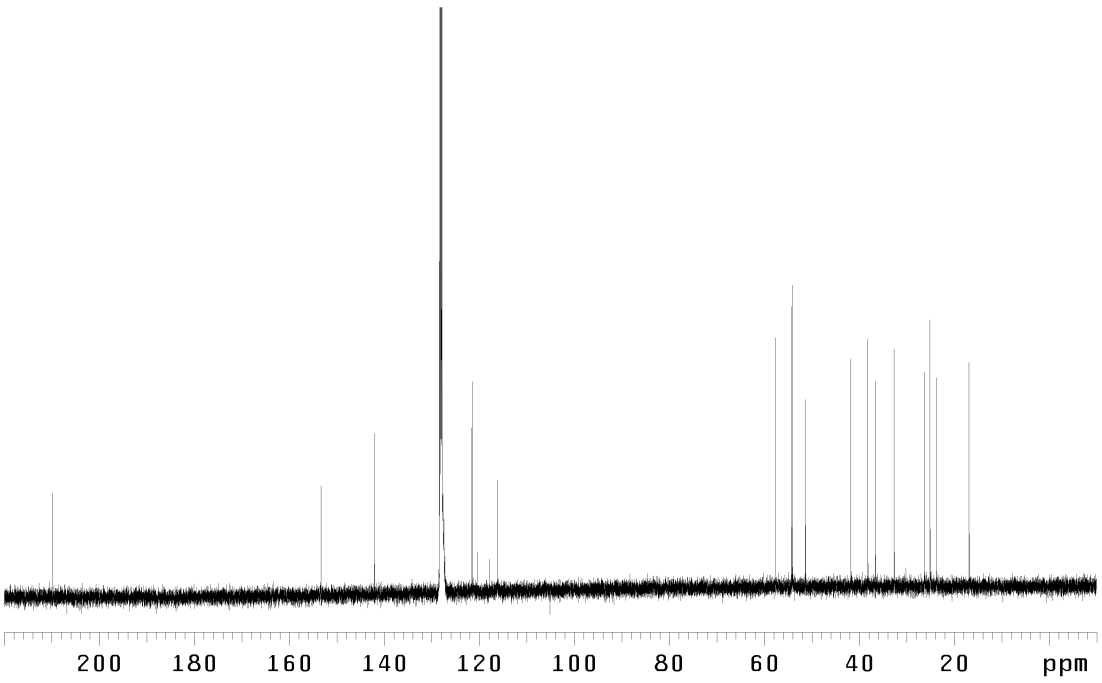

Figure A2.54 ^{13}C NMR (125 MHz, C_6D_6) of tricyclic triflate **217**.

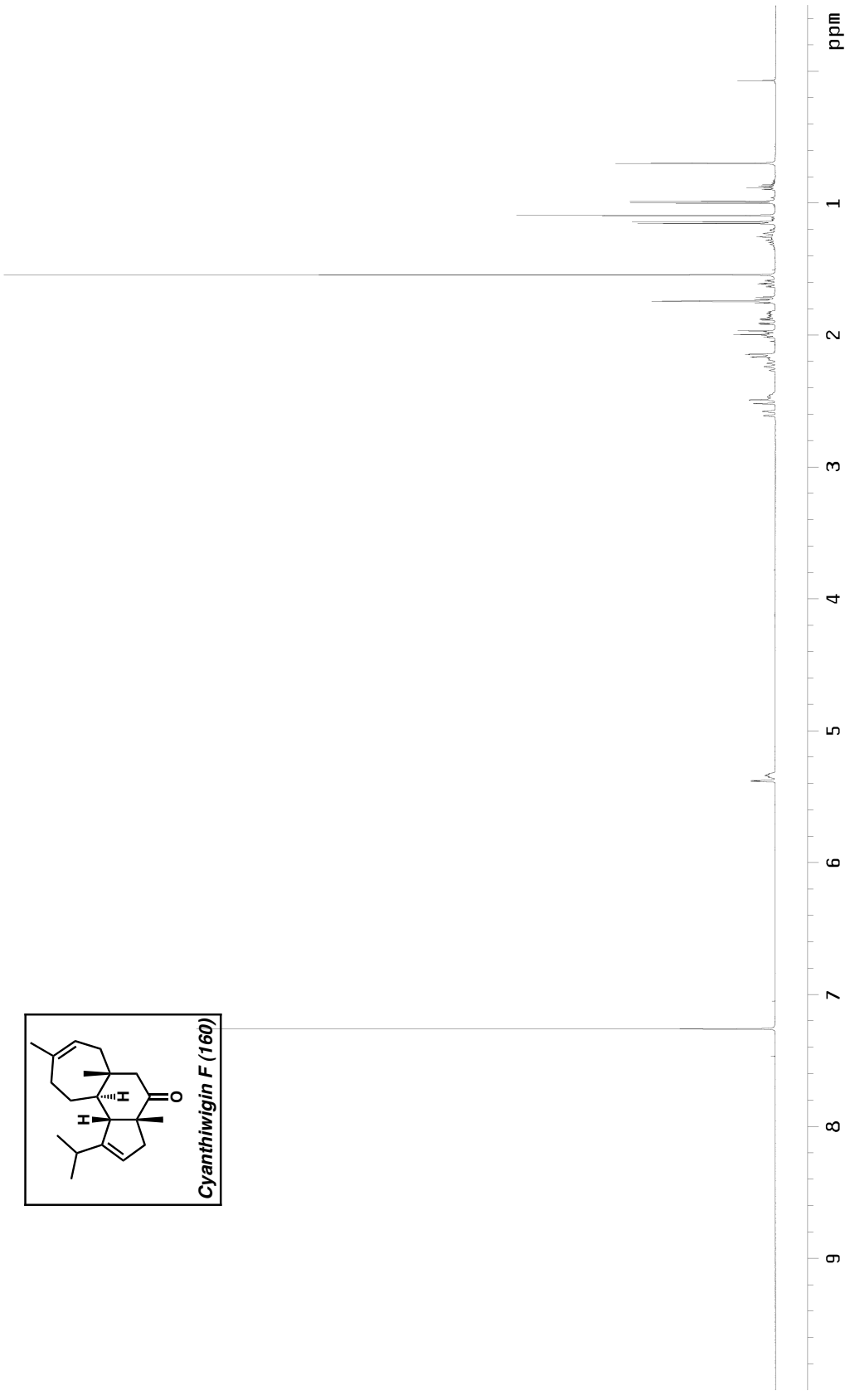

Figure A2.55 ^{1}H NMR (500 MHz, $CDCl_3$) of cyanthiwigin F (**160**).

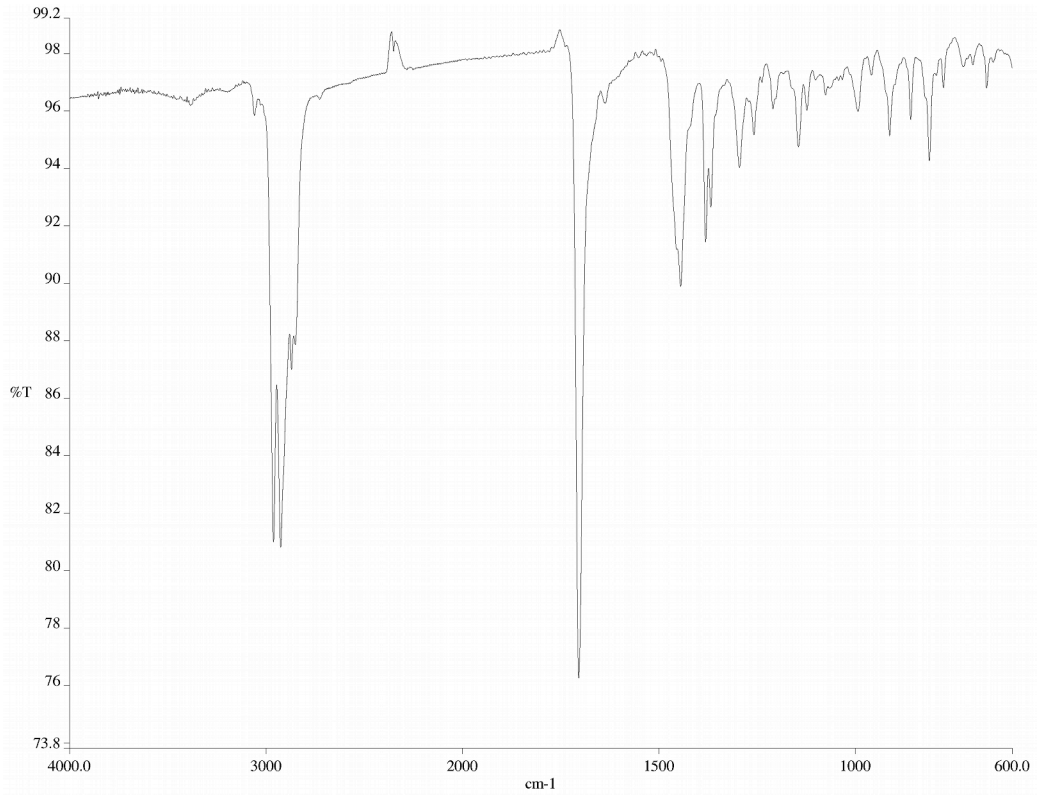

Figure A2.56 Infrared spectrum (thin film/NaCl) of cyanthiwigin F (**160**).

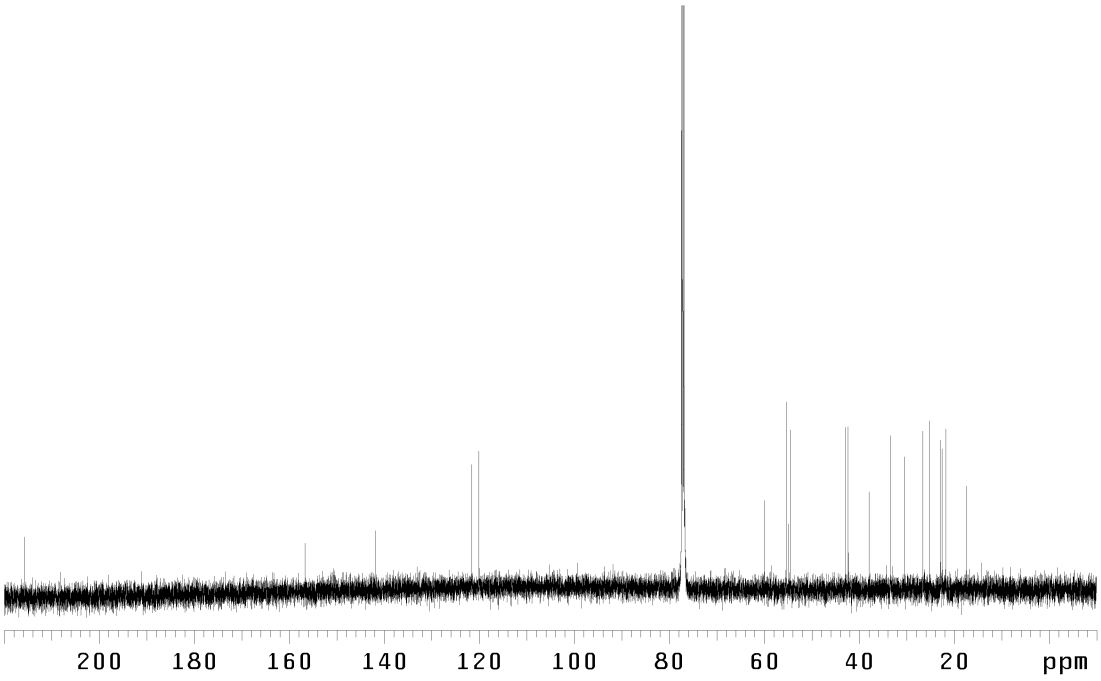

Figure A2.57 ^{13}C NMR (125 MHz, $CDCl_3$) of cyanthiwigin F (**160**).

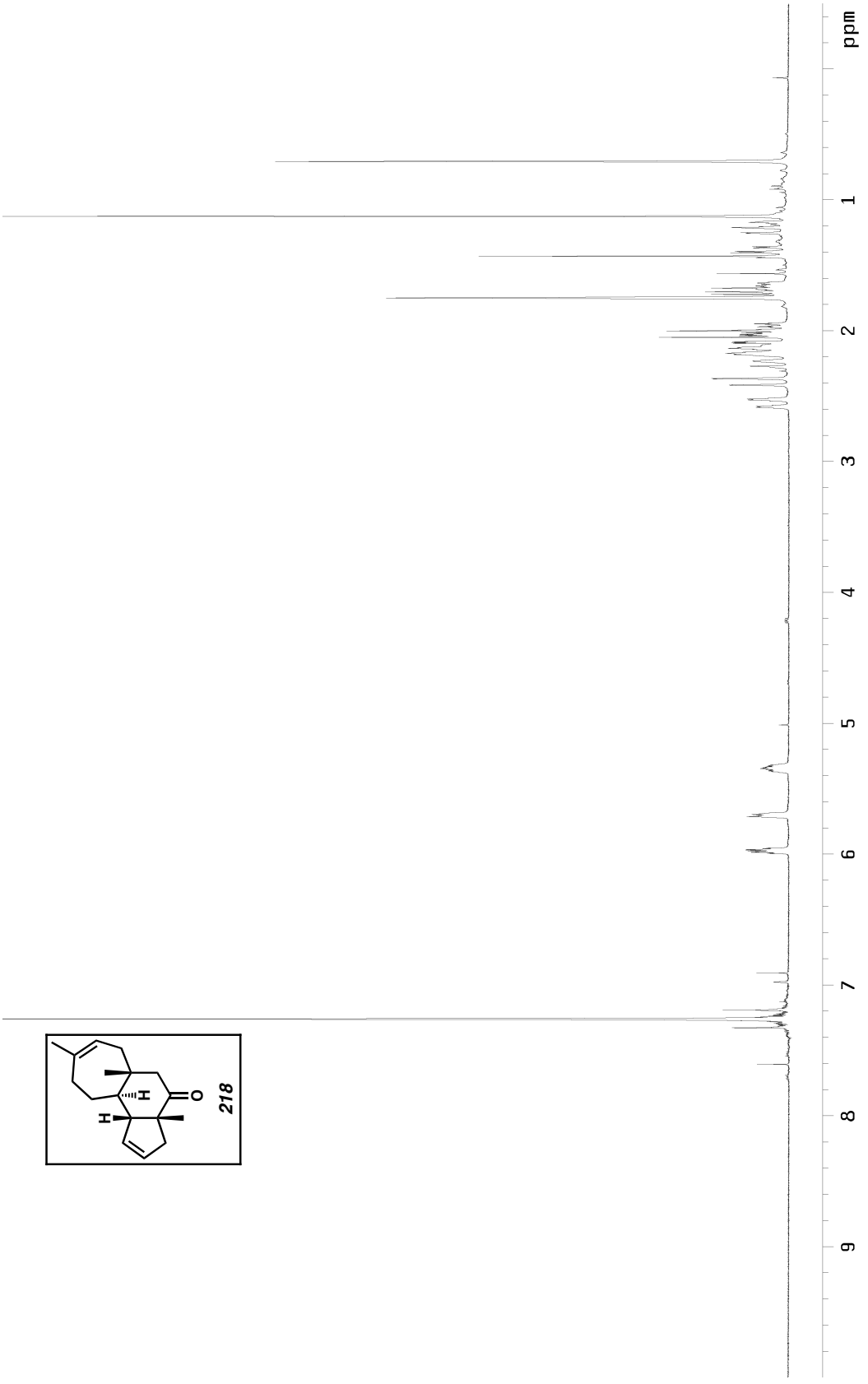

Figure A2.58 ^{1}H NMR (500 MHz, $CDCl_3$) of tricyclic ketone **218**.

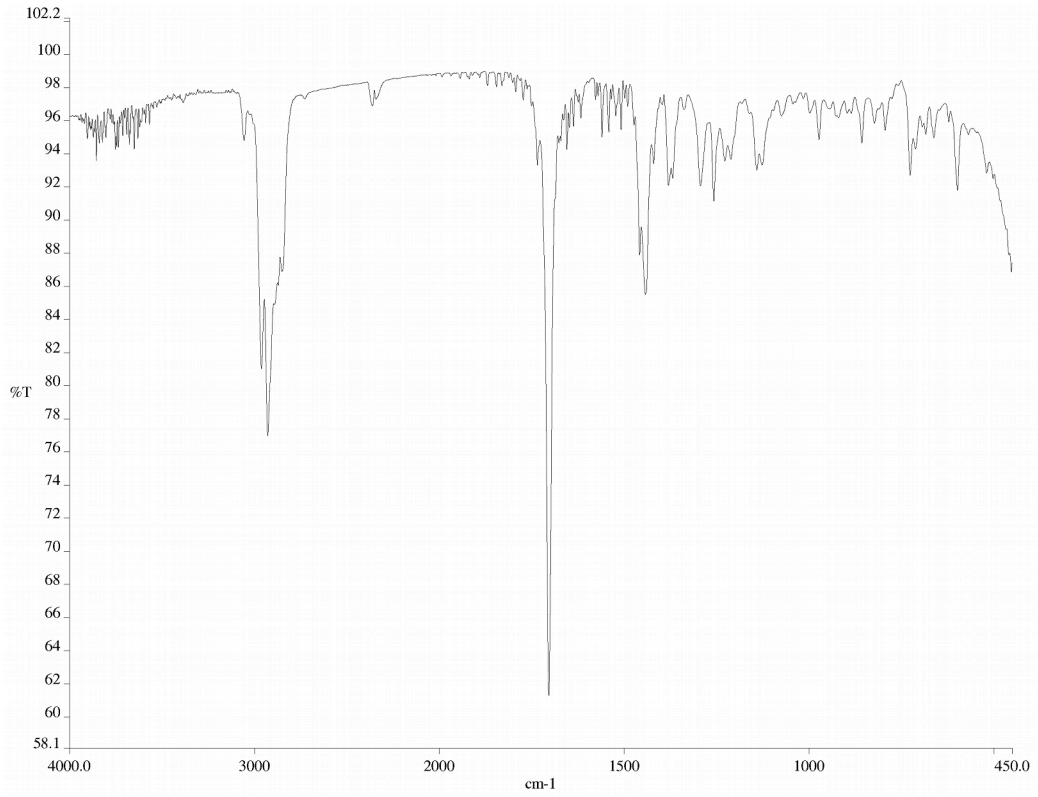

Figure A2.59 Infrared spectrum (thin film/NaCl) of tricyclic ketone **218**.

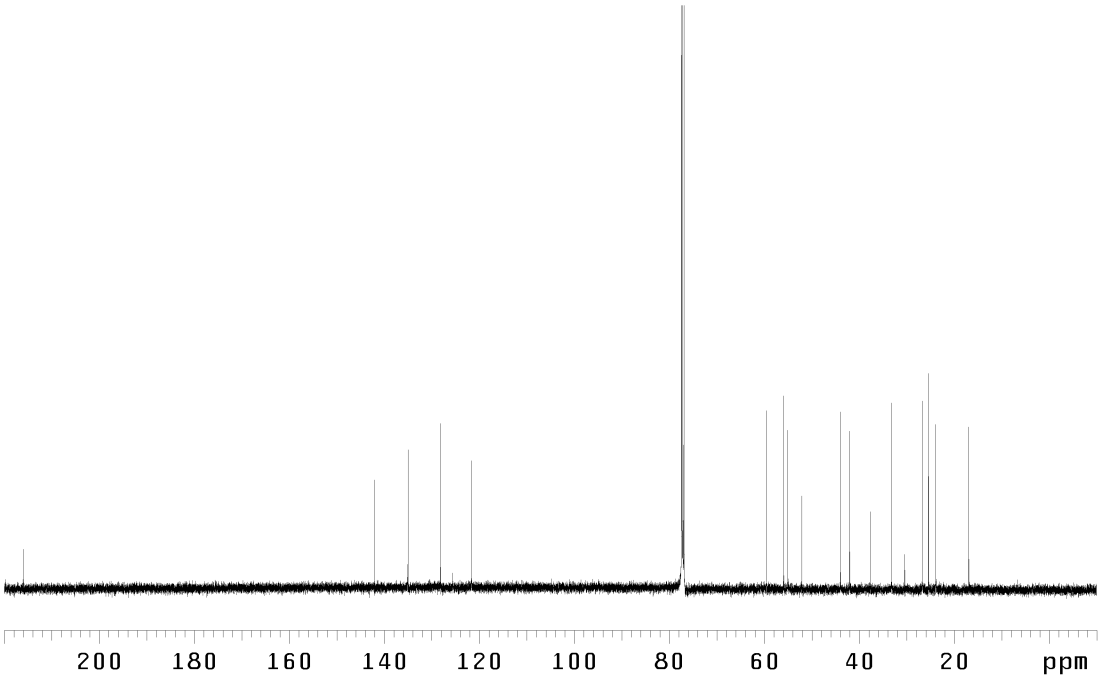

Figure A2.60 ^{13}C NMR (125 MHz, $CDCl_3$) of tricyclic ketone **218**.

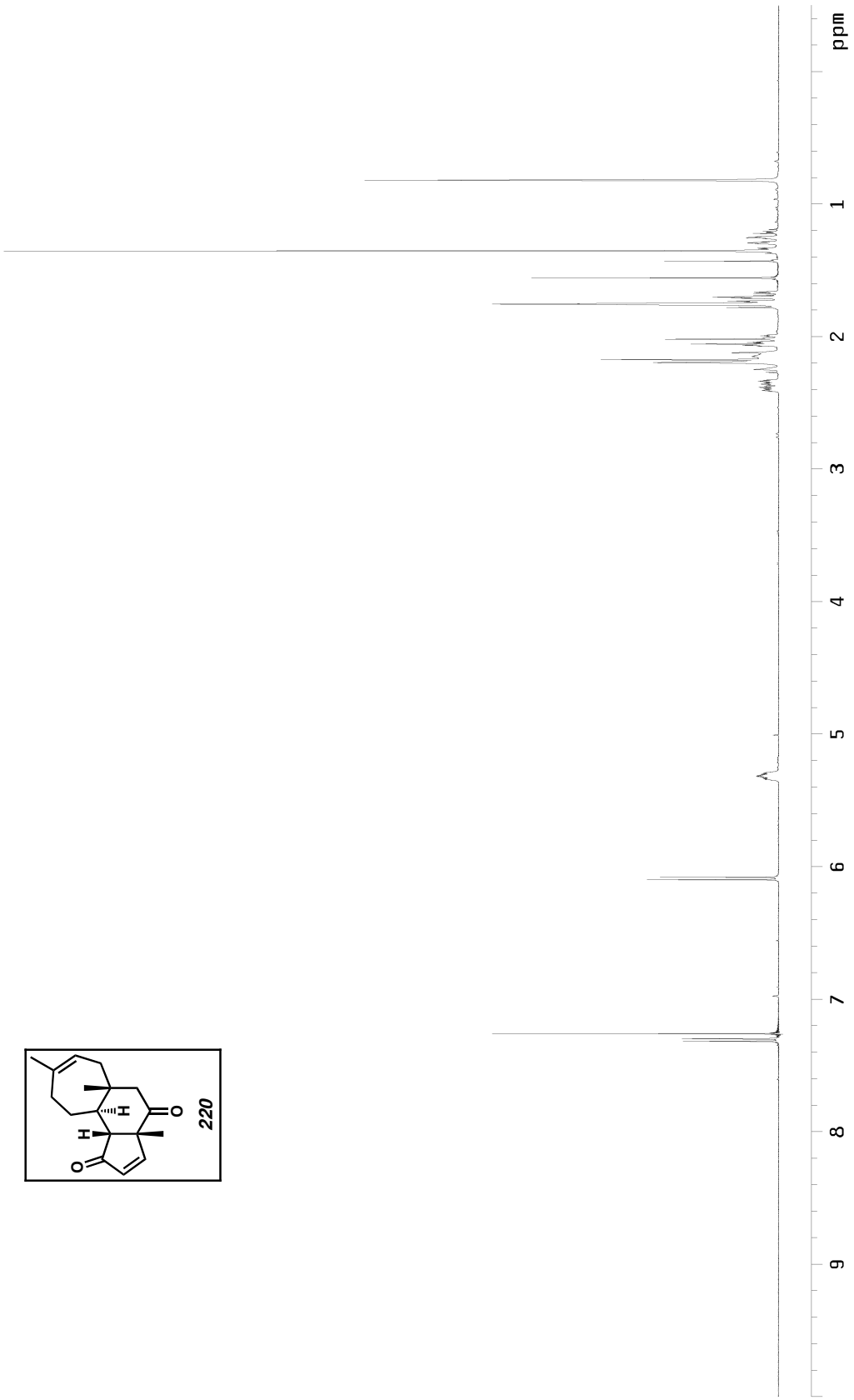

Figure A2.61 ^{1}H NMR (500 MHz, $CDCl_3$) of tricyclic enone **220**.

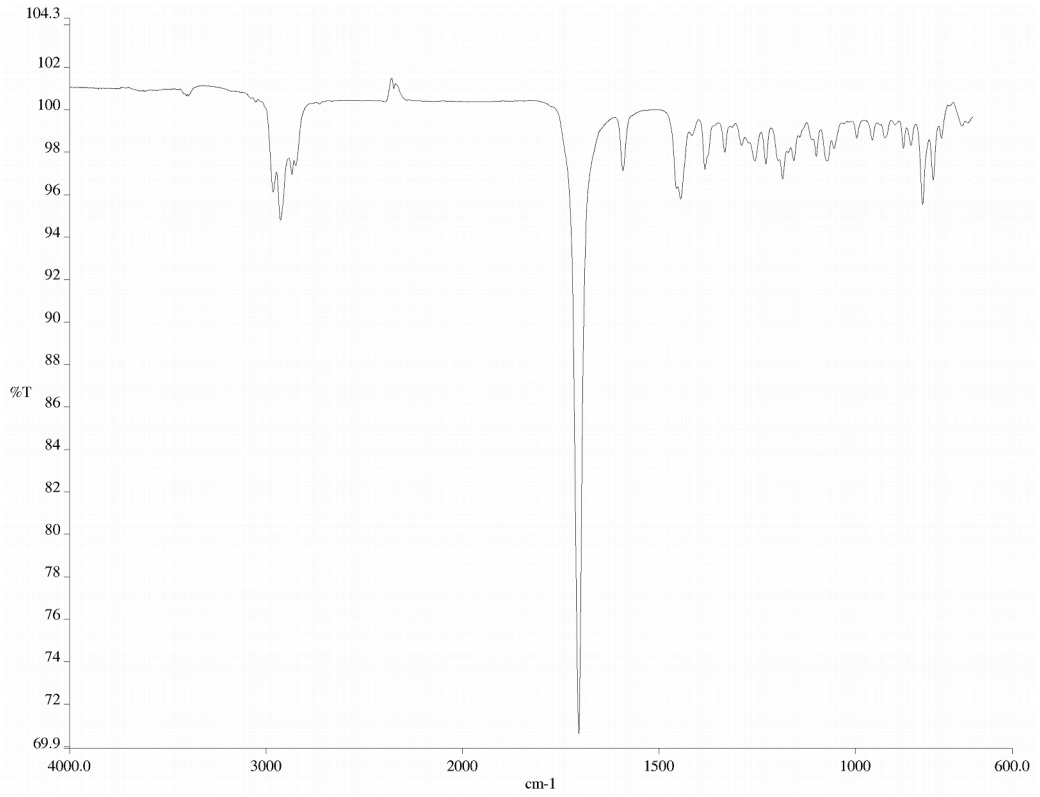

Figure A2.62 Infrared spectrum (thin film/NaCl) of tricyclic enone **220**.

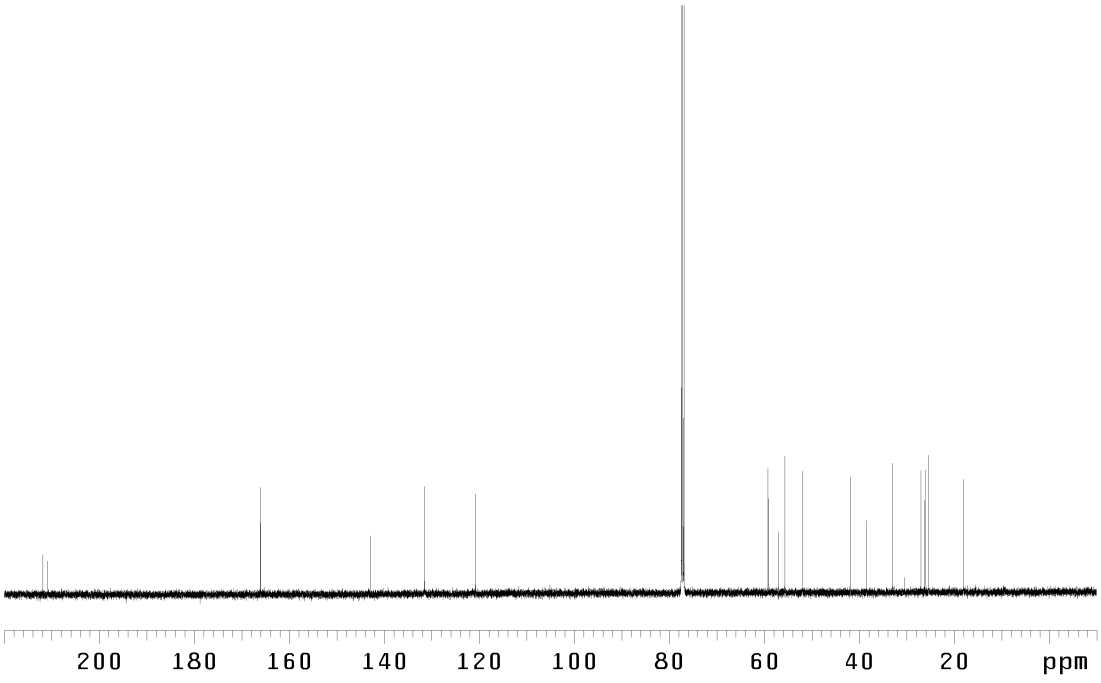

Figure A2.63 ^{13}C NMR (125 MHz, $CDCl_3$) of tricyclic enone **220**.

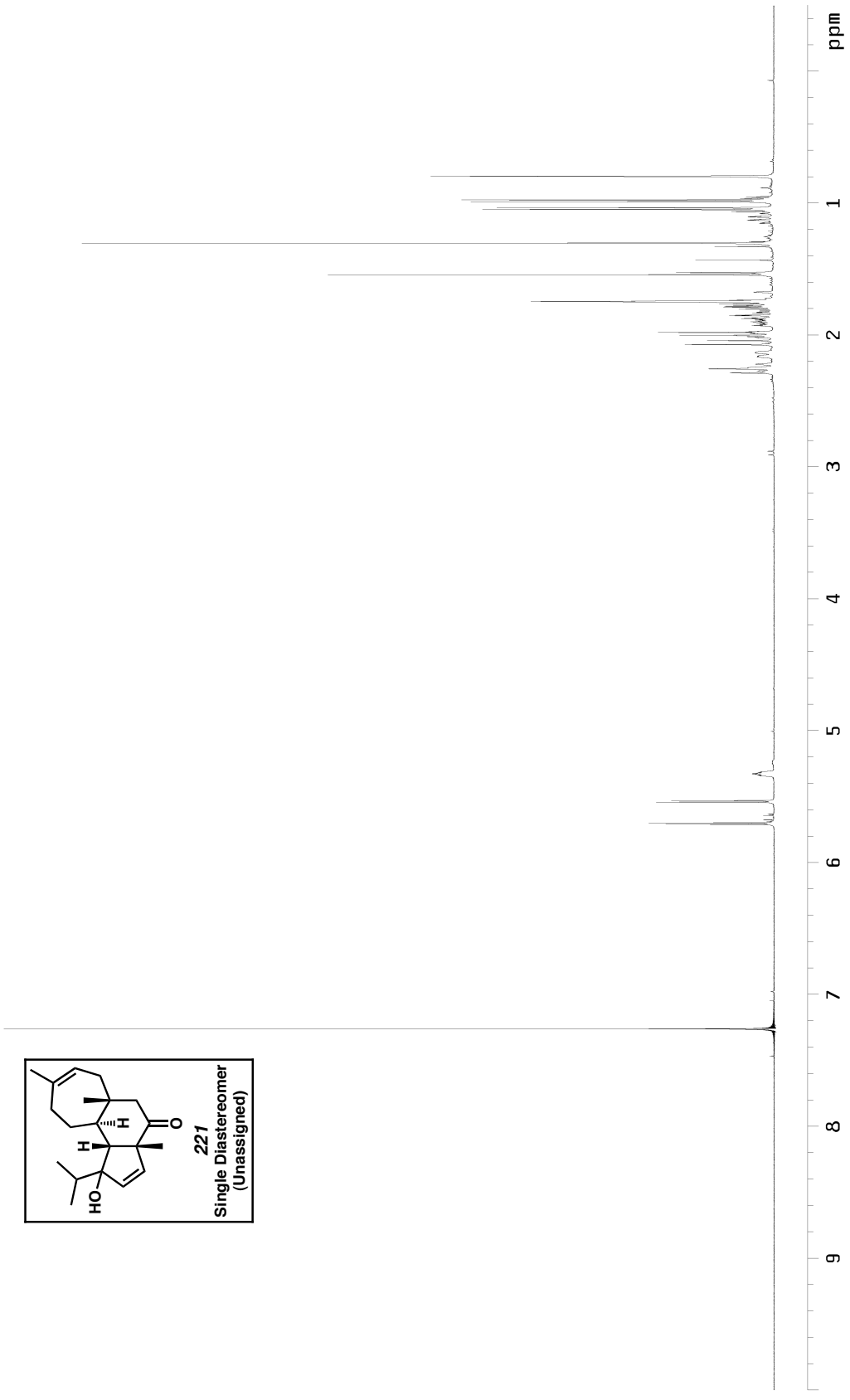

Figure A2.64 ^{1}H NMR (500 MHz, $CDCl_3$) of allylic alcohol **221(A)**.

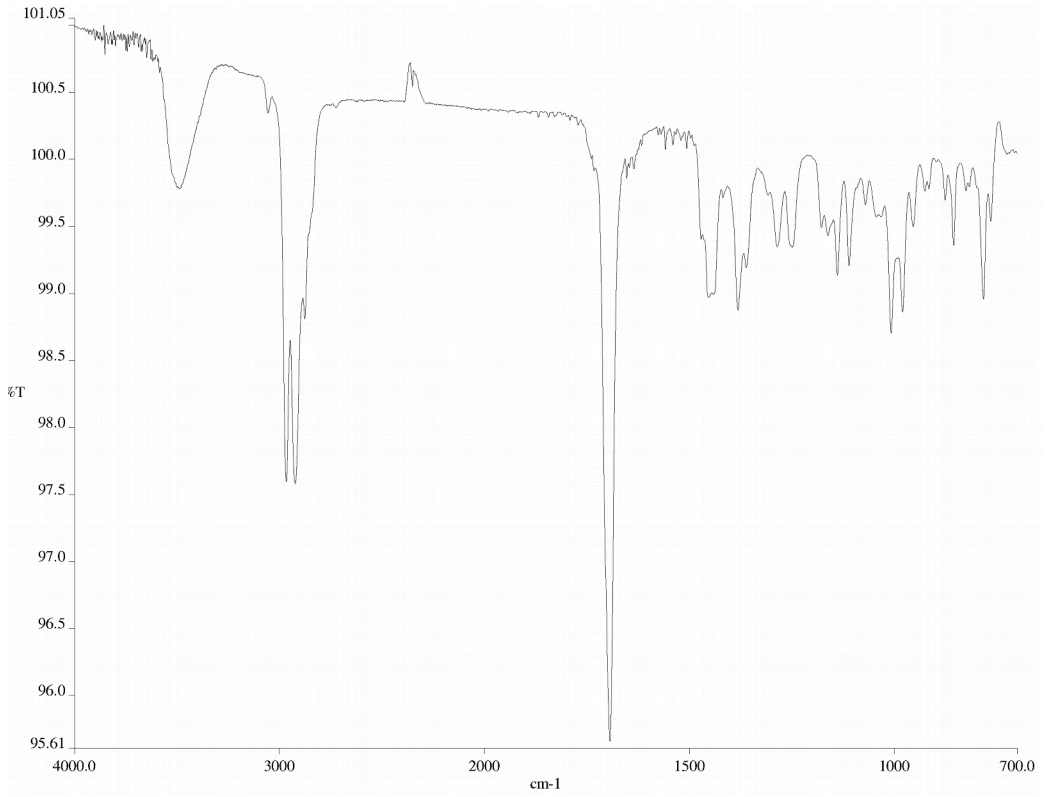

Figure A2.65 Infrared spectrum (thin film/NaCl) of allylic alcohol **221(A)**.

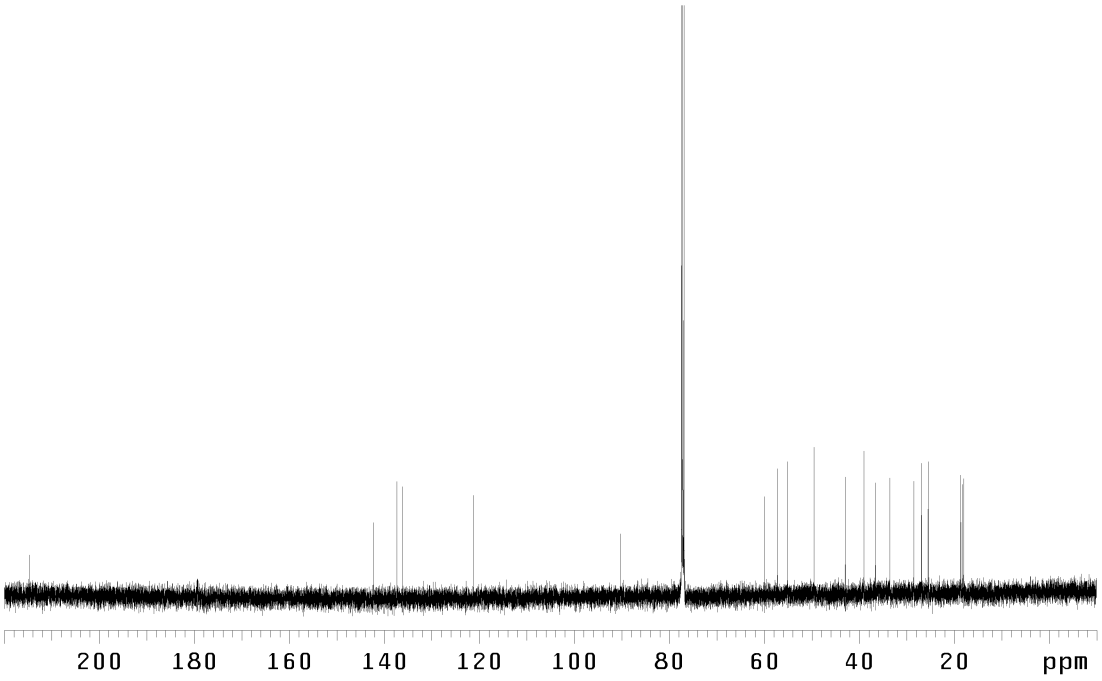

Figure A2.66 ^{13}C NMR (125 MHz, $CDCl_3$) of allylic alcohol **221(A)**.

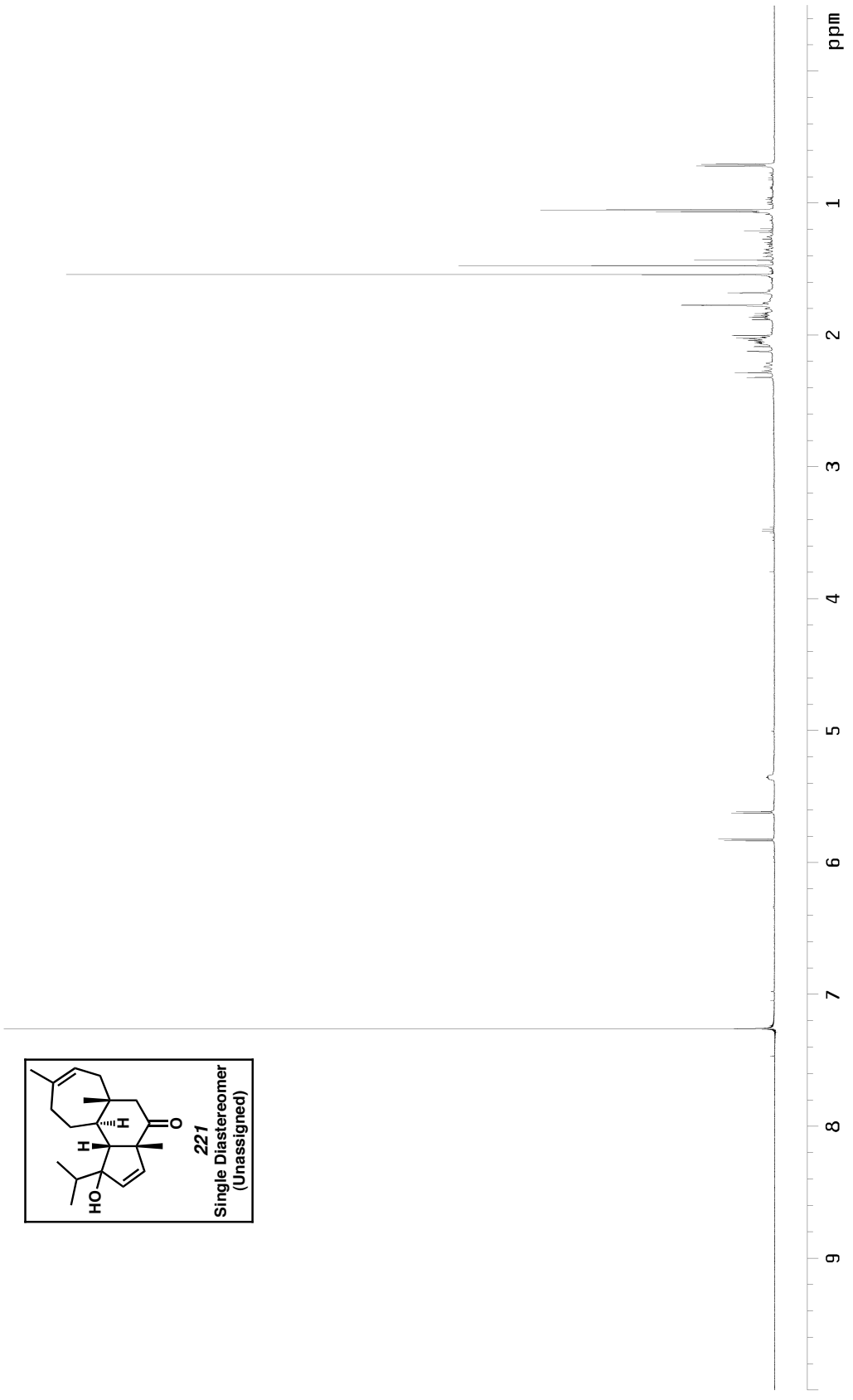

Figure A2.67 ^{1}H NMR (500 MHz, $CDCl_3$) of allylic alcohol **221(B)**.

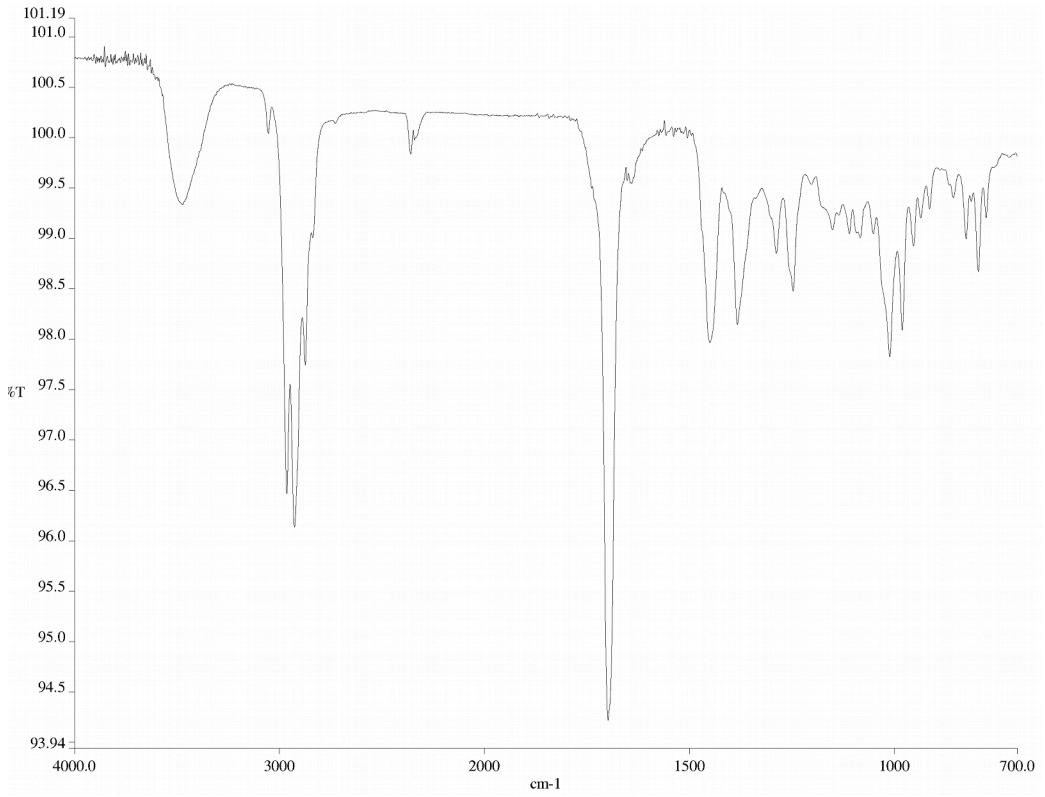

Figure A2.68 Infrared spectrum (thin film/NaCl) of allylic alcohol **221(B)**.

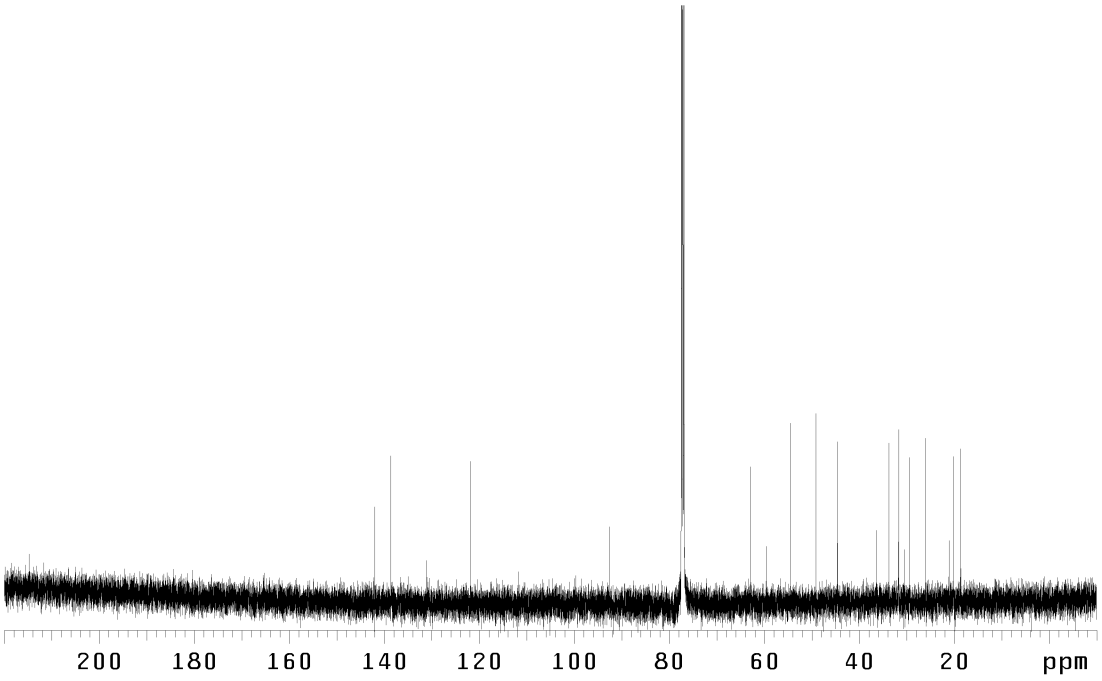

Figure A2.69 ^{13}C NMR (125 MHz, $CDCl_3$) of allylic alcohol **221(B)**.

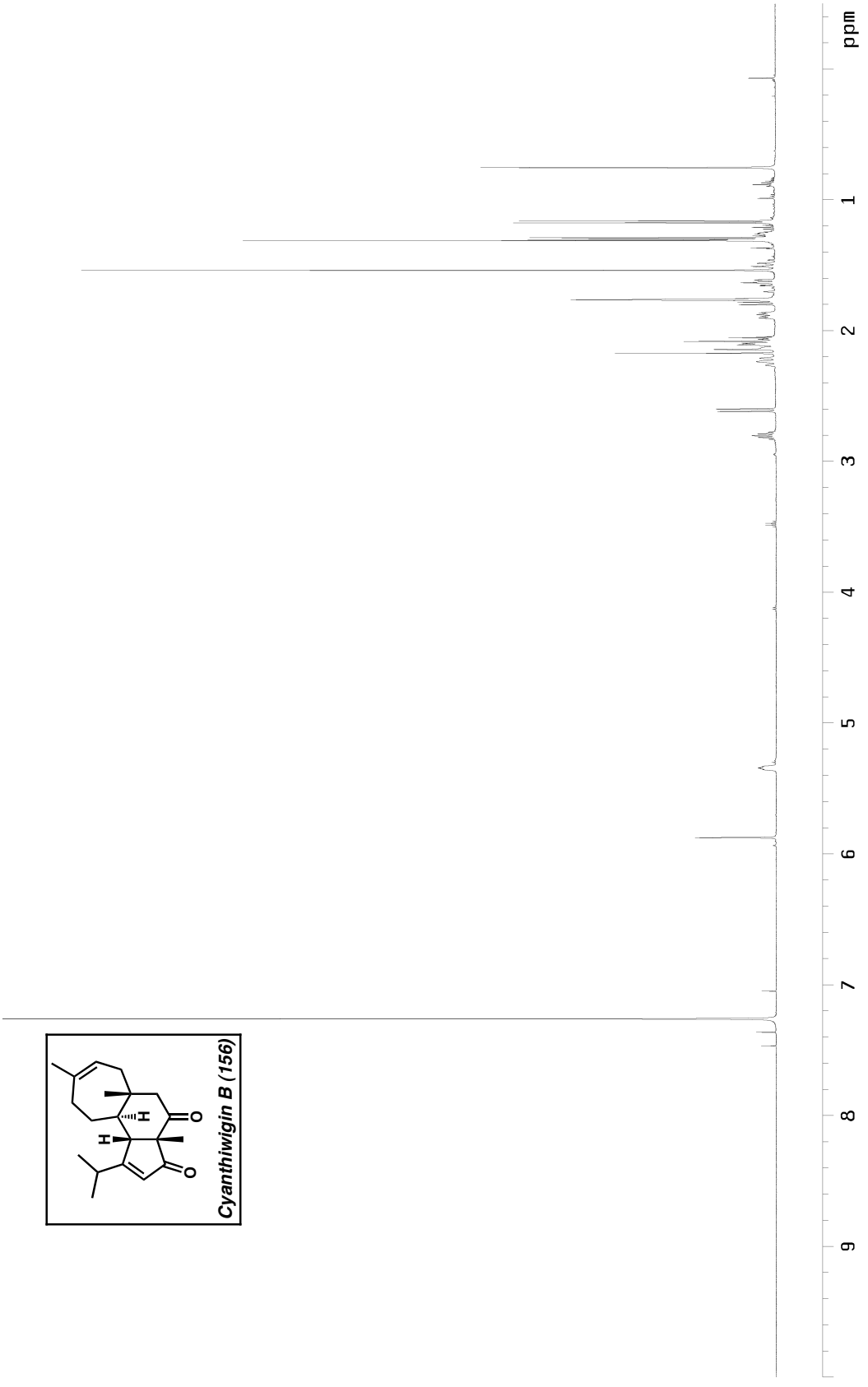

Figure A2.70 ^{1}H NMR (125 MHz, $CDCl_3$) of cyanthiwigin B (**156**).

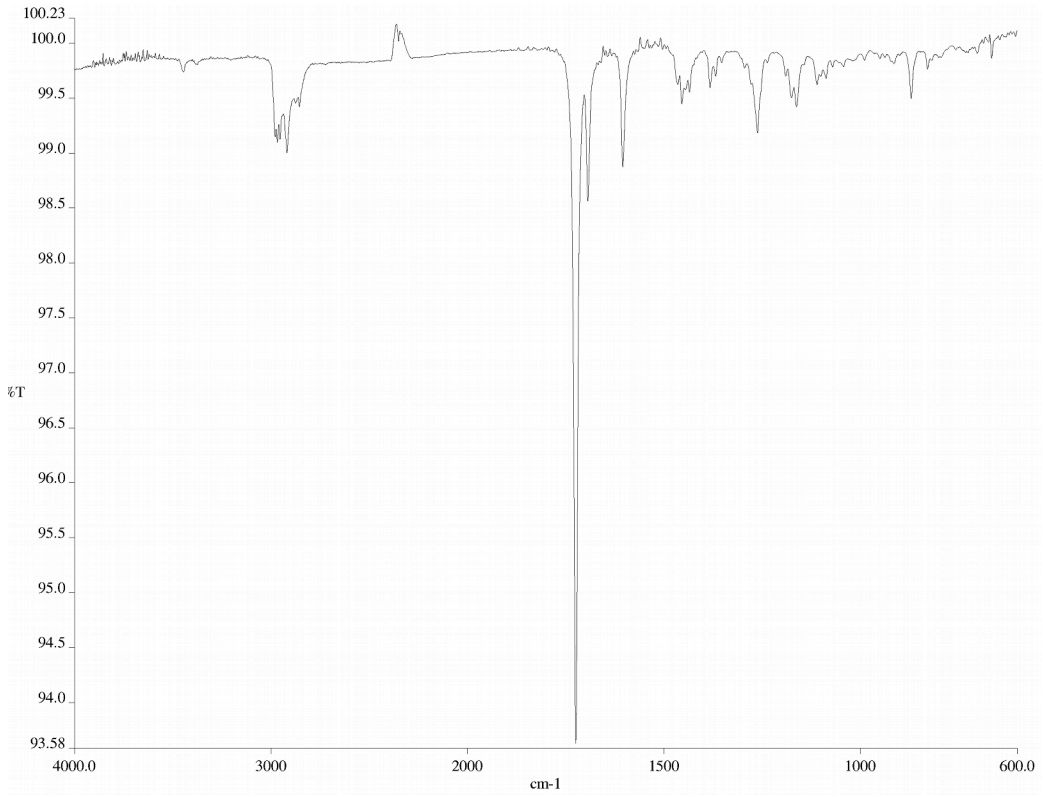

Figure A2.71 Infrared spectrum (thin film/NaCl) of cyanthiwigin B (**156**).

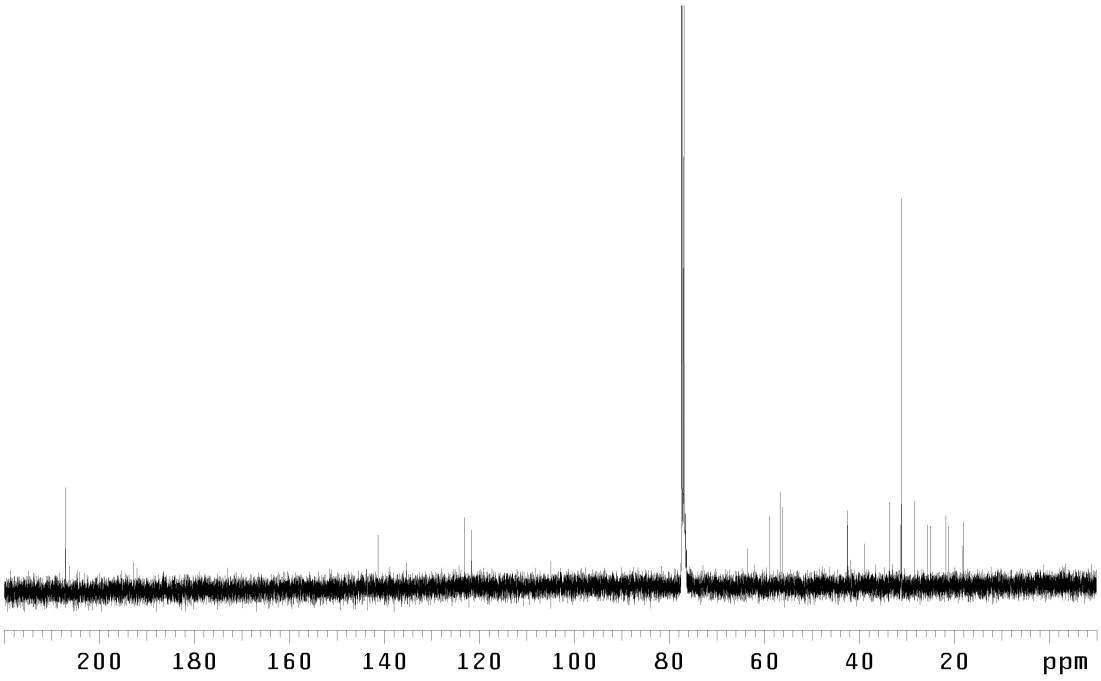

Figure A2.72 ^{13}C NMR (125 MHz, $CDCl_3$) of cyanthiwigin B (**156**).

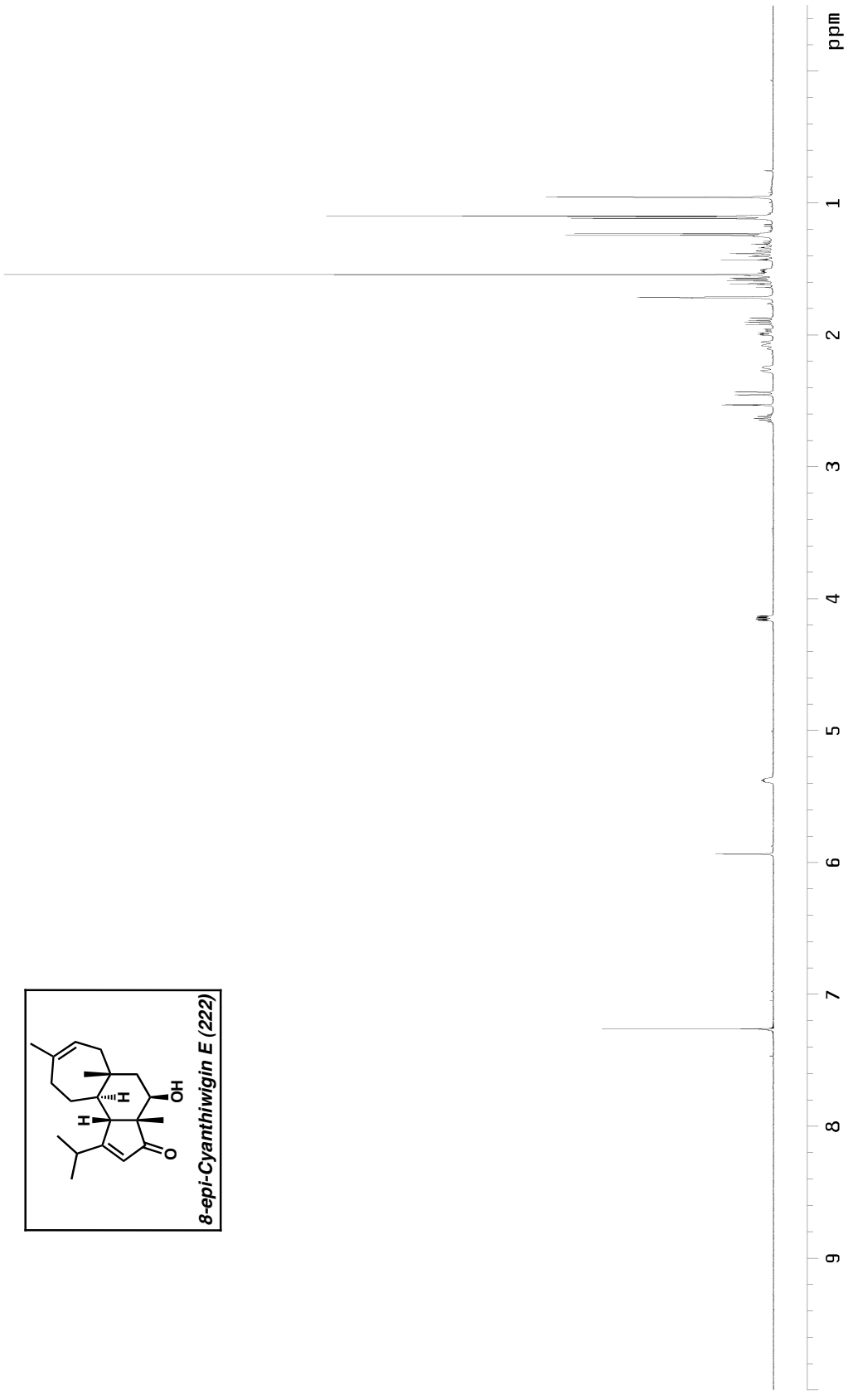

Figure A2.73 ^{1}H NMR (500 MHz, $CDCl_3$) of 8-*epi*-cyanthiwigin E (**222**).

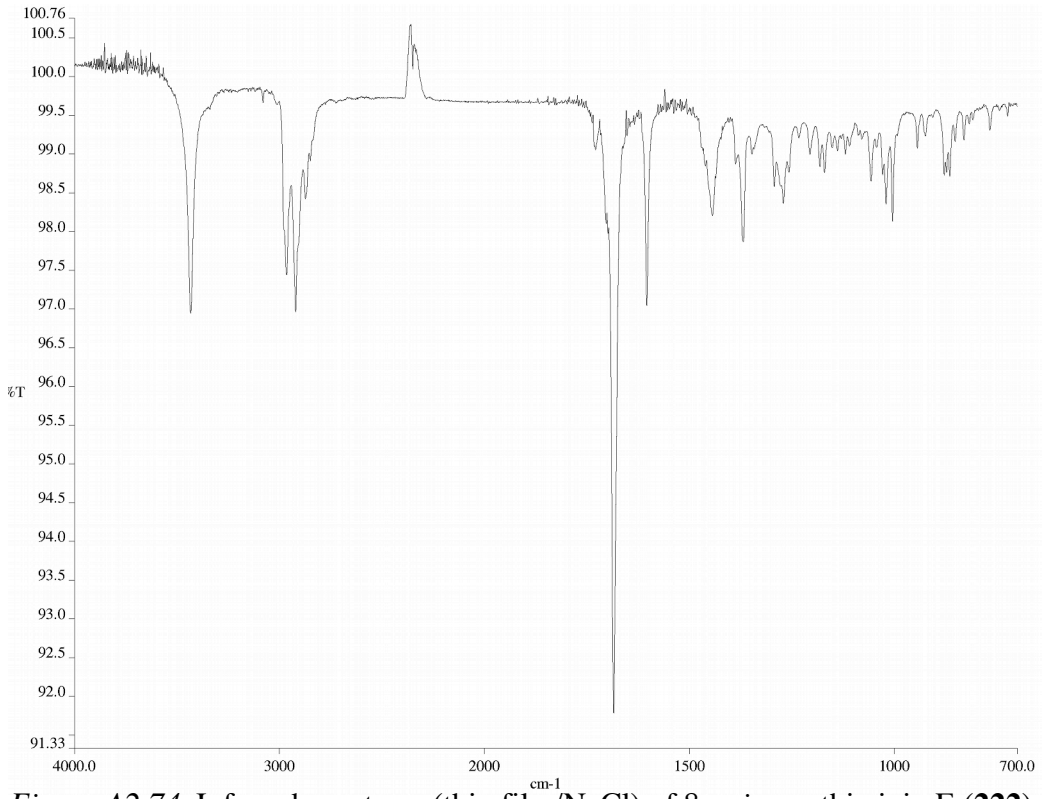

Figure A2.74 Infrared spectrum (thin film/NaCl) of 8-*epi*-cyanthiwigin E (**222**).

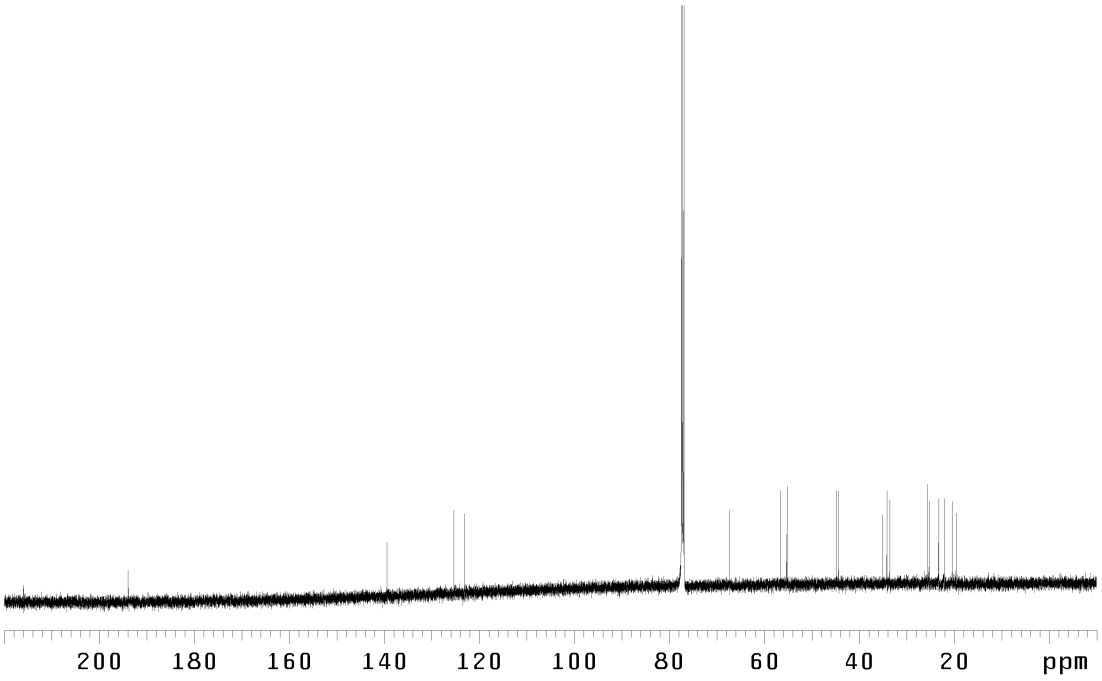

Figure A2.75 ^{13}C NMR (125 MHz, $CDCl_3$) of 8-*epi*-cyanthiwigin E (**222**).

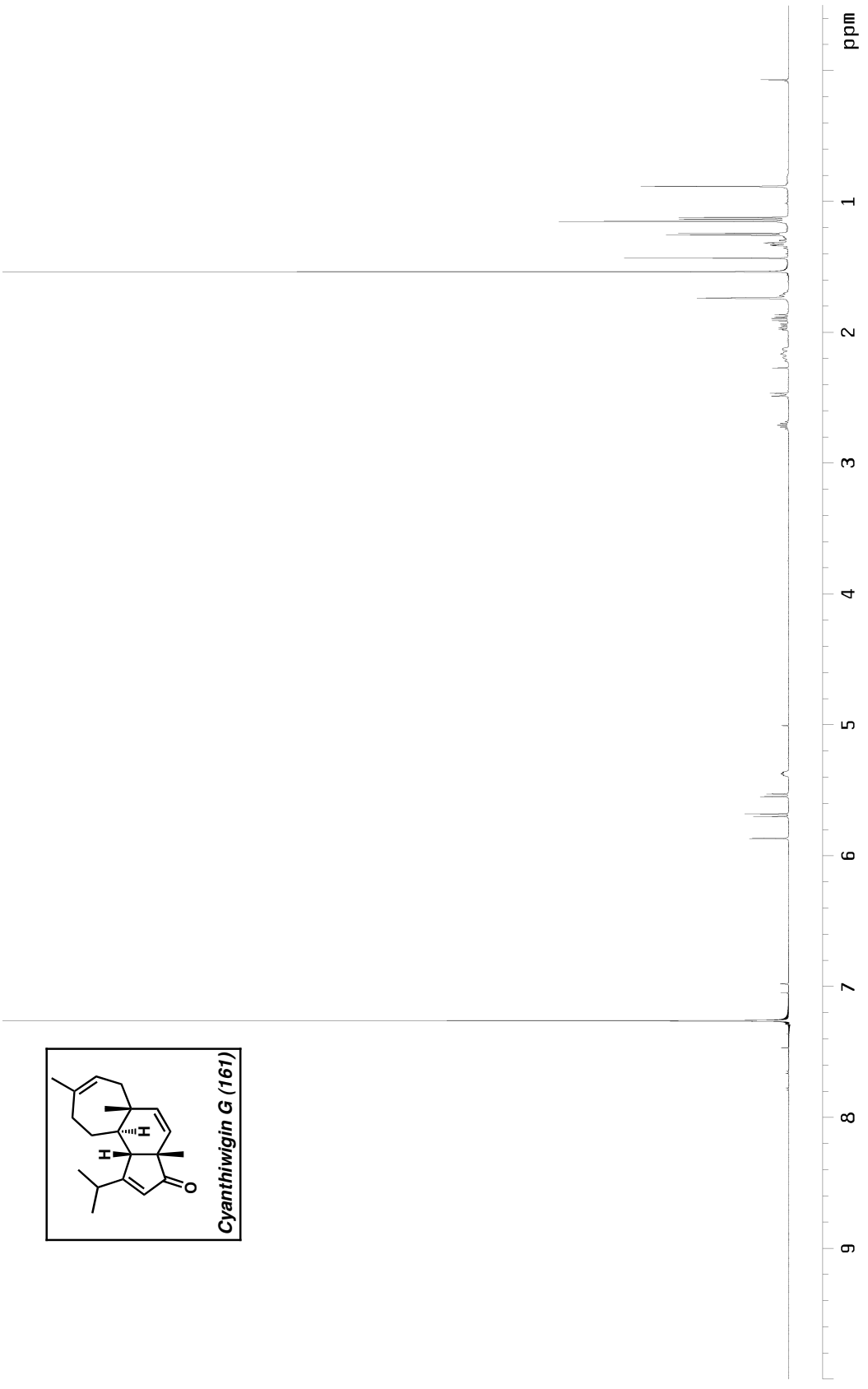

Figure A2.76 ^{1}H NMR (500 MHz, $CDCl_3$) of cyanthiwigin G (**161**).

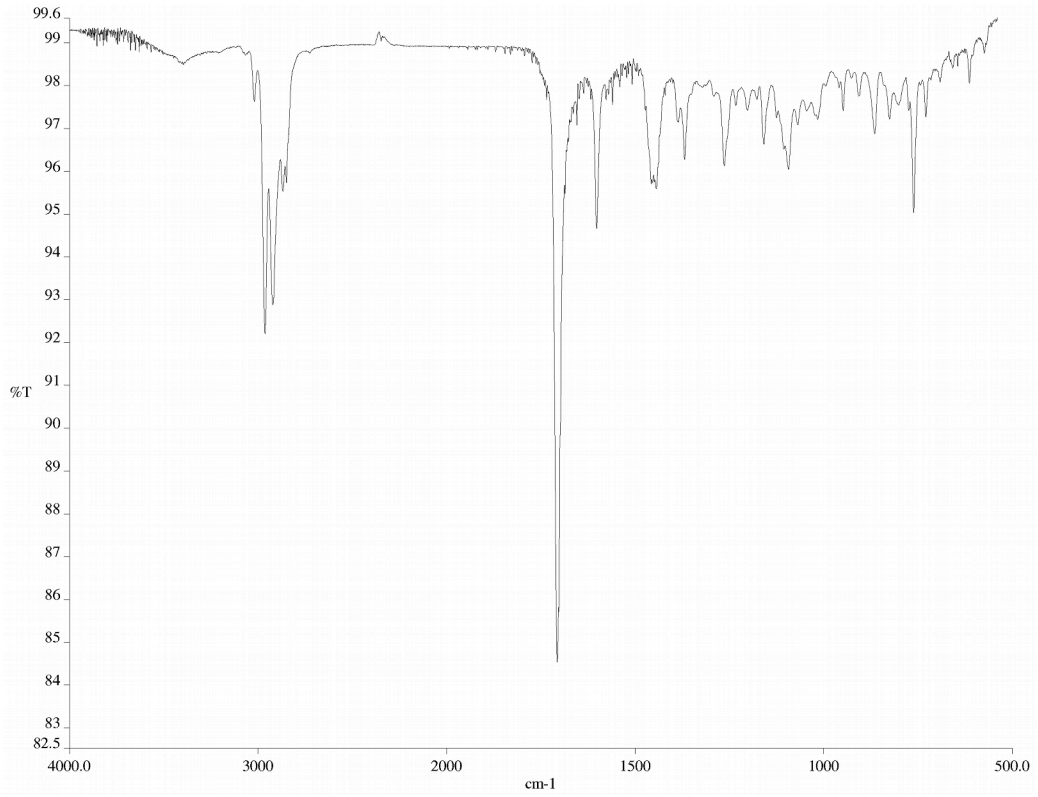

Figure A2.77 Infrared spectrum (thin film/NaCl) of cyanthiwigin G (**161**).

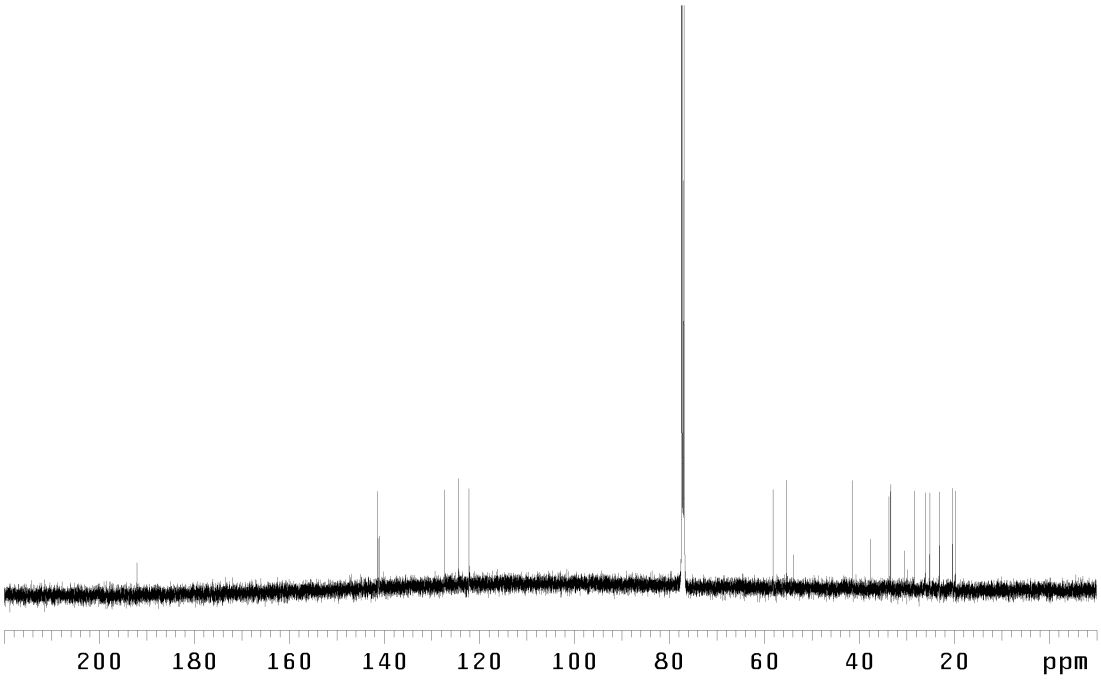

Figure A2.78 ^{13}C NMR (125 MHz, $CDCl_3$) of cyanthiwigin G (**161**).

APPENDIX 3

X-ray Crystallography Reports Relevant to Chapter 2

A3.1 CRYSTAL STRUCTURE ANALYSIS OF DIKETONE *214*

*Figure A3.1 ORTEP drawing of tricyclic diketone **214** (shown with 50% probability ellipsoids).*

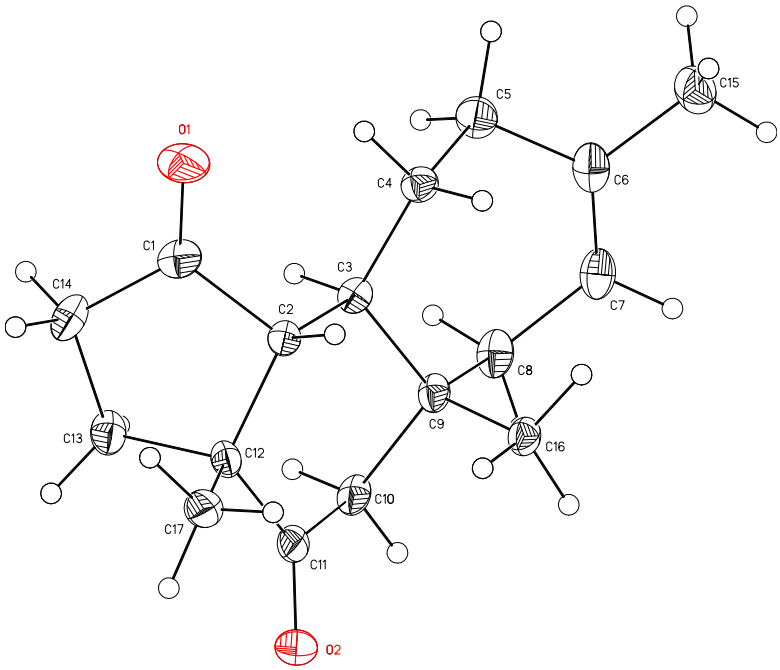

Crystallographic data have been deposited at the CCDC, 12 Union Road, Cambridge CB2 1EZ, UK and copies can be obtained on request, free of charge, by quoting the publication citation and the deposition number 664430.

*Table A3.1 Crystal data and structure refinement for tricyclic diketone **214** (CCDC 664430).*

Empirical formula	$C_{17}H_{24}O_2$
Formula weight	260.36
Crystallization Solvent	Water/acetonitrile
Crystal Habit	Fragment
Crystal size	0.39 x 0.28 x 0.09 mm^3
Crystal color	Colorless

Data Collection

Type of diffractometer	Bruker SMART 1000
Wavelength	1.54178 Å CuKα
Data Collection Temperature	100(2) K
θ range for 5024 reflections used in lattice determination	4.12 to 65.79°
Unit cell dimensions	a = 7.4937(2) Å b = 9.0345(2) Å c = 21.4487(5) Å
Volume	1452.12(6) $Å^3$
Z	4
Crystal system	Orthorhombic
Space group	$P2_12_12_1$
Density (calculated)	1.191 Mg/m^3
F(000)	568
Data collection program	Bruker SMART v5.630
θ range for data collection	4.12 to 65.79°
Completeness to θ = 65.79°	96.1 %
Index ranges	$-7 \leq h \leq 8$, $-10 \leq k \leq 8$, $-21 \leq l \leq 24$
Data collection scan type	ω scans at 7 ϕ settings
Data reduction program	Bruker SAINT v6.45A
Reflections collected	7914
Independent reflections	2344 [R_{int}= 0.0753]
Absorption coefficient	0.593 mm^{-1}
Absorption correction	None
Max. and min. transmission	0.9486 and 0.8017

Table A3.1 (cont.)

Structure solution and Refinement

Structure solution program	SHELXS-97 (Sheldrick, 1990)
Primary solution method	Direct methods
Secondary solution method	Difference Fourier map
Hydrogen placement	Difference Fourier map
Structure refinement program	SHELXL-97 (Sheldrick, 1997)
Refinement method	Full matrix least-squares on F^2
Data / restraints / parameters	2344 / 0 / 268
Treatment of hydrogen atoms	Unrestrained
Goodness-of-fit on F^2	1.394
Final R indices [I>2σ(I), 2083 reflections]	R1 = 0.0335, *w*R2 = 0.0669
R indices (all data)	R1 = 0.0391, *w*R2 = 0.0686
Type of weighting scheme used	Sigma
Weighting scheme used	$w=1/\sigma^2(Fo^2)$
Max shift/error	0.000
Average shift/error	0.000
Absolute structure determination	Anomalous differences
Absolute structure parameter	0.2(2)
Largest diff. peak and hole	0.142 and -0.155 e.Å^{-3}

Special Refinement Details

Refinement of F^2 against ALL reflections. The weighted R-factor (*w*R) and goodness of fit (S) are based on F^2, conventional R-factors (R) are based on F, with F set to zero for negative F^2. The threshold expression of $F^2 > 2\sigma(F^2)$ is used only for calculating R-factors(gt) etc. and is not relevant to the choice of reflections for refinement. R-factors based on F^2 are statistically about twice as large as those based on F, and R-factors based on ALL data will be even larger.

All esds (except the esd in the dihedral angle between two l.s. planes) are estimated using the full covariance matrix. The cell esds are taken into account individually in the estimation of esds in distances, angles and torsion angles; correlations between esds in cell parameters are only used when they are defined by crystal symmetry. An approximate (isotropic) treatment of cell esds is used for estimating esds involving l.s. planes.

*Figure A3.2 Tricyclic diketone **214** (CCDC 664430)*

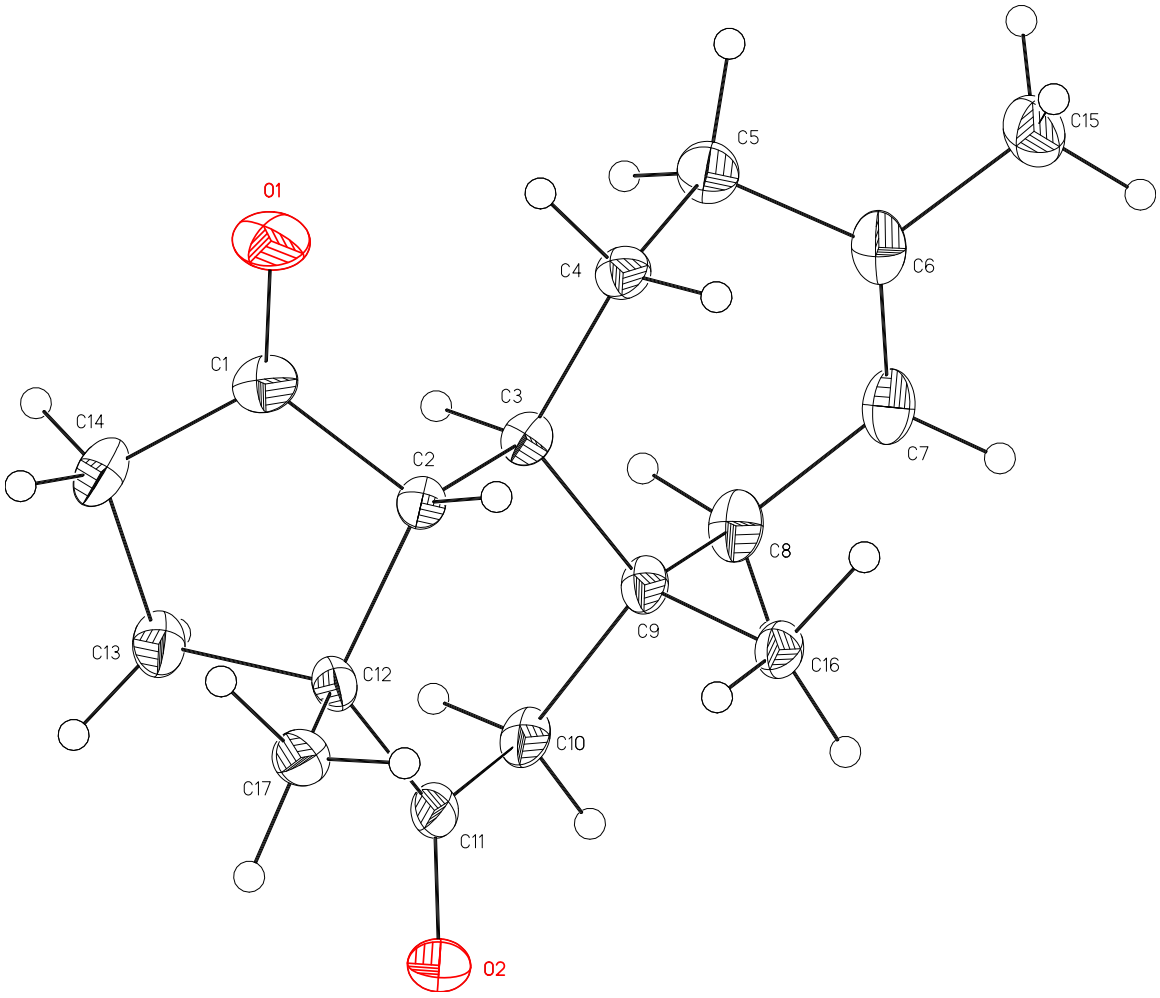

Table A3.2 Atomic coordinates (x 10^4) and equivalent isotropic displacement parameters ($Å^2$x 10^3) for diketone ***214*** *(CCDC 664430). U(eq) is defined as the trace of the orthogonalized U^{ij} tensor.*

	x	y	z	U_{eq}
O(1)	8369(2)	2053(2)	7466(1)	32(1)
O(2)	13478(2)	3487(2)	5446(1)	29(1)
C(1)	9211(2)	2001(2)	6981(1)	21(1)
C(2)	10059(2)	3336(2)	6653(1)	15(1)
C(3)	8595(2)	4237(2)	6306(1)	15(1)
C(4)	7465(3)	5062(2)	6791(1)	18(1)
C(5)	5740(3)	5787(2)	6542(1)	25(1)
C(6)	6041(2)	7246(2)	6214(1)	23(1)
C(7)	7053(3)	7331(2)	5712(1)	24(1)
C(8)	7949(3)	6025(2)	5407(1)	22(1)
C(9)	9420(3)	5246(2)	5792(1)	17(1)
C(10)	10444(3)	4224(2)	5340(1)	20(1)
C(11)	11962(2)	3449(2)	5658(1)	20(1)
C(12)	11518(2)	2593(2)	6244(1)	17(1)
C(13)	10651(3)	1092(2)	6049(1)	22(1)
C(14)	9615(3)	599(2)	6620(1)	24(1)
C(15)	5143(3)	8573(3)	6497(1)	30(1)
C(16)	10728(3)	6397(2)	6053(1)	19(1)
C(17)	13190(3)	2308(2)	6637(1)	23(1)

*Table A3.3. Bond lengths [Å] and angles [°] for diketone **214** (CCDC 664430)*

O(1)-C(1)	1.219(2)	C(1)-C(2)-C(3)	109.78(14)
O(2)-C(11)	1.224(2)	C(12)-C(2)-C(3)	116.84(14)
C(1)-C(14)	1.514(3)	C(1)-C(2)-H(2)	108.8(9)
C(1)-C(2)	1.533(2)	C(12)-C(2)-H(2)	111.2(9)
C(2)-C(12)	1.554(2)	C(3)-C(2)-H(2)	107.8(9)
C(2)-C(3)	1.556(2)	C(4)-C(3)-C(2)	108.61(14)
C(2)-H(2)	0.972(16)	C(4)-C(3)-C(9)	114.51(15)
C(3)-C(4)	1.534(3)	C(2)-C(3)-C(9)	111.44(14)
C(3)-C(9)	1.559(2)	C(4)-C(3)-H(3)	107.6(9)
C(3)-H(3)	1.050(16)	C(2)-C(3)-H(3)	106.6(9)
C(4)-C(5)	1.544(3)	C(9)-C(3)-H(3)	107.7(8)
C(4)-H(4A)	1.008(19)	C(3)-C(4)-C(5)	115.75(16)
C(4)-H(4B)	0.995(18)	C(3)-C(4)-H(4A)	111.3(11)
C(5)-C(6)	1.511(3)	C(5)-C(4)-H(4A)	107.4(11)
C(5)-H(5A)	0.994(19)	C(3)-C(4)-H(4B)	108.6(10)
C(5)-H(5B)	1.06(2)	C(5)-C(4)-H(4B)	107.8(10)
C(6)-C(7)	1.320(3)	H(4A)-C(4)-H(4B)	105.5(14)
C(6)-C(15)	1.503(3)	C(6)-C(5)-C(4)	113.95(17)
C(7)-C(8)	1.507(3)	C(6)-C(5)-H(5A)	109.1(11)
C(7)-H(7)	0.99(2)	C(4)-C(5)-H(5A)	106.3(11)
C(8)-C(9)	1.547(3)	C(6)-C(5)-H(5B)	108.4(12)
C(8)-H(8A)	1.046(19)	C(4)-C(5)-H(5B)	107.8(11)
C(8)-H(8B)	1.013(19)	H(5A)-C(5)-H(5B)	111.3(15)
C(9)-C(16)	1.535(2)	C(7)-C(6)-C(15)	122.73(18)
C(9)-C(10)	1.543(2)	C(7)-C(6)-C(5)	121.05(18)
C(10)-C(11)	1.500(3)	C(15)-C(6)-C(5)	116.21(18)
C(10)-H(10A)	1.008(19)	C(6)-C(7)-C(8)	124.41(19)
C(10)-H(10B)	0.94(2)	C(6)-C(7)-H(7)	121.8(11)
C(11)-C(12)	1.514(2)	C(8)-C(7)-H(7)	113.8(11)
C(12)-C(17)	1.532(3)	C(7)-C(8)-C(9)	116.25(16)
C(12)-C(13)	1.561(3)	C(7)-C(8)-H(8A)	109.8(11)
C(13)-C(14)	1.518(3)	C(9)-C(8)-H(8A)	108.7(11)
C(13)-H(13A)	0.966(18)	C(7)-C(8)-H(8B)	110.5(10)
C(13)-H(13B)	0.973(19)	C(9)-C(8)-H(8B)	105.5(10)
C(14)-H(14A)	0.99(2)	H(8A)-C(8)-H(8B)	105.5(15)
C(14)-H(14B)	1.00(2)	C(16)-C(9)-C(10)	108.47(16)
C(15)-H(15A)	1.00(2)	C(16)-C(9)-C(8)	109.99(15)
C(15)-H(15B)	1.01(2)	C(10)-C(9)-C(8)	106.98(15)
C(15)-H(15C)	0.96(2)	C(16)-C(9)-C(3)	112.96(14)
C(16)-H(16A)	1.03(2)	C(10)-C(9)-C(3)	106.99(14)
C(16)-H(16B)	1.000(19)	C(8)-C(9)-C(3)	111.19(15)
C(16)-H(16C)	1.036(19)	C(11)-C(10)-C(9)	111.79(15)
C(17)-H(17A)	1.00(2)	C(11)-C(10)-H(10A)	107.4(10)
C(17)-H(17B)	1.01(2)	C(9)-C(10)-H(10A)	110.6(10)
C(17)-H(17C)	0.95(2)	C(11)-C(10)-H(10B)	110.2(12)
		C(9)-C(10)-H(10B)	109.6(12)
O(1)-C(1)-C(14)	124.84(18)	H(10A)-C(10)-H(10B)	107.0(15)
O(1)-C(1)-C(2)	125.15(17)	O(2)-C(11)-C(10)	121.45(17)
C(14)-C(1)-C(2)	109.99(15)	O(2)-C(11)-C(12)	121.84(17)
C(1)-C(2)-C(12)	102.14(14)	C(10)-C(11)-C(12)	116.70(15)

C(11)-C(12)-C(17)	111.27(16)	C(6)-C(15)-H(15B)	110.4(12)
C(11)-C(12)-C(2)	113.80(14)	H(15A)-C(15)-H(15B)	106.7(18)
C(17)-C(12)-C(2)	109.74(15)	C(6)-C(15)-H(15C)	114.4(14)
C(11)-C(12)-C(13)	108.17(14)	H(15A)-C(15)-H(15C)	112.7(19)
C(17)-C(12)-C(13)	110.00(16)	H(15B)-C(15)-H(15C)	102.7(17)
C(2)-C(12)-C(13)	103.55(15)	C(9)-C(16)-H(16A)	109.4(11)
C(14)-C(13)-C(12)	104.54(15)	C(9)-C(16)-H(16B)	111.8(11)
C(14)-C(13)-H(13A)	110.1(10)	H(16A)-C(16)-H(16B)	111.5(15)
C(12)-C(13)-H(13A)	110.7(11)	C(9)-C(16)-H(16C)	107.7(10)
C(14)-C(13)-H(13B)	111.8(11)	H(16A)-C(16)-H(16C)	107.4(15)
C(12)-C(13)-H(13B)	112.1(12)	H(16B)-C(16)-H(16C)	108.8(14)
H(13A)-C(13)-H(13B)	107.6(15)	C(12)-C(17)-H(17A)	110.3(11)
C(1)-C(14)-C(13)	105.56(16)	C(12)-C(17)-H(17B)	112.1(12)
C(1)-C(14)-H(14A)	113.1(12)	H(17A)-C(17)-H(17B)	108.9(16)
C(13)-C(14)-H(14A)	111.2(12)	C(12)-C(17)-H(17C)	111.9(11)
C(1)-C(14)-H(14B)	109.3(12)	H(17A)-C(17)-H(17C)	109.2(16)
C(13)-C(14)-H(14B)	112.8(12)	H(17B)-C(17)-H(17C)	104.2(15)
H(14A)-C(14)-H(14B)	105.1(17)		
C(6)-C(15)-H(15A)	109.6(13)		

*Table A3.4 Anisotropic displacement parameters ($Å^2 x\ 10^4$) for diketone **214** (CCDC 664430). The anisotropic displacement factor exponent takes the form: $-2\pi^2 [h^2 a^{*2} U^{11} + ... + 2 h k a^* b^* U^{12}]$*

	U^{11}	U^{22}	U^{33}	U^{23}	U^{13}	U^{12}
O(1)	372(9)	382(9)	203(8)	136(6)	113(6)	108(7)
O(2)	332(8)	252(8)	275(8)	-7(6)	149(6)	2(7)
C(1)	202(11)	268(11)	149(10)	90(8)	-25(8)	30(8)
C(2)	203(10)	152(10)	94(10)	-6(7)	-6(7)	-11(7)
C(3)	175(10)	170(10)	115(10)	12(7)	-25(7)	-14(8)
C(4)	183(11)	195(11)	170(11)	27(9)	1(8)	1(8)
C(5)	173(11)	242(12)	320(13)	9(9)	-27(10)	14(9)
C(6)	199(12)	187(10)	317(12)	2(9)	-117(9)	9(8)
C(7)	306(12)	175(11)	231(12)	53(8)	-85(9)	15(9)
C(8)	312(11)	188(11)	165(11)	37(8)	-69(9)	3(9)
C(9)	252(11)	141(10)	124(10)	15(7)	-2(8)	-2(8)
C(10)	332(12)	160(11)	98(10)	17(8)	33(8)	-30(9)
C(11)	296(12)	142(11)	163(11)	-59(7)	66(8)	-34(8)
C(12)	211(11)	130(10)	157(10)	1(7)	5(7)	26(7)
C(13)	340(12)	174(11)	160(11)	-5(8)	4(9)	-7(9)
C(14)	308(13)	197(11)	213(12)	38(8)	-22(9)	-82(9)
C(15)	233(12)	241(12)	421(15)	3(11)	-34(10)	51(9)
C(16)	244(11)	150(10)	178(11)	-20(8)	16(8)	-29(9)
C(17)	212(12)	212(12)	262(12)	30(9)	28(9)	30(9)

*Table A3.5 Hydrogen coordinates (x 10^4) and isotropic displacement parameters ($Å^2$x 10^{-3}) for diketone **214** (CCDC 664430)*

	x	y	z	U_{iso}
H(2)	10590(20)	3978(18)	6967(7)	5(4)
H(3)	7760(20)	3463(18)	6085(7)	7(4)
H(7)	7290(20)	8280(20)	5503(9)	29(5)
H(4A)	8180(20)	5860(20)	7005(8)	21(5)
H(5A)	5210(20)	5070(20)	6242(9)	24(5)
H(8A)	8490(30)	6340(20)	4977(9)	33(5)
H(10A)	9630(20)	3440(20)	5166(8)	22(5)
H(13A)	9850(20)	1230(20)	5701(9)	19(5)
H(14A)	8530(30)	40(20)	6501(9)	33(6)
H(15A)	5460(30)	9480(30)	6252(10)	46(7)
H(16A)	11750(30)	5860(20)	6279(9)	31(6)
H(17A)	14160(30)	1860(20)	6372(9)	30(5)
H(4B)	7120(20)	4350(20)	7125(8)	16(5)
H(5B)	4880(30)	5970(20)	6926(10)	41(6)
H(8B)	7040(20)	5230(20)	5307(8)	17(5)
H(10B)	10870(20)	4780(20)	5001(9)	26(5)
H(13B)	11540(30)	360(20)	5925(9)	24(6)
H(14B)	10310(30)	-90(20)	6890(10)	36(6)
H(15B)	5590(30)	8740(20)	6937(9)	34(6)
H(16B)	10120(20)	7120(20)	6333(8)	26(5)
H(17B)	12940(30)	1620(20)	7000(9)	37(6)
H(15C)	3890(30)	8470(30)	6556(10)	43(6)
H(16C)	11280(20)	6960(20)	5679(9)	22(5)
H(17C)	13620(20)	3190(20)	6827(8)	17(5)

CHAPTER 3

A Mathematical Examination of Multiple Asymmetric Transformations:

Statistical Amplification and the Horeau Principle.

3.1 INTRODUCTION

Multiple asymmetric transformations are powerful reactions that establish multiple stereocenters in a single synthetic transformation. The ability to sequentially and selectively execute more than one bond-forming event in a single operation is undeniably advantageous to any complicated multistep synthesis. In addition to the expediency gained in bond construction, this technique also holds the potential to impart beneficial amplification to the enantiomeric purity of the terminal product. However, whereas the course of solitary enantioselective transformations are very well understood, the impact of more than one such reaction upon a single substrate is typically more complicated. This is particularly true with regard to prediction and analysis of the eventual enantio- and diastereomeric enrichment of the final product. The following chapter examines the impact of compound dimerization events and multiple asymmetric transformations with a specific focus on the stereochemical outcome of these reactions, as well as the possible

pathways relevant to the course of these reactions. The nature of statistical amplification and its benefits in complex molecular synthesis are explored mathematically and empirically, with particular attention paid to the effect known as the Horeau Principle.

3.1.1 PRELIMINARY RESULTS AND INITIAL INTEREST

Recently, our group completed the total synthesis of the marine diterpenoid natural product cyanthiwigin F.[1] Vital to the success of our synthetic route was the use of an early-stage double asymmetric catalytic alkylation reaction to simultaneously set two all-carbon quaternary stereocenters.[2] By subjecting bis(β-ketoester) (**186**) to a catalyst comprised of palladium(0) and (*S*)-*t*-BuPHOX (**193**), it was possible to realize the synthesis of diketone (*R*, *R*)-**185** in 78% yield, with an exceptional *ee* of 99% and a dr of 4.4:1 (Scheme 3.1). While we were delighted to obtain such a high level of enantioselectivity, the modest diastereomeric ratio observed in this reaction was not anticipated. Our experience concerning the catalytic enantioselective alkylation of isolated, single β-ketoester substrates routinely yielded products with roughly 95 : 5 selectivity. As such, it was our expectation that the double stereoselective alkylation would afford the desired product with a high level of diastereoselectivity. Indeed, because the reaction was selective to the point of affording essentially enantiopure (*R*,*R*)-**185**, we anticipated that the process would also strongly favor the formation of C_2 symmetric isomer (*R*,*R*)-**185** over the *meso* diastereomer of diketone **185**.

Scheme 3.1 Double asymmetric catalytic alkylation

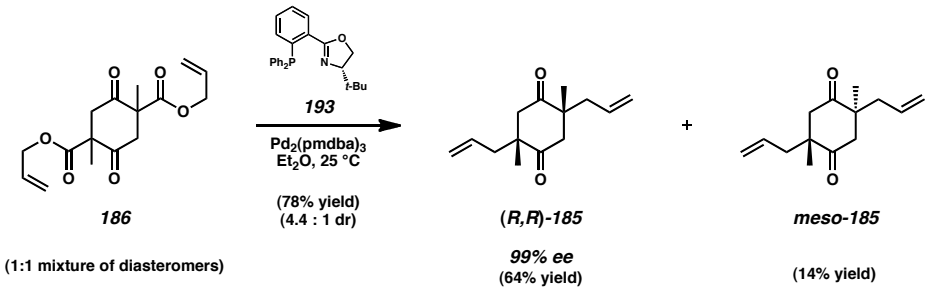

In order to examine other cases of double asymmetric alkylation, we desired to develop alternative substrates with which to probe these processes. Though bis(β-ketoester) **186** had proven to be an efficient substrate for the synthesis of the cyanthiwigin natural products, the nature of its preparation obviated the potential to efficiently separate the primary and secondary alkylation processes. Therefore, we sought a different class of double alkylation substrate that, with appropriate substitution, would allow the two alkylation steps to be cleanly and predictably differentiated from one another. For example, carbonate (±)-**223** was designed specifically as a substrate for such a double allylation reaction (Scheme 3.2).[3] Not only does ester **223** contain a reactive enol carbonate functionality, but it also boasts a latent β-ketoester moiety, a group that is only revealed upon conclusion of the first alkylation process. Treatment of enol carbonate **223** with palladium(0) and ligand **193** provided smooth access to cyclohexanone **224** in 76% yield and 92% *ee*. However, just as the case of bis(β-ketoester) **224** the diastereomeric ratio of C_2 symmetric ketone (*S*,*S*)-**224** to *meso* ketone **224** was mediocre (4.0 : 1).

Scheme 3.2 Double asymmetric catalytic alkylation of an enol carbonate ester substrate

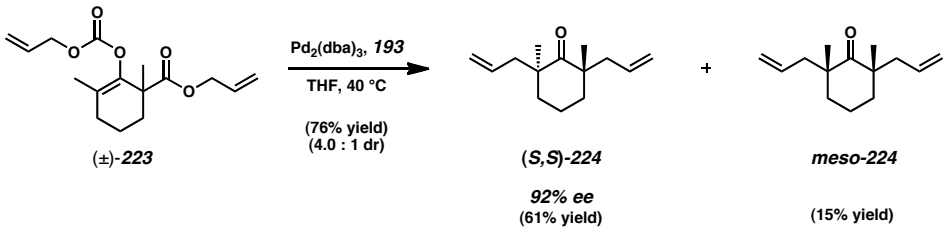

With these results in hand, we reasoned that optimization of the diastereomeric ratio resulting from these transformations would require a deeper understanding of the course of the reaction. Toward this end, we became interested in thoroughly scrutinizing the selectivity of alkylation at each independent C–C bond-formation step for any given double stereoselective process. Ideally, we sought a method to determine these desired selectivity values from the three observable stereochemical values of the final product of a double stereoselective transformation, namely the diastereomeric ratio (dr) and the enantiomeric excess of both isolated diastereomers (ee_A and ee_B).[4] As we quickly came to understand, a thorough investigation of multiple asymmetric processes required a historical review of the literature, as well as a mathematical representation of the stereoisomers involved.

3.2 DUPLICATION AND MULTIPLE ASYMMETRIC PROCESSES

The following sections investigate the historical and mathematical aspects of statistical amplification as it relates to both duplication reactions and multiple asymmetric transformations. A brief history of scalemic dimerization is followed by a presentation of the pertinent equations related to this phenomenon. The same treatment is then given to multiple asymmetric reactions, with a specific focus on double asymmetric processes.

3.2.1 THE HISTORY OF STATISTICAL AMPLIFICATION

The fundamental concepts related to the statistical amplification of enantiomeric excess in multiple asymmetric reactions were first investigated in relation to non-enantioselective transformations. Indeed, one of the earliest reported examples of this enantioenrichment phenomenon utilized no external chiral reagents whatsoever, but instead involved the dimerization of a scalemic mixture of starting materials.

In 1936, Langenbeck and coworkers conducted a series of experiments in an effort to understand the mechanisms maintaining the enantiopurity of naturally occurring compounds.[5] He observed that "with every synthesis of an optically active compound from inactive starting materials, a degradation in optical purity takes place; that is, the newly formed compound is less optically active than the compound from which the optical activity was derived." Langenbeck further elaborated his postulate by explaining that, "If an enzyme is synthesized using another optically active enzyme, the newly formed product cannot be optically pure. The infinite repetition of these processes over a geological time period would have led to a complete loss of optical activity in enzymes (and therefore of all naturally occurring compounds) if the degradation in optical purity were not compensated for by an increase in optical purity in a different process."[5]

In order to seek out and study this enantiopurity preservation process, Langenbeck and coworkers subjected multiple samples of L-menthol (L-**225**) (each with varying degrees of enantioenrichment) to a process of dimerization with oxalyl chloride (**226**, Scheme 3.3A). Upon measuring the optical rotation of the resulting dimers (**227**) obtained from increasingly enantiopure samples of alcohol L-**225**, nonlinear deviations were observed that did not match the expected behavior (Scheme 3.3B). Curve I depicts

the optical rotation measured for the individual samples of L-menthol employed, while curve II represents the optical rotation of the resulting dimer formed from each of these samples. In nearly every instance, Langenbeck observed that the optical rotation of the dimer was significantly different than the optical rotation of the corresponding menthol monomer employed. Repetition of this experiment while employing modern HPLC techniques has verified that the *ee* of the dimer is greater than that of the starting material for every experiment run.[5b]

*Scheme 3.3 (A) Langenbeck's initial experiment (B) Curves depicting the optical rotation of samples of (I) L-**225** and (II) **227** vs enantioenrichment of L-menthol starting material*

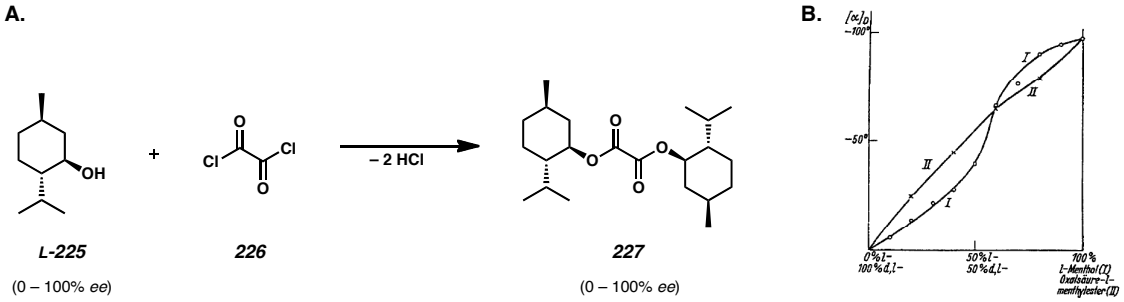

The amplification in enantiopurity measured in the product dimers when compared to their relative starting materials was puzzling. Because no enantioenriched materials beyond L-menthol (L-**225**) were employed in the reaction, it was not immediately clear how the *ee* of the product obtained could exceed that of the starting material used. To rationalize this observation, Langenbeck concluded that the increase in observed *ee* of the product must be the result of a statistical phenomenon.

If one examines the course of this transformation, initial reaction of a scalemic mixture of L-menthol (L-**225**) with oxalyl chloride (**226**) would necessarily produce intermediate acid halide species (*R*,*R*,*S*)-**228** (Scheme 3.4). Depending on the level of

enantiopurity of the menthol used in this reaction, some quantity of D-menthol (D-**225**) would be present in the reaction mixture, and thus would be expected to react in a corresponding manner to give acid halide (*S*,*S*,*R*)-**228**. Intermediate acid chlorides (*R*,*R*,*S*)-**228** and (*S*,*S*,*R*)-**228** would then undergo reaction with an additional equivalent of either L- or D-menthol, ultimately producing one of three stereoisomeric products. In the event that either ester (*R*,*R*,*S*)-**228** or ester (*S*,*S*,*R*)-**228** react with another molecule of menthol of the same enantiomeric sense as the first reaction, then homochiral isomers (L,L)-bis-menthyl oxylate (L,L-**227**) or (D,D)-bis-menthyl oxylate (D,D-**227**) will result. If either intermediate (*R*,*R*,*S*)-**228** or (*S*,*S*,*R*)-**228** react instead with the opposite enantiomer of menthol, the heterochiral (*meso*)-bis-menthyl oxylate (*meso*-**227**) will be afforded.

Scheme 3.4 Product pathways for Langenbeck's duplication experiment

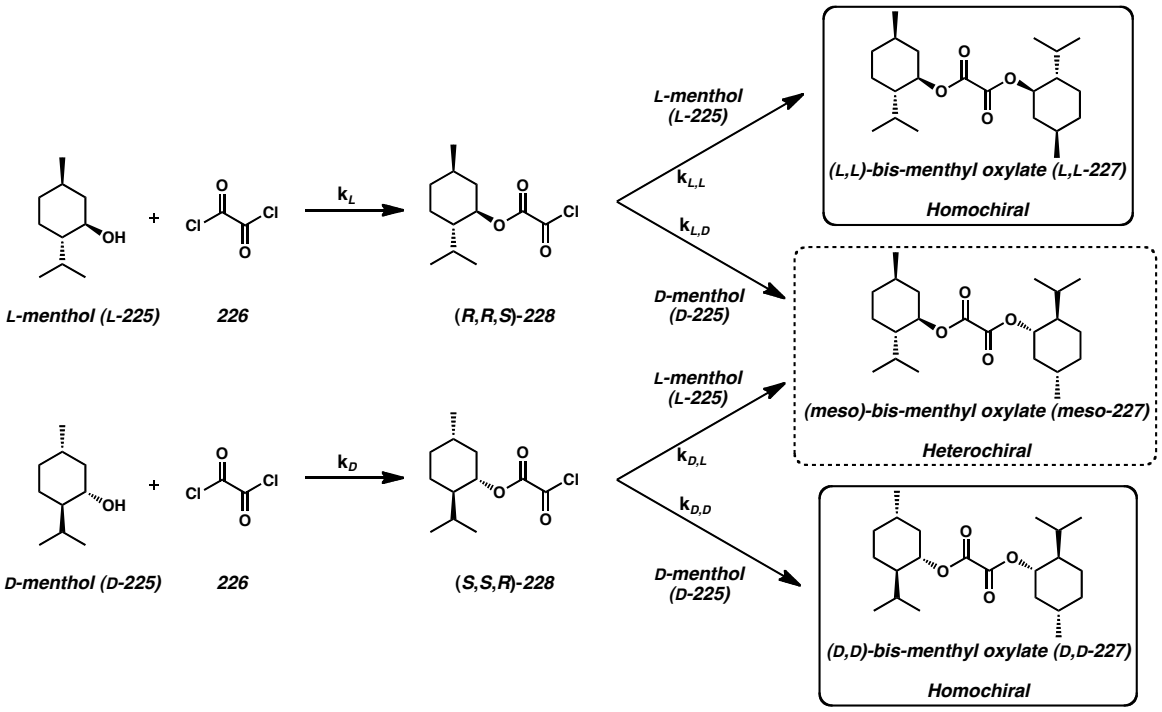

At the time of his initial experiment, Langenbeck surmised that the observed deviation in optical purity was a consequence of the distribution between the diastereomers formed as the eventual reaction products. Because the *meso* diastereomer is composed of one D- and one L-isomer of menthol, and because this diastereomer cannot rotate polarized light, the formation of this dimer in Lagenbeck's experiment effectively represented the removal of racemic menthol from the observable system. Though he had no way to effect the physical separation of these diastereomers, Langenbeck nevertheless hypothesized that "If it were possible to separate the *meso* ester quantitatively, then it would be expected that even with the use of L-menthol with a low *ee* value, an increase in the optical purity of the product would be observed."[5]

Over 40 years after the publication of Langenbeck's findings, Horeau and coworkers revisited the concept of enantiomeric amplification via duplication.[6] With the benefit of improved purification techniques, Horeau was able to perform his own dimerization experiments in order to further elucidate the nature of this phenomenon. Using a system similar to the dimerization of L-menthol, Horeau *et al*. investigated the reaction of scalemic *sec*-phenethyl alcohol (**229**, 60% *ee*) with diethyl carbonate under alkaline conditions (Scheme 3.5).

Scheme 3.5 Duplication of sec*-phenethyl alcohol by Horeau*

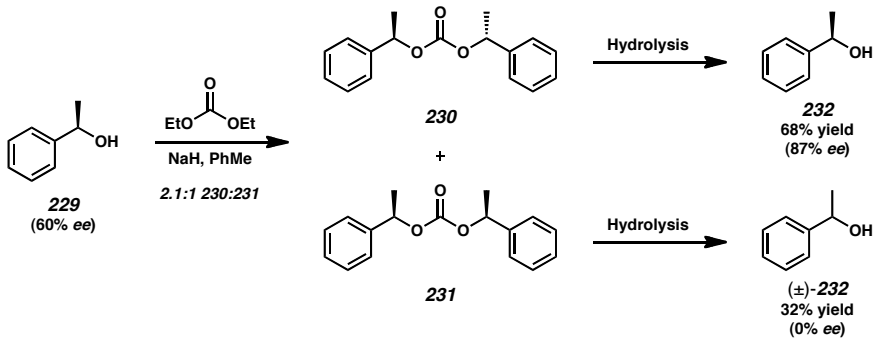

Dimerization of *sec*-phenethyl alcohol (**229**) afforded both the homochiral carbonate **230** and the heterochiral carbonate **231**, in a 2.1 : 1 ratio. After purification, separation, and hydrolysis of these diastereomeric products, two different samples of *sec*-phenethyl alcohol were isolated.[7] The alcohol product **232** obtained from the heterochiral diastereomer (**231**) was observed to be completely racemic, whereas saponification of the homochiral diastereomer (**230**) afforded enantioenriched alcohol **232** in 87% *ee*. This result represented a statistical amplification of *ee* without the use of external chiral reagents, as *sec*-phenethyl alcohol was enriched by 27% *ee* via simple dimerization of the starting material. These results experimentally confirmed Langenbeck's previous hypothesis, as the duplication process effectively allowed for the removal of racemic substrate via the separation of diastereomeric intermediates.

3.2.2 MATHEMATICAL REPRESENTATION OF HOREAU DUPLICATION

In order to extrapolate his experimental findings into a useful, predictive model, Horeau subsequently addressed the duplication phenomenon from a mathematical perspective. For any scalemic material for which one arbitrarily assigns that the *R*

enantiomer (**233**) predominates over the *S* enantiomer (**234**), the relative mol fraction of the two isomers is represented by x for the *R* enantiomer and 1 – x for the *S* enantiomer (Scheme 3.6A). If the possible reactive pathways toward complete dimerization are followed, reaction of either enantiomer with a dimerization linker (**235**) will afford either the *R*-substituted (**236**) or *S*-substituted (**237**) intermediate. Further reaction of these intermediates with the remaining monomeric components thereafter furnishes the expected dimers in four different stereoisomeric forms. The *R*-derived intermediate **236** can further react with either enantiomer of the starting material to furnish the homochiral (**238**) or the heterochiral (**239**) diastereomer. Similarly, the *S*-derived intermediate **237** can also produce heterochiral (**240**) and homochiral (**241**) products.

If a number of assumptions are applied to this system, two very useful equations can be applied to the duplication phenomenon. The reaction pathways illustrated below contain six different transformations, each with its own distinct rate constant. In order for the obtained mathematical representations to be manageable, it is assumed that all six of these rate constants are reasonably similar ($k_R \cong k_S \cong k_{RR} \cong k_{RS} \cong k_{SR} \cong k_{RR}$). This precludes the possibility of kinetic resolution at any point in the reaction process, and additionally presumes that no chiral recognition or asymmetric induction occurs between the chiral intermediates **236** or **237** and the monomeric starting materials **233** and **234**. Although this assumption may appear at first to be extreme, if the nature of the dimerization linker **235** is such that the two reactive centers are sufficiently removed from one another, these simplifications become quite appropriate. Additionally, all reactions are assumed to proceed to completion, so that all molecules of starting material (**233** and **234**) and intermediate (**236** and **237**) are consumed in this process.

Scheme 3.6 (A) Reaction pathways for Horeau-type dimerization and (B) mathematical representations of relevent stereoisomeric quantities

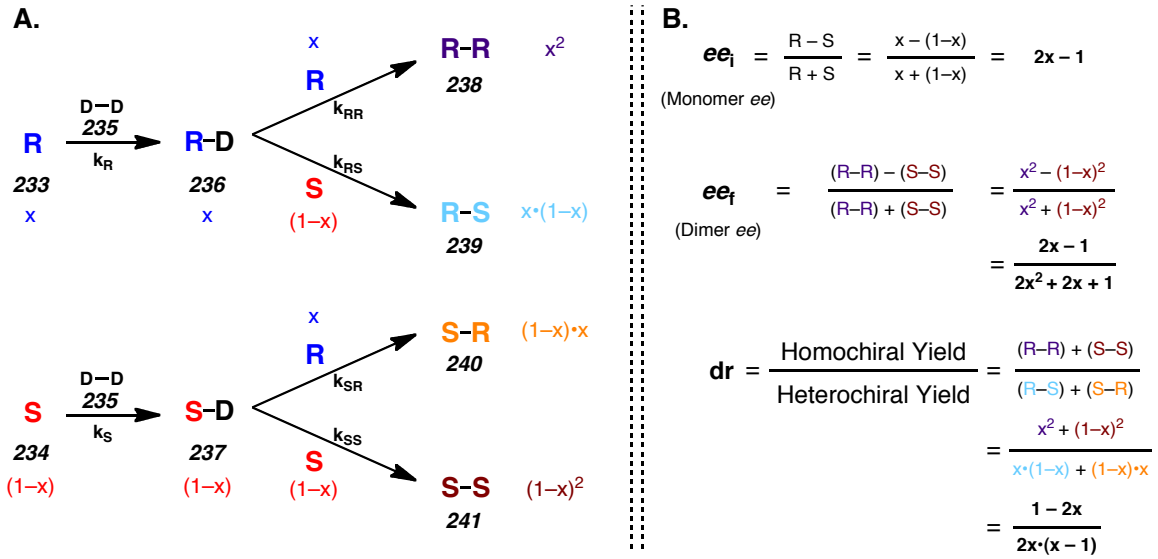

With these assumptions in place, it is possible to leverage the expressions for the mol fraction of the starting material *R* and *S* enantiomers in order to derive expected yields for all four stereoisomers of product. These values can thereafter be used in expressions for the diastereomeric ratio and enantiomeric excess of the product mixture (Scheme 3.6B). By exploiting the relationship between the mol fraction of the major enantiomer (x) and the initial enantiomeric excess of the scalemic starting material ($ee_i = 2x - 1$), further substitution and manipulation provide two simple and extremely useful expressions for the diastereomeric ratio (dr) and enantiomeric excess (ee_f) of the product dimer.

$$dr = \frac{1 + (ee_i)^2}{1 - (ee_i)^2} \quad (1) \qquad ee_f = \frac{2 \cdot ee_i}{1 + (ee_i)^2} \quad (2)$$

Though these equations are greatly simplified due to the assumption of rate equivalence, they nevertheless provide valuable insight into the behavior of enantiomeric amplification in Horeau-type duplications. After converting equation (1) from a

relationship in terms of diastereomeric ratio into an expression representing diastereomeric excess, it is possible to plot the final dimer enantiomeric excess (ee_f) and diastereomeric excess (*de*) of the product dimer versus the initial enantiomeric excess of the scalemic starting material (ee_i).[8] Additionally, the total yield of the heterochiral diastereomer as it relates to ee_i can also be calculated (Figure 3.1). As expected, the value of ee_f displays a rapid and positive nonlinear deviation when compared to the ee_i value of the starting material. Indeed, even with an initial ee_i as low as 50%, an enantiomeric excess of roughly 80% is predicted for ee_f after duplication, a value that represents a considerable increase in enantioenrichment.

In addition to the obvious gains imparted by this technique, these equations also illustrate the inherent cost of Horeau-type duplication. The value for diastereomeric excess increases much more slowly relative to the value of ee_f for similar increases in ee_i. This pronounced negative nonlinear deviation represents the quantity of racemic starting material separated from the mixture in the form of the heterochiral diastereomer (For example, **239** and **240**, Scheme 3.6). Hence, any duplication technique of this type necessarily incurs a synthetic penalty, in that the overall yield of enantioenriched material obtained will be negatively impacted. For example, the case of a 50% value for ee_i would afford the homochiral diastereomer in approximately 80% ee_f. However, this same reaction would also generate a diastereomeric ratio of 1.7 : 1 dr (25% *de*). These results correlate to roughly 37% of the original scalemic material that must be sacrificed in order to achieve enantioenrichment. Despite this drawback, Figure 3.1 clearly illustrates that for larger values of ee_i the benefits of Horeau-type duplication remain high, while the costs in terms of yield become vanishingly small.

Figure 3.1 A graphical representation of the impact of Horeau duplication

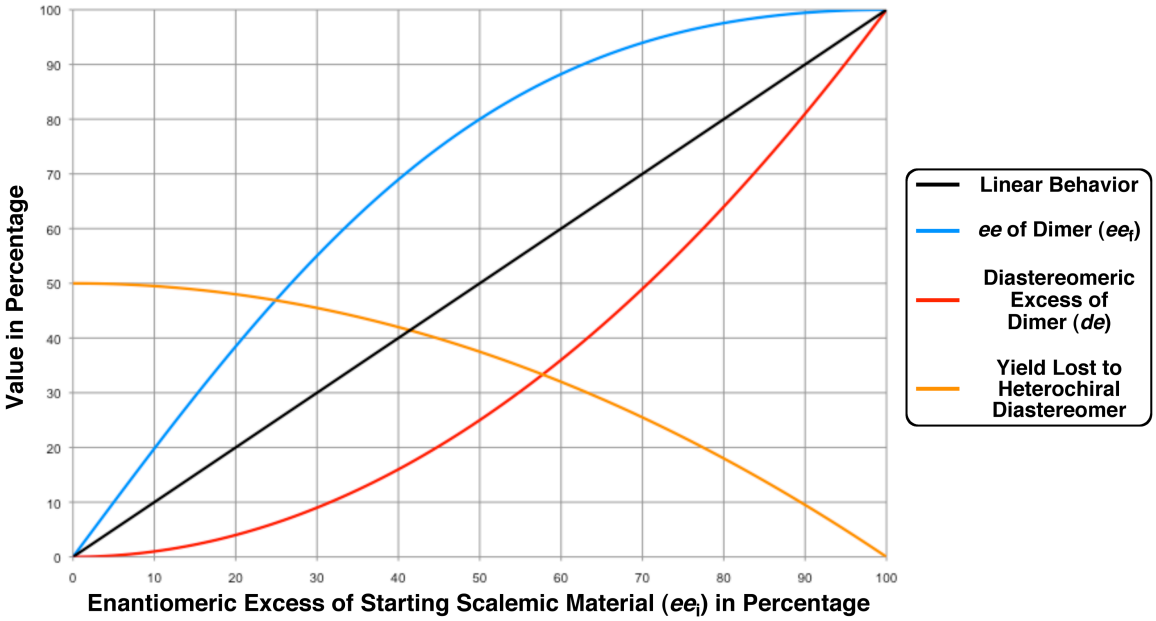

Encouragingly, application of these equations to Horeau's experimental duplication of *sec*-phenethyl alcohol is in excellent agreement with the observed data. For starting material of 60% ee_i, the expressions (1) and (2) afford values for ee_f and dr of 88% and 2.13:1, respectively. When compared to the physically determined values of 87% ee_f and 2.10:1 dr, the approximations above appear to be quite reasonable in predicting the outcome of simplistic dimerizations.

Overall, Horeau-type duplications are a useful way to approach the enantioenrichment of a scalemic mixture without requiring traditional chiral resolution techniques. Provided that no chiral recognition or asymmetric induction occurs during dimerization, these reactions provide a very quick route toward exceptional ee_f values by sequestering racemic material within a heterochiral diastereomer. This undesired material can then be separated from the homochiral diastereomer via traditional purification methods to impart enantioenrichment. However, it should always be noted

that the removal of the heterochiral diastereomer incurs a synthetic penalty in the form of lost yield, and the dr of Horeau-type duplications are typically sluggish to increase to acceptable levels.

3.2.3 SYNTHETIC APPLICATIONS OF THE HOREAU DUPLICATION

In the time since Horeau's explanatory report concerning duplication as a method for enantioenrichment, this technique has been used to approach numerous synthetic problems. For instance, the non-linear behavior of these duplication events provides an expedient and transparent method for the excellent enantioenrichment of scalemic intermediates in the course of a complex natural products synthesis.

One notable example of this phenomenon can be found in the total synthesis of the carpenter bee hormone 2,8-dimethyl-1,7-dioxaspiro[5.5]undecane (**247**), and the controversy surrounding its preparation. In 1981, Mori and coworkers reported the preparation of this particular bee hormone from ethyl acetoacetate (**242**, Scheme 3.7).[9] Their synthesis leveraged a reduction of ketone **242** via the action of baker's yeast to afford enantioenriched 3-hydroxy-butanoate (**243**) in 92% *ee*. This material was thereafter advanced several steps to protected iodide substrate **244**.

Scheme 3.7 Initial steps toward Mori's synthesis of 2,8-dimethyl-1,7-dioxaspiro[5.5]undecane

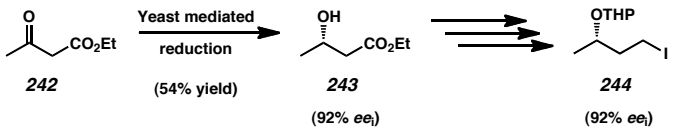

With iodide **244** in hand, Mori *et al*. were then able to complete the total synthesis of 2,8-dimethyl-1,7-dioxaspiro[5.5]undecane by leveraging a Horeau-type duplication. Treatment of ethyl acetoacetate (**242**) under strongly alkaline conditions was thereafter followed by exposure to enantioenriched iodine **244** (Scheme 3.8). Coupling of these two fragments proceeded smoothly to give β-ketoester **245**, which was subsequently alkylated with a second equivalent of iodide **244**. After saponification and decarboxylation, an acidic workup served to remove of both the alcohol protecting groups and furnish diol **246**. However, before ketone **246** could be isolated, this compound spontaneously underwent spiroacetal formation, thus generating the desired natural products **247** and **248**.

Scheme 3.8 Horeau duplication in Mori's bee hormone synthesis

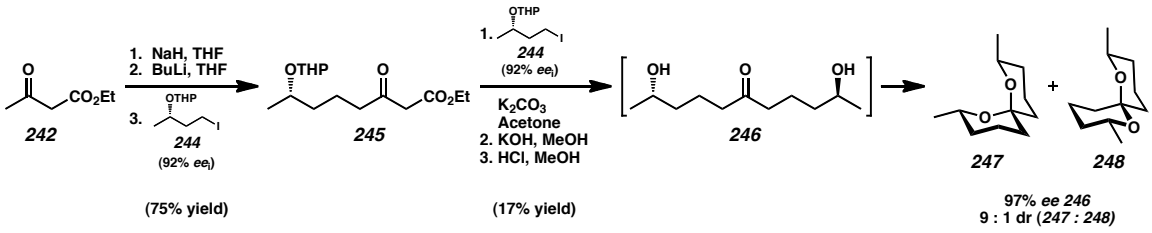

Despite having begun the synthesis with material of 92% ee_i, the Horeau-type dimerization of **244** onto **242** afforded the final natural product in an amplified 97% ee_f and a 9:1 ratio of **247** to **248**. If the initial value of 92% ee_i is substituted into both equations (1) and (2), the final calculated values of 99% for ee_f and 12 : 1 for dr are within acceptable agreement with the experimental data. Nevertheless, the increased ee_f observed by Mori later became a point of dispute. In 1984 Isaksson *et al*. contested the validity of Mori's reported optical rotation values for acetal **247** on the grounds that the

starting iodide **244** was not enantiopure.[10] In order to address these concerns, Mori revisited the synthesis of the hormone **247** using two different samples of iodide **244**, one of which was enantioenriched to 100% ee_i and the other possessing an ee_i of only 85% (Table 3.1). While the enantiopure approach confirmed the optical rotation values reported in Mori's initial synthesis, the lower ee_i sample once again confirmed the Horeau-type duplication phenomenon. With an ee_i of 85% for iodide **244**, the ee_f and dr observed for hormone **247** were 97% and 6.4:1, respectively. Once again, these values are in very good agreement with predictions based on equations (1) and (2).

Table 3.1 Stereochemical summary of Mori's synthetic efforts

ee_i of *244*	Experimentally Determined		Calculated, Predicted Values	
	ee_f of *247*	dr of *247 : 248*	ee_f of *247*	dr of *247 : 248*
85%	97%	6.4:1	99%	6.2:1
92%	99%	9:1	99%	12:1
100%	100%	N/A	100%	N/A

Another example of the Horeau-type duplication approach to enantioenrichment in total synthesis can be found in Corey's preparation of the lignan natural product (–)-wodeshiol.[11] Starting from bromoenone **249**, enantioselective 1,2-reduction of the carbonyl moiety afforded the desired allylic alcohol in high yield, but in only 88% ee_i (Scheme 3.9). Further functionalization of vinyl bromide **250** via lithium-halogen exchange and trapping with chlorotributylstannane provided access to vinyl stannane **251**. This material was subsequently dimerized under palladium–catalyzed homocoupling conditions to generate dimer **252**. Notably, this bis-allylic alcohol was isolated in 99% ee_f and 8.0:1 dr, an impressive enantioenrichment that can be attributed to the statistical amplification of dimerization. Both of these values are predicted

extremely well by equations (1) and (2) based on an 88% value for ee_i. In this particular example, the yield lost to the undesired heterochiral diastereomer is roughly 10%, a value low enough to make the sacrifice synthetically viable. From this point, Corey *et al*. were able to easily complete the total synthesis of (–)-wodeshiol (**253**).

Scheme 3.9. Corey's total synthesis of (–)-wodeshiol via Horeau-type duplication

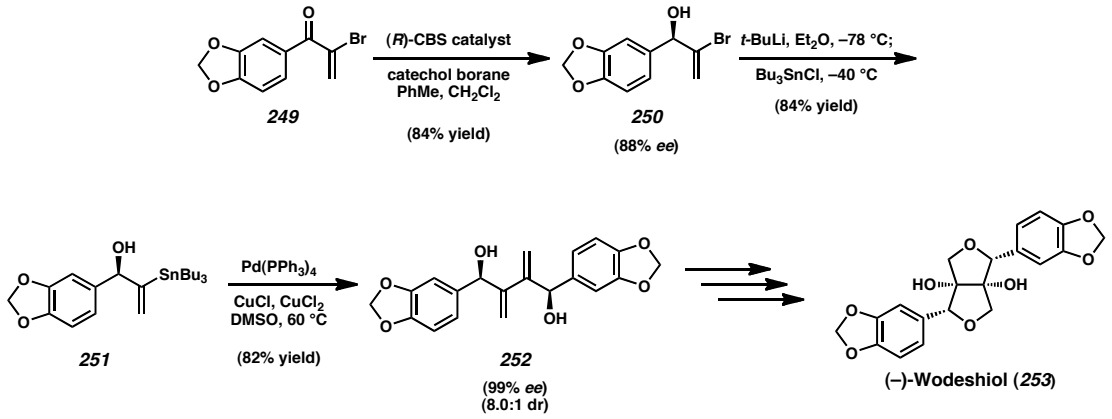

Though Horeau-type duplications have found much application in the direct enantioenrichment of synthetic intermediates, this phenomenon has also been employed toward many other purposes. This technique has facilitated the synthesis of ligands and reagents for further enantioselective synthesis,[12] served as an alternative to traditional resolution with chiral reagents,[13] enabled the development of new analytical methods for the ^{1}H NMR analysis of reagent enantiopurity,[14] and facilitated prediction of the selectivity of an enantioenriched catalyst from its racemic mixture.[15]

The dimerization of scalemic mixtures is an efficient method for the enantioenrichment of modest *ee* material. Provided that the dimerization technique employed obviates the possibility of chiral recognition or kinetic resolution, the outcome of such a reaction can be understood as a consequence of statistical distribution, and thus

can be predicted with simple expressions. However, Horeau-type duplication is not a method of enantioinduction, as all chirality must necessarily be present prior to the dimerization event. Far more complicated are those processes that involve multiple asymmetric transformations.

3.2.4 MULTIPLE ASYMMERTRIC TRANSFORMATIONS

Rather than simply joining two enantioenriched fragments onto a central molecule, multiple asymmetric transformations are processes that construct more than one asymmetric center in a single operation. For example, the interaction of an achiral substrate bearing two prochiral reactive sites with a chiral substrate or a chiral catalyst has the potential to forge four stereoisomeric products in one synthetic process. These transformations hold the potential to efficiently construct multiple key bonds with a high degree of selectivity. Such reactions can also be valuable under circumstances where the desired stereocenters are considerably distal from one another, a circumstance that renders the intramolecular relay of stereochemical information from one stereocenter to a prochiral reactive group quite difficult.

Unfortunately, despite their myriad benefits, multiple asymmetric transformations are significantly more complex than those corresponding reactions that forge a single stereocenter. Indeed, it can be quite difficult to troubleshoot or optimize a multiple asymmetric transformation, due to convoluted reaction pathways and unpredictable substrate-catalyst interactions. Additionally, a rigorous mathematical model of such processes can quickly become overwhelming, a fact that often renders predictive models either cumbersome or inaccessible. Despite these complications, it is possible, via the

application of reasonable assumptions and simplifications, to arrive at expressions for the prediction and analysis of stereoisomeric distributions in these transformations.

In 1994, Kagan *et al*. published an impressively thorough mathematical treatment of double enantioselective transformations.[16] In order to illustrate the numerous variables involved in multiple asymmetric catalysis, Kagan considered the reaction of an enantioselective hydrogenation catalyst with a single molecule bearing two distinct, prochiral olefin moieties. Starting from completely achiral bis-olefin [1*P*, 2*P*] (**254**), complete reaction at both prochiral sites would yield two diastereomeric products (hereafter referred to as diastereomer A and diastereomer B), with each diastereomer possessing a distinct *ee* value (ee_A and ee_B, respectively, Scheme 3.10).[17] In terms of the course of this reaction, hydrogenation can initially occur at either olefin (1) or olefin (2).[18]

For the case where initial hydrogenation transpires at olefin (1), two enantiomeric intermediates are generated prior to subsequent reduction of olefin (2). If catalyst selectivity is large enough to ensure a non-racemic product, the intermediate [1*R*, 2*P*] (**255**) will predominate over the unfavored [1*S*, 2*P*] (**256**) isomer. In order to gauge the efficacy of this first bond-forming transformation, the value "r" is introduced as a measure of relative selectivity for this reaction to produce **255** relative to **256**. Closely mirroring *ee* in structure, the r term represents the local selectivity of the first transformation only, and varies in size from zero to one. A value of zero denotes a complete lack of selectivity in the reaction, and value of unity signifies exclusive generation of the [1*R*, 2*P*] (**255**) isomer.

Scheme 3.10 Pathways for double asymmetric transformation, route 1

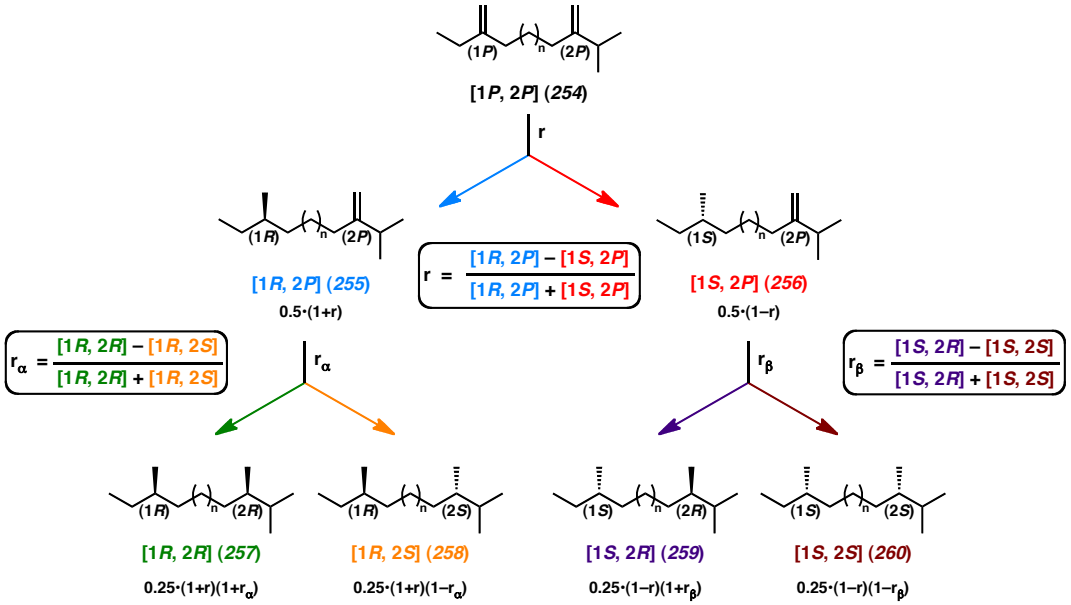

If the reaction is followed further forward, both intermediates **255** and **256** possess one enantioenriched and one reactive prochiral site. Because of this, any additional interaction with the enantioselective catalyst necessarily involves the formation of a diastereomeric catalyst-substrate complex. Thus, in order to fully represent the course of this reaction, two additional selectivity values must be considered, one for either of these possible complexes. Toward this end, the value r_α represents the relative selectivity for formation of the [1*R*, 2*R*] isomer (**257**) over the [1*R*, 2*S*] (**258**) stereoisomeric product starting from the [1*R*, 2*P*] (**255**) intermediate. Similarly, the r_β variable describes the same relationship between [1*S*, 2*R*] (**259**) and [1*S*, 2*S*] (**260**) molecules, as products from the [1*S*, 2*P*] (**256**) intermediate.

It is critical to note that the values for intermediates [1*R*, 2*P*] (**255**) and [1*S*, 2*P*] (**256**) do not reflect isolated yields of the compounds generated in this reaction. Instead, these variables represent the relative quantities of material that pass through each of these

intermediates on the path toward the final products. Additionally, the values [1*R*, 2*R*] (**257**), [1*R*, 2*S*] (**258**), [1*S*, 2*R*] (**259**), and [1*S*, 2*S*] (**260**) represent the quantities of these compounds afforded via route 1 only, rather than the combined total yields of these isomers from the final reaction.

The possibilities explored above (Scheme 3.10) outline the routes that lead to all potential stereoisomeric products in this envisioned reaction. Both products [1*R*, 2*R*] (**257**) and [1*S*, 2*S*] (**260**) contribute to the yield of diastereomer A, and their relative quantities dictate the value ee_A. Similarly, products [1*R*, 2*S*] (**258**) and [1*S*, 2*R*] (**259**) add to the total yield of diastereomer B, and their relative quantities contribute to ee_B. However, the three final values of dr, ee_A, and ee_B cannot be determined from these variables alone. Whereas the situation considered above (Scheme 3.10) initiates with the enantioselective hydrogenation of olefin (1), the possibility also exists that the overall reaction commences with the reduction of olefin (2) (Scheme 3.11). In this situation, the initial intermediates [1*P*, 2*R*]' (**261**) and [1*P*, 2*S*]' (**262**) provide distinct diastereotopic prochiral reactive sites for further enantioselective reduction, which are unique from those intercepted in route 1. As such, a further three selectivity terms are required in order to address the complete set of stereochemical paths available to this reaction. These additional terms (defined as r', r_α', and r_β') are analogous to their route 1 counterparts above.

Scheme 3.11 Pathways for double asymmetric transformation, route 2

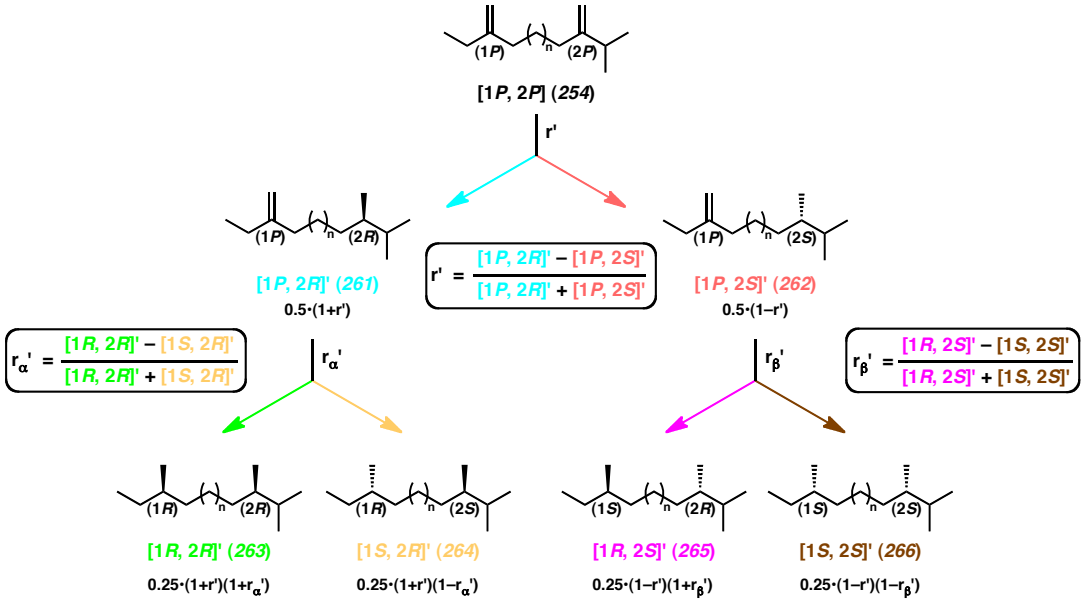

To be able to describe the course of a double asymmetric transformation as thoroughly as possible, another selectivity factor is required in addition to the six r type variables defined above. Because route 1 and route 2 both contribute competitively toward the final outcome of the reaction, the variable *i* must be established to determine the relative selectivity of the reaction for one route over the other. The *i* value is defined as the ratio between the quantity of material that reacts via route 1 and the total quantity of material that reacts via both routes 1 and 2. The *i* term is represented mathematically as follows:[16]

$$i = \frac{[1R, 2P] + [1S,2P]}{[1R, 2P] + [1S,2P] + [1P, 2R]' + [1P,2S]'} \quad (3)$$

A value of unity denotes complete selectivity for route 1, while a value of zero indicates complete selectivity toward route 2. An *i* value of 0.5 represents that equal portions of the starting material react along both available paths. With a total of seven selectivity variables defined, four stereoisomeric products to consider, and eight distinct

paths possible over the course of the reaction, a complete mathematical representation can be compiled. The relative contribution of each unique reaction pathway can be related to the values of dr, ee_A and ee_B.

$$ee_A = \frac{([1R, 2R] + [1R, 2R]') - ([1S, 2S] + [1S, 2S]')}{([1R, 2R] + [1R, 2R]') + ([1S, 2S] + [1S, 2S]')} = \frac{[i(1+r)(1+r_\alpha) + (1-i)(1+r')(1+r_\alpha')] - [i(1-r)(1-r_\beta) + (1-i)(1-r')(1-r_\beta')]}{[i(1+r)(1+r_\alpha) + (1-i)(1+r')(1+r_\alpha')] + [i(1-r)(1-r_\beta) + (1-i)(1-r')(1-r_\beta')]} \quad (4)$$

$$ee_B = \frac{([1R, 2S] + [1R, 2S]') - ([1S, 2R] + [1S, 2R]')}{([1R, 2S] + [1R, 2S]') + ([1S, 2R] + [1S, 2R]')} = \frac{[i(1+r)(1-r_\alpha) - (1-i)(1-r')(1+r_\beta')] - [i(1-r)(1+r_\beta) - (1-i)(1+r')(1-r_\alpha')]}{[i(1+r)(1-r_\alpha) - (1-i)(1-r')(1+r_\beta')] + [i(1-r)(1+r_\beta) - (1-i)(1+r')(1-r_\alpha')]} \quad (5)$$

$$dr = \frac{([1R, 2R] + [1R, 2R]') + ([1S, 2S] + [1S, 2S]')}{([1R, 2S] + [1R, 2S]') + ([1S, 2R] + [1S, 2R]')} = \frac{[i(1+r)(1+r_\alpha) + (1-i)(1+r')(1+r_\alpha')] + [i(1-r)(1-r_\beta) + (1-i)(1-r')(1-r_\beta')]}{[i(1+r)(1-r_\alpha) + (1-i)(1+r')(1-r_\alpha')] + [i(1-r)(1+r_\beta) - (1-i)(1-r')(1+r_\beta')]} \quad (6)$$

Equations (4), (5), and (6) are the most exhaustive mathematical representations of dr, ee_A, and ee_B available for any double asymmetric transformation. These complicated expressions allow for different selectivity values at every stage of the reaction, and thus account for every possible diastereomeric catalyst-substrate interaction. Because of this, these equations are ideal for situations where the influence of the substrate overpowers or complicates catalyst control.

In principle, manipulation of equations (4) through (6) should allow for examination of the various intermediate selectivity r values. Extracting these selectivity constants from observable data can provide insight into the total course of a double asymmetric transformation. Specifically, calculation of each r term could elucidate those phases of the reaction that operate with low or no selectivity. In light of this fact, attaining expressions for each individual r value could assist greatly in the optimization and understanding of these versatile processes. Unfortunately, while equations (4) through (6) do provide a maximum amount of theoretical information regarding every possible selectivity value, the number of variables employed in these expressions renders them intractable. With three equations, ten variables, and only three values readily attainable

from experimental observation, this most rigorous mathematic treatment is also impractical. In order to achieve a useful mathematical model, several simplifying assumptions must be made.

If the catalyst employed acts upon olefin (1) and olefin (2) with equal or reasonably similar efficacy, then each of the selectivity factors along route 2 can be assumed to be identical to the same r terms of route 1. In other words, each of the corresponding pairs of r values between the two routes can be taken as equal ($r = r'$, $r_\alpha = r_\alpha'$, and $r_\beta = r_\beta'$). Under this assumption, equations (4), (5), and (6), are reduced to the much more manageable expressions (7), (8), and (9). While these relationships are much less complicated than the alternatives presented above, they are nevertheless still difficult to engage realistically. The persistence of the *i* term in addition to the three r values, and the difficulty inherent in directly measuring any of these selectivity factors, once again provides a system of equations for which a solution is not attainable from the observable data.

$$ee_A = \frac{(1+r_\alpha)(1+r) - (1-r_\beta)(1-r)}{(1+r_\alpha)(1+r) + (1-r_\beta)(1-r)} \quad (7)$$

$$ee_B = (2i-1)\frac{(1-r_\alpha)(1+r) - (1+r_\beta)(1-r)}{(1-r_\alpha)(1+r) + (1+r_\beta)(1-r)} \quad (8)$$

$$dr = \frac{(1+r_\alpha)(1+r) + (1-r_\beta)(1-r)}{(1-r_\alpha)(1+r) + (1+r_\beta)(1-r)} \quad (9)$$

$i = 1$ ⇒

$$ee_A = \frac{(1+r_\alpha)(1+r) - (1-r_\beta)(1-r)}{(1+r_\alpha)(1+r) + (1-r_\beta)(1-r)} \quad (7)$$

$$ee_B = \frac{(1-r_\alpha)(1+r) - (1+r_\beta)(1-r)}{(1-r_\alpha)(1+r) + (1+r_\beta)(1-r)} \quad (10)$$

$$dr = \frac{(1+r_\alpha)(1+r) + (1-r_\beta)(1-r)}{(1-r_\alpha)(1+r) + (1+r_\beta)(1-r)} \quad (9)$$

⇒

$$r = \frac{dr \cdot ee_A + ee_B}{1 + dr} \quad (11)$$

$$r_\alpha = \frac{dr + dr \cdot ee_A - ee_B - 1}{dr + dr \cdot ee_A + ee_B + 1} \quad (12)$$

$$r_\beta = \frac{dr - dr \cdot ee_A + ee_B - 1}{dr \cdot ee_A - dr + ee_B - 1} \quad (13)$$

An important case to consider is the situation where the reaction displays total selectivity for either route 1 or route 2. Under these circumstances the value of *i* can be taken as 1, and the course of the reaction can be described fully via the use of only a single route (i.e., exclusively Scheme 3.10). This simplifies the situation to a system involving only the three selectivity factors (r, r_α, and r_β), and the three observable

stereoisomeric ratios (ee_A, ee_B, and dr). With the assumption of route exclusivity in place, equation (8) can be reduced to expression (10). Notably, the relationships described by (7), (9), and (10) can also be derived directly from the original expressions (4), (5), and (6) by assuming route selectivity ($i = 1$).

Further algebraic manipulation of equations (7), (9), and (10) provides access to expressions (11), (12), and (13), which describe the value of each selectivity factor in terms of the measurable quantities of ee_A, ee_B, and dr. Thus, under these limiting conditions the value of each intermediary selectivity variable can be evaluated and studied via directly observed experimental data. These mathematical representations therefore provide a method by which to scrutinize and optimize double asymmetric transformations by allowing the identification of mid-reaction processes with low or mediocre r values.

One further simplifying case that can be applied to equations (4)–(6) is a situation where the catalyst exerts a large influence on the reaction, but displays dissimilar selectivity values for transformation at either prochiral reactive site. In this system, it is assumed that two r variables representing the selectivity of reaction at either the 1P or 2P prochiral centers (r_1 and r_2, respectively) are sufficient to describe the course of a double asymmetric process (Scheme 3.12). The variable r_1 represents the selectivity of the transformation at the 1P center, regardless of the order in which the reactions occur. Whether considering the conversion of substrate **254** in route 1, or scrutinizing the reaction of intermediates **261** and **262** in route 2, every one of these processes is accepted to progress with a selectivity of r_1. The variable r_2 is defined similarly, and corresponds

to the selectivity of transformation at the 2P prochiral reactive site regardless of the route followed.

Scheme 3.12 Double asymmetric transformation via two variable simplification

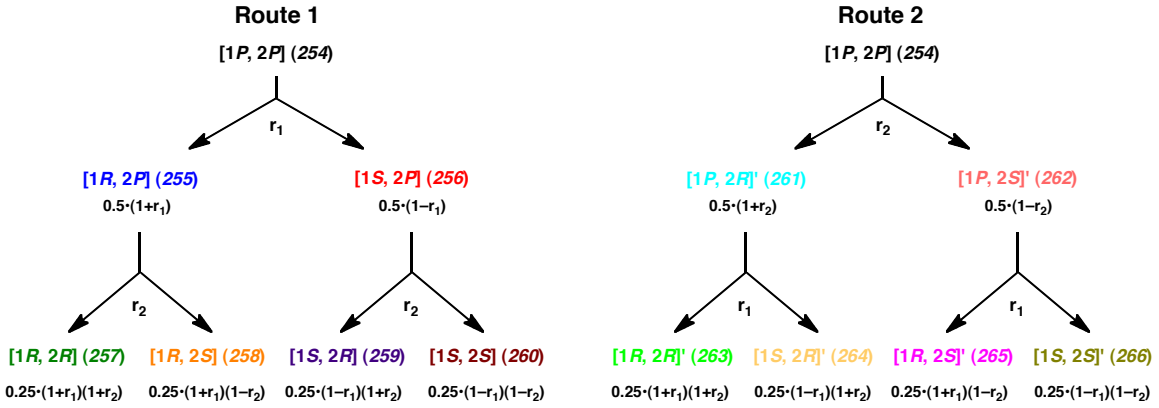

Using these relationships, it is possible to define expressions for ee_A, ee_B, and dr in terms of both the r_1 and r_2 variables. Examination of both routes 1 and 2 reveal that the final quantities of each stereoisomer afforded via either pathway are identical (i.e., [1R, 2S] = [1R, 2S]'). Because of this equivalence, the relationship between the selectivity variables and ee_A, ee_B, or dr are completely independent of the *i* term. This fact can be confirmed by using the quantities defined in Scheme 3.12 to calculate the three pertinent stereoisomeric ratios, thus attaining equations (14), (15), and (16), none of which display any dependence upon *i*. More importantly, these three expressions relate the measurable quantities of ee_A, ee_B, and dr to the value of r_1 and r_2, thereby reducing the system of multiple asymmetric transformations to a model involving only two unobservable variables. Notably, these same three equations may also be derived via direct substitution of the simplified r values ($r = r_1$, $r_\alpha = r_\beta = r_2$) into equations (4), (5), and (6).

$$ee_A = \frac{[i(1+r_1)(1+r_2) + (1-i)(1+r_1)(1+r_2)] - [i(1-r_1)(1-r_2) + (1-i)(1-r_1)(1-r_2)]}{[i(1+r_1)(1+r_2) + (1-i)(1+r_1)(1+r_2)] + [i(1-r_1)(1-r_2) + (1-i)(1-r_1)(1-r_2)]} = \frac{(1+r_1)(1+r_2) - (1-r_1)(1-r_2)}{(1+r_1)(1+r_2) + (1-r_1)(1-r_2)} = \boxed{\frac{r_1 + r_2}{1 + r_1 r_2}} \quad (14)$$

$$ee_B = \frac{[i(1+r_1)(1-r_2) + (1-i)(1+r_1)(1-r_2)] - [i(1-r_1)(1+r_2) + (1-i)(1-r_1)(1+r_2)]}{[i(1+r_1)(1-r_2) + (1-i)(1+r_1)(1-r_2)] + [i(1-r_1)(1+r_2) + (1-i)(1-r_1)(1+r_2)]} = \frac{(1+r_1)(1-r_2) - (1-r_1)(1+r_2)}{(1+r_1)(1-r_2) + (1-r_1)(1+r_2)} = \boxed{\frac{r_1 - r_2}{1 - r_1 r_2}} \quad (15)$$

$$dr = \frac{[i(1+r_1)(1+r_2) + (1-i)(1+r_1)(1+r_2)] + [i(1-r_1)(1-r_2) + (1-i)(1-r_1)(1-r_2)]}{[i(1+r_1)(1-r_2) + (1-i)(1+r_1)(1-r_2)] + [i(1-r_1)(1+r_2) + (1-i)(1-r_1)(1+r_2)]} = \frac{(1+r_1)(1+r_2) + (1-r_1)(1-r_2)}{(1+r_1)(1-r_2) + (1-r_1)(1+r_2)} = \boxed{\frac{1 + r_1 r_2}{1 - r_1 r_2}} \quad (16)$$

The most extreme limiting case to consider for equations (4)–(6) is the situation in which the catalyst employed exercises complete and identical control over all stages of enantioselective bond construction. Such an assumption would be reasonable for substrates where both of the reactive sites are considerably removed from one another and are similarly reactive. Under these circumstances, all selectivity values can be taken as equal ($r = r_\alpha = r_\beta = r' = r_\alpha' = r_\beta'$). If route selectivity is once again considered exclusive ($i = 1$), then equations (4)–(6) are easily reduced to two simple expressions, with the value of ee_B being equal to zero in all cases.

$$\boxed{ee_A = \frac{2r}{1 + r^2}} \quad (17) \qquad ee_B = 0 \quad (18) \qquad \boxed{dr = \frac{1 + r^2}{1 - r^2}} \quad (19)$$

Equations (17) and (19) closely resemble the mathematical representation of the Horeau principle described by expressions (1) and (2), with the selectivity factor r taking the place of the monomer enantiomeric excess (ee_i). Because these relationships represent an extremely aggressive reduction of equations (4), (5), and (6), their application should only be appealed to after careful consideration of the simplifying assumptions in use. Specifically, great confidence must be placed in the ability of the catalyst to operate upon all prochiral sites with equal efficacy and selectivity.

The relationship between the selectivity factors employed in the equations above and the final values of ee_A, ee_B, and dr are not immediately obvious from their mathematical

representations. In order to better depict the influence of the r values upon the stereoisomeric ratios of the products, the simplified expressions presented in equations (14), (15), and (16) can be represented graphically.

Because the value of ee_A and dr are most often of interest in double asymmetric transformations, their relationship to values r_1 and r_2 are represented below (Figure 3.2, 3.3). Examination of these three-dimensional plots reveals a striking similarity to the plotted behavior of the ee_f and *de* values for the expressions of the Horeau duplication (Figure 3.1). Plotting equation (16) illustrates the diastereomeric enrichment of the reaction product as it relates to either selectivity factor, and from this graph one can observe a negative non-linear deviation in *de* relative to both r values (Figure 3.2A).[19] Indeed, in these cases, the ultimate *de* of the reaction product is always less than either of the selectivity factors alone. As either r_1 or r_2 approaches zero, the product *de* drops precipitously, and does so regardless of the remaining r value. Because of this, only in situations where both r_1 and r_2 are simultaneously large will the dr of the reaction be reasonably high.

Investigation of the behavior of ee_A as it relates to the r_1 and r_2 selectivity terms (i.e., plotting equation (14) in three dimensions) reveals a relationship similar to the positive non-linear deviations calculated for Horeau-type duplications. In fact, if a substitution is made where both r terms are equal, this relationship reduces exactly to the Horeau-type model (i.e., setting $r_1 = r_2$ in expression (14) will afford the ee_f graph of Figure 3.1). The graph depicted in Figure 3.2B illustrates the impact of both selectivity values upon the overall enantioenrichment of the major diastereomer in a double asymmetric process. This plot clearly demonstrates that the value of ee_A rises rapidly in response to any

increase in either r_1 or r_2 alone. Scrutiny of both the graphical and mathematical representations of ee_A clearly demonstrates that the lower bound for this term is defined by the highest r value in operation. Indeed, when both r terms are nonzero values, the final value of ee_A will always exceed both of the independent selectivity factors, and thus rapidly approach unity.[20]

Figure 3.2 Product (A) ee_A*, (B)* de*, and (C) both plotted as a function of* r_1 *and* r_2 *selectivity factors*

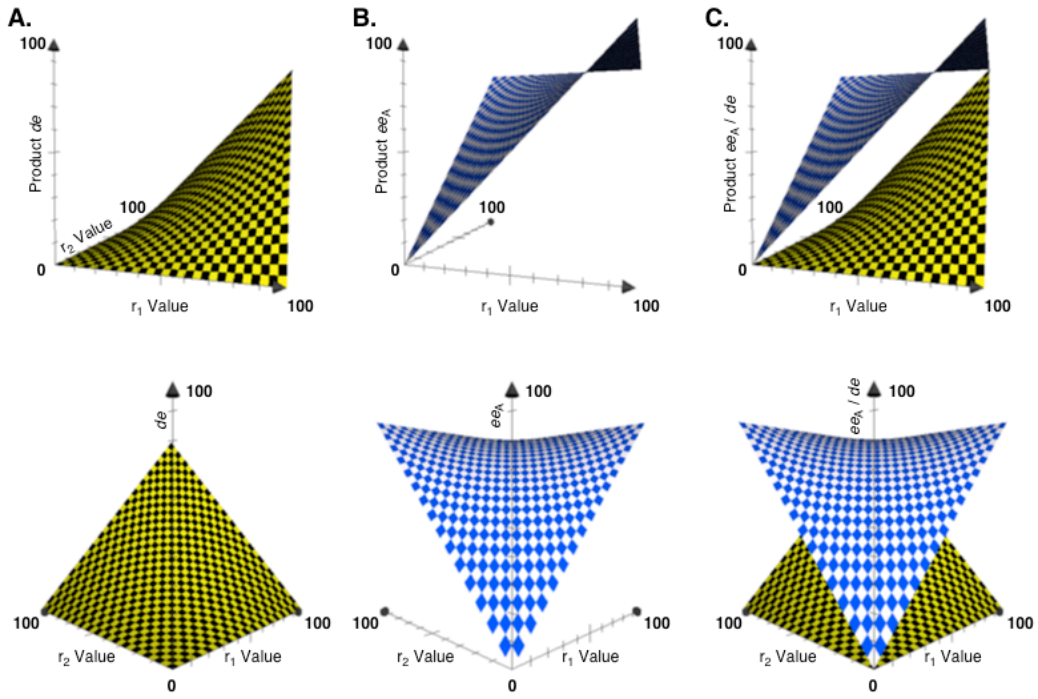

The graphs in this figure include: (A) Three-dimensional plot of an adaptation of equation (16), relating r_1 and r_2 to final product *de*, (B) Three-dimensional plot of equation (14), relating r_1 and r_2 to final product ee_A, and (C) Simultaneous three-dimensional plot of both equations (14) and (16). All values are presented in terms of percentage.

By simultaneously plotting the surfaces representing ee_A and *de* as they relate to any value of r_1 and r_2, the costs and benefits of multiple asymmetric transformation are clearly displayed (Figure 3.2C). Exceptions levels of enantioenrichment in the major diastereomer can be attained with even modest selectivity, but the corresponding values

of *de* increase much more slowly. Just as in the case of Horeau duplication, high product enantioselectivity is attained in a multiple asymmetric transformation at the cost of yield sacrificed to the minor diastereomer.[21]

To better illustrate the interplay between the r terms and the values of ee_A and dr, it is useful to consider the case wherein one enantioselective process occurs with total selectivity, and the other occurs with none whatsoever (Scheme 3.13). If the initial bond-forming reaction establishes the new stereocenter with an r value of 1, then the prochiral starting material [1P, 2P] (**254**) will be exclusively converted into intermediate [1R, 2P] (**255**). Regardless of the selectivity encountered in the subsequent reaction, because no possibility exists for the formation of the [1S, 2S] isomer, ee_A will always be 100%. However, because it is assumed that the subsequent transformation occurs with no preference for either diastereomer, both [1R, 2R] (**257**) and [1R, 2S] (**258**) isomers are produced in equal quantities, yielding a dr of 1 : 1 for the final product.

Scheme 3.13 Double asymmetric transformation where $r_1 = 1.0$ and $r_2 = 0$

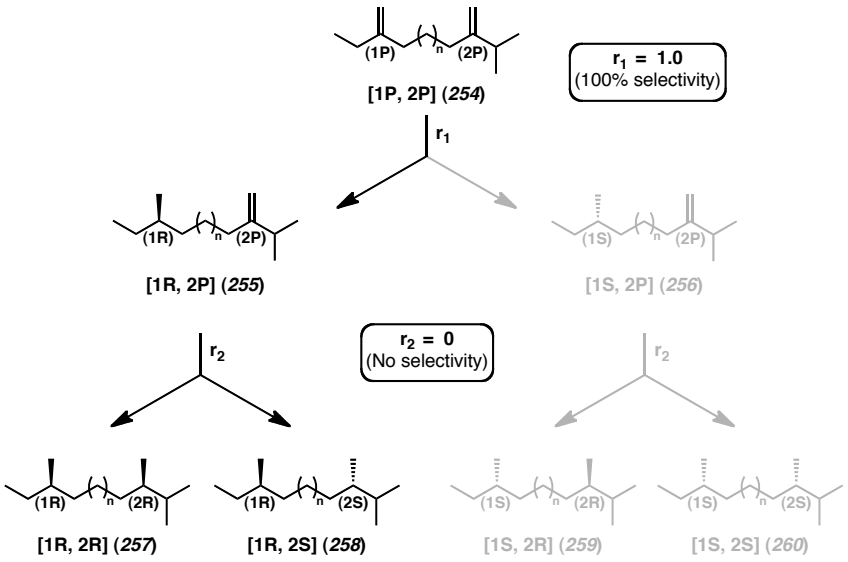

In the situation where the initial bond-forming reaction occurs with no selectivity ($r_1 = 0$), equal portions of [1R, 2P] (**255**) and [1S, 2P] (**256**) are afforded (Scheme 3.14). However, in this theoretical case it is assumed that both intermediates subsequently undergo an asymmetric reaction that occurs with total selectivity ($r_2 = 1$). Therefore, stereoisomers [1R, 2R] (**257**) and [1S, 2R] (**259**) are produced as the sole products of reaction, and in equal quantities. Again, while the final dr value resulting from this transformation is 1 : 1, the ultimate ee_A is 100%. Just as in the case of the Horeau-type duplications, the positive amplification observed in product *ee* can be attributed to the creation and removal of an undesired diastereomeric product. Thus, even in the case of multiple asymmetric transformations, increased *ee* comes at the cost of decreased dr and sacrificed yield. Also, whereas ee_A shows a dependence upon only one of the r terms in operation, the value of dr relies heavily upon both r_1 and r_2 together.

Scheme 3.14 Double asymmetric transformation where $r_1 = 0.0$, and $r_2 = 1.0$

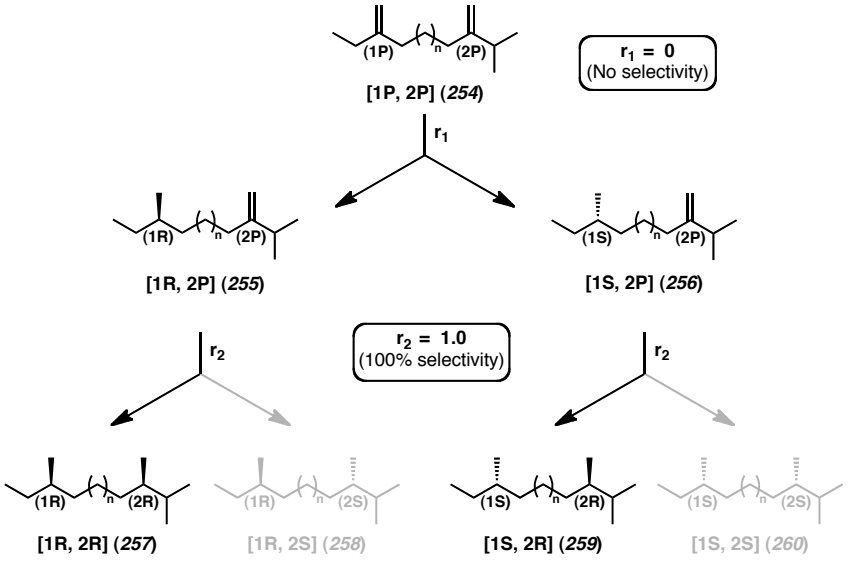

Further examples of the interplay between r_1 and r_2 with the value of ee_A and dr are summarized in Table 3.2 below. Notably, these theoretical cases illustrate the relative insensitivity of the ee_A term with regard to either selectivity value, and the much greater dependence of dr upon r_1 and r_2 simultaneously. Indeed, only when both selectivity terms achieve a value of 95% does the dr reach a level of 20 : 1, a number typically regarded as being excellent.

Table 3.2 Selected examples of r_1 and r_2 values, and their impact on ee *and* de

r_1 (%)	r_2 (%)	ee_A (%)	de (%)	dr	yield lost (%)
0	100	100	0	1 : 1	50
100	0	100	0	1 : 1	50
50	50	80	25	1.7 : 1	38
50	75	91	38	2.2 : 1	31
50	90	96	45	2.6 : 1	28
75	90	98	68	5.2 : 1	16
90	90	99	81	9.5 : 1	10
95	95	>99	90	20 : 1	5

It is important to note that the equations presented above cover a wide range of possible circumstances, and that care must be taken to apply the most appropriate formulae for a given reaction. While equations (17) and (19) are undeniably the most mathematically accessible expressions, these expressions should only be employed in situations where the degree of catalyst control is exceptionally high. These simplified expressions can also be applied when both of the prochiral reactive sites are very similar in terms of reactivity, and are also sufficiently distal from one another, so as to preclude intramolecular interference. For circumstances where catalyst control is anticipated to be high, but nevertheless operate with dissimilar selectivity at different prochiral reactive sites, equations (14)–(16) should be used. In those situations where catalyst control is not

absolute, but the order of transformation is limited to a single route exclusively, equations (11)–(13) should be used to investigate the three distinct selectivity values involved. Under conditions where substrate-catalyst interactions are likely to have a significant influence upon selectivity at all stages of bond construction, the rigorous equations (4)–(6) must be employed.

3.2.5 SYNTHETIC APPLICATIONS OF MULTIPLE ASYMMETRIC TRANSFORMATIONS

Multiple asymmetric transformations have proven to be a powerful and efficient technique when employed in the context of natural products total synthesis. Several groups have reported the use of highly selective catalysts for the rapid, simultaneous construction of key bonds in critical synthetic intermediates. These powerful, concurrent bond-forming processes have facilitated the preparation of complicated molecules with a minimal investment of time and effort.[22,23,24]

One impressive example of a practical double asymmetric transformation in total synthesis can be found in Overman's approach toward quadrigemine C.[25] Starting with dibutenanilide **267**, treatment with palladium acetate and (*R*)-Tol-BINAP initiated two simultaneous, stereocontrolled Heck reactions (Scheme 3.15). The eventual product of this transformation was dioxindole **268**, which was isolated in 90% *ee* and as a 3 : 1 ratio with the undesired *meso* diastereomer. The rapid construction of two all-carbon quaternary stereocenters in high enantiopurity made the completion of the total synthesis possible in only two additional steps. In this situation, it is notable that nearly 20% of the dibutenanilide **267** was lost to the *meso* diastereomer generated in the course of reaction,

once again illustrating the costs inherent to multiple asymmetric transformations. Nevertheless, both the speed and selectivity with which Overman is able to conclude the total synthesis of quadrigemine C (**269**) justify this sacrifice.

Scheme 3.15 Double asymmetric catalytic transformation toward quadrigemine C

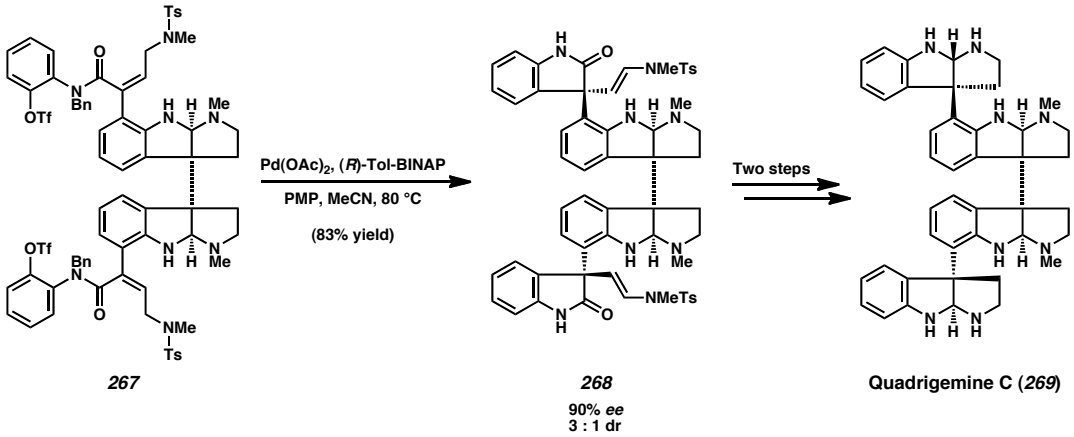

The drawbacks of multiple asymmetric transformations can be overcome under circumstances where the catalyst employed exerts a high degree of control at all stages of bond construction. An impressive example of catalyst preference overriding substrate interference across multiple bond-forming events can be found in the total synthesis of glabrescol (**273**) performed by Corey and coworkers (Scheme 3.16).[26] Exposure of tetraol **270** to Shi's chiral dioxirane conditions[27] smoothly afforded tetraepoxide product **272** in 66% yield and an estimated 80% diastereomeric purity. In light of the fact that four asymmetric processes must occur to form all eight of the new stereocenters found in tetraol **272**, each epoxidation step in this reaction must have transpired with greater than 20 : 1 selectivity (r = 90%) in order to attain the experimentally observed level of diastereoselection. Given the number of distinct diastereomeric intermediates possible throughout the course of this reaction, as well as the potential for deleterious catalyst-

substrate interactions to deteriorate the desired selectivity, the ability of the Shi catalyst to exert this level of control is impressive. By leveraging this powerfully selective technique, Corey was able to set eight of the ten stereocenters of glabrescol in a single, efficient procedure. Conclusion of the synthesis was thereafter attained in only three additional steps.

Scheme 3.16 Total synthesis of glabrescol by Corey

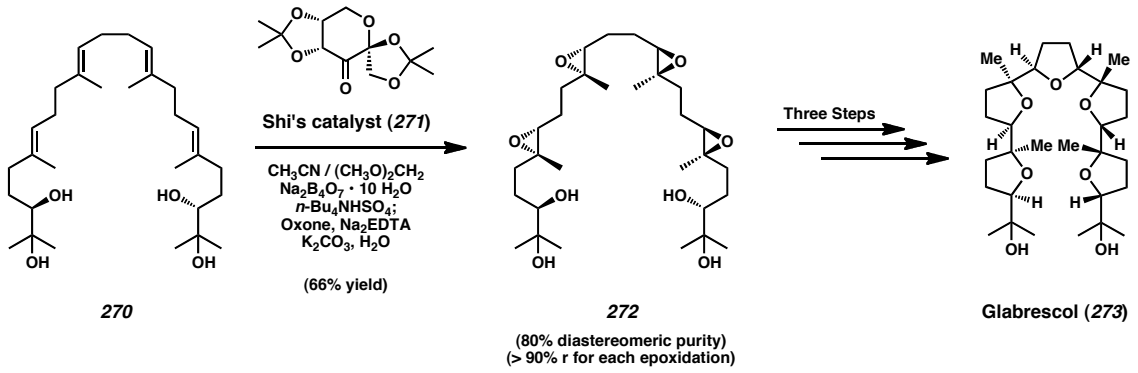

The same approach that Corey proved to be effective toward the total synthesis of glabrescol was later applied toward the preparation of the oxasqualenoid natural product omaezakianol (**276**, Scheme 3.17).[28] Starting from pentaolefin substrate **274**, use of the Shi catalyst to generate enantioenriched pentaepoxide **275** was followed by treatment under acidic conditions and subsequent exposure to sodium metal. This three-step process afforded access to omaezakianol (**276**) in 16% yield as a single, enantiopure diastereomer. The efficiency of this synthetic sequence, as well as the stereopurity of its eventual product, would not be possible without the application of a refined multiple asymmetric transformation.

Scheme 3.17 Total synthesis of omaezakianol by Corey

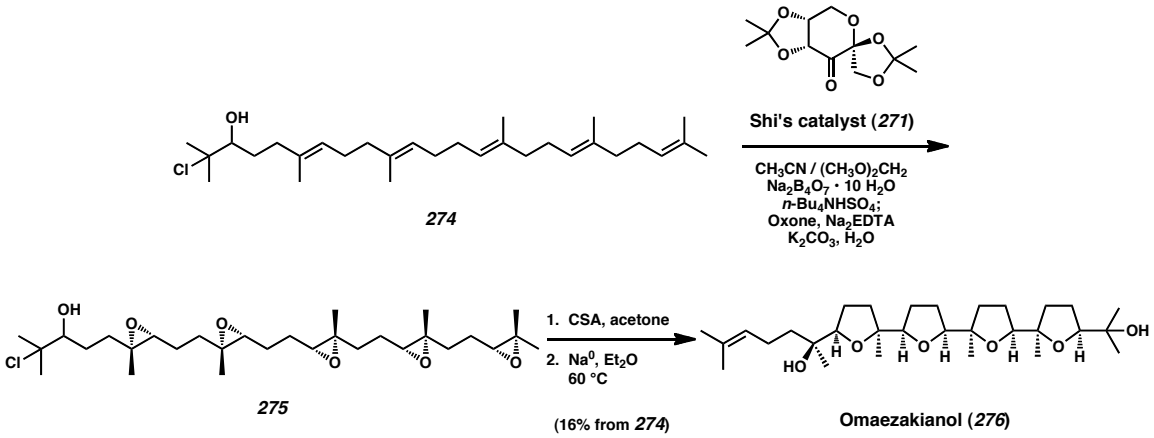

3.3 EXPERIMENTAL INVESTIGATION OF MULTIPLE ASYMMETRIC TRANSFORMATIONS

After having scrutinized the literature for a thorough mathematical explanation of multiple asymmetric transformations and Horeau duplications, we turned our focus once more toward the case of our double asymmetric catalytic alkylation reactions (Schemes 3.18A, 3.18B). With equations (17) and (18) in mind, we reasoned that the lower than desired diastereomeric ratio obtained in the generation of diketone **185** and cyclohexanone **224** must be the result of a less than optimal r_1 or r_2 value. A mediocre selectivity operating at one or both of the alkylation steps in these reactions could be responsible for lower than anticipated dr values observed, while still providing exceptional enantiopurity in the desired products.

Scheme 3.18 Examples of double asymmetric catalytic alkylation

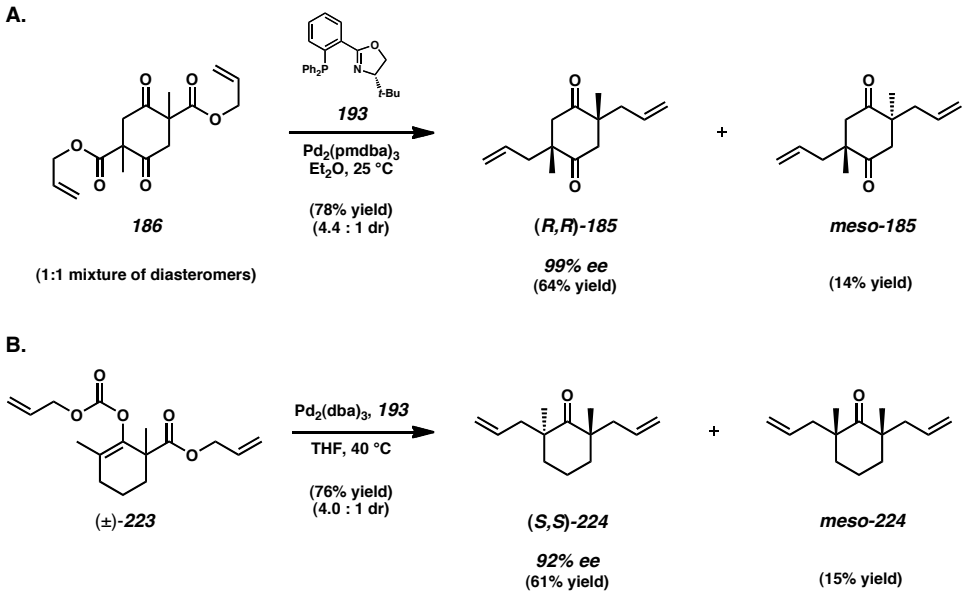

In order to optimize our results to achieve higher dr values, we hoped to use data extracted from the mathematical relationships described in the preceding sections to determine at which point in the reaction process the selectivity was less than desired. Unfortunately, due to the symmetric and achiral nature of the minor *meso* diastereomer in these reactions, it is not possible to collect data concerning ee_B in either of these reactions. Because of this fact, we were unable to implement equations (4)–(6), (11)–(13), or (14)–(16) to obtain data concerning the selectivity of the primary or secondary bond-forming events. Instead, we appealed to limiting cases of expressions (17) and (19) to gain insight into the possible range of values that either r term might possess. For example, if a value of 80% were in operation for both r_1 and r_2 variables, this would result in an ee_A of 98%, and a dr of 4.5 : 1. Additionally, if the r_1 and r_2 selectivities had dissimilar values of 95% and 65%, respectively, this would result in an ee_A of 99%, and a dr of 4.2 : 1. Both sets of possible r values are reasonably close to the experimentally observed results for both transformations. However, in the absence of a measurable ee_B

value, a clear understanding of the selectivities in operation cannot be calculated with confidence.

An additional point of complication involved with the double alkylation of either bis(β-ketoester) **186** (Scheme 3.18A) or enol carbonate (±)-**223** (Scheme 3.18B) is the presence of a pre-existing stereocenter during both asymmetric transformations. Initial decarboxylation of either of these substrates will lead to reactive ketone enolate intermediate bearing a "spectator" stereocenter (**277** or **279**).[29] During the first enantioselective bond formation, either intermediate **227** or **279** will be present in solution as a racemic mixture.

*Scheme 3.19 Schematic representation of intermediates in the double asymmetric alkylation of (A) substrate **186**, and (B) substrate (±)-**223***

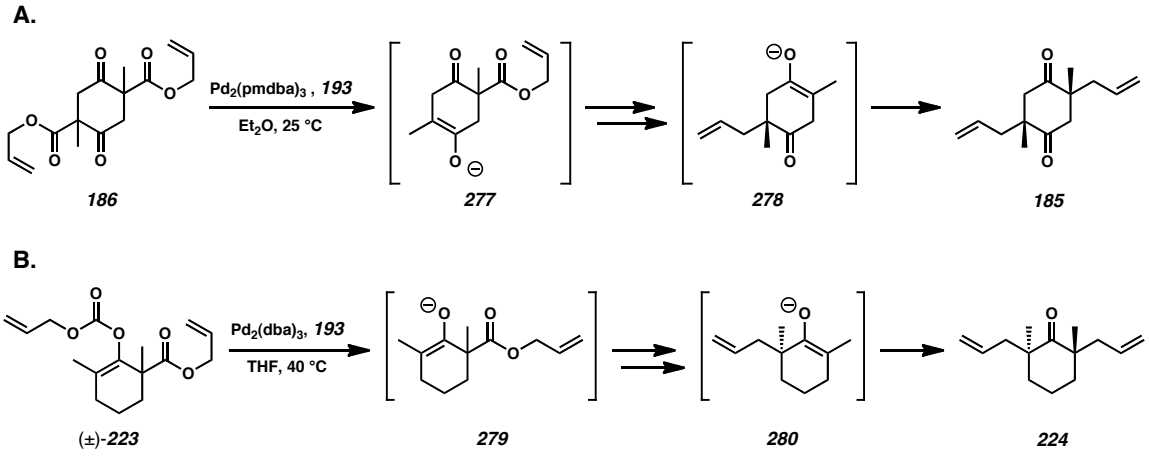

After alkylation of the transient enolate and subsequent decarboxylation of the remaining β-ketoester, the resulting enolate intermediates **278** and **280** still possess a "spectator" stereocenter. However, unlike the previous alkylation process, at this point in the reaction anionic intermediates **278** and **280** are enantioenriched to some extent by the action of the previously selective bond formation. Because the primary alkylation acts

upon a racemic mixture, whereas the secondary alkylation engages an enantioenriched substrate, the corresponding r values for each step are anticipated to be dissimilar due to their different stereochemical features. In order to better understand the impact of pre-existing stereocenters upon a double asymmetric transformation, we decided to first investigate the stereoselective alkylation of a racemic substrate. Toward this end, we synthesized enol carbonate (±)-**281**, and subjected this material to the conditions of asymmetric alkylation to afford a mixture of racemic cyclohexanone diastereomers (**282**, Scheme 3.19A).

*Scheme 3.20 (A) Alkylation of racemic enol carbonate (±)-**281** and (B) mathematical treatment thereof*

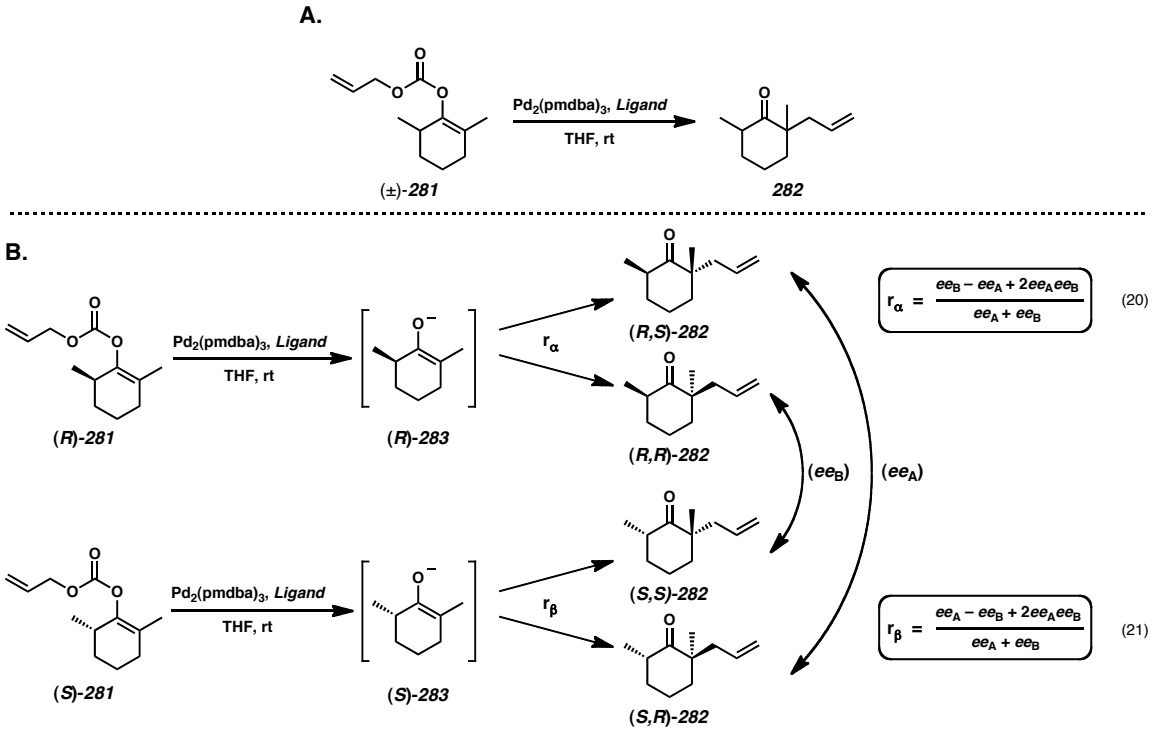

Starting from the racemic enol carbonate (±)-**281**, it is possible to represent the possible stereochemical pathways of the reaction mathematically (Scheme 3.19B). As a

racemate, carbonate (±)-**281** must enter the reaction as a 1 : 1 mixture of enol enantiomers (*R*)-**281** and (*S*)-**281**. Upon initiation of the reaction, both of these stereoisomers undergo decarboxylation to afford an enantiomeric pair of ketone enolate intermediates ((*R*)-**283** and (*S*)-**283**). Interaction of these intermediates with an enantioenriched catalyst thereafter generates a pair of diastereomeric catalyst-substrate complexes, both of which undergo the alkylation process with a distinct selectivity value (r_α and r_β, as defined in Scheme 3.19B). By analyzing the magnitude of ee_A and ee_B, as well as both the r_α and r_β values, information about the interplay between catalyst and substrate can be extracted from experimental data. Interestingly, the mathematical representation of this reaction can be considered a special case of equations (7), (9), and (10), wherein the selectivity for the primary alkylation is taken to be zero (r = 0). This affords expressions for ee_A, ee_B, and dr that rely exclusively upon the r_α and r_β terms. Algebraic manipulation of these formulae yields expressions (20) and (21), relationships that allow for the calculation of either selectivity factor from observable *ee* data.

Under conditions involving a high degree of catalyst control, it would be expected that the values of both r_α and r_β would approach unity, in accordance with ligand-guided bond construction. In such a situation, the reaction would afford a 1 : 1 mixture of enantiopure diastereomers ((*R*,*S*)-**282** and (*S*,*S*)-**282**, exclusively). However, the possibility exists that alkylation of enolates (*R*)-**283** and (*S*)-**283**) may operate with an overwhelming substrate preference for a particular relative stereochemical configuration (favoring either (*R*,*S*)-**282** and (*S*,*R*)-**282**, or (*R*,*R*)-**282** and (*S*,*S*)-**282**). In this case, the substrate interference would overpower catalyst selectivity to yield a very large dr, as well as one r term much larger than the other ($r_\alpha > r_\beta$, or $r_\alpha < r_\beta$). This would result in one

matched, and one mismatched, catalyst-substrate interaction. Such a process would be expected to generate exceptionally high levels of dr, but afford minimal values for either *ee*.

Subjecting enol carbonate (±)-**281** to the conditions of the enantioselective alkylation allowed us to gain some insight into the behavior of this reaction in the presence of pre-existing stereocenters. Substrate (±)-**281** was alkylated in the presence of numerous different ligands, a small subset of which results are summarized below (Table 3.3).

Table 3.3 Study on the effect of a pre-existing stereocenter upon asymmetric alkylation[a]

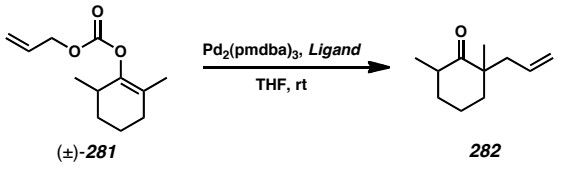

(±)-***281*** ***282***

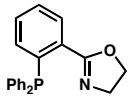

284

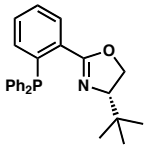

193

Ligand	Yield (%)	dr	ee_1	ee_2	r_α	r_β
PPh_3	49%	4.5:1	-	-	64%	–64%
284	79%	24:1	-	-	92%	–92%
193	81%	2.7:1	40%	99%	99%	10%
285	48%	2.2:1	36%	79%	87%	12%
286	-	15:1	5.9%	78%	97%	–78%

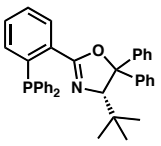

285

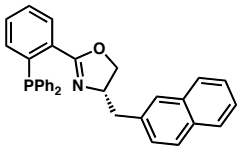

286

[a] All values presented were measured from collected GC data, rather than expressions (20) or (21).

Based on the data collected from these experiments, the r_α value appears to be large across most cases. Regardless of the ligand employed, the ratio of alkylation for intermediate (*R*)-**283** appears to strongly favor (*R*,*R*)-**282** over (*R*,*S*)-**282**, suggesting a matched catalyst-substrate situation. Conversely, the r_β value was observed to be disappointingly low for many of these experiments, often favoring the formation of stereoisomer (*S*,*R*)-**282** against catalyst preference. This trend in r_β suggests that the substrate interferes directly and considerably with the catalyst system over the course of

the enantioselective bond-forming event. In order to further evaluate these findings, the alkylation of an enantioenriched substrate bearing a pre-existing stereocenter was examined.

To more thoroughly study the impact of pre-existing stereocenters upon the course of a double asymmetric alkylation reaction, the enantiopure β-ketoester **287** was prepared as a mixture of diastereomers (Scheme 3.20). Exposure of **287** to the previously described allylation conditions afforded cyclohexanone **224** in greater than 50 : 1 dr (C_2 : *meso*). This diastereomeric ratio indicates that the selectivity of alkylation on **287** proceeds with an r value of approximately 96%.[30] Repeating this experiment with (*R*)-*t*-BuPHOX instead of (*S*)-*t*-BuPHOX provided cyclohexanone **224** in a 1 : 6.7 dr (C_2 : *meso*). If this diastereomeric ratio is converted to an alkylation selectivity value, an r term equal to –74% is obtained.[31] Though this reversal of selectivity indicates some measure of catalyst control during bond formation, the reduced magnitude of the diastereomeric ratio reveals that catalyst preference is not operating uncontested.

Scheme 3.21 Asymmetric alkylation of an enantioenriched substrate[a]

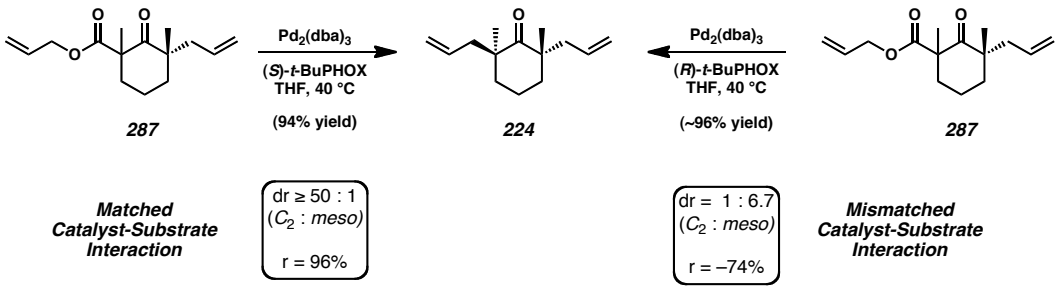

[a] For the reaction involving (*S*)-*t*-BuPHOX, use of either isolated, pure diastereomer of β-ketoeseter ***287*** afforded cyclohexanone ***224*** in excess of 50 : 1 dr. Additionally, a 1 : 1 mixture of both possible diastereomers of ***287*** achieved the same result. For the reaction involving (*R*)-*t*-BuPHOX, use of a pure diastereomer of ***287*** or a 1 : 1 mixture of diastereomers gave cyclohexanone **224** in a 1 : 6.7 dr. Relative stereochemistry of the isomers of ***287*** was not assigned.

Overall, the exceptionally high dr observed with the use of (*S*)-*t*-BuPHOX and β-ketoester **287** strongly suggests a matched catalyst-substrate situation, whereas the lower selectivity observed when (*R*)-*t*-BuPHOX is employed indicates some degree of mismatched interference. With these findings in mind, it is likely that the development of deleterious catalyst-substrate interactions due to the presence of pre-existing stereocenters, in combination with negative non-linear (Horeau-type) statistical effects, are the factors responsible for the lower than anticipated diastereomeric ratio values observed in our double-alkylation experiments. However, given the exceptional level of diastereoselectivity observed in these reactions when (*S*)-*t*-BuPHOX is employed, the results strongly suggest that undesired interactions influence the initial alkylation process, rather than the secondary allylation. If the allylation of enolate **279** (Scheme 3.19) in the double asymmetric alkylation were to proceed with high catalyst selectivity, the reaction would necessarily intercept an intermediate similar to β-ketoester **287** in the course to the final reaction product. In keeping with the results presented above, an exceptional dr would be anticipated under these conditions. Because the double asymmetric alkylation of (±)-**223** was observed to afford a 4.0 : 1 value for dr, these experiments suggest that the primary allylation occurs with mediocre selectivity.

To further strengthen our understanding of double asymmetric alkylation processes, additional investigations were performed using the racemic enol carbonates (±)-**288** and (±)-**290** (Scheme 3.21). Though very similar to the previously discussed enol carbonate (±)-**223**, these modified substrates possess differential substitution on either side of the latent ketone functionality. This critical addition provides two analytical advantages over the more symmetric ester (±)-**223**. First, due to the structural nature of these

differentially substituted, masked β-ketoester compounds, it is possible to control the order in which the alkylation events occur, thus restricting the course of the reaction to a single route (i = 1). Second, double alkylation of either (±)-**288** or (±)-**290** yields cyclohexanone **289** as the terminal product, allowing for direct comparison of results between the two orders of alkylation. Lastly, when considering the four stereoisomers of cyclohexanone **289** that can be afforded by these reactions, none of the possible diastereomers predicted are *meso* in nature, thus allowing for direct observation of ee_B. Because of this, more complicated mathematical expressions can be applied to the system in order to extract selectivity data, rather than relying upon the oversimplified equations (17) and (19).

Scheme 3.22 Substrates for double asymmetric catalytic alkylation studies

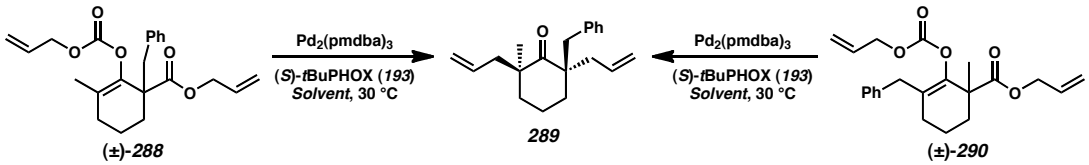

Both esters (±)-**288** and (±)-**290** were exposed to a palladium(0) precatalyst and (*S*)-*t*-BuPHOX (**193**) across twelve solvents at two concentrations (Scheme 3.22). The results of these reactions were scrutinized for the critical values of ee_A, ee_B, and diastereomeric ratio.[32] Because the β-ketoester moiety nested in both substrates (±)-**288** and (±)-**290** is effectively masked, reaction of either molecule can be assumed to first occur from the enol carbonate functionality. This reduces the possible number of selectivity factors encountered to three, thus allowing equations (11) – (13) to be implemented when calculating the value of these r terms. It is critical to note that equations (11) – (13)

facilitate more complicated calculations, provide more detailed data, and involve fewer simplifying assumptions than expressions (14)–(16), because of their inclusion of an additional r term. As such, the following case is no way comparable to the graphs presented in Figure 3.2.

Scheme 3.23 Stereochemical course of double alkylation for a differentially substituted carbonate

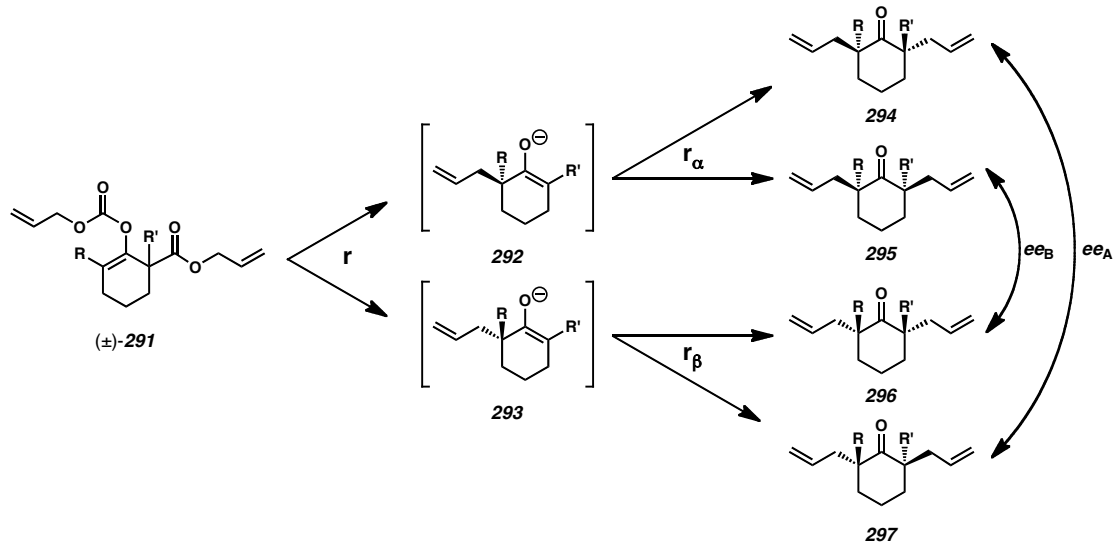

$$r = \frac{292 - 293}{292 + 293} = \frac{dr \cdot ee_A + ee_B}{1 + dr} \quad (11)$$

$$r_\alpha = \frac{294 - 295}{294 + 295} = \frac{dr + dr \cdot ee_A - ee_B - 1}{dr + dr \cdot ee_A + ee_B + 1} \quad (12)$$

$$r_\beta = \frac{296 - 297}{296 + 297} = \frac{dr - dr \cdot ee_A + ee_B - 1}{dr \cdot ee_A - dr + ee_B - 1} \quad (13)$$

Examination of the data resulting from these reactions provided surprising insight into the course of the double asymmetric catalytic alkylation (Scheme 3.24). Nearly every reaction run displayed a large value of ee_A, typically between 85 and 90 percent. The value of ee_B in all cases was only slightly lower, averaging between 75 and 85 percent. Across all experiments performed, the diastereomeric ratio observed ranged from 1.5 : 1 to 6.2 : 1, with the vast majority of results between 2.5 : 1 and 3.5 : 1. These

data are consistent with literature precedent regarding the positive non-linear effects anticipated for the value of ee_A and the negative non-linear effects anticipated for dr.

Scheme 3.24 Averaged selectivity values for double asymmetric catalytic alkylation

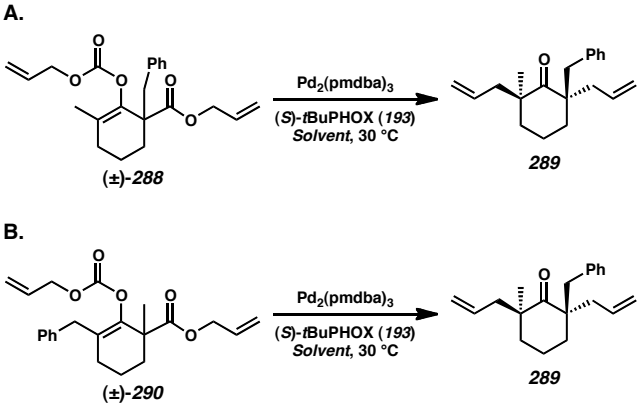

Average Values							
[0.03 M]				[0.01 M]			
ee_A	89.1%	r	87.1%	ee_A	90.6%	r	89.2%
ee_B	81.2%	r_α	42.8%	ee_B	84.6%	r_α	42.6%
dr	2.5:1	r_β	–14.8%	dr	2.6:1	r_β	–10.2%

Average Values							
[0.03 M]				[0.01 M]			
ee_A	83.0%	r	82.6%	ee_A	85.1%	r	84.5%
ee_B	78.8%	r_α	56.6%	ee_B	80.6%	r_α	56.0%
dr	3.9:1	r_β	–45.0%	dr	3.8:1	r_β	–39.6%

Using the data obtained from these experiments in combination with the equations discussed previously, values for all three selectivity terms can be derived. In all reactions examined the value of the r term averages above 80%, and typically falls within the range between 85 and 90%. This finding implies two important facts about the course of the double alkylation reaction. First, these data indicate that the initial bond-forming event proceeds with the close to the expected degree of catalyst control. Second, because the value of r is large, the total quantity of intermediate enolate **293** present throughout the reaction is very small (Scheme 3.23). It should be noted that a majority of the calculated r_β values afford negative results, indicating a preference for the generation of cyclohexanone **297** over diallyl species **296** during the final bond-forming transformation. However, due to the sparingly small quantity of enolate **293** produced from the previous alkylation, the influence of r_β upon the overall outcome of the reaction

is minimized. As such, no trend is easily observable between the value of r_β and either ee_A or dr.

In light of the consistently large selectivity for r, and the consequent insignificance of r_β, the r_α term appears to be much more important to the eventual ee_A and dr of the total reaction. The observed values for r_α across multiple reactions were calculated in the range of 40 to 55%, an observation that suggests an unanticipated amount of cyclohexanone product **295** is produced during the final alkylation of enolate **292**. Notably, this low selectivity and undesired accumulation of diallyl product **295** has no impact upon ee_A, which remains large for all reactions examined. However, because this second alkylation occurs with lower efficiency than desired, the formation of cyclohexanone **295** at the expense of desired product **294** leads to a reduction in dr. Interestingly, these findings suggest the disappointing diastereomeric ratios observed for some of our double alkylation reactions are partly due to ineffective catalyst control at the second stage of bond formation, a conclusion that contradicts our earlier experiments employing enantioenriched β-ketoester substrates.

An additional experiment to further investigate the impact of the primary and secondary alkylation selectivities in these reactions would help resolve this observed contradiction. In particular, performing an alkylation from an enol carbonate substrate in the presence of a racemic β-ketoester stereocenter would provide an excellent system to probe the selectivity of the primary alkylation process. Starting from known β-ketoester **298**, hydrogenation of the allyl group, followed by methylation of the α-position, will afford cyclohexanone **299**. After installation of an appropriate enol carbonate moiety to achieve carbonate-ester substrate **300**, this material will be subjected to the conditions of

the stereoselective catalytic alkylation to ultimately generate β-ketoester **301**. By measuring the resulting dr of propyl ester **301**, data complementary to that observed in the alkylation of β-ketoester **287** (Scheme 3.21) will be attained, thus providing access to a more complete set of data for the process of double stereoselective alkylation. If a dr near 1 : 1 is observed for this proposed reaction, the evidence would suggest that the primary alkylation proceeds with very high catalyst control. If the value of dr is observed to deviate significantly from a 1 : 1 ratio, this result would imply considerable substrate interference with catalyst activity and consequent low selectivity for the primary alkylation.

Scheme 3.25 Experiment proposed for further investigation of double asymmetric alkylation

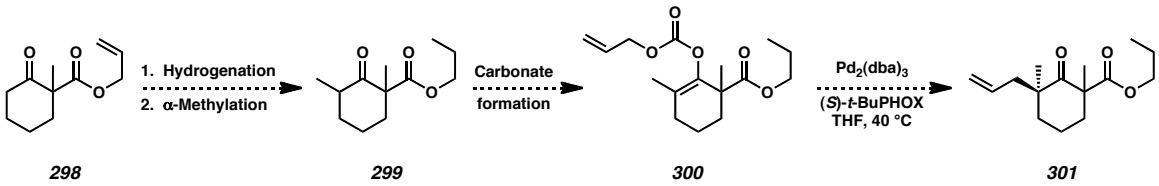

It should be noted that the studies conducted above exclusively focused on the 2,6-substituted substrates that react to form diallyl cyclohexanone **224**. Many of the conclusions concerning these experiments may be specific to double alkylation reactions of compounds with similar substitution patterns.

3.4 CONCLUSION

Multiple asymmetric transformations are powerful techniques that rapidly build molecular complexity via the concurrent installation of two or more stereocenters under

catalyst or reagent control. By leveraging these versatile reactions, not only is it possible to efficiently construct structurally difficult compounds, but it is also possible to garner an impressive boost in the *ee* of the desired product via statistical amplification. Indeed, multiple asymmetric reactions are able to produce very high levels of enantioenrichment in the major diastereomer of reaction. This is largely because the minor diastereomer produced in the course of such a transformation serves as a "buffer" against accumulation of the opposite enantiomer of the major diastereomer. Thus, high values attained for *ee* in these reactions are always accompanied by lower than anticipated diastereomeric ratios.

While multiple asymmetric transformations are powerful tools with which to approach a variety of synthetic challenges, their optimization is often made cumbersome due to the difficulty of analyzing multiple, convoluted reaction pathways. However, depending on the degree to which substrate interference impacts catalyst control, a wide variety of simplified mathematical representations are available for the extraction of crucial selectivity data from the values of ee_A, ee_B, and dr. By appealing to expressions most suitable for the situations in question, our group has been able to deconstruct the various stages of a double asymmetric alkylation. In so doing, we found that the secondary alkylation process is prone to experience deleterious catalyst-substrate interactions. This valuable data has provided valuable insight into the behavior of the reaction, and further refinement of our technology based on these findings is currently underway.

3.5 EXPERIMENTAL SECTION

3.5.1 MATERIALS AND METHODS

All reactions were performed at ambient temperature (22 °C) unless otherwise noted. Reactions requiring external heat were modulated to the specified temperatures indicated by using an IKAmag temperature controller. All reactions were performed in glassware flame dried under vacuum and allowed to cool under nitrogen or argon. Solvents were dried by passage over a column of activated alumina with an overpressure of argon gas. Tetrahydrofuran was distilled directly over benzophenone and sodium, or else was dried by passage over a column of activated alumina with an overpressure of argon gas. (*S*)-*t*-BuPHOX (**193**) was prepared according to known methods.[33,34] All other chemicals and reagents were used as received. Compounds purified by flash chromatography utilized ICN silica gel (particle size 0.032-0.063 mm) or SiliCycle® Silia*Flash*® P60 Academic Silica Gel (particle size 40-63 μm; pore diameter 60 Å). Thin-layer chromatography (TLC) was performed using E. Merck silica gel 60 F254 pre-coated plates (0.25 mm) and visualized by UV, *p*-anisaldehyde, or alkaline permanganate staining. NMR spectra were recorded on a Varian Mercury 300 (at 300 MHz for ^{1}H NMR and 75 MHz for ^{13}C), Varian Inova 500 (at 500 MHz for ^{1}H NMR and 125 for ^{13}C), or Varian Inova 600 (at 600 MHz for 1H NMR only) instrument, and are reported relative to residual $CHCl_3$ (δ 7.26 for ^{1}H NMR, δ 77.16 for ^{13}C) or C_6H_6 (δ 7.16 for ^{1}H NMR, δ 128.06 for ^{13}C). The following format is used for the reporting of ^{1}H NMR data: chemical shift (δ ppm), multiplicity, coupling constant (Hz), and integration. Data for ^{13}C NMR spectra are reported in terms of chemical shift. IR spectra were recorded on a Perkin Elmer

Spectrum Paragon 1000 spectrometer, and data are reported in frequency of absorption (cm^{-1}). High-resolution mass spectra were obtained from the Caltech Mass Spectral Facility, or else were acquired using an Agilent 6200 Series TOF mass spectrometer with an Agilent G1978A Multimode source in ESI, APCI, or MM (ESI/APCI) ionization mode. Analytical chiral gas chromatography was performed with an Agilent 6850 GC using a G-TA (30 m x 0.25 mm) column (1.0 mL/min carrier gas flow). Analytical achiral gas chromatography was performed with an Agilent 6850 GC using a DB-WAX (30 x 0.25 mm) column (1.0 mL/min carrier gas flow). Analytical chiral super critical fluid chromatography was performed with a Mettler supercritical CO_2 analytical chromatography system equipped with a CTC analytics HTC PAL autosampler, utilizing a Chiracel OD/OD-H column with a flow rate of 2.5 mL/min. Analytical chiral super critical fluid chromatography runs were visualized with a UV-visible detector operating at 210 nm. Automated experiments were performed with a Symex Core Module while inside a nitrogen-filled glovebox. Optical rotations were measured with a Jasco P-1010 polarimeter at 589 nm using a 100 mm path-length cell.

3.5.2 PREPARATIVE PROCEDURES

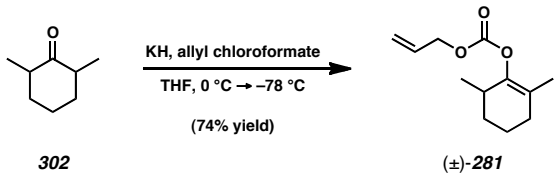

302 (±)-***281***

Enol Carbonate (281). To a flame dried flask under argon was added KH (30% in mineral oil, 0.552 g, 4.13 mmol, 1.04 equiv). The KH was suspended in dry hexanes (ca. 6.5 mL), stirred briefly, and then the hexanes were removed via syringe without disturbing the KH sediment. This process was repeated two additional times, and the residual solid was then dried under high vacuum for 10 min. The washed KH powder was then suspended in THF (12.5 mL) and cooled to 0 °C. Once cooled, 2,6-dimethylcyclohexanone (**302**, 0.500 mL, 3.96 mmol, 1.00 equiv) was added dropwise via syringe. The reaction was allowed to slowly reach room temperature, and then was allowed to deprotonate over 10 h. After this time had elapsed, the reaction was cooled to –78 °C, and a single portion of allyl chloroformate (0.430 mL, 4.05 mmol, 1.02 equiv) was added dropwise. After a further 15 min of reaction at –78 °C, the flask was allowed to reach room temperature. The reaction was quenched via the addition of saturated $NH_4Cl_{(aq)}$ (10 mL), and the phases were thereafter separated. The aqueous phase was extracted with Et_2O (4 x 20 mL). The combined organic layers were washed with brine (20 mL), dried over $MgSO_4$, filtered, and then concentrated in vacuo. The resulting material was thereafter purified over silica gel using 2% ethyl acetate in hexanes as eluent. This afforded (±)-**281** as a clear, colorless oil (0.619 g, 74% yield): ^{1}H NMR (500 MHz, $CDCl_3$) δ 5.96 (app ddt, J = 17.2, 10.5, 5.7 Hz, 1H), 5.38 (app dq, J = 17.2, 1.5 Hz, 1H), 5.28 (app dq, J = 10.5, 1.2 Hz, 1H), 4.66 (ddd, J = 5.7, 2.6, 1.2 Hz, 2H),

2.52–2.42 (m, 1H), 2.07–2.01 (m, 2H), 1.86 (dddd, J = 12.8, 8.8, 8.5, 3.1 Hz, 1H), 1.66 (app dddt, J = 17.7, 9.0, 6.0, 3.1 Hz, 1H), 1.61–1.52 (m, 1H), 1.56–1.55 (m, 3H), 1.45–1.37 (m, 1H), 1.02 (d, J = 7.0 Hz, 3H); ^{13}C NMR (125 MHz, $CDCl_3$) δ 153.3, 146.1, 131.7, 121.3, 118.9, 68.7, 31.9, 31.4, 30.8, 20.1, 18.3, 16.2; IR (Neat film, NaCl) 2934, 2875, 1756, 1701, 1650, 1455, 1366, 1292, 1248, 1156, 1132, 1035, 994, 981, 940 cm^{-1}; HRMS (EI) *m/z* calc'd for $C_{12}H_{18}O_3$ $[M]^+$: 210.1256, found 210.1259.

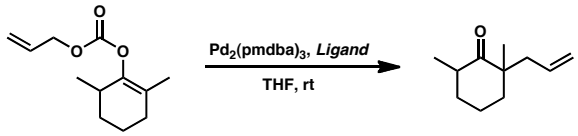

(±)-***281*** ***282***

Cyclohexanone (282). A representative procedure for the synthesis of cyclohexanone **282** is as follows: To a flame dried flask under argon was added 0.004 g $Pd_2(pmdba)_3$ (0.004 g, 0.004 mmol, 0.025 equiv) and a corresponding amount (0.009 mmol, 0.06 equiv) of a given PHOX ligand derivative. These solids were briefly vacuum purged in the flask, before being backfilled with argon. To these solids was added a single portion of THF (4.3 mL), and the reaction was allowed to pre-complex over 30 min. After this time had elapsed, the reaction was treated with neat enol carbonate (±)-**281** (0.030g, 0.143 mmol, 1.00 equiv). The reaction was allowed to proceed for 3 h. The solvent was then removed in vacuo, and the resulting crude material was purified directly over silica using 1% Et_2O in pentane as eluent. Cyclohexanone **282** was isolated as a clear oil (inseparable mixture of diastereomers): Chiral GC assay (GTA column): 90 °C isothermal method over 40 min, t_r (Enantiomer A, diastereomer A) = 25.3 min; t_r (Enantiomer B, diastereomer A) = 26.7 min; t_r (Enantiomer A, diastereomer B) = 27.5

min; t_r (Enantiomer B, diastereomer B) 32.0 min. ^{1}H NMR (500 MHz, $CDCl_3$) δ 5.60 (dddd, *J* = 14.7, 13.7, 9.5, 7.4 Hz, 1H), 5.07–4.98 (comp. m, 2H), 2.65–2.56 (m, 1H), 2.53 (dd, *J* = 13.9, 7.4 Hz, 1H), 2.52–2.21 (m, 1H), 2.17 (dd, *J* = 13.9, 7.4 Hz, 1H), 2.09–2.00 (m, 1H), 1.97–1.82 (m, 1H), 1.74–1.56 (m, 1H), 1.53–1.45 (m, 1H), 1.38–1.28 (m, 1H), 1.01 (s, 3H), 0.99 (d, *J* = 6.5 Hz, 3H); ^{13}C NMR (125 MHz, $CDCl_3$) δ 216.5, 133.3, 118.1, 48.9, 41.9, 41.5, 40.0, 36.8, 22.7, 21.2, 15.1; IR (Neat film, NaCl) 3077, 2969, 2931, 2870, 2854, 1706, 1640, 1456, 1377, 1316, 1126, 999, 958, 914, 856 cm^{-1}; HRMS (EI) *m/z* calc'd for $C_{11}H_{18}O$ $[M]^+$: 166.1358, found 116.1357; $[\alpha]^{25}_D$ –21.2 (*c* 1.14, CH_2Cl_2).

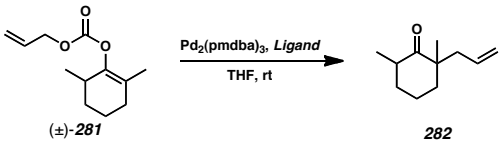

Ligand	ee_A (%)	ee_B (%)	*de* (%)	dr (X : 1)	r_α (%)	r_β (%)
PPh_3	-	-	63.6	4.5	63.6	–63.6
dppp	-	-	42.4	2.5	42.6	–42.6
284	-	-	92.1	24	92.1	–92.1
193	40.2	98.9	46.2	2.7	99.4	10.0
303	–39.5	–98.9	50.1	3.0	–4.4	–99.5
304	22.2	96.3	66.5	5.0	98.8	–32.6
305	38.6	97.1	46.1	2.7	98.5	8.5
286	5.9	78.0	87.8	15	97.3	–78.1
306	–13.0	–88.5	85.7	13	71.5	–98.5
285	35.9	78.8	37.6	2.2	86.8	11.7
307	45.8	87.1	56.2	3.6	95.1	–1.6
308	–35.3	–81.8	57.1	3.7	13.2	–92.9
309	17.4	90.7	73.3	6.5	97.6	–46.5
310	–15.6	–76.1	71.5	6.0	48.5	–93.3

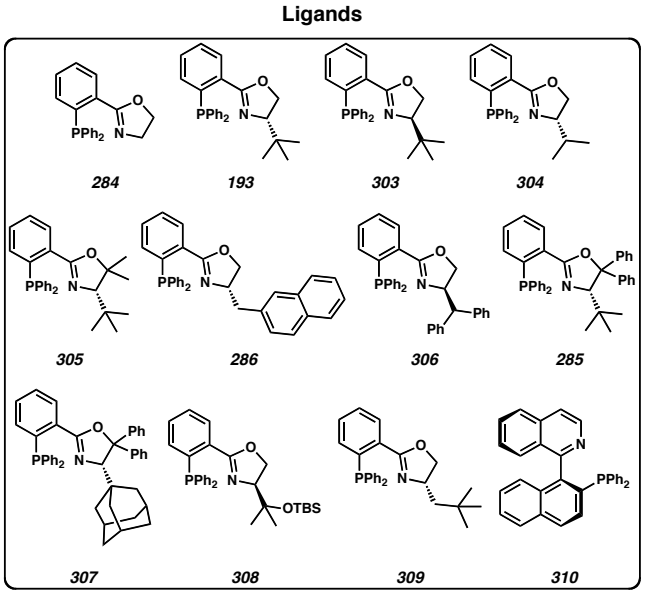

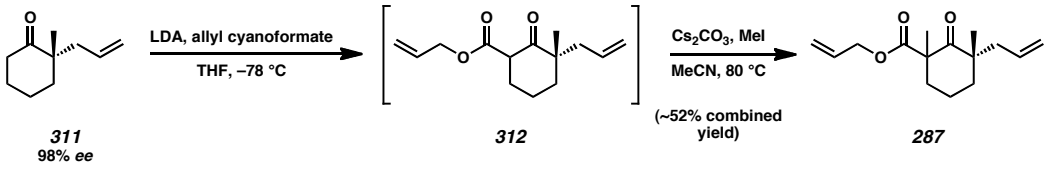

β-ketoester (287). To a flame dried flask was added THF (50 mL) and diisopropyl amine (1.76 mL, 12.3 mmol, 1.25 equiv). This solution was cooled to 0 °C, before being treated with *n*-BuLi (5.14 mL, 2.3 M in hexanes, 11.8 mmol, 1.20 equiv). The solution was allowed to stir for 30 min at this temperature, before being cooled to –78 °C. After this temperature was reached, neat cyclohexanone **311** (1.50 g, 9.85 mmol, 1.00 equiv) was added dropwise. Deprotonation was allowed at –78 °C over 30 min, after which time the reaction was treated with a single portion of neat allyl cyanoformate (1.42 mL, 12.8 mmol, 1.30 equiv). The reaction was allowed to slowly reach room temperature by warming in the bath over 6 h. After the reaction had reached room temperature it was quenched via the addition of saturated $NH_4Cl_{(aq)}$ (30 mL). The phases were separated, and the aqueous layer was extracted with ethyl acetate (3 x 40 mL). Combined organics were washed with brine (40 mL), dried over $MgSO_4$, and filtered. The material resultant from this process was passed over a plug of silica using 20% ethyl acetate in hexanes as eluent, and then was used directly in the next reaction.

To a flame dried Schlenk flask was added Cs_2CO_3 (3.89 g, 11.8 mmol, 1.20 equiv). This material was vacuum purged briefly, before being backfilled with nitrogen. To this flask was added 50 mL of MeCN containing the crude product of the previous sequence (ca. 2.33g, 9.85 mmol, 1.00 equiv). The reaction was treated with MeI (1.90 mL, 30.5 mmol, 3.10 equiv) and the reaction vessel was sealed. The reaction was then heated to 80 °C for 12 h. After this time had elapsed, the reaction was cooled to room temperature and filtered to remove excess solid Cs_2CO_3. The filtrate was diluted with saturated

$NH_4Cl_{(aq)}$ (40 mL) and the two phases were then separated. The aqueous phase was extracted with ethyl acetate (4 x 20 mL), and the combined organic phases were washed with brine (40 mL). The organic layers were dried over $MgSO_4$, filtered, and concentrated in vacuo. The resulting material was purified twice over silica using a gradient of 0 → 5% Et_2O in pentane as eluent. This afforded β-ketoester **287** as a mixture of diasteromers, isolated as a clear, colorless oil (1.28 g, 52% combined yield). Analytically pure samples of each diastereomer were obtained via preparatory HPLC separation, using 0 → 3.5% *tert*-butyl methyl ether.

Diastereomer A: ^{1}H NMR (500 MHz, $CDCl_3$) δ 5.87 (app ddt, *J* = 17.2, 10.4, 5.8 Hz, 1H), 5.75 (dddd, *J* = 17.2, 10.2, 7.6, 7.1 Hz, 1H), 5.30 (app dq, *J* = 17.2, 1.5 Hz, 1H), 5.22 (app dq, *J* = 10.4, 1.2 Hz, 1H), 5.03 (app dddt, *J* = 18.4, 17.0, 2.5, 1.1 Hz, 2H), 4.61 (app ddt, *J* = 13.2, 5.8, 1.4 Hz, 1H), 4.52 (app ddt, *J* = 13.2, 5.8, 1.4 Hz, 1H), 2.55–2.50 (m, 1H), 2.29 (app ddt, *J* = 13.8, 7.0, 1.1 Hz, 1H), 2.25–2.19 (m, 1H), 2.01–1.90 (m, 1H), 1.68–1.60 (comp. m, 3H), 1.45–1.38 (m, 1H), 1.32 (s, 3H), 1.04 (s, 3H); ^{13}C NMR (125 MHz, $CDCl_3$) δ 210.9, 172.6, 134.7, 131.6, 118.9, 118.1, 65.9, 55.5, 49.0, 43.7, 37.4, 36.7, 23.7, 23.6, 18.4; IR (Neat film, NaCl) 3076, 2978, 2937, 1738, 1706, 1639, 1459, 1377, 1237, 1204, 1175, 1141, 1062, 994, 917 cm^{-1}; HRMS (EI) *m/z* calc'd for $C_{15}H_{22}O_3$ $[M+H]^+$: 251.1642, found 251.1642; $[\alpha]^{25}_D$ –97.6 (*c* 0.61, CH_2Cl_2). **Diastereomer B**: ^{1}H NMR (500 MHz, $CDCl_3$) δ 5.87 (app ddt, *J* = 17.2, 10.4, 5.8 Hz, 1H), 5.61 (dddd, *J* = 16.8, 10.2, 7.9, 6.5 Hz, 1H), 5.31 (app dq, *J* = 17.2, 1.5 Hz, 1H), 5.23 (ddd, *J* = 10.4, 2.5, 1.2 Hz, 1H), 5.07–4.98 (m, 2H), 4.64 (app ddt, *J* = 13.1, 5.8, 1.4 Hz, 1H), 4.48 (app ddt, *J* = 13.1, 5.8, 1.4 Hz, 1H), 2.52 (app dtd, *J* = 13.8, 4.5, 2.1 Hz, 1H), 2.24–2.15 (m, 2H), 2.00–1.90 (m, 1H), 1.85 (dddd, *J* = 13.9, 6.0, 4.1, 2.1 Hz, 1H), 1.66–1.59 (m, 1H), 1.51

(dddd, J = 13.8, 11.1, 6.3, 4.5 Hz, 2H), 1.35 (s, 3H), 1.04 (s, 3H); ^{13}C NMR (125 MHz, $CDCl_3$) δ 211.3, 172.5, 133.8, 131.6, 119.1, 118.4, 66.0, 55.6, 48.9, 41.9, 37.4, 36.4, 24.1, 23.9, 18.0; IR (Neat film, NaCl) 2935, 2874, 1734, 1705, 1456, 1377, 1241, 1169, 1145, 1118, 1080, 994, 974, 918, 868 cm^{-1}; HRMS (EI) *m/z* calc'd for $C_{15}H_{22}O_3$ $[M+H]^+$: 251.1642, found 251.1643; $[\alpha]^{25}_D$ +51.7 (*c* 0.80, CH_2Cl_2).

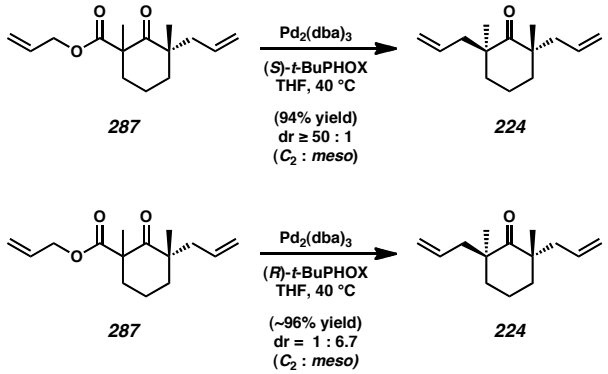

Diallyl cyclohexanone (224). To a flame dried flask under argon was added $Pd_2(dba)_3$ (0.003 g, 0.004 mmol, 0.04 equiv) and of either (*R*) or (*S*)-*t*-BuPHOX (0.003 g, 0.008 mmol, 0.08 equiv). These solids were briefly vacuum purged in the flask before being backfilled with argon. To these solids were added 3 mL of THF, and the reaction was allowed to precomplex at 40 °C over 30 min. After this time had elapsed, the reaction was treated with a single portion of neat β-ketoester **287** (0.025 g, 0.100 mmol, 1.00 equiv). The reaction was allowed to proceed for 3 h. The solvent was then removed in vacuo, and the resulting crude material was purified directly over silica using 2% Et_2O in pentane as eluent. This afforded cyclohexanone **224** as a clear, colorless oil (19.3 mg, 94% yield). Characterization data was identical to that reported in reference 3: ^{1}H NMR (300 MHz, $CDCl_3$) δ 5.65 (m, 2H), 5.10–4.95 (m, 4H), 2.33 (dd, J = 13.8, 6.9 Hz, 2H), 2.18 (dd, J = 13.8, 7.8 Hz, 2H), 1.87–1.68 (m, 4H), 1.59–1.48 (m, 2H), 1.06 (s, 6H); ^{13}C

NMR (75 MHz, $CDCl_3$) δ 218.6, 134.4, 118.0, 47.6, 43.9, 36.4, 25.0, 17.3; IR (Neat film, NaCl) 3076, 2930, 1694, 1639, 1461, 1374, 992, 914 cm^{-1}; HRMS (EI) *m/z* calc'd for $C_{14}H_{22}O$ $[M]^+$: 206.1671, found 206.1675; $[\alpha]^{25}_D$ –54.0 (*c* 0.95, hexane).

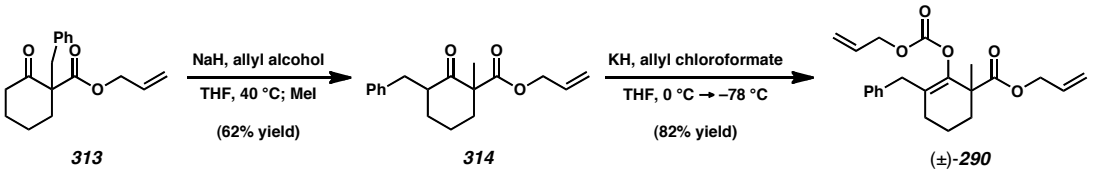

313 ***314*** (±)-***290***

Enol carbonate (290). To a flame dried vial under argon was added NaH (60% in mineral oil, 0.299 g, 7.48 mmol, 2.04 equiv) and THF (20 mL). This suspension was cooled to 0 °C, and then was treated with allyl alcohol (0.550 mL, 8.09 mmol, 2.20 equiv). After gas evolution had halted the reaction was treated with neat cyclohexanone **313** (1.00 g, 3.67 mmol, 1.0 equiv) and was heated to 40 °C. After stirring for 3 h at 40 °C, the reaction was cooled to room temperature and treated with a single portion of MeI (0.510 mL, 8.19 mmol, 2.23 equiv). The reaction was thereafter heated to 40 °C for an additional 12 h. After this time had elapsed, the reaction was cooled to room temperature and quenched with saturated $NH_4Cl_{(aq)}$ (40 mL). The phases were separated, and the aqueous layer was extracted with Et_2O (3 x 20 mL). The combined organic layers were washed with brine (40 mL), dried over $MgSO_4$ and filtered. After removal of the solvent in vacuo, the crude material obtained was purified over silica gel using 3% ethyl acetate in hexanes. Because the resulting material isolated was not of sufficient purity for characterization, this mixture of diasteromeric β-ketoesters was carried into the next transformation directly.

To a flame dried flask under argon was added KH (30% in mineral oil, 0.280 g, 2.09 mmol, 1.20 equiv). The KH was suspended in dry hexanes (ca. 4.0 mL), stirred briefly, and then was allowed to settle. The hexanes layer was carefully removed via syringe while taking precautions not to disturb the KH sediment. This process was repeated two additional times, and the residual solid was then dried under high vacuum for 10 min. The washed KH powder was then suspended in THF (5.8 mL). To this was added, dropwise via syringe, the material obtained from the preceding step (ca. 0.500 g, 1.75 mmol, 1.0 equiv). The reaction was allowed to deprotonate at room temperature over 1 h. After this time had elapsed, the reaction was cooled to –78 °C, and a single portion of allyl chloroformate (0.222 mL, 2.10 mmol, 1.20 equiv) was added dropwise. After a further 1.5 h of reaction at –78 °C, the flask was allowed to reach room temperature. The reaction was quenched via the addition of saturated $NH_4Cl_{(aq)}$ (10 mL), and the phases were separated. The aqueous phase was extracted with Et_2O (4 x 20 mL). The combined organic layers were washed with brine (20 mL), dried over $MgSO_4$, filtered, and then concentrated in vacuo. The resulting material was thereafter purified over silica gel using 5% ethyl acetate in hexanes as eluent. This afforded **290** as a clear, colorless oil (0.530 g, 51% yield from **313**). ^{1}H NMR (500 MHz, $CDCl_3$) δ 7.28–7.24 (comp. m, 2H), 7.22–7.17 (comp. m, 3H), 5.93 (app dddt, *J* = 17.2, 10.4, 5.7, 2.8 Hz, 2H), 5.35 (app ddq, *J* = 17.2, 12.2, 1.5 Hz, 2H), 5.25 (app ddq, *J* = 14.3, 10.5, 1.3 Hz, 2H), 4.65–4.60 (m, 4H), 3.41 (d, *J* = 14.9 Hz, 1H), 3.19 (d, *J* = 14.9 Hz, 1H), 2.20–2.14 (m, 1H), 2.01–1.98 (m, 2H), 1.67–1.59 (comp. m, 3H), 1.40 (s, 3H); ^{13}C NMR (125 MHz, $CDCl_3$) δ 174.8, 153.6, 143.1, 138.9, 132.3, 131.5, 129.1, 128.5, 127.7, 126.3, 119.3, 118.1, 69.0, 65.8, 47.2, 36.8, 36.1, 28.2, 22.5, 19.3; IR (Neat film, NaCl) 3026, 2942, 1759, 1733, 1649,

1602, 1496, 1434, 1365, 1238, 1166, 1108, 1024, 994, 940 cm^{-1}; HRMS (EI) *m/z* calc'd for $C_{22}H_{26}O_5$ $[M]^+$: 370.1780, found 370.1788.

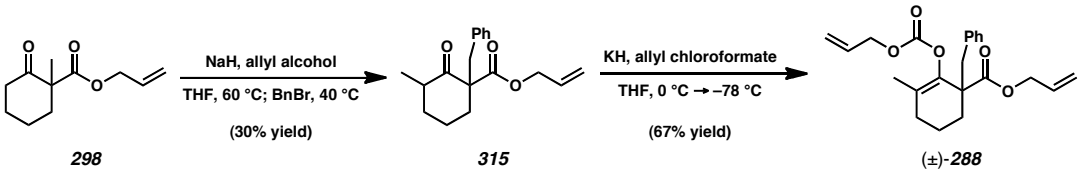

298 ***315*** (±)-***288***

Enol carbonate (288). To a flame dried vial under argon was added NaH (60% in mineral oil, 1.05 g, 26.3 mmol, 2.07 equiv) and THF (64 mL). This suspension was cooled to 0 °C, and then was treated with allyl alcohol (3.12 mL, 46.2 mmol, 3.64 equiv). After gas evolution had halted, the reaction was treated with neat cyclohexanone **298** (2.50 g, 12.7 mmol, 1.0 equiv) and was heated to 60 °C. After stirring for 12 h at 60 °C, the reaction was cooled to 40 °C and treated with neat BnBr (3.20 mL, 26.9 mmol, 2.12 equiv). The reaction was stirred at 40 °C for three additional hours, but complete conversion was not observed. An additional portion of BnBr (2.0 mL, 16.8 mmol, 1.33 equiv) was introduced to the flask, and the reaction was allowed to continue for 12 h more. After this time had elapsed, the reaction was cooled to room temperature and quenched with saturated $NH_4Cl_{(aq)}$ (40 mL). The phases were separated, and the aqueous layer was extracted with Et_2O (3 x 40 mL). The combined organic layers were washed with brine (40 mL), dried over $MgSO_4$, and were filtered. After removal of the solvent in vacuo, the crude material obtained was purified over silica gel using 3% ethyl acetate in hexanes. Because the resulting material isolated was not of sufficient purity for characterization, this mixture of diasteromeric β-ketoesters was carried into the next transformation directly.

To a flame dried flask under argon was added KH (30% in mineral oil, 0.291 g, 2.18 mmol, 1.24 equiv). The KH was suspended dry hexanes (ca. 4.0 mL), stirred briefly, and then was allowed to settle. The hexanes layer was carefully removed via syringe while taking precautions not to disturb the KH sediment. This process was repeated two additional times, and the residual solid was then dried under high vacuum for 10 min. The washed KH powder was then suspended in THF (6.0 mL). To this suspension was added, dropwise via syringe, the material obtained from the preceding step (ca. 0.500 g, 1.75 mmol, 1.0 equiv). The reaction was allowed to deprotonate at room temperature over 5 h. After this time had elapsed, the reaction was cooled to –78 °C, and a single portion of allyl chloroformate (0.225 mL, 2.10 mmol, 1.20 equiv) was added dropwise. After a further 4 h of reaction at –78 °C, the flask was allowed to reach room temperature. The reaction was quenched via the addition of saturated $NH_4Cl_{(aq)}$ (10 mL), and the phases were separated. The aqueous phase was extracted with Et_2O (4 x 25 mL). The combined organic layers were washed with brine (20 mL), dried over $MgSO_4$, filtered, and concentrated in vacuo. The resulting material was purified over silica gel using 5% ethyl acetate in hexanes as eluent. This afforded **288** as a clear, colorless oil (0.493 g, 20% yield from **298**). ^{1}H NMR (500 MHz, $CDCl_3$) δ 7.25–7.18 (comp. m, 3H), 7.16–7.13 (comp. m, 2H), 5.95 (app dddt, *J* = 34.7, 17.2, 10.5, 5.7 Hz, 2H), 5.42 (app dq, *J* = 17.2, 1.5 Hz, 1H), 5.34 (app dq, *J* = 17.2, 1.5 Hz, 1H), 5.30 (app dq, *J* = 10.5, 1.3 Hz, 1H), 5.23 (app dq, 10.5, 1.3 Hz, 1H), 4.67 (app ddt, *J* = 12.2, 5.8, 1.4 Hz, 1H), 4.64–4.60 (comp. m, 2H), 4.49 (app ddt, *J* = 13.4, 5.8, 1.4 Hz, 1H), 3.30 (d, *J* = 13.5 Hz, 1H), 3.02 (d, *J* = 13.5 Hz, 1H), 2.13–1.92 (comp. m, 3H), 1.78–1.68 (m, 1H), 1.58 (s, 3H), 1.58–1.54 (m, 1H), 1.49–1.41 (m, 1H); ^{13}C NMR (125 MHz, $CDCl_3$) δ 172.9, 152.7, 140.3,

137.0, 132.3, 131.8, 130.6, 128.1, 127.7, 126.7, 119.1, 118.2, 68.9, 65.9, 50.9, 41.9, 31.3, 30.9, 19.4, 17.4; IR (Neat film, NaCl) 3029, 2942, 1761, 1732, 1649, 1604, 1496, 1454, 1365, 1230, 1176, 1155, 1094, 1032, 993, 937 cm^{-1}; HRMS (EI) *m/z* calc'd for $C_{22}H_{26}O_5$ $[M]^+$: 370.1780, found 370.1770.

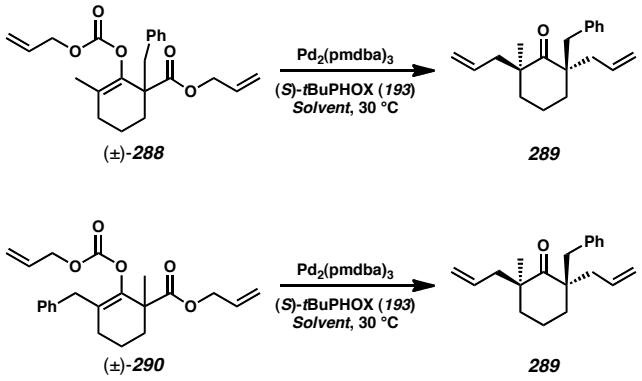

Diallyl cyclohexanone (289). The following series of experiments were run simultaneously inside of a glovebox under a nitrogen atmosphere. To each of 48 vials in two 24-well plates was added solution of $Pd_2(pmdba)_3$ (62.5 μL, 3.60 mM in THF, 0.225 μmol, 0.025 equiv). The solvent was removed from the vials in vacuo, and to each vial was added of (*S*)-*t*-BuPHOX in a (20 μL, 27.9 mM solution of a 1 : 1 mixture of PhMe : Hex, 0.559 μmol, 0.062 equiv). To each vial was then added a portion of the appropriate solvent (160 μL) to be used in the solvent screen. Each vial was then allowed to stir for 40 min at 30 °C in order to allow the palladium and ligand to precomplex. After this time had elapsed, either **289** or **290** (20 μL, 0.450 M solution of a 1 : 1 mixture of PhMe : Hex, 8.99 μmol) were added to each vial. Each of the 24 vials of the first plate (Plate A) were charged with **288**. Each of the 24 vials of the second plate (Plate B) were charged with **290**. The vials were then treated with an additional volume of solvent such that the

first 12 vials of each plate achieved a final concentration of 0.03 M, while the last twelve vials of each plate achieved a final concentration of 0.01 M. All reactions were tightly capped, and then run for 70 h at 30 °C inside the glovebox. After this time had elapsed, each reaction was passed over a small plug of silica using Et_2O as eluent. Afterward all solvents were removed in vacuo, and each reaction was assayed by ^1H NMR and analytical SFC. Values for *ee* and dr were collected via analytical supercritical fluid chromatography over a Chiralcel OD/OD-H column at a flow rate of 2.5 mL/min using an isocratic elution of 3% *i*-PrOH in CO_2: t_r (major diastereomer, major enantiomer) = 7.8 min; t_r (minor diastereomer, minor enantiomer) = 8.5 min; t_r (major diastereomer, minor enantiomer) = 9.2 min; t_r (minor diastereomer, major enantiomer) = 9.8 min. ^1H NMR (500 MHz, $CDCl_3$) δ 7.27–7.17 (comp. m, 3H), 7.12–7.09 (m, 2H), 5.76–5.62 (m, 1H), 5.58–5.49 (m, 1H), 5.12–5.08 (m, 1H), 5.08–5.01 (m, 1H), 4.99–4.93 (m, 2H), 3.15 (d, *J* = 13.3 Hz, 1H), 2.52 (d, *J* = 13.3 Hz, 1H), 2.39 (dd, *J* = 14.1, 7.0, 1H), 2.29 (dd, *J* = 13.7, 6.7 Hz, 1H), 2.20 (dd, *J* = 14.0, 7.5 Hz, 1H), 2.07 (dd, *J* = 13.7, 8.0, 1H), 1.80–1.59 (comp. m, 4H), 1.55–1.39 (comp. m, 2H), 1.09 (s, 3H); ^{13}C NMR (125 MHz, $CDCl_3$) δ 217.9, 138.0, 134.6, 134.3, 131.4, 128.0, 126.4, 118.5, 118.1, 52.6, 47.5, 44.2, 42.8, 42.6, 35.5, 32.1, 25.6, 17.3; IR (Neat film, NaCl) 3075, 2933, 2869, 1692, 1638, 1496, 1454, 1373, 1072, 994, 916, 743 cm^{-1}; HRMS (EI) *m/z* calc'd for $C_{20}H_{26}O$ $[M]^+$: 282.1984, found 282.1972; $[\alpha]^{25}_D$ –8.6 (*c* 1.05, CH_2Cl_2).

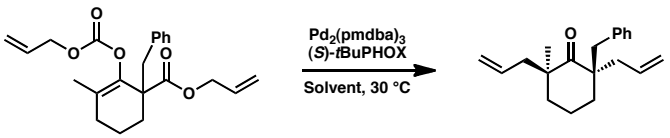

(±)-***288*** ***289***

0.03 M Concentration

Solvent	ee_A (%)	ee_B (%)	*de* (%)	dr (X : 1)	yield lost (%)	r (%)	r_α (%)	r_β (%)
Dioxane	50.2	62.3	47.4	2.8	26.3	53.4	44.3	–57.4
DME	83.3	88.3	44.4	2.6	27.8	84.7	43.4	–57.5
Et_2O	92.7	83.9	66.1	4.9	16.9	91.2	67.4	–37.9
Et_2O / Hex	93.4	79.4	69.7	5.6	15.2	91.3	71.6	–28.4
PhH	87.4	82.5	59.2	3.9	20.4	86.4	60.0	–47.5
PhF	76.2	88.1	35.5	2.1	32.3	80.0	32.6	–61.5
PhMe	91.4	81.1	63.6	4.5	18.2	92.6	65.3	–34.4
PhMe / Hex	91.2	79.3	68.7	5.4	15.6	89.3	70.4	–39.3
t-BuOMe	90.8	82.8	61.5	4.2	19.2	89.3	62.9	–38.4
THF[a]	86.6	85.6	44.4	2.6	27.8	86.3	44.7	–41.5
THF[b]	84.7	83.6	42.9	2.5	28.6	84.4	43.1	–40.0
THF / Hex[a]	68.0	48.9	70.1	5.7	14.9	65.1	73.1	–56.2

0.01 M Concentration

Solvent	ee_A (%)	ee_B (%)	*de* (%)	dr (X : 1)	yield lost (%)	r (%)	r_α (%)	r_β (%)
Dioxane	57.4	62.3	45.9	2.7	27.0	58.7	44.7	–57.4
DME	82.9	84.4	41.2	2.4	29.4	83.3	40.8	–44.9
Et_2O	95.6	71.6	65.5	4.8	17.2	91.5	69.1	14.7
Et_2O / Hex	89.6	93.2	72.2	6.2	13.9	90.1	71.8	–80.9
PhH	91.9	80.1	54.5	3.4	22.7	89.2	56.7	–16.1
PhF	71.6	83.2	41.1	2.4	29.4	75.0	38.4	–60.5
PhMe	90.4	71.7	62.2	4.3	18.9	86.9	65.3	–18.7
PhMe / Hex	92.5	76.5	70.1	5.7	14.9	90.1	72.3	–29.1
t-BuOMe	91.1	85.3	59.2	3.9	20.4	89.9	60.2	–40.5
THF[a]	80.9	89.3	44.4	2.6	27.8	83.2	42.3	–64.5
THF[b]	86.8	84.2	47.4	2.8	26.3	86.1	47.9	–40.1
THF / Hex[a]	91.0	85.2	61.5	4.2	19.2	89.9	62.5	–43.7

[a] The THF employed in these reactions was dried by passing the solvent over a column of activated alumina with an argon overpressure. [b] The THF employed in these reactions was dried via distillation over benzophenone and sodium metal.

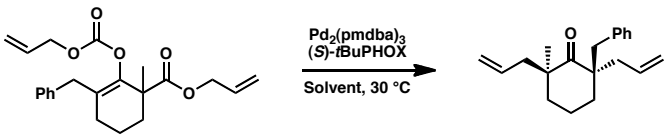

(±)-***290*** ***289***

0.03 M Concentration

Solvent	ee_A (%)	ee_B (%)	*de* (%)	dr (X : 1)	yield lost (%)	r (%)	r_α (%)	r_β (%)
Dioxane	66.2	76.1	23.1	1.6	38.5	67.5	19.1	–43.4
DME	93.4	86.1	31.0	1.9	34.5	90.9	32.8	5.1
Et_2O	89.5	63.7	45.9	2.7	27.0	82.5	51.5	12.3
Et_2O / Hex	92.4	58.9	50.0	3.0	25.0	84.0	56.8	28.6
PhH	92.5	81.7	48.7	2.9	25.6	89.7	50.9	–7.8
PhF	87.9	86.2	20.0	1.5	40.0	87.2	20.4	–13.6
PhMe	94.3	87.0	52.4	3.2	23.8	92.6	53.8	–16.8
PhMe / Hex	92.1	90.4	54.5	3.4	22.7	91.7	54.9	–47.3
t-BuOMe	91.6	79.9	44.4	2.6	27.8	88.4	46.9	–4.1
THF[a]	90.6	93.2	37.5	2.2	31.3	91.4	36.9	–50.5
THF[b]	88.8	88.4	37.5	2.2	31.3	88.7	37.6	–36.0
THF / Hex[a]	93.9	83.0	50.0	3.0	25.0	91.2	52.1	–3.7

0.01 M Concentration

Solvent	ee_A (%)	ee_B (%)	*de* (%)	dr (X : 1)	yield lost (%)	r (%)	r_α (%)	r_β (%)
Dioxane	64.4	74.7	23.1	1.6	38.5	68.4	20.2	–38.5
DME	95.1	77.1	28.6	1.8	35.7	88.7	33.0	44.4
Et_2O[c]	-	-	-	-	-	-	-	-
Et_2O / Hex	93.2	80.5	53.4	3.3	23.3	90.2	55.9	–7.0
PhH	93.4	88.9	55.5	3.5	22.2	92.4	56.4	–35.1
PhF	82.4	88.3	20.0	1.5	40.0	84.8	18.5	–38.6
PhMe	94.5	82.8	56.5	3.6	21.7	92.0	58.6	–7.0
PhMe / Hex	95.1	87.1	59.2	3.9	20.4	93.5	60.5	–19.4
t-BuOMe	95.1	90.3	47.4	2.8	26.3	93.8	48.3	–17.2
THF[a]	92.4	90.8	33.3	2.0	33.3	91.9	33.7	–24.6
THF[b]	95.7	90.5	33.3	2.0	33.3	94.0	34.5	5.0
THF / Hex[a]	95.7	81.0	45.9	2.7	27.0	91.5	49.2	26.3

[a] The THF employed in these reactions was dried by passing the solvent over a column of activated alumina with an argon overpressure. [b] The THF employed in these reactions was dried via distillation over benzophenone and sodium metal. [c] This reaction failed to afford measurable quantities of product.

3.6 NOTES AND REFERENCES

(1) Enquist, J. A., Jr.; Stoltz, B. M. *Nature* **2008**, *453*, 1228–1231.

(2) See chapter 2 for a thorough explaination of our synthetic endeavors toward the cyanthiwigin natural products.

(3) Mohr, J. T.; Behenna, D. C.; Harned, A. M.; Stoltz, B. M. *Angew. Chem., Int. Ed.* **2005**, *44*, 6924–6927.

(4) The value of ee_B is defined as the enantiomeric excess of the minor diastereomer of a double asymmetric transformation. If the minor diastereomer of such a reaction is *meso* in nature, this value is equal to zero under all conditions.

(5) (a) Langenbeck, W.; Triem, G. *Z. Phys. Chem. A* **1936**, *117*, 401–409. (b) Heller, D.; Drexler, H.-J.; Fischer, C.; Buschmann, H.; Baumann, W.; Heller, B. *Angew. Chem., Int. Ed.* **2000**, *39*, 495–499.

(6) Vigneron, J. P.; Dhaenens, M.; Horeau, A. *Tetrahedron Lett.* **1973**, *29*, 1055–1059.

(7) The intial yield, as well as the method of saponification of the carbonate species, was not specified.

(8) The value of diastereomeric exccess (*de*) is employed in place of dr for these graphical representations to achieve a scale comparable to *ee*. While calculated

values for dr range between zero and infinity, *de* varies only between zero and unity for the situations we consider. The value of *de* is calculated similarly to *ee*, and can be represented as the difference between the quantities of major and minor diastereomer produce, divided by the total material affored by the reaction:

$$de = \frac{[\text{Quantity of major diastereomer} - \text{quantity of minor diastereomer}]}{[\text{Quantity of major diastereomer} + \text{quantity of minor diastereomer}]}$$

(9) (a) Mori, K.; Tanida, K. *Tetrahedron* **1981**, *37*, 3221–3225. (b) Mori, K.; Watanabe, H. *Tetrahedron* **1986**, *42*, 295–304.

(10) Isaksson, R.; Liljefors, T.; Reinholdsson, P. *J. Chem. Soc., Chem. Commun.* **1984**, *3*, 137–138.

(11) Han, X.; Corey, E. J. *Org. Lett.* **1999**, *1*, 1871–1872.

(12) (a) Brown, H. C.; Singaram, B. *J. Org. Chem.* **1984**, *49*, 945–947. (b) Mathre, D. J.; Thompson, A. S.; Douglas, A. W.; Hoogsteen, J.; Carroll, J. D.; Corley, E. G.; Grabowki, E. J. *J. Org. Chem.* **1993**, *58*, 2880–2888. (c) Schwink, L.; Knochel, P. *Chem. Eur. J.* **1998**, *4*, 950–968.

(13) (a) Jadhav, P. K.; Prasad, J. V. N. V.; Brown, H. C. *J. Org. Chem.* **1985**, *50*, 3203–3206. (b) Toda, F.; Tanaka, K. *Chem. Lett.* **1986**, 1905–1908. (c) Brown, H. C.; Joshi, N. N. *J. Org. Chem.* **1988**, *53*, 4059–4062. (d) Venkatraman, L.; Periasamy, M. *Tetrahedron: Asymm.* **1996**, *7*, 2471–2474. (e) Periasamy, M; Venkatraman, L.; Thomas, K. R. J. *J. Org. Chem.* **1997**, *62*, 4302–4306.

(14) (a) Reuben, J. *J. Am. Chem. Soc.* **1980**, *102*, 2232–2237. (b) Feringa, B. L.; Smaardijk, A.; Wynberg, H. *J. Am. Chem. Soc.* **1985**, *107*, 4798–4799. (c) Pasquier, M.; Marty, W. *Angew. Chem., Int. Ed. Engl.* **1985**, *24*, 315–316. (d) Feringa, B. L.; Strijtveen, B.; Kellogg, R. M. *J. Org. Chem.* **1986**, *51*, 5485–5489. (e) Feringa, B. L. *J. Chem. Soc., Chem. Commun.* **1987**, 695–696. (f) Ouryupin, A. B.; Kadyko, M. I.; Petrovskii, P. V.; Fedin, E. I. *Chirality* **1994**, *6*, 1–4. (g) Platzer, N.; Rudler, H.; Alvarez, C.; Barkaoui, L.; Denise, B.; Goasdoué, N.; Rager, M.-N.; Vaissermann, J.; Daran, J.-C. *Bull. Soc. Chim. Fr.* **1995**, *132*, 95–113. (h) Hulst, R.; Kellogg, R. M.; Feringa, B. L. *Recl. Trav. Chim. Pay-B.* **1995**, *114*, 115–138. (i) Grotjahn, D. B.; Joubran, C. *Tetrahedron: Asymm.* **1995**, *6*, 745–752. (j) Cawley, A.; Duxbury, J. P.; Kee, T. P. *Tetrahedron: Asymm.* **1998**, *9*, 1947–1949. (k) Laverde, A., Jr.; Miranda, D. S.; Conceição, G. J. A.; Schirmer, H.; Pilli, R. A.; Meijere, A.; Marsaioli, A. J. *J. Brazil Chem. Soc.* **1999**, *10*, 293–298.

(15) Lagasse, F.; Tsukamoto, M.; Welch, C. J.; Kagan, H. B. *J. Am. Chem. Soc.* **2003**, *125*, 7490–7491.

(16) The following publication is the source of all mathmatical expressions in this section, with the exception of equations (11), (12), and (13): Baba, S. E.; Sartor, K.; Poulin, J.-C.; Kagan, H. *Bull. Soc. Chim. Fr.* **1994**, *131*, 525–533.

(17) In the following section, the configuration of each stereocenter for the isomers presented is represented in the format [1*P*, 2*P*], [1*S*, 2*S*], [1*R*, 2*R*], etc., for all possible combinations. The leading number (1 or 2) denotes the position of the

stereocenter as corresponding to either olefin (1) or (2) as shown in Scheme 3.10. The trailing letter corresponds to the configuration of that stereocenter as either *R* or *S*. Those centers referred to as *P* are prochiral, and have yet to undergo transformation.

(18) In the examples provided, the enantioselective catalyst employed is arbitrarily assumed to favor generation of the *R* enantiomer at each reactive center.

(19) The graphical representations depicted in Figure 3.2 utilize an expression for dr which has been converted to *de* in order to keep the scale of the curves consistant.

(20) For an alternative mathematical treatment of this system that reaches the same conclusion, see: Soai, K.; Hori, H.; Kawahara, M. *J. Chem. Soc., Chem. Commun.* **1992**, 106–108.

(21) The relationship between the enantiomeric excess of the minor diastereomer (ee_B) and either selectivity term can also be plotted. In this case, the value of ee_B varies between 1 and –1, indicating that the minor diastereomer can yield either sense of enantiomeric product depending upon the dominance of either the r_1 or r_2 term. Interestingly, the magnitude of the r terms alone does not dictate the final value of ee_B. Instead, the determining factor is the overall difference between the values of r_1 and r_2. Under all conditions where both r_1 and r_2 are equal, ee_B will be zero. If r_1 and r_2 are very close in value, ee_B will be very small. Only in situations where a large disparity exists between r_1 and r_2 will ee_B display a correspondingly large

value. In contrast to the behavior of ee_A, under no circumstances will ee_B ever exceed the value of either r_1 or r_2.

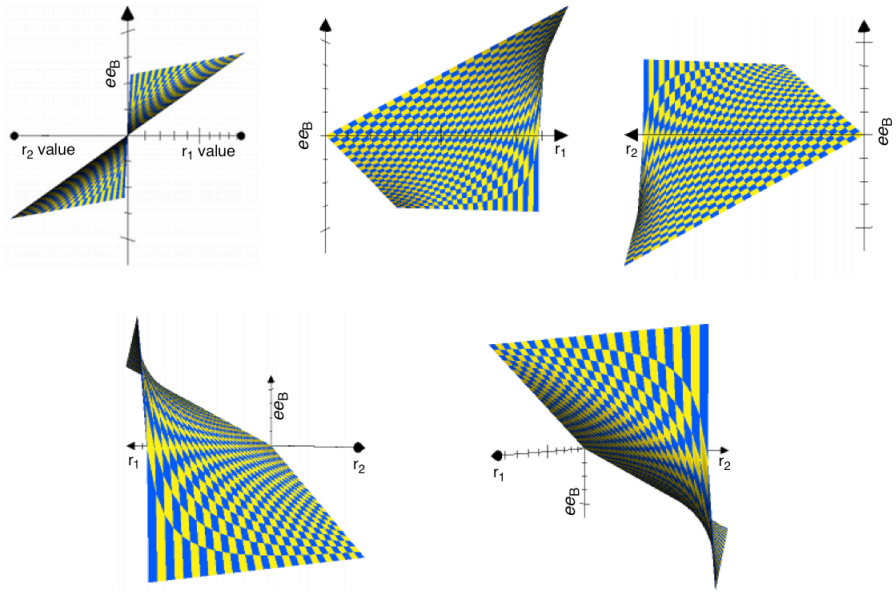

(22) Taylor, M. S.; Jacobsen, E. N. *Pro. Natl. Acad. Sci. U.S.A.* **2004**, *101*, 5368–5373.

(23) Examples of multiple stereoselective catalysis in which five or more stereocenters are set simultaneously have been reported. Though the general trends in enantioselectivity and diastereoselectivity are the same as observed in double asymmetric transformations, the mathematically complex nature of these reactions precludes a rigorous treatment here.

(24) For examples of multiple asymmetric processes that are not related to total synthetic efforts, see: (a) Hoye, T. R.; Suhadolnik, J. C. *Tetrahedron* **1986**, *42*, 2855–2862. (b) Crispino, G. A.; Sharpless, K. B. *Tetrahedron Letters* **1992**, *33*,

4273–4274. (c) Crispino, G. A.; Ho, P. T.; Sharpless, K. B. *Science* **1993**, *259*, 64–65.

(25) Lebsack, A. D.; Link, J. T.; Overman, L. E.; Steams, B. A. *J. Am. Chem. Soc.* **2002**, *124*, 9008–9009.

(26) Xiong, Z.; Corey, E. J. *J. Am. Chem. Soc.* **2000**, *122*, 9328–9329.

(27) Wang, Z.-X.; Tu, Y.; Frohn, M.; Zhang, J.-R.; Shi, Y. *J. Am. Chem. Soc.* **1997**, *119*, 11224–11235.

(28) Xiong, Z.; Busch, R.; Corey, E. J. *Org. Lett.* **2010,** *12*, 1512–1514.

(29) The alkylation of either substrate **189** or **233** is unlikely to involve a discrete ketone enolate. In spite of this, intermediates **277–280** are depicted in this manner in order to provide a schematic representation of the reaction course.

(30) This experiment was run with a 1 : 1 mixture of diastereomers of **287** as the starting material, and was also repeated twice more with either pure diastereomer of **287**. In all three reactions, the results obtained showed a dr in excess of 50 : 1 regardless of the starting diastereomer employed.

(31) In this case, the negative value obtained for the r term is assigned via relative comparison to the diastereomers observed in the (*S*)-*t*-BuPHOX case.

(32) To see the results of all 48 experiments in this screen, please see the experimental section of this chapter.

(33) (a) Helmchen, G.; Pfaltz, A. *Acc. Chem. Res.* **2000**, *33*, 336–345. (b) Tani, K.; Behenna, D. C.; McFadden, R. M.; Stoltz, B. M. *Org. Lett.* **2007**, *9*, 2529–2531.

(34) Peer, M.; de Jong, J. C.; Kiefer, M.; Langer, T.; Rieck, H.; Schell, H.; Sennhenn, P.; Sprinz, J.; Steinhagen, H.; Wiese, B.; Helmchen, G. *Tetrahedron* **1996**, *52*, 7547–7583.

APPENDIX 4

Spectra Relevant to Chapter 3

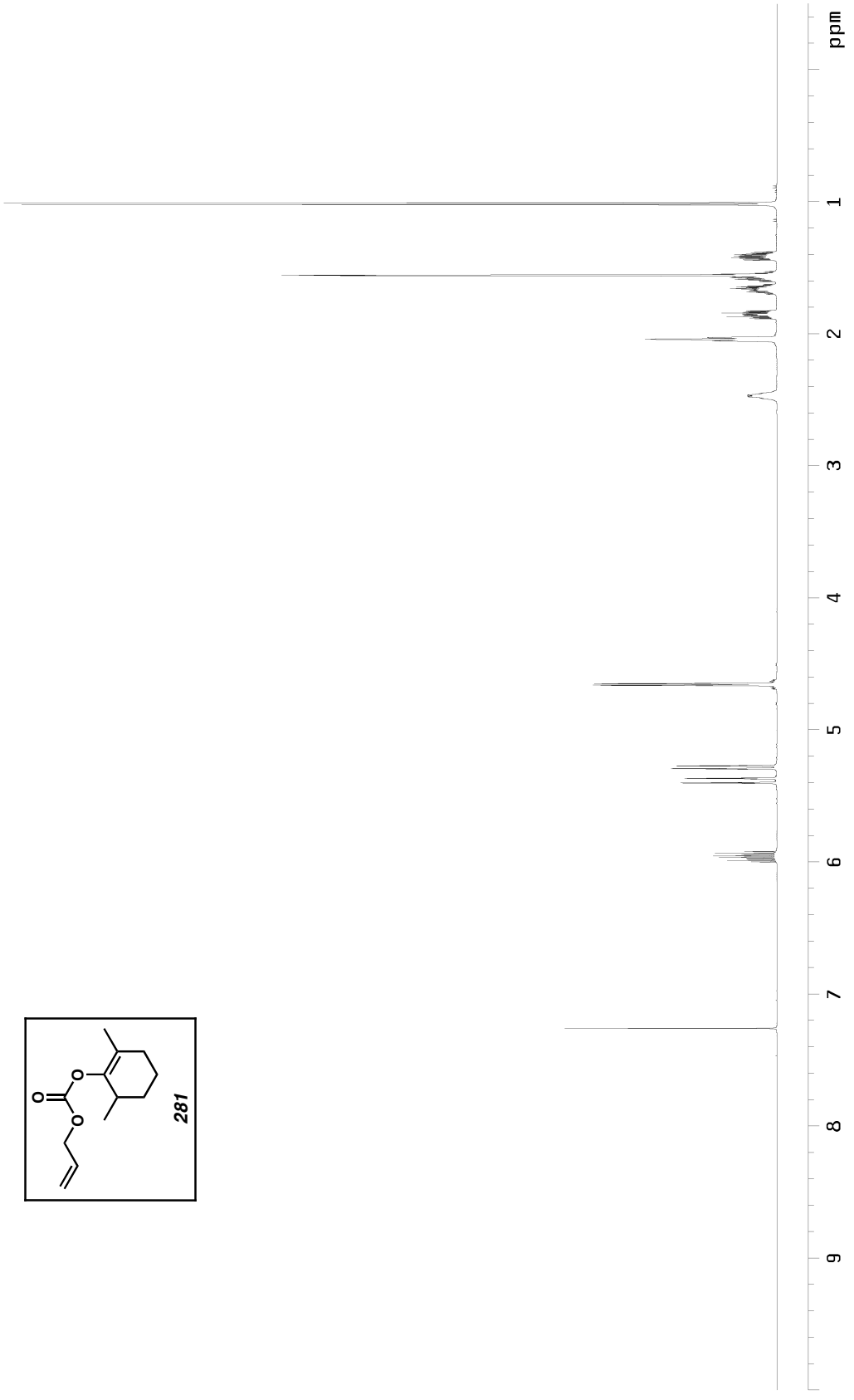

Figure A4.1 ^{1}H NMR (500 MHz, $CDCl_3$) of carbonate **281**.

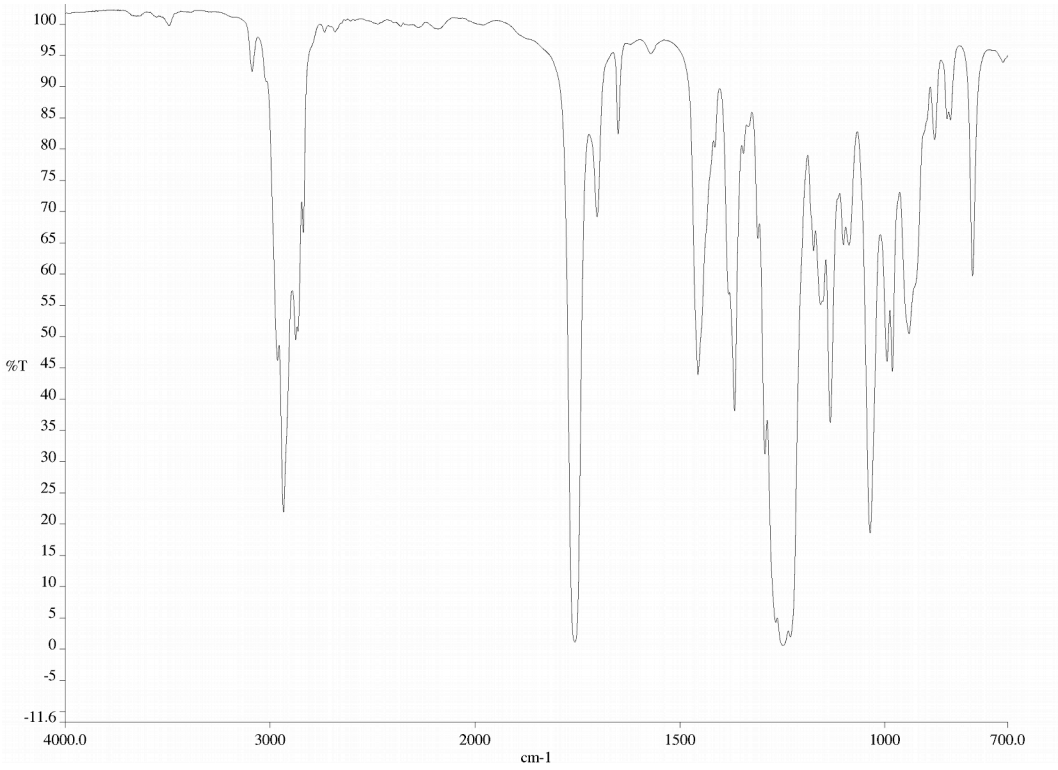

Figure A4.2 Infrared spectrum (thin film/NaCl) of carbonate **281**.

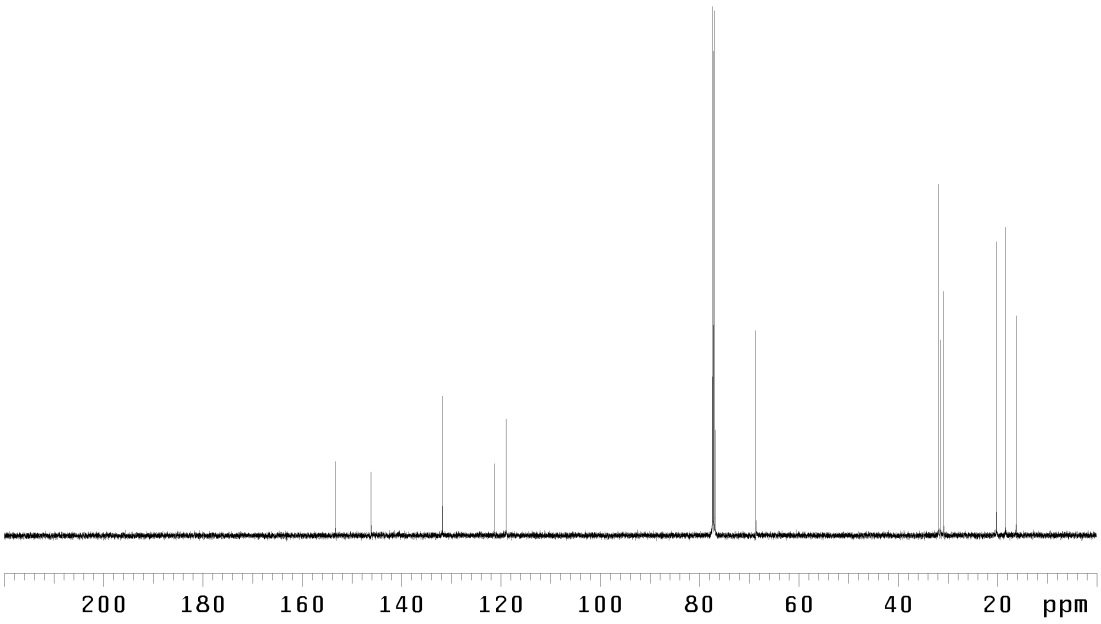

Figure A4.3 ^{13}C NMR (125 MHz, $CDCl_3$) of carbonate **281**.

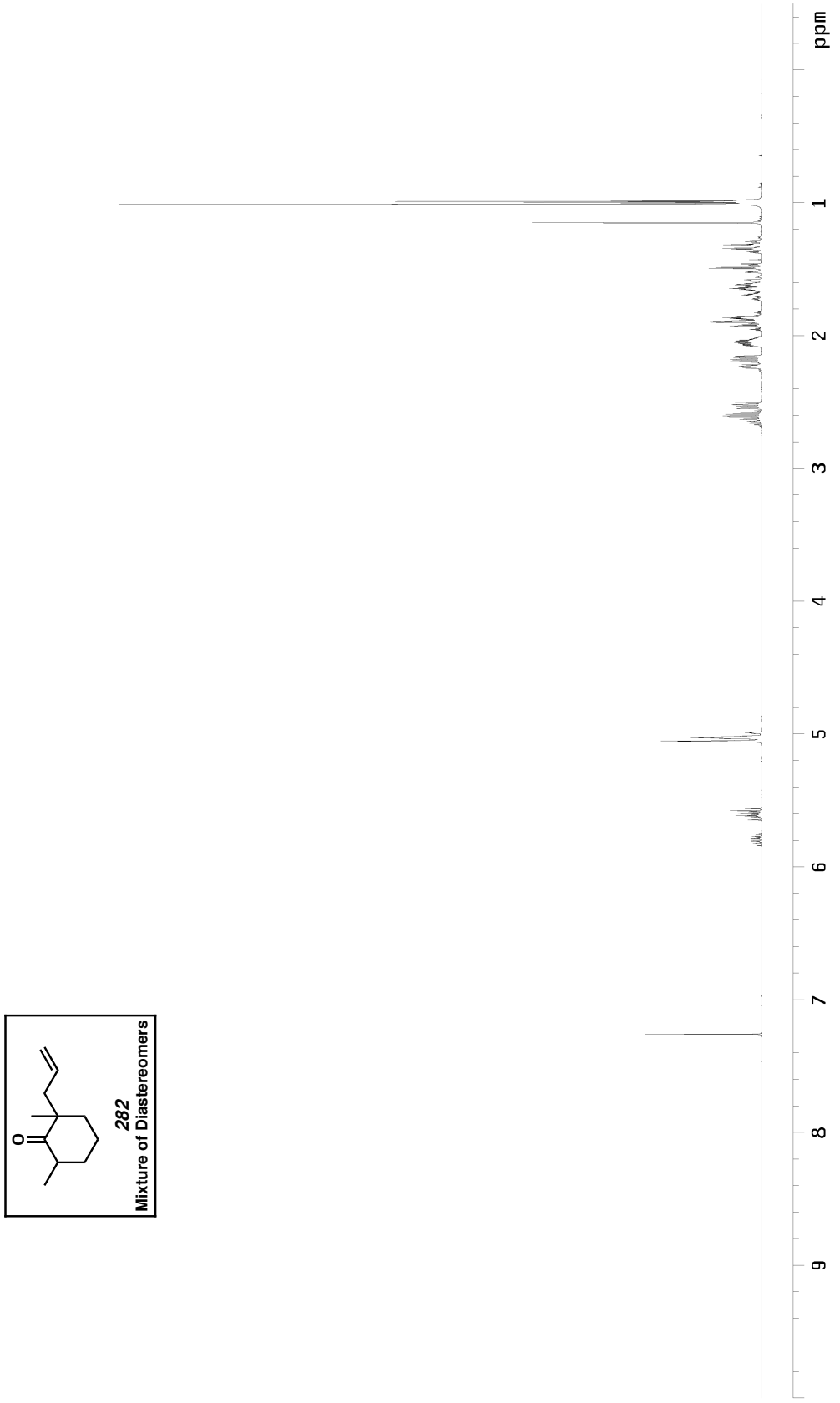

Figure A4.4 ^{1}H NMR (500 MHz, $CDCl_3$) of allyl ketone **282**.

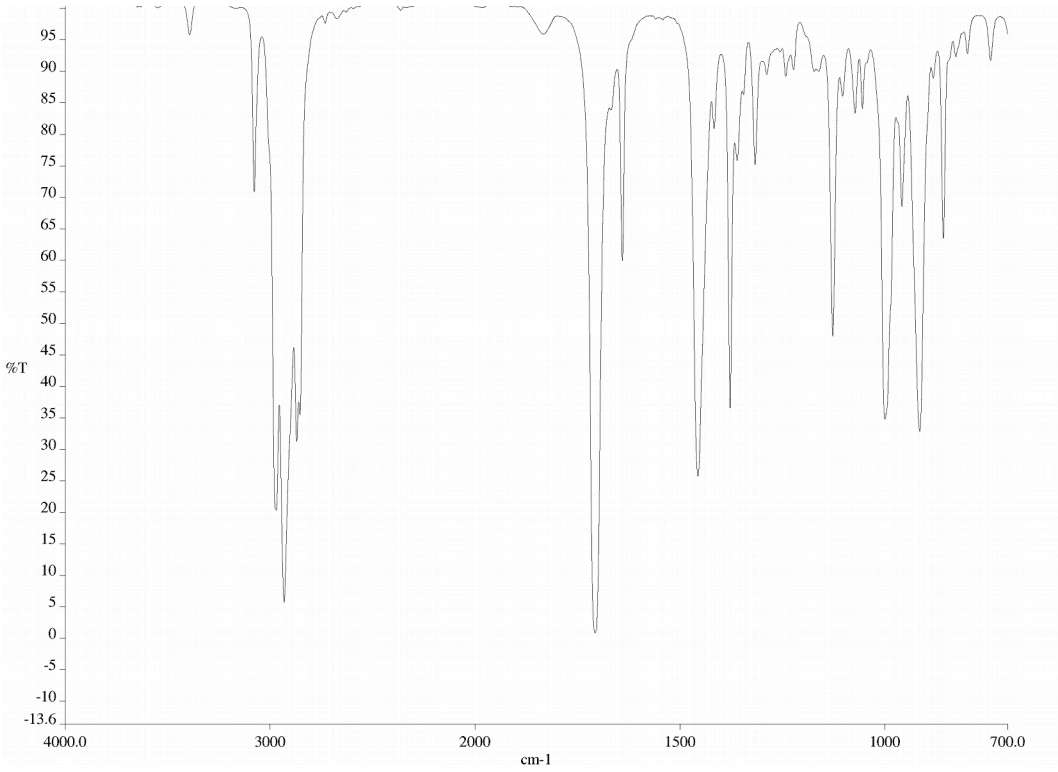

Figure A4.5 Infrared spectrum (thin film/NaCl) of allyl ketone **282**.

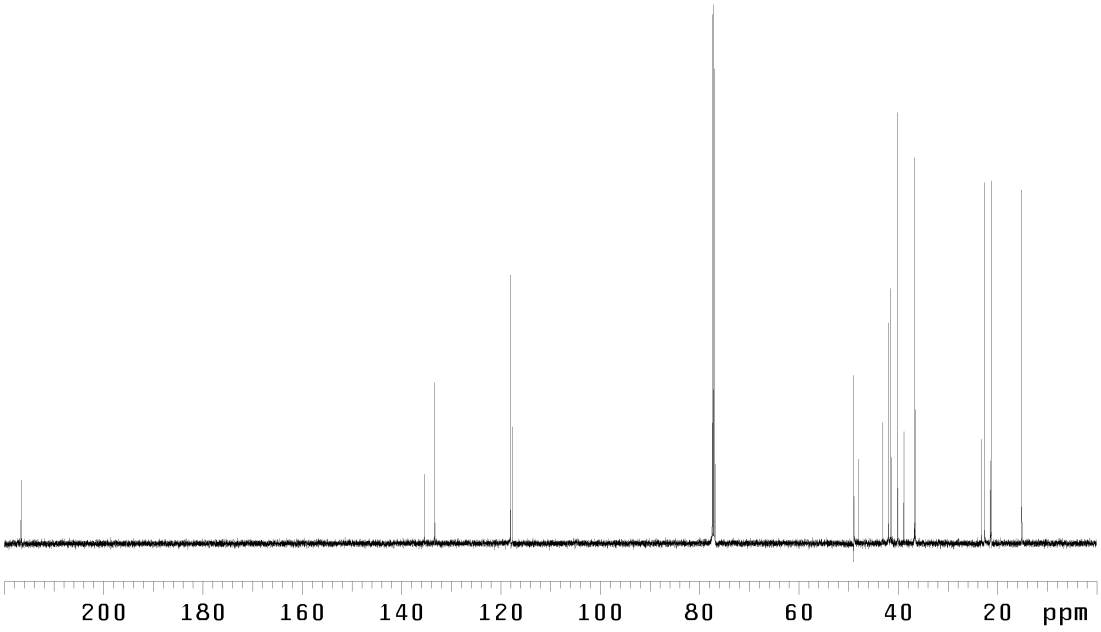

Figure A4.6 ^{13}C NMR (125 MHz, $CDCl_3$) of allyl ketone **282**.

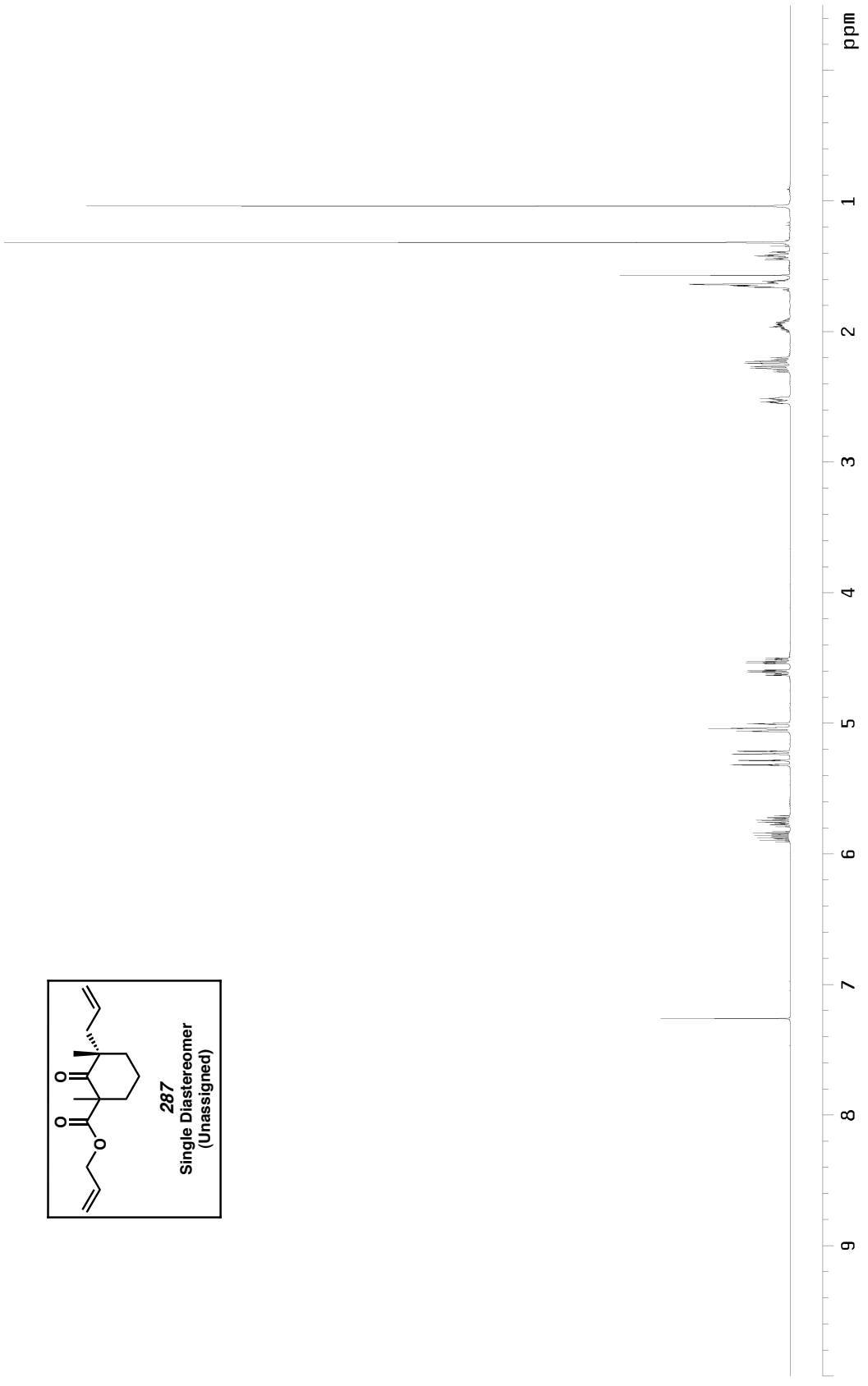

Figure A4.7 ^{1}H NMR (500 MHz, $CDCl_3$) of β-ketoester **287(A)**.

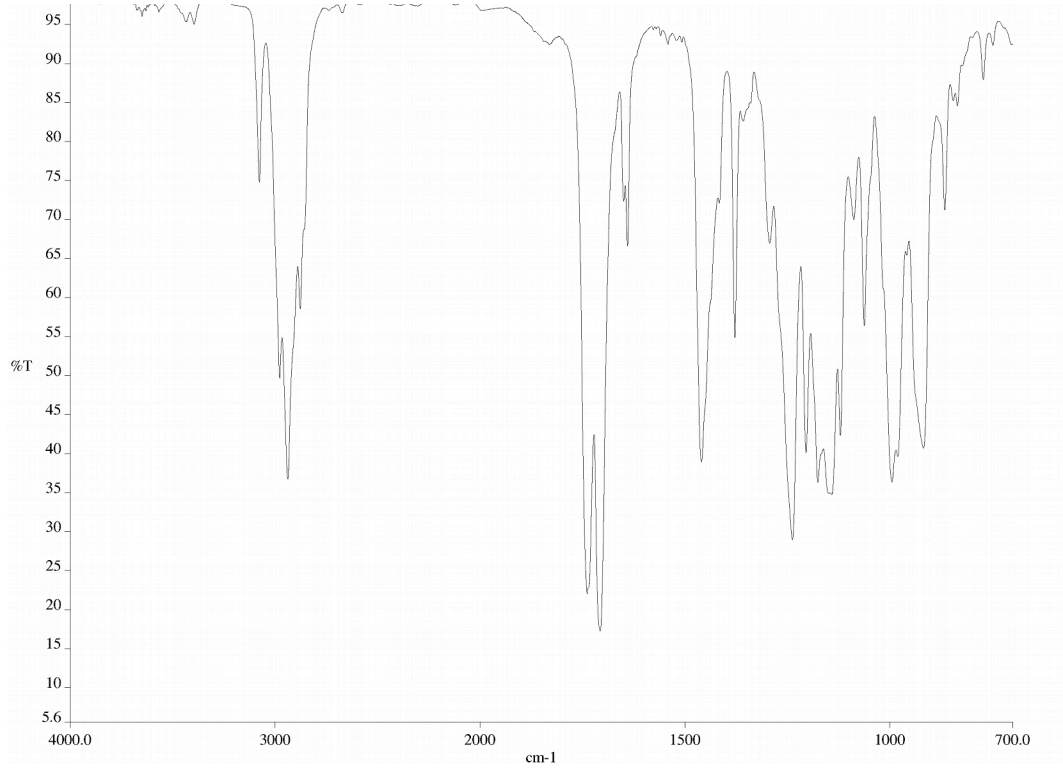

Figure A4.8 Infrared spectrum (thin film/NaCl) of β-ketoester **287(A)**.

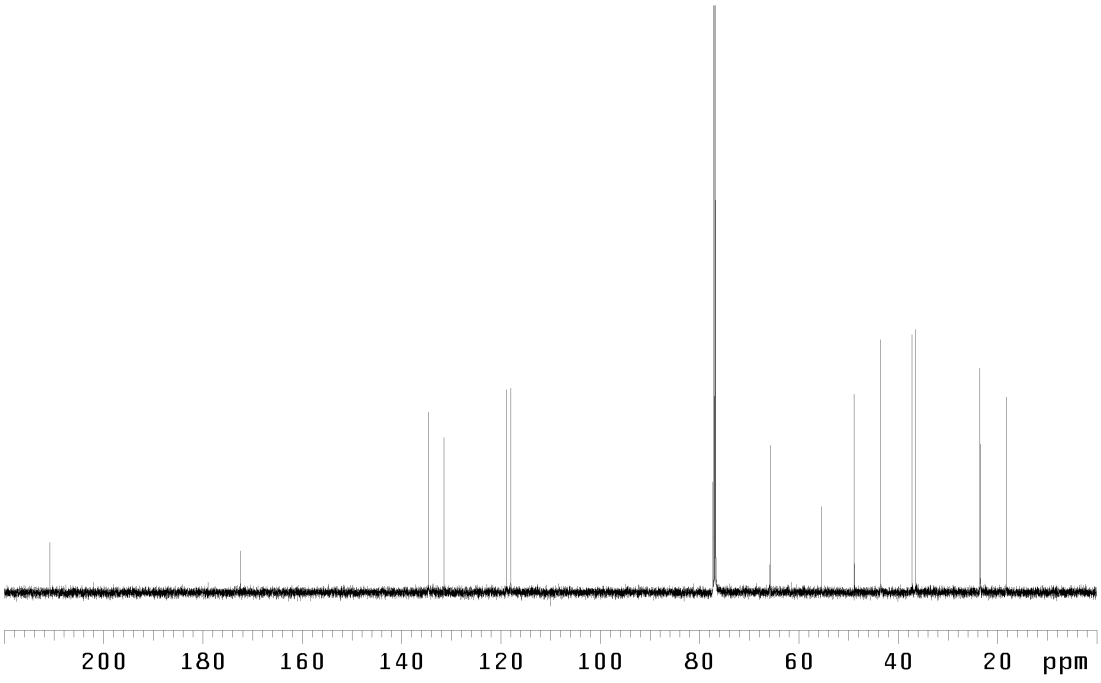

Figure A4.9 ^{13}C NMR (125 MHz, $CDCl_3$) of β-ketoester **287(A)**.

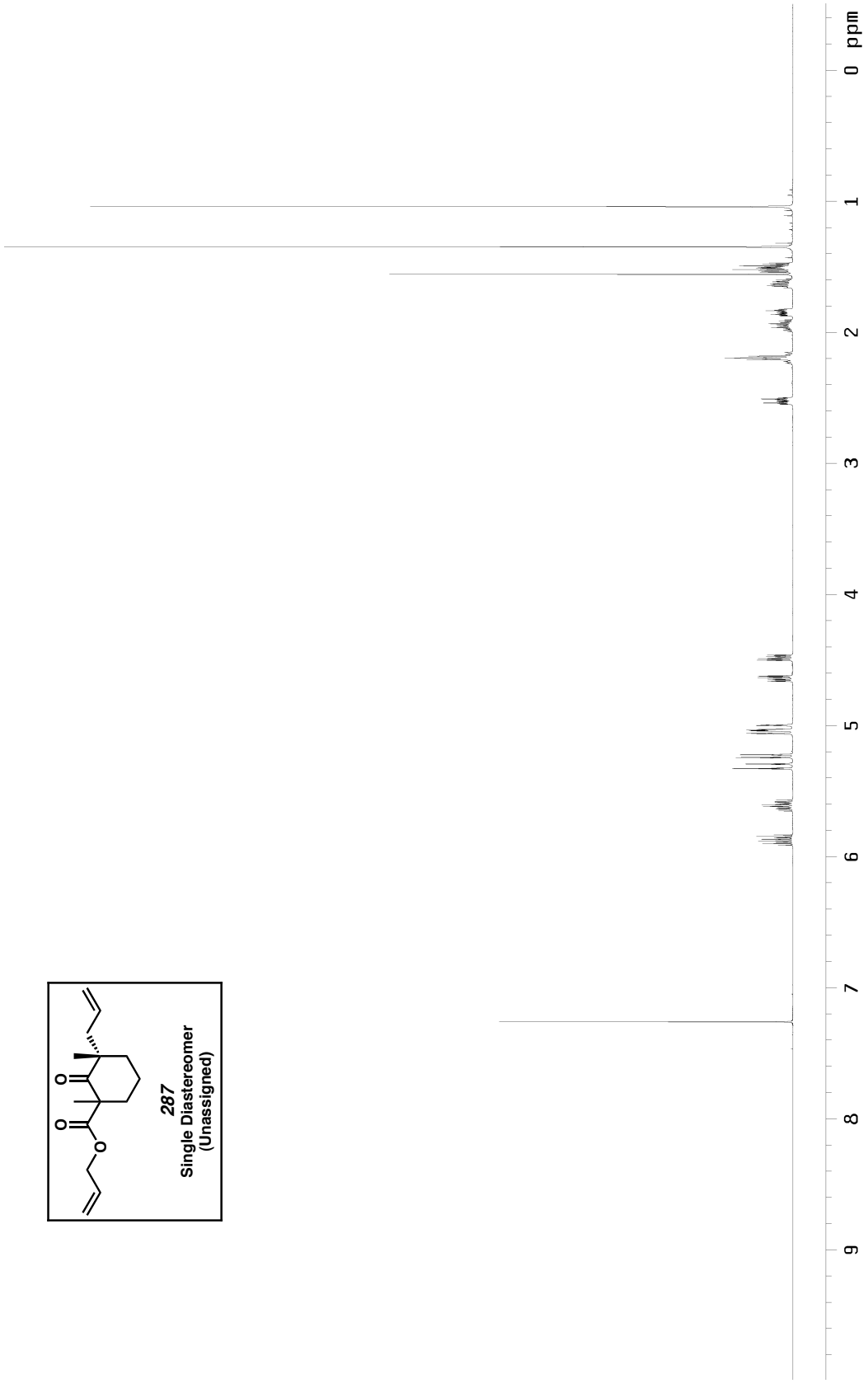

Figure A4.10 ^{1}H NMR (500 MHz, $CDCl_3$) of β-ketoester **287(B)**.

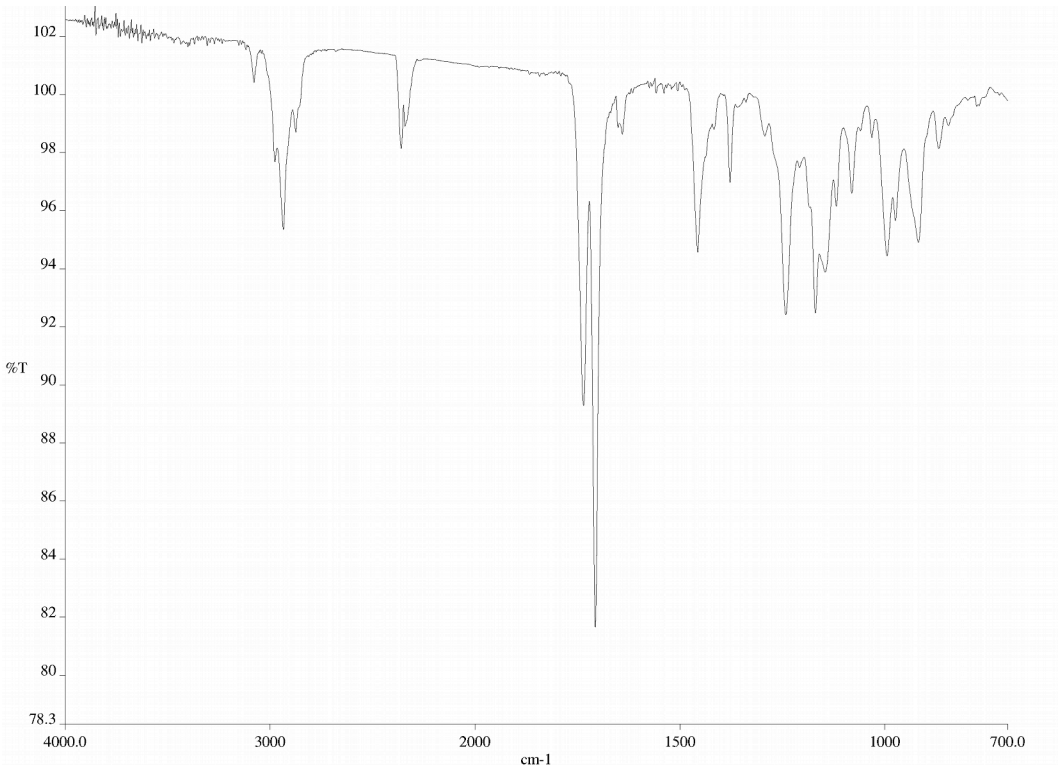

Figure A4.11 Infrared spectrum (thin film/NaCl) of β-ketoester **287(B)**.

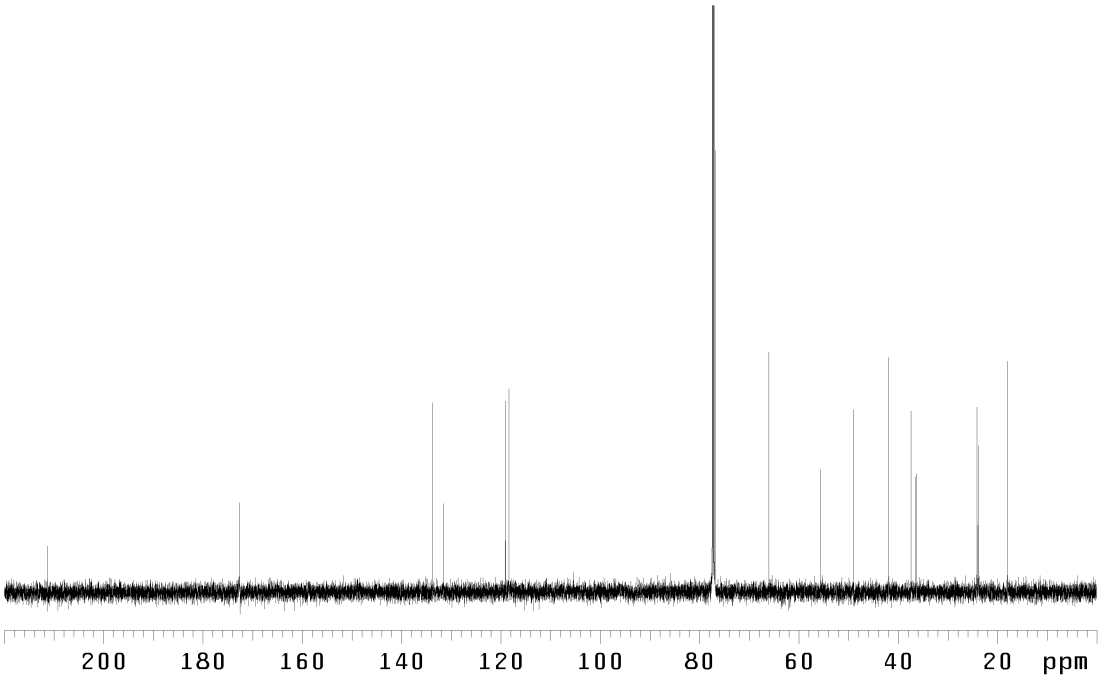

Figure A4.12 ^{13}C NMR (125 MHz, $CDCl_3$) of β-ketoester **287(B)**.

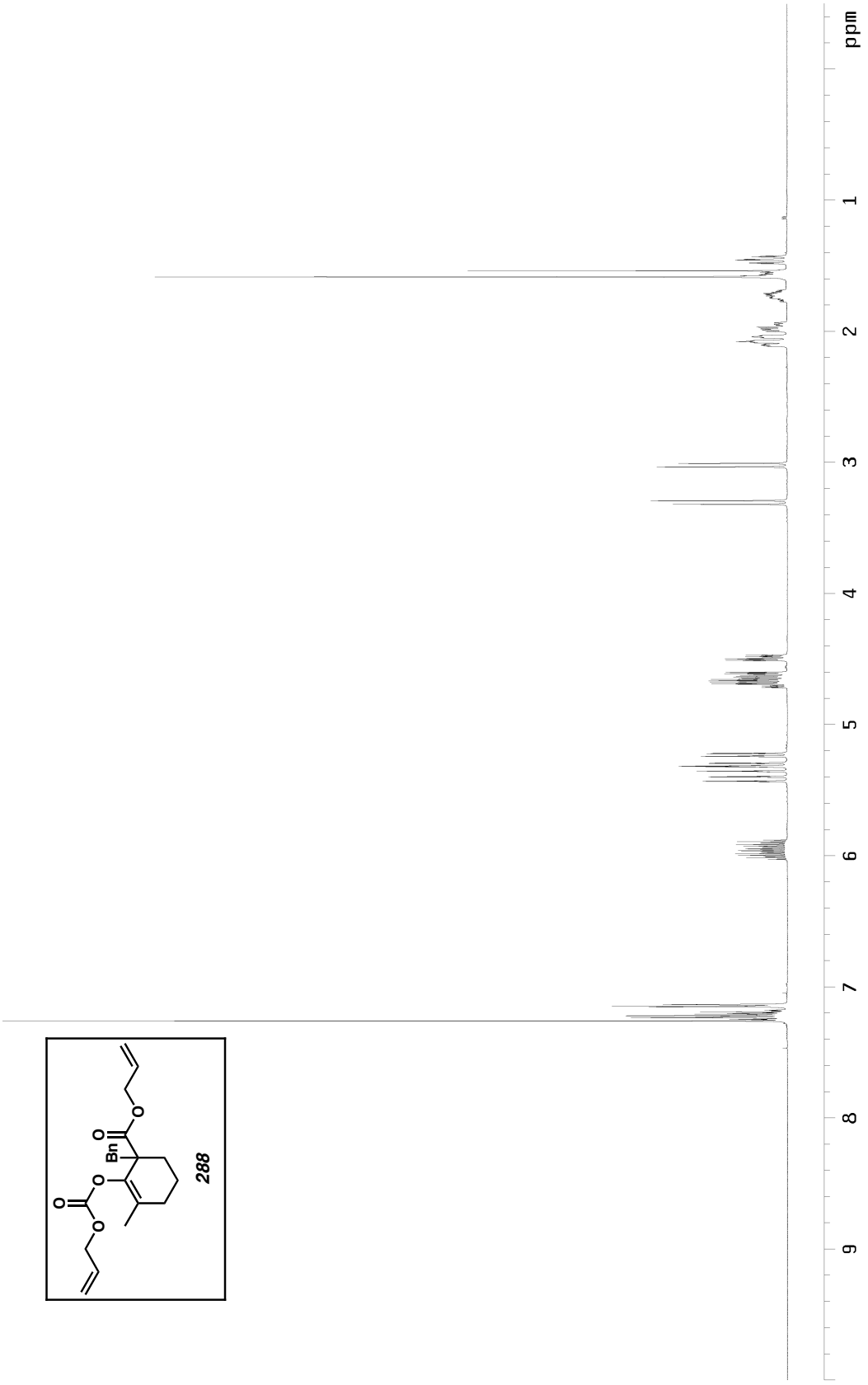

Figure A4.13 ^{1}H NMR (500 MHz, $CDCl_3$) of carbonate ester **288**.

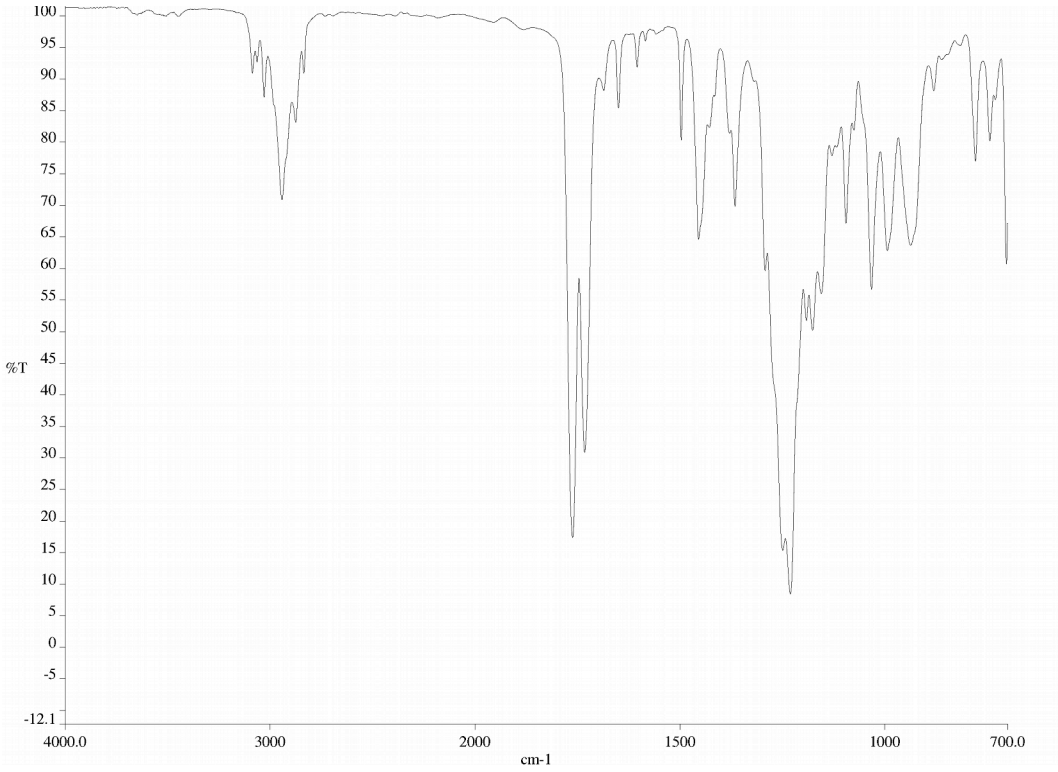

Figure A4.14 Infrared spectrum (thin film/NaCl) of carbonate ester **288**.

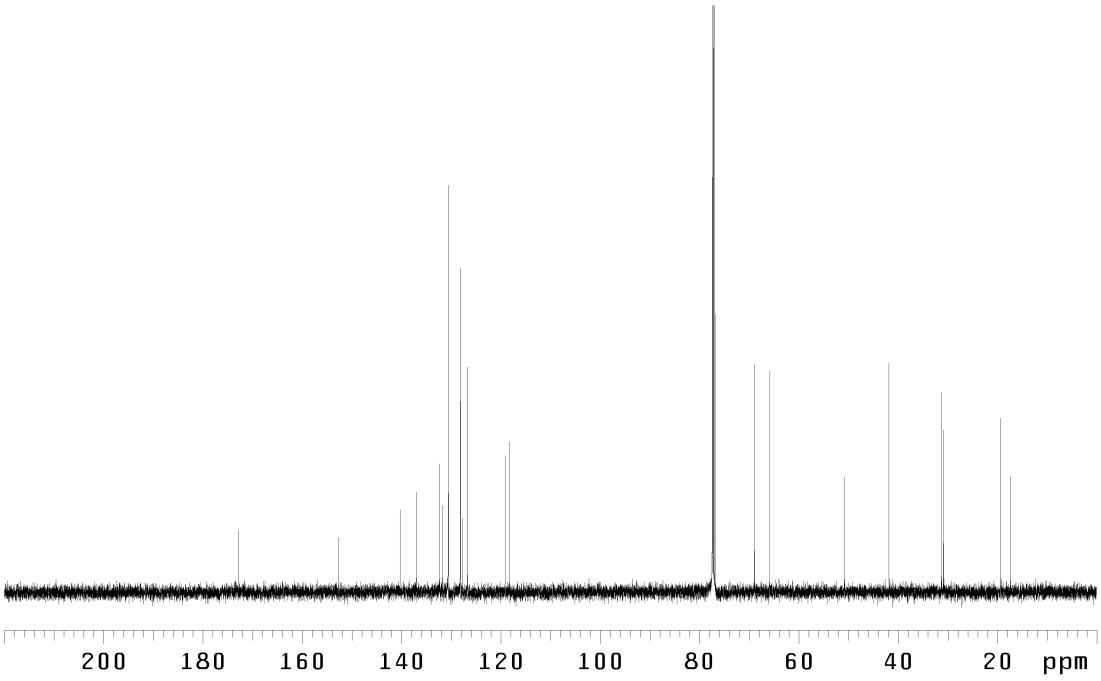

Figure A4.15 ^{13}C NMR (125 MHz, $CDCl_3$) of carbonate ester **288**.

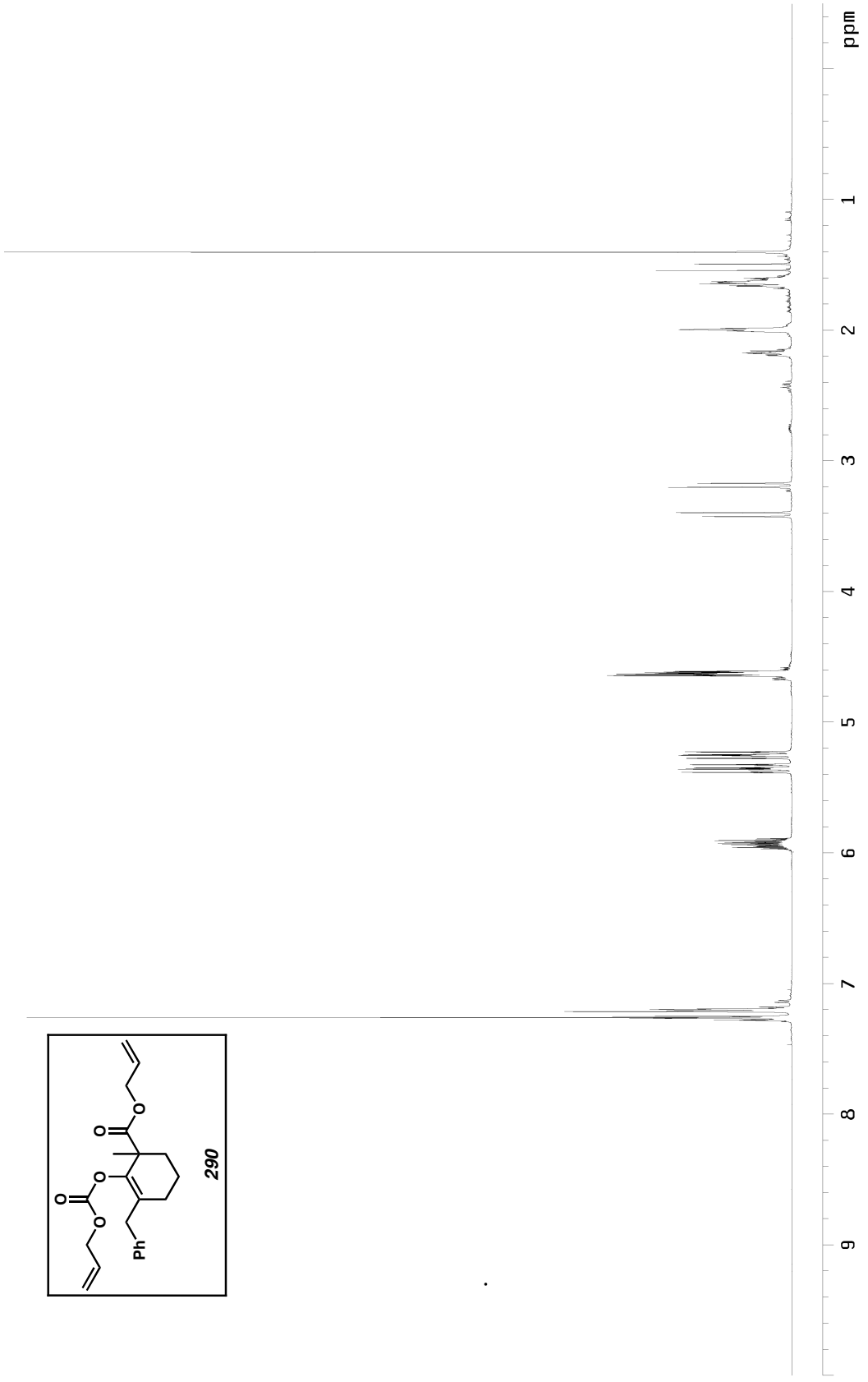

Figure A4.16 ^{1}H NMR (500 MHz, $CDCl_3$) of carbonate ester **290**.

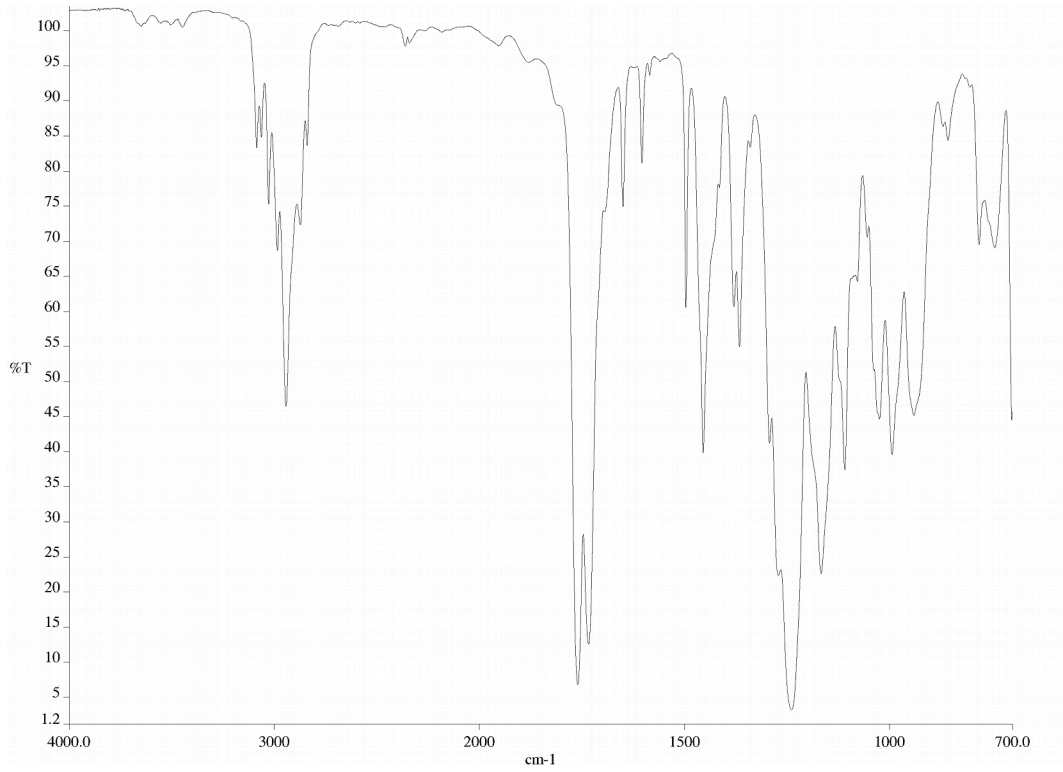

Figure A4.17 Infrared spectrum (thin film/NaCl) of carbonate ester **290**.

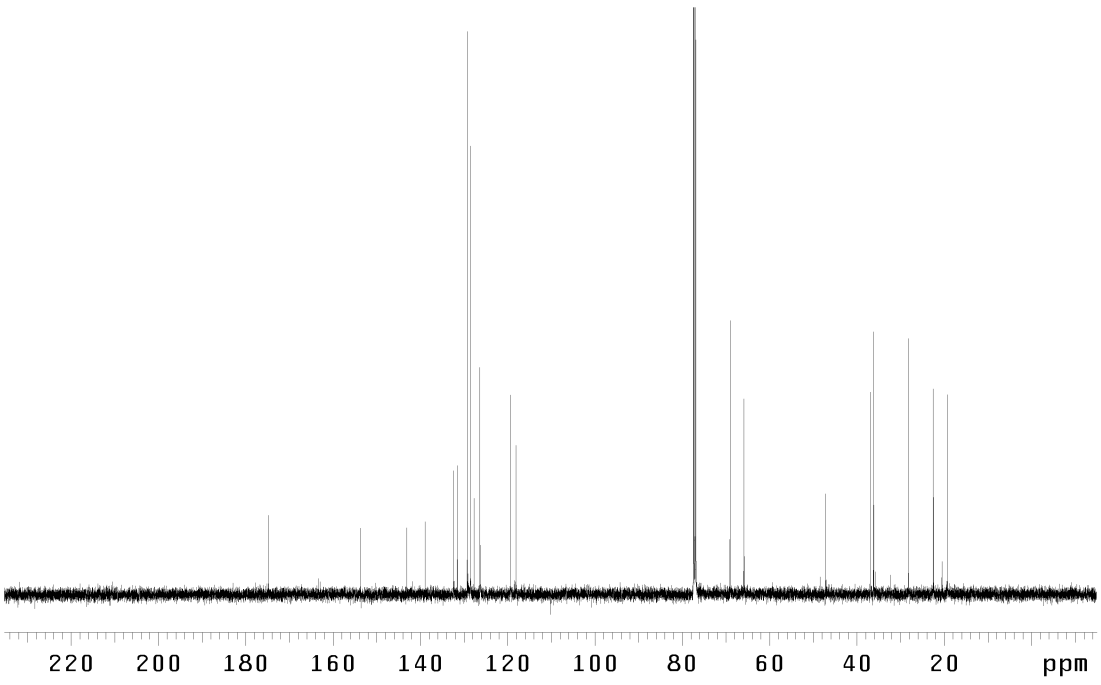

Figure A4.18 ^{13}C NMR (125 MHz, $CDCl_3$) of carbonate ester **290**.

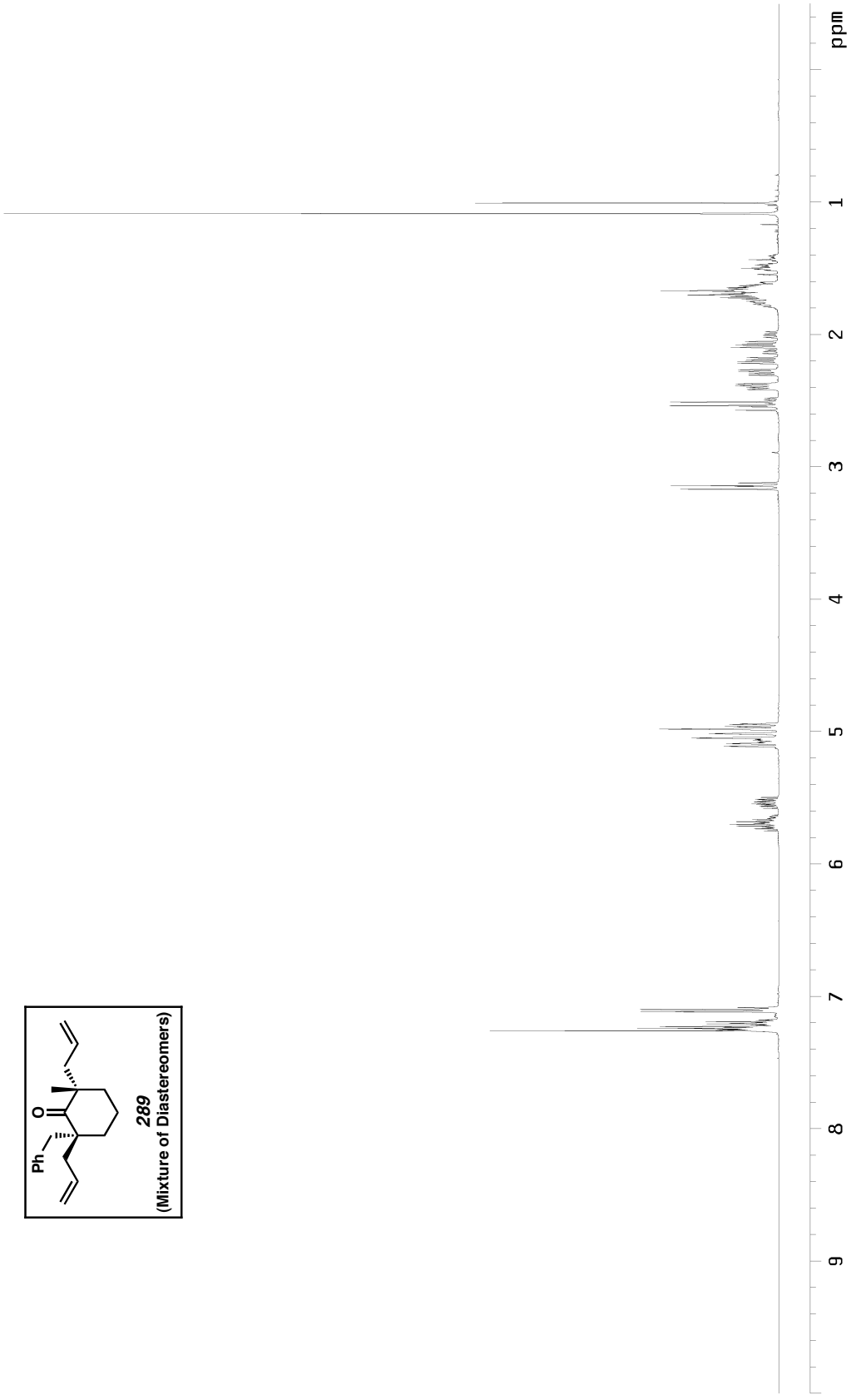

Figure A4.19 ^{1}H NMR (500 MHz, $CDCl_3$) of diallyl cyclohexanone **289**.

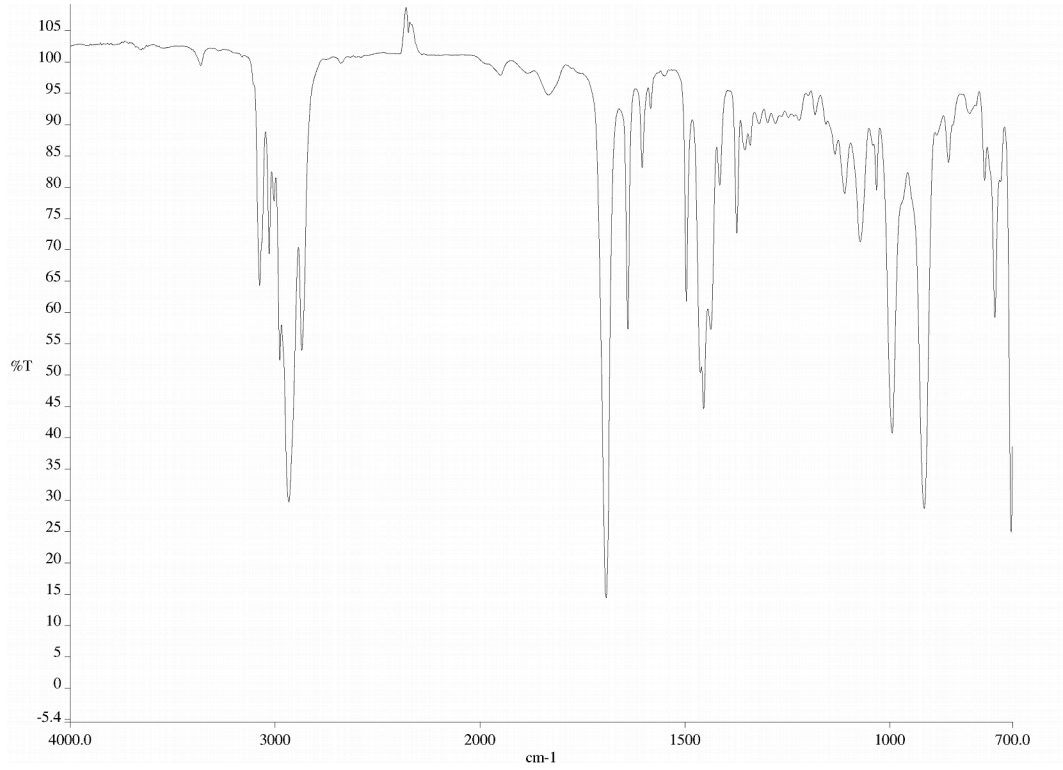

Figure A4.20 Infrared spectrum (thin film/NaCl) of diallyl cyclohexanone **289**.

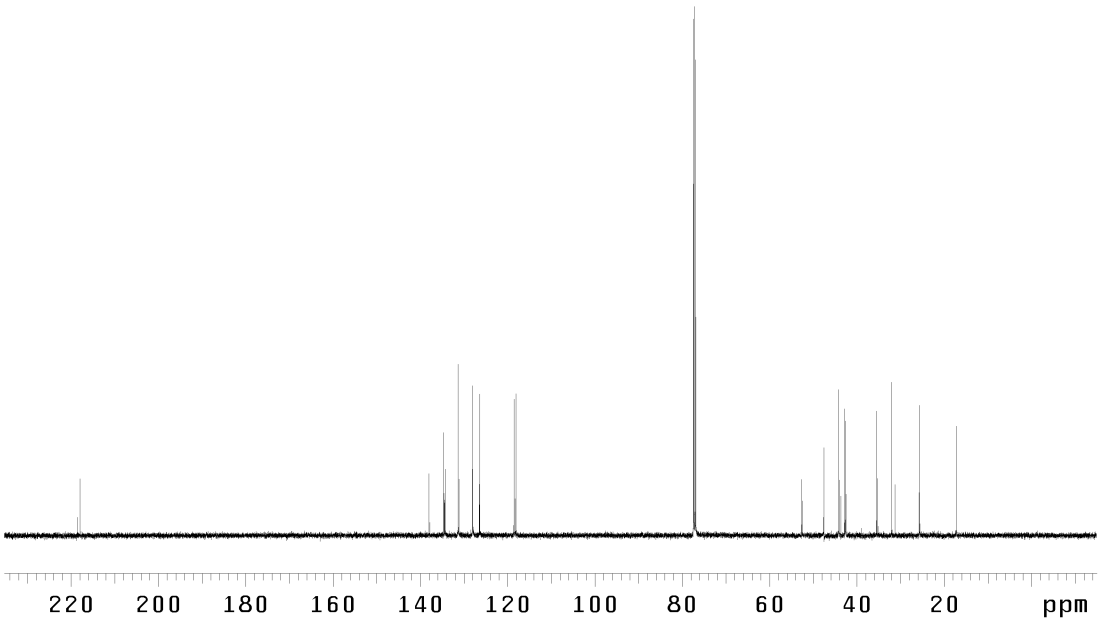

Figure A4.21 ^{13}C NMR (125 MHz, $CDCl_3$) of diallyl cyclohexanone **289**.

APPENDIX 5

Notebook Cross-Reference

NOTEBOOK CROSS-REFERENCE FOR NEW COMPOUNDS

The following cross-reference provides the file name for each piece of original spectroscopic data obtained for the compounds presented in this thesis. For each compound, both hard copy and electronic characterization folders containing the original ^{1}H NMR, ^{13}C NMR, and IR spectra have been created. All notebooks and spectroscopic data are stored in the Stoltz research group archive.

Table A5.1 Compounds in Chapter 2 – Enantioselective Total Synthesis of Cyanthiwigin Diterpenoids

Compound	^{1}H NMR	^{13}C NMR	IR
187	JAEVIII-157A	JAEVIII-157A-13C	JAEVIII-157A
189	JAEVIII-161B	JAEVIII-161B-13C	JAEVIII-161B
186	JAEVIII-183B	JAEVIII-183B-13C	JAEVIII-183B
185	JAEVII-301X	JAEVII-301X-13C	JAEVII-301X
194	JAEVIII-211C	JAEXIV-195X-13C	JAEVIII-211C
195	JAE-Enoate-X-1H	JAE-Enoate-X-13C	JAE Enoate B
196	JAE-XIV-Carb-Heck-B-1H	JAE-XIV-Carb-Heck-B-13C	JAEXIV-Carb Heck B
197	JAE-Carb-Heck-C-1H	JAE-Carb-Heck-C-13C	JAE-Carb Heck C
198	JAE-Alkyne-B-1H	JAE-Alkyne-B-13C	JAE Alkyne B
200	JAE-Ketone-B-1H	JAE-Ketone-B-13C	JAE Ketone B
204(A)	JAE-Stille-Enone-C-1H	JAE-Stille-Enone-C-13C	JAE-Stille-Enone-C
204(B)	JAE-Stille-Enone-D-1H	JAE-Stille-Enone-D-13C	JAE Stille Enone D
183	JAEVIII-89B	JAEVIII-89B-13C	JAEVIII-89B
181	JAEVIII-131B	JAEXIV-199X-13C	JAEVIII-131B
209	JAEXIV-299B	JAEXIV-299B-13C	JAEXIV-299B
208	JAEVIII-91B	JAEVIII-91B-13C	JAEVIII-131DI
214	JAEVIII-159H	JAEVIII-159H-13C	JAEVII-299D
217	JAEVIII-203B	JAEVIII-203B-13C	JAEVIII-203B

160	JAEVIII-79C	JAEVIII-79C-13C	JAEVIII-79C
218	JAEIX-43B	JAEIX-43B-13C	JAEVIII-33B
220	JAEXIII-51B	JAEXIII-51B-13C	JAEXIII-57B
221(A)	JAEXIII-59C2	JAEXIII-59C2-13C	JAEXIII-59C2
221(B)	JAEXIII-59D2	JAEXIII-59D2-13C	JAEXIII-59D2
156	JAEXI-69B	JAEXI-69B-13C	CyanF-C
222	JAEXIII-187C	JAEXIII-187C-13C	JAEXIII-187C
161	JAEXIII-203BII	JAEXIII-203BII-13C	JAEXIII-203BII

Table A5.2 Compounds in Chapter 3 – A Mathematical Examination of Multiple Asymmetric Transformations: Statistical Amplification and the Horeau Principle

Compound	^{1}H NMR	^{13}C NMR	IR
281	JAEXIII-159B	JAEXIII-159B-13C	JAEXIII-159B
282	JAEXIV-223B	JAEXIV-223B-13C	JAEXIV-223B
287(A)	JAEXIV-205F	JAEXIV-205F-13C	JAEXIV-205DA
287(B)	JAEXIV-205G	JAEXIV-205G-13C	JAEXIV-205DBx
290	JAEXI-285B	JAEXI-285B-13C	JAEXIV-285B
288	JAEXI-291B	JAEXI-291B-13C	JAEXI-291B
289	JAEXIV-227B	JAEXIV-227B-13C	JAEXIV-227B

COMPREHENSIVE BIBLIOGRAPHY

Allbutt, A. D.; Ayer, W. A.; Brodie, H. J.; Johri, B. N.; Taube, H. *Can. J. Microbiol.* **1971**, *17*, 1401–1407.

Arhart, R. J.; Martin, J. C. *J. Am. Chem. Soc.* **1972**, *94*, 5003–5010.

Artman, G. D., III; Weinreb, S. M. *Org. Lett.* **2003**, *5*, 1523–1526.

Ayer, W. A.; Ling, S. P. *Can. J. Chem.* **1979**, *57*, 3332–3337.

Ayer, W. A.; Ling, S. P.; Nakashima, T. T. *Can. J. Chem.* **1979**, *57*, 3338–3343.

Ayer, W. A.; Taube, H. *Can. J. Chem.* **1973**, *51*, 3842–3854.

Ayer, W. A.; Taube, H. *Tetrahedron Lett.* **1972**, 1917–1920.

Ayer, W. A.; Ward, D. E.; Browne, L. M.; Delbaere, L. T. J.; Hoyano, Y. *Can. J. Chem.* **1981**, *59*, 2665–2672.

Baba, S. E.; Sartor, K.; Poulin, J.; Kagan, H. *Bull. Soc. Chim. Fr.* **1994**, *131*, 525–533.

Behenna, D. C.; Stoltz, B. M. *J. Am. Chem. Soc.* **2004**, *126*, 15044–15045.

Brown, H. C.; Joshi, N. N. *J. Org. Chem.* **1988**, *53*, 4059–4062.

Brown, H. C.; Singaram, B. *J. Org. Chem.* **1984**, *49*, 945–947.

Cawley, A.; Duxbury, J. P.; Kee, T. P. *Tetrahedron: Asymm.* **1998**, *9*, 1947–1949.

Conner, B.; Dragunow, M. *Brain Res. Rev.* **1998**, *27*, 1–39.

Crabbé, P.; Garcia, G. A.; Rius, C. *J. Chem. Soc., Perkin Trans. 1* **1973**, 810–816.

Crispino, G. A.; Ho, P. T.; Sharpless, K. B. *Science* **1993**, *259*, 64–65.

Crispino, G. A.; Sharpless, K. B. *Tetrahedron Letters* **1992**, *33*, 4273–4274.

Drège, E.; Morgant, G.; Desmaële, D. *Tetrahedron Lett.* **2005**, *46*, 7263–7266.

Drège, E.; Tominiaux, C.; Morgant, G.; Desmaële, D. *Eur. J. Org. Chem.* **2006**, 4825–4840.

Ebert, H. *Liebigs Ann. Chem.* **1885**, *229*, 45–88.

Eckhardt, M.; Brückner, R.; Suffert, J. *Tetrahedron Lett.* **1995**, *36*, 5167–5170.

Eliel, E. L.; Wilen, S. H. *Stereochemistry of Organic Compounds*; John Wiley & Sons, Inc.: New York, 1994; pp 965–971.

Enquist, J. A., Jr.; Stoltz, B. M. *Nat. Prod. Rep.* **2009**, *26*, 661–680.

Enquist, J. A., Jr.; Stoltz, B. M. *Nature* **2008**, *453*, 1228–1230.

Feringa, B. L. *J. Chem. Soc., Chem. Commun.* **1987**, 695–696.

Feringa, B. L.; Smaardijk, A.; Wynberg, H. *J. Am. Chem. Soc.* **1985**, *107*, 4798–4799.

Feringa, B. L.; Strijtveen, B.; Kellogg, R. M. *J. Org. Chem.* **1986**, *51*, 5485–5489.

Gensler, W. J.; Johnson, F.; Sloan, A. D. B. *J. Am. Chem. Soc.* **1960**, *82*, 6074–6081.

Green, D.; Goldberg, I.; Stein, Z.; Ilan, M.; Kashman, Y. *Nat. Prod. Lett.* **1992**, *1*, 193–199.

Grotjahn, D. B.; Joubran, C. *Tetrahedron: Asymm.* **1995**, *6*, 745–752.

Guerrero, A.; Parrilla, A.; Camps, F. *Tetrahedron Lett.* **1990**, *31*, 1873–1876.

Han, X.; Corey, E. J. *Org. Lett.* **1999**, *1*, 1871–1872.

Han, X.; Stoltz, B. M.; Corey, E. J. *J. Am. Chem. Soc.* **1999**, *121*, 7600–7605.

Hasegawa, E.; Kitazume, T.; Suzuki, K.; Tosaka, E. *Tetrahedron Lett.* **1998**, *39*, 4059–4062.

Hayashi, T.; Tang, J.; Kato, K. *Org. Lett.* **1999**, *1*, 1487–1489.

Heller, D.; Drexler, H.-J.; Fischer, C.; Buschmann, H.; Baumann, W.; Heller, B. *Angew. Chem., Int. Ed.* **2000**, *39*, 495–499.

Helmboldt, H.; Köhler, D.; Hiersemann, M. *Org. Lett.* **2006**, *8*, 1573–1576.

Helmchen, G.; Pfaltz, A. *Acc. Chem. Res.* **2000**, *33*, 336–345.

Honma, M.; Sawada, T.; Fujisawa, Y.; Utsugi, M.; Watanabe, H.; Umino, A.; Matsumura, T.; Hagihara, T.; Takano, M.; Nakada, M. *J. Am. Chem. Soc.* **2003**, *125*, 2860–2861.

Hoye, T. R.; Suhadolnik, J. C. *Tetrahedron* **1986**, *42*, 2855–2862.

Hulst, R.; Kellogg, R. M.; Feringa, B. L. *Recl. Trav. Chim. Pay-B.* **1995**, *114*, 115–138.

Isaksson, R.; Liljefors, T.; Reinholdsson, P. *J. Chem. Soc., Chem. Commun.* **1984**, *3*, 137–138.

Iwasawa, N.; Satoh, H. *J. Am. Chem. Soc.* **1999**, *121*, 7951–7952.

Iwamoto, M.; Kawada, H.; Tanaka, T.; Nakada, M. *Tetrahedron Lett.* **2003**, *44*, 7239–7243.

Jadhav, P. K.; Prasad, J. V. N. V.; Brown, H. C. *J. Org. Chem.* **1985**, *50*, 3203–3206.

Kagan, H. *Tetrahedron* **2001**, 57, 2449–2468.

Kawagishi, H.; Shimada, A.; Hosokawa, S.; Mori, H.; Sakamoto, H.; Ishiguro, Y.; Sakemi, S.; Bordner, J.; Kojima, N.; Furukawa, S. *Tetrahedron Lett.* **1996**, *37*, 7399–7402.

Kawagishi, H.; Shimada, A.; Shirai, R.; Okamoto, K.; Ojima, F.; Sakamoto, H.; Ishiguro, Y.; Furukawa, S. *Tetrahedron Lett.* **1994**, *35*, 1569–1572.

Kharasch, W. H.; Urry, W. H.; Kuderna, B. M. *J. Org. Chem.* **1949**, *14*, 248–253.

Kim, K.; Cha, J. K. *Angew. Chem., Int. Ed.* **2009**, *48*, 5334–5336.

King, A. O.; Okukado, N.; Negishi, E.-I. *J. Chem. Soc., Chem. Commun.* **1977**, 683–684.

Kita, T.; Takaya, Y.; Oshima, Y.; Ohta, T. *Tetrahedron* **1998**, *54*, 11877–11886.

Kolodiazhnyi, O. I. *Tetrahedron* **2003**, *59*, 5953–6018.

Lagasse, F.; Tsukamoto, M.; Welch, C. J.; Kagan, H. B. *J. Am. Chem. Soc.* **2003**, *125*, 7490–7491.

Langenbeck, W.; Triem, G. *Z. Phys. Chem. A* **1936**, *117*, 401–409.

Laverde, A., Jr.; Miranda, D. S.; Conceição, G. J. A.; Schirmer, H.; Pilli, R. A.; Meijere, A.; Marsaioli, A. J. *J. Brazil Chem. Soc.* **1999**, *10*, 293–298.

Lebsack, A. D.; Link, J. T.; Overmann, L. E.; Stearns, B. A. *J. Am. Chem. Soc.* **2002**, *124*, 9008–9009.

Ma, B.-J.; Zhu, H.-J.; Liu, J.-K. *Helv. Chim. Acta* **2004**, *87*, 2877–2881.

Martin, J. C.; Franz, J. A.; Arhart, R. J. *J. Am. Chem. Soc.* **1974**, *96*, 4604–4611.

Maruoka, K.; Concepcion, A. B.; Yamamoto, H. *J. Org. Chem.* **1994**, *59*, 4725–4726.

Maruoka, K.; Concepcion, A. B.; Yamamoto, H. *Synthesis* **1994**, 1283–1290.

Masamune, S.; Choy, W.; Peterson, J.; Sita, L. *Angew. Chem. Int., Ed. Engl.* **1985**, *24*, 1–30.

Mathre, D. J.; Thompson, A. S.; Douglas, A. W.; Hoogsteen, J.; Carroll, J. D.; Corley, E. G.; Grabowki, E. J. *J. Org. Chem.* **1993**, *58*, 2880–2888.

Matsuura, T.; Overmann, L. E.; Poon, D. J. *J. Am. Chem. Soc.* **1998**, *120*, 6500–6503.

Mikami, K.; Motoyama, Y.; Terada, M. *J. Am. Chem. Soc.* **1994**, *116*, 2812–2820.

Miller, L. C.; Ndungu, J. M.; Sarpong, R. *Angew. Chem., Int. Ed.* **2009**, *48*, 2398–2402.

Minami, I.; Takahashi, K.; Shimizu, I.; Kimura, T.; Tsuji, J. *Tetrahedron* **1986**, *42*, 2971–2977.

Mohr, J. T.; Behenna, D. C.; Harned, A. M.; Stoltz, B. M. *Angew. Chem., Int. Ed. Engl.* **2004**, *44*, 6924–6927.

Mohr, J. T.; Ebner, D. C.; Stoltz, B. M. *Org. Biomol. Chem.* **2007**, *5*, 3571–3576.

Mohr, J. T.; Krout, M. R.; Stoltz, B. M. *Org. Synth.* **2009**, *86*, 194–211.

Molander, G. A.; Kenny, C. *J. Org. Chem.* **1991**, *56*, 1439–1445.

Molander, G. A.; McKie, J. A. *J. Org. Chem.* **1992**, *57*, 3132–3139.

Mori, K.; Tanida, K. *Tetrahedron* **1981**, *37*, 3221–3225.

Mori, K.; Watanabe, H. *Tetrahedron* **1986**, *42*, 295–304.

Morrill, C.; Funk, T. W.; Grubbs, R. H. *Tetrahedron Lett.* **2004**, *45*, 7733–7736.

Morrill, C.; Grubbs, R. H. *J. Org. Chem.* **2003**, *68*, 6031–6034.

Nagata, W.; Mitsuru, Y.; Masayuk, M. *J. Am. Chem. Soc.* **1972**, *94*, 4644–4653.

Nakashima, K.; Fujisaki, N.; Inoue, K.; Minami, A.; Nagaya, C.; Sono, M.; Tori, M. *Bull. Chem. Soc. Jpn.* **2006**, *79*, 1955–1962.

Namy, J. L.; Souppe, J.; Kagan, H. B. *Tetrahedron Lett.* **1983**, *24*, 765–766.

Negishi, E.-I.; Ma, S.; Amanfu, J.; Copéret, C.; Miller, J. A.; Tour, J. M. *J. Am. Chem. Soc.* **1996**, *118*, 5919–5913.

Nicolaou, K. C.; Zhong, Y.-L.; Baran, P. S. *J. Am. Chem. Soc.* **2000**, *122*, 7596–7597.

Njardarson, J. T.; Biswas, K.; Danishefsky, S. J. *Chem. Commun.* **2002**, 2759–2761.

Obara, Y.; Kobayashi, H.; Ohta, T.; Ohizumi, Y.; Nakahata, N. *Mol. Pharmacol.* **2001**, *59*, 1287–1297.

Obara, Y.; Nakahata, N.; Kita, T.; Takaya, Y.; Kobayashi, H.; Hosoi, S.; Kiuchi, S.; Ohta, T.; Oshima, Y.; Ohizumi, Y. *Eur. J. Pharmacol.* **1999**, *370*, 79–84.

Ohta, T.; Kita, T.; Kobayashi, N.; Obara, Y.; Nakahata, N.; Ohizumi, Y.; Takaya, Y.; Oshima, Y. *Tetrahedron Lett.* **1998**, *39*, 6229–6232.

Ouryupin, A. B.; Kadyko, M. I.; Petrovskii, P. V.; Fedin, E. I. *Chirality* **1994**, *6*, 1–4.

Palomo, C.; Oiarbide, M.; García, J. M.; González, A.; Lecumberri, A.; Linden, A. *J. Am. Chem. Soc.* **2002**, *124*, 10288–10289.

Pasquier, M.; Marty, W. *Angew. Chem., Int. Ed. Engl.* **1985**, *24*, 315–316.

Peer, M.; de Jong, J. C.; Kiefer, M.; Langer, T.; Rieck, H.; Schell, H.; Sennhenn, P.; Sprinz, J.; Steinhagen, H.; Wiese, B.; Helmchen, G. *Tetrahedron* **1996**, *52*, 7547–7583.

Peng, J.; Avery, M. A.; Hamann, M. T. *Org. Lett.* **2003**, *5*, 4575–4578.

Peng, J.; Kasanah, N.; Stanley, C. E.; Chadwick, J.; Fronczek, M.; Hamann, M. T. *J. Nat. Prod.* **2006**, *69*, 727–730.

Peng, J.; Walsh, K.; Weedman, V.; Bergthold, J. D.; Lynch, J.; Lieu, K. L.; Braude, I. A.; Kelly, M.; Hamann, M. T. *Tetrahedron* **2002**, *58*, 7809–7819.

Periasamy, M; Venkatraman, L.; Thomas, K. R. J. *J. Org. Chem.* **1997**, *62*, 4302–4306.

Pfau, M.; Revial, G.; d'Angelo, J.; Desmaële, D.; Dumas, F.; Guingant, A. *Tetrahedron: Asymm.* **1992**, *3*, 459–505.

Pfau, M.; Revial, G.; d'Angelo, J.; Guingant, A. *J. Am. Chem. Soc.* **1985**, *107*, 273–274.

Pfeiffer, M. W. B.; Phillips, A. J. *J. Am. Chem. Soc.* **2005**, *127*, 5334–5335.

Pfeiffer, M. W. B.; Phillips, A. J. *Tetrahedron Lett.* **2008**, *49*, 6860–6861.

Piers, E.; Gilbert, M.; Cook, K. L. *Org. Lett.* **2000**, *2*, 1407–1410.

Piers, E.; Yeung, B. K. A.; Fleming, F. F. *Can. J. Chem.* **1993**, *71*, 280–286.

Platzer, N.; Rudler, H.; Alvarez, C.; Barkaoui, L.; Denise, B.; Goasdoué, N.; Rager, M.-N.; Vaissermann, J.; Daran, J.-C. *Bull. Soc. Chim. Fr.* **1995**, *132*, 95–113.

Poss, C. S.; Schreiber, S. L. *Acc. Chem. Res.* **1994**, *27*, 9–17.

Rautentrauch, V. *Bull. Soc. Chim. Fr.* **1994**, *131*, 515–524.

Rawat, D. S.; Gibbs, R. A. *Org. Lett.* **2002**, *4*, 3027–3030.

Reddy, T. J.; Bordeau, G.; Trimble, L. *Org. Lett.* **2006**, *8*, 5585–5588.

Reuben, J. *J. Am. Chem. Soc.* **1980**, *102*, 2232–2237.

Rieck, H.; Helmchen, G. *Angew. Chem., Int. Ed. Engl.* **1995**, *34*, 2687–2689.

Satoh, T.; Itaya, T.; Okuro, K.; Miura, M.; Nomura, M. *J. Org. Chem.* **1996**, *60*, 7267–7271.

Saito, T.; Aoki, F.; Hirai, H.; Inagaki, T.; Matsunaga, Y.; Sakakibara, T.; Sakemi, S.; Suzuki, Y.; Watanabe, S.; Suga, O.; Sujaku, T.; Smogowicz, A. A.; Truesdell, S. J.; Wong, J. W.; Nagahisa, A.; Kojima, Y.; Kojima, N. *J. Antibiot. (Tokyo)* **2003**, *51*, 983–990.

Schwink, L.; Knochel, P. *Chem. Eur. J.* **1998**, *4*, 950–968.

Sennett, S. H.; Pomponi, S. A.; Wright, A. E. *J. Nat. Prod.* **1992**, *55*, 1421–1429.

Shibata, H.; Tokunaga, T.; Karasawa, D.; Hirota, A.; Nakayama, M.; Nozaki, H.; Taka, T. *Agric. Biol. Chem.* **1989**, *53*, 3373–3375.

Shimizu, I.; Minami, I.; Tsuji, J. *Tetrahedron Lett.* **1983**, *24*, 1797–1800.

Shimizu, I.; Tsuji, J. *J. Am. Chem. Soc.* **1982**, *104*, 5844–5846.

Snider, B. B. *Comprehensive Organic Synthesis*; Pergamon: Oxford, 1991; Vol. 2, p 527.

Snider, B. B.; Rodini, D. J.; van Straten, J. *J. Am. Chem. Soc.* **1980**, *102*, 5872–5880.

Snider, B. B.; Vo, N. H.; O'Neil, S. V. *J. Org. Chem.* **1998**, *63*, 4732–4740.

Soai, K.; Hori, H.; Kawahara, M. *J. Chem. Soc, Chem. Commun.* **1992**, 106–108.

Snider, B. B.; Vo, N. H.; O'Neil, S. V.; Foxman, B. M. *J. Am. Chem. Soc.* **1996**, *118*, 7644–7645.

Snider, B. B.; Yang, K. J. *J. Org. Chem.* **1990**, *55*, 4392–4399.

Sonogashira, K.; Tohda, Y.; Hagihara, N. *Tetrahedron Lett*. **1975**, *16*, 4467–4470.

Starker, L. N.; Cosulich, D. B.; Smith, J. M., Jr. *J. Am. Chem. Soc*. **1955**, *77*, 2534–2536.

Stetter, H.; Kuhlmann, H. *Tetrahedron Lett*. **1974**, *15*, 4505–4508.

Stewart, I. C.; Ung, T.; Pletnev, A. A.; Berlin, J. M.; Grubbs, R. H.; Schrodi, Y. *Org. Lett*. **2007**, *9*, 1589–1592.

Still, W. C.; Mitra, A. *J. Am. Chem. Soc*. **1978**, *100*, 1927–1928.

Taishi, T.; Takechi, S.; Mori, S. *Tetrahedron Lett*. **1998**, *39*, 4347–4350.

Takano, M.; Umino, A.; Nakada, M. *Org. Lett*. **2004**, *6*, 4897–4900.

Takeda, K.; Nakajima, A.; Takeda, M.; Okamoto, Y.; Sato, T.; Yoshii, E.; Koizumi, T.; Shiro, M. *J. Am. Chem. Soc*. **1998**, *120*, 4947–4959.

Takeda, K.; Nakane, D.; Takeda, M. *Org. Lett*. **2000**, *2*, 1903–1905.

Tamao, K.; Sumitani, K.; Kiso, Y.; Zembayashi, M.; Fujioka, H.; Kodama, S.-I.; Nakajima, I.; Minato, A.; Kumada, M. *Bull. Chem. Soc. Jpn*. **1976**, *49*, 1958–1969.

Tani, K.; Behenna, D. C.; McFadden, R. M.; Stoltz, B. M. *Org. Lett*. **2007**, *9*, 2529–2531.

Taylor, M. S.; Jacobsen, E. N. *Proc. Natl. Acad. Sci. U.S.A*. **2004**, *101*, 5368–5373.

Thominiaux, C.; Chiarnoi, A.; Desmaële, D. *Tetrahedron Lett*. **2002**, *43*, 4107–4110.

Tivola, P. B.; Deagostino, A.; Prandi, C.; Venturello, P. *J. Chem. Soc., Perkin Trans. 1* **2001**, 437–441.

Toda, F.; Tanaka, K. *Chem. Lett.* **1986**, 1905–1908.

Tori, M.; Toyoda, N.; Sono, M. *J. Org. Chem.* **1998**, *63*, 306–313.

Trost, B. M.; Dong, L.; Schroeder, G. M. *J. Am. Chem. Soc.* **2005**, *127*, 2844–2845.

Trost, B. M.; Dong, L.; Schroeder, G. M. *J. Am. Chem. Soc.* **2005**, *127*, 10259–10268.

Trost, B. M.; Mallert, S. *Tetrahedron Lett.* **1993**, *34*, 8025–8028.

Trost, B. M.; Schroeder, G. M. *J. Am. Chem. Soc.* **1999**, *121*, 6759–6760.

Trost, B. M.; Schroeder, G. M.; Kristensen, J. *Angew. Chem., Int. Ed.* **2002**, *41*, 3492–3495.

Trost, B. M.; Toste, F. D.; Pinkerton, A. B. *Chem. Rev.* **2001**, *101*, 2067–2096.

Venkatraman, L.; Periasamy, M. *Tetrahedron: Asymm.* **1996**, *7*, 2471–2474.

Vigneron, J. P.; Dhaenens, M.; Horeau, A. *Tetrahedron* **1973**, *29*, 1055–1059.

Wang, Z.-X.; Tu, Y.; Frohn, M.; Zhang, J.-R.; Shi, Y. *J. Am. Chem. Soc.* **1997**, *119*, 11224–11235.

Watanabe, H.; Nakada, M. *J. Am. Chem. Soc.* **2008**, *130*, 1150–1151.

Watanabe, H.; Nakada, M. *Tetrahedron Lett.* **2008**, *49*, 1518–1522.

Watanabe, H.; Takano, M.; Umino, A.; Ito, T.; Ishikawa, H.; Nakada, M. *Org. Lett.* **2007**, *9*, 359–362.

Ward, D. E. *Can. J. Chem.* **1987**, *65*, 2380–2384.

Ward, D. E.; Gai, Y.; Qiao, Q. *Org. Lett.* **2000**, *2*, 2125–2127.

Ward, D. E.; Rhee, C. K. *Can. J. Chem.* **1989**, *67*, 1206–1211.

Ward, D. E.; Shen, J. *Org. Lett.* **2007**, *9*, 2843–2846.

Waters, S. P.; Tian, Y.; Li, Y.-M.; Danishefsky, S. J. *J. Am. Chem. Soc.* **2005**, *127*, 13514–13515.

Weichert, A.; Bauer, M.; Wirsig, P. *Synlett* **1996**, 473–474.

Welter, C.; Dahnz, A.; Brunner, B.; Streiff, S.; Dübon, P.; Helmchen, G. *Org. Lett.* **2005**, *7*, 1239–1242.

Wender, P. A.; Bi, F. C.; Brodney, M. A.; Gosseln, F. *Org. Lett.* **2001**, *3*, 2105–2108.

Wender, P. A.; Dyckman, A. J.; Husfeld, C. O.; Kadereit, D.; Love, J. A.; Rieck, H. *J. Am. Chem. Soc.* **1999**, *121*, 10442–10443.

Wender, P. A.; Husfeld, C. O.; Langkopf, E.; Love, J. A. *J. Am. Chem. Soc.* **1998**, *120*, 1940–1941.

Wender, P. A.; Takahashi, H.; Witulski, B. *J. Am. Chem. Soc.* **1995**, *117*, 4720–4721.

Wright, D. L.; Whitehead, C. R. *Org. Prep. Proced. Int.* **2000**, *32*, 309–330.

Wu, X.-F.; Neumann, H.; Beller, M. *Angew. Chem. Int. Ed.* **2010**, *49*, 5284–5288.

Wu, X.; Nilsson, P.; Larhed, M. *J. Org. Chem.* **2005**, *70*, 346–349.

Xiong, Z.; Busch, R.; Corey, E. J. *Org. Lett.* **2010,** *12*, 1512–1514.

Xiong, Z.; Corey, E. J. *J. Am. Chem. Soc.* **2000**, *122*, 9328–9329.

Yang, S.; Hungerhoff, B.; Metz, P. *Tetrahedron Lett.* **1998**, *39*, 2097–2098.

Yeh, M.-C. P.; Wang, F.-C.; Tu, J.-J.; Chang, S.-C.; Chou, C.-C.; Liao, J.-W. *Organometallics* **1998**, *17*, 5656–5662.

Yong, K.; Lotoski, J. A.; Chong, J. M. *J. Org. Chem.* **2001**, *66*, 8248–8251.

Yoshikai, K.; Hayama, T.; Nishimura, K.; Yamada, K.; Tomioka, K. *J. Org. Chem.* **2005**, *70*, 681–683.

INDEX

A

α-quaternary.....2, 8, 9, 13, 19, 21–24, 26–28, 30, 33–34, 36–39, 43, 54, 56, 58, 60, 62, 64, 66, 68–74, 76–78, 84–85, 87–90, 92–92, 95, 98–101, 103–105, 107–108, 110–112, 114, 190–191, 221, 224–226, 228–229, 231–233, 240–242, 244–245, 247, 249, 251–252

Acylation.....20, 25, 242

Allyation.....*See* Alkylation

Allocyathin B_2.....2–5, 18–21, 27–29, 33–35

Allocyathin B_3.....2, 5, 23–25

Alyklation.....9, 21, 33, 40, 56–63, 79, 87, 189–191, 223–236, 240–241, 244, 249

Asymmetric.....26, 33, 38, 57, 59, 60, 62, 79, 188–192, 197, 200, 205–210, 212–213, 215–218, 220–226, 228–233, 235–236

B

β-ketoester.....23, 57–61, 79, 84–85, 189–190, 202, 225, 229–231, 234–235, 242–245, 247

B-ring.....2, 7, 9, 12, 14, 28–29, 33–34, 78

Biological activity.....3, 5, 54–55

Biosynthesis.....5–6

Boronate cross-metathesis.....69–70, 101–102

C

Carbonylative reaction.....18–19, 25, 64–66

Claisen condensation.....56–57, 86

Claisen rearrangement.....10

Cha.....8, 42–43

Cross metathesis.....69–70

Crystal structure.....74, 179–187

Cyanthiwigins.....2, 4–5, 9, 17, 37–39, 40–41, 52–56, 75–79, 105, 111, 114

Cyanthiwigin B.....54, 77–78, 111–112

Cyanthiwigin F.....54–56, 76–77, 105–106

Cyanthiwigin G.....54, 78, 114–115

Cyanthiwigin U.....2, 4, 37–38

Cyanthiwigin W.....37–39, 54

Cyanthiwigin Z.....37–39, 54

Cyathane core, preparation of.....2, 10–17, 19, 21, 23–24, 27–28, 30, 35, 37–38, 43, 72–74, 103

Cyathanes 1–10
Cyathins 2–3, 5–6
Cyathin A_3 ..... 2, 26–27, 42–43
Cyathin B_2 42–43
Cycloaddition 7, 10–12, 23–24, 26, 38
Cycloisomerization 33–35

D

Danishefsky 7–8, 35–37
Decarboxylation 56–63, 79, 202, 224–236
Desmaële 7–8, 12–14
Desymmetrization 14, 63–66
Dieckmann cyclization 56–57, 85–86
2,3-Dimethyl-1,7-dioxasprio[5.5]undecane 201–203
Double asymmetric alkylation 57, 59–60, 62, 189–191, 207, 209-210, 212–213, 215, 217–218, 220–221, 223–226, 229–233, 235–236

E

Enantioselective 26–27, 56, 58, 62–63, 87, 188–189, 203–204, 206–208, 214, 217, 225, 228–229
Enol carbonate 59, 77, 190–191, 225–226, 228, 230–231, 234, 239, 245, 247
Enolate 9, 13, 15, 32, 35–36, 42, 61, 64, 77, 225, 227, 230, 233–234
Erinacines 2, 4–5
Erinacine A 2, 18–20
Erinacine B 2, 29–31
Erinacine E 2, 31–32

G

Germane 22
Glabrescol 221–222
Graphs 200, 216
Grubbs catalyst 21, 39, 42, 67–70, 95–97, 99–102

H

Hajos–Parrish 16, 40

Heck reaction 7, 12–14, 65–65, 220
Horeau 63, 195–196
Horeau Principle 63, 189, 195–205, 214–215, 217–218, 223, 230

I

Iodide 9, 13, 22–23, 27–29, 32, 58, 68–69, 75, 84, 201–203
Isaksson 202–203

K

Kagan 63, 206

L

Langenbeck 192–195

M

Methoxycarbonylation 65–66
Mori 201–203

N

Nakada 9, 27–32
Nazarov cyclization 7, 36
Negishi reaction 68–69, 98

O

Omaezakianol 222–223

P

Palladium 7, 14, 18–19, 25, 27, 33, 35, 59, 61–62, 64–66, 68–69, 75–77, 87, 89–90, 92–93, 98, 105–109, 189–191, 203–204, 220–221, 224–226, 228–229, 231, 233, 235, 240–241, 244, 249, 251–252
Pathways for double asymmetric reactions 60, 194, 198, 207, 209, 213, 217–218, 226, 232
Piers 9, 21–23
Phillips 8, 37–39

Q

Quadrigemine C 220–221

Quaternary 2, 8, 9, 13, 19, 21–24, 26–28, 30, 33–34, 36–39, 43, 54, 56, 58, 60, 62, 64, 66, 68–74, 76–78, 84–85, 87–90, 92–92, 95, 98–101, 103–105, 107–108, 110–112, 114, 190–191, 221, 224–226, 228–229, 231–233, 240–242, 244–245, 247, 249, 251–252

R

Radical cyclization 70–74

Reddy 9, 40–41

Ring-closing metathesis 7, 21, 38–39, 42, 56, 67–70, 99–102

Ring-expansion 11–12, 23, 28–29, 36–37

Ruthenium catalysis 33–35, 38–39, 42, 68–70, 101–102

S

Sarcodonin G 2, 4, 21–23

Sarpong 8, 16–17

Samarium iodide 28–30, 120–121

Scabronine 2, 4–5, 35–37

Snider 7–8, 18–20

Sonogashira reaction 66

Spirocycle 5, 9, 40–41, 43, 65–66, 92, 201–202

Stannane 66–67, 71, 94–97

Stereoselective 10, 56, 58–59, 61–62, 189, 191, 221, 226, 235

Stille cross-coupling 66–67, 94–97

T

Takeda 9, 15–16

Tori 9, 20–21

Trost 7–8, 33–35

V

V-40 initiator 72

W

Ward 8–9, 23–27

Wender 7–8, 10–12

X

X-ray structure 74, 179–187

Z

Zinc 68, 98

ABOUT THE AUTHOR

John Andrew Enquist, Jr. was born in Santa Rosa, California on February 24th, 1982 to Cynthia and John Enquist. His early years were spent growing up and attending school in Rohnert Park, with frequent visits to the Santa Rosa area. Though he was born an only child, he was fortunate enough to spend his childhood with his stepmother Janet, his stepfather Mike, his four stepsisters (Tracy, Tiffany, Christy, and Jenna), and his three stepbrothers (Dave, Ryan, and Ben). Much of his early youth was spent playing card, board, and video games with his friends. He also passed much time riding his bike and developing a keen interest in computers. In elementary school, John learned to play the trombone. He maintained this practice throughout middle school, and upon entering Rancho Cotate high school as a freshman, he joined their performance and marching band. At Rancho Cotate John was introduce to the International Baccalaureate program, and it was this class sequence that helped to foster his interest in math and science.

In the fall of the year 2000, John relocated several hundred miles south to attend the University of California in San Diego. As a freshman he was intimidated by the UCSD Chem 141 sequence, but the skillful teaching and powerful enthusiasm of Professor Jay Siegel soon transformed this apprehension into excitement. Over the years, John would attend multiple classes taught by Professor Siegel, as well as courses lead by Professors Charles Perrin, Karsten Meyer, Yoshihisa Kobayashi, John Wheeler, and Marjorie Casserio. Their dynamic and challenging lessons pertaining to all matters of chemistry helped to fuel John's interest in organic synthesis. Though John passed a year as an undergraduate assistant in the molecular biology laboratories of Professor Daniel Donoughe, he was later given the opportunity to join the organic chemistry labs of Professor Yitzhak Tor. In Professor Tor's group, John learned the fundamentals of synthesis, and learned much from Dr. Haim Weizman.

After graduating from UCSD in 2004, John travelled to Pasadena, California to enter the graduate program at the California Institute of Technology. He was fortunate enough to join the group of Professor Brian Stoltz, where his research efforts have focused on the enantioselective total synthesis of the cyanthiwigin diterpenoid molecules. John will begin a postdoctoral position in the laboratories of Professor John Wood at Colorado State University in late 2010.